Design, Synthesis and Evaluation of 1,3-Diaryl Pyrazoles as Inhibitors of GGTase-I, a Target for Anti-cancer Drugs

BY

MUHAMMAD MANSHA

A Dissertation Presented to the

DEANSHIP OF GRADUATE STUDIES

KING FAHD UNIVERSITY OF PETROLEUM & MINERALS

DHAHRAN, SAUDI ARABIA

In Partial Fulfillment of the

Requirements for the Degree of

DOCTOR OF PHILOSOPHY

In

CHEMISTRY

MAY 2017

KING FAHD UNIVERSITY OF PETROLEUM & MINERALS

DHAHRAN- 31261, SAUDI ARABIA

DEANSHIP OF GRADUATE STUDIES

This thesis, written by MUHAMMAD MANSHA under the direction of his thesis advisor and approved by his thesis committee, has been presented and accepted by the Dean of Graduate Studies, in partial fulfillment of the requirements for the degree of **DOCTOR OF PHILOSOPHY IN CHEMISTRY.**

Dr. Nisar Ullah
(Advisor)

22/5/2017

Dr. Abdulaziz Al-Saadi
Department Chairman

Sk. Asrof Ali

Dr. Shaikh Asrof Ali
(Member)

Dr. Salam A. Zummo
Dean of Graduate Studies

Dr. Anvarhusein A. Isab
(Member)

7/6/17

Date

Dr. Hassan Ali Saleh Al-Muallem
(Member)

Dr. Basheer Chanbasha
(Member)

DEDICATION

Dedicated to my mentor and an affectionate brother **Major (R) Zulfiqar Ali Chohan,** a source of inspiration and encouragement for me.

ACKNOWLEDGMENTS

All praise is to **ALLAH** to Most Gracious, Merciful and Almighty who bestowed me with potential and ability to complete this research work. His peace and blessings be upon his messenger **MUHAMMAD (S.A.W.)** who is forever a torch of guidance and knowledge for humanity.

After gratefulness of Almighty ALLAH, I would like to express my sincere appreciation to my parents for their devotion, dedication and self-sacrificing support for putting me on the path of learning. It is highly imperative for me to mention here every support provided by my brothers, sisters and other family members during my college and university days. I could not ever forget their assistance, encouragement and prayers for my every success in life.

I would not miss the opportunity to express special thanks to my supervisor Prof Dr. Nisar Ullah**,** Department of Chemistry, King Fahd University of Petroleum and Minerals, KFUPM, for his enormous assistance, time dedication, encouraging attitude, and invaluable suggestions that helped me a lot to accomplish this research work. I found him a personality having a blend of character, competence and courage. I learned from him the secrecies to spend a well-managed, organized, and reputable life.

I would also like to express my sincere gratitude to committee members Dr. Shaikh Asrof Ali, Dr. Anvarhusein A. Isab, Dr. Hassan Ali Saleh Al-Muallem, and Dr. Basheer Chanbasha for their contributions to enhance the quality of my thesis. Further, I also appreciate the role of all faculty members of Chemistry Department, KFUPM, for teaching up-to-date and modern chemistry courses and constituting my scholarly personality.

Last but not the least, no words can be satisfying enough to express my cordial thanks to my colleagues and co-workers. Especially I would like to thank Ibrahim Khan, Muhammad Naeem Younas, Muhammad Ibrar Ahmed, Abdul Waheed, Muhammad Sajid, Sajid Jillani, Muhammad Monim-ul-Mehboob, Yasir Abbas, Azeem Rana and Nadeem Baig for their cooperation and caring behavior for me. In the end, I salute the dignity of my beloved Mother (Late) and Father who supported and prayed for my success throughout my life.

TABLE OF CONTENTS

LIST OF SCHEMES

LIST OF TABLES

LIST OF FIGURES

LIST OF ABBREVIATIONS

FTase	:	Farnesyltransferase
GGTase-I	:	Geranylgeranyltransferase
Ser.	:	Serine
Met.	:	Methionine
Gln.	:	Glutamine
Cys.	:	Cysteine
Ala.	:	Alanine
Leu.	:	Leucine
Rce1	:	Ras Converting Enzyme
Icmt	:	Isoprenyl-cysteine Carboxylmethyltransferase
FTIs	:	Farnesyltransferase Inhibitors
GGTIs	:	Geranylgeranyltransferase Inhibitors
FPP	:	Farnesyl Diphosphate
GGPP	:	Geranylgeranyl Diphosphate
DPIs	:	Dual Prenylated Inhibitors
QSAR	:	Quantitative Structure-Activity Relationship
MIR	:	Multiple Isomorphous Replacement
SIRAS	:	Single Isomorphous Replacement with Anomalous Scattering
PDB	:	Protein Data Bank
1FT1	:	Name of Protein (Farnesyltransferase)

1N4P	:	Name of Protein (Geranylgeranyltransferase-I)
SCC	:	Squamous Cell Carcinoma
AML	:	Acute Myeloid Leukemia
MTT	:	3-(4,5-Dimethylthiazol-2-yl)-2,5-Diphenyltetrazolium Bromide
Formazan	:	1,3,5-Triphenyltetrazolium Formazan
HEPES	:	2-[4-(2-hydroxyethyl)piperazin-1-yl]ethanesulfonic acid
PVDF	:	Polyvinylidene Difluoride
Tris-HCl	:	2-Amino-2-(hydroxymethyl)-1,3-propanediol hydrochloride
EDTA	:	Ethylenediaminetetraacetic Acid
DMSO	:	Dimethyl Sulfoxide
GSP	:	Glide Standard Precision
GXP	:	Glide Extra Precision
OPLS	:	Optimized Potentials for Liquid Simulations

ABSTRACT

Full Name : MUHAMMAD MANSHA

Thesis Title : Design, Synthesis and Evaluation of 1,3-Diaryl Pyrazoles as Inhibitors of GGTase-I, a Target for Anti-cancer Drugs

Major Field : CHEMISTRY

Date of Degree : May 2017

Ras and Rho proteins, involve in the pathogenesis of more than half of all forms of cancer, undergo posttranslational modification with an isoprenyl lipid catalyzed by protein farnesyltransferase (FTase) or protein geranylgeranyltransferase-I (GGTase-I). This posttranslational modification is termed as prenylation. The attached lipid is required for proper function of the modified protein, either as a mediator of membrane association, a determinant for specific protein-protein interactions, or both. Accordingly, inhibitors for both of these enzymes have been developed. However, farnesyltransferase inhibitors (FTIs) have not performed up to expectation in solid tumors and failed to respond in many types of cancer. When FTase is inhibited, the human oncogenic Ras isoform K-RasB is geranylgeranylated by protein GGTase-I. GGTase-I is the enzyme that catalyzes geranylgeranylation, which in turn is important to the function of the majority of Rho GTPases and several other regulatory proteins. Earlier studies have demonstrated that many of these proteins contribute to tumor development and metastasis. Thus to effectively block Ras processing, the development of selective inhibitors of GGTase-I (GGTIs) is required. In addition to their potential to suppress alternate prenylation of K-Ras and hence impact on K-Ras-dependent oncogensis, GGTIs have been proposed as potential drugs for anti-angiogenic therapy and for inhibiting metastatic progression of cancers (via impact on

proteins such as RhoA/C), inflammatory disorders and those of vascular system, and for hepatitis C.

In this study, a series of pyrazole-based GGTIs, structural analogues of GGTI-DU40, **2-16** have been synthesized and biologically evaluated for their GGTas-1 and farnesyltransferase (FTase) inhibition. The screening results revealed that **2** (IC_{50} = 2.4 μM) and **5** (IC_{50} = 3.1 μM) are potent inhibitors of GGTase-I, possessing higher inhibitory activity compared to the control compound **1** (GGTI-DU40, IC_{50} = 3.3 μM). The anti-proliferative efficacies against MDA-MB-231 cells line of target compounds demonstrated a significantly higher activity of **2** (IC_{50} = 7.6 μM) compared to **1** (IC_{50} = 23.0 μM). The efficiency of the target compounds was further validated by western blot analysis in MDA-MB-231 cell line, which revealed very high inhibitory cellular activity of **2** and **5**, demonstrating their capacity to inhibit prenylation of endogenous proteins. Molecular docking studies of **2** with the crystal structure of GGTase-I complexed with a geranylgeranyl pyrophosphate (GGPP) Analog and a CaaX (C = cysteine, aa = aliphatic amino acids, and X = any amino acid) portion of the KKKSKTKCVIL peptide substrate revealed several H-bonding interactions and π-π contacts between **2** and the binding pocket of GGTase-I. Therefore, highly potent in vitro activity of **2** merits its extensive in vivo investigation.

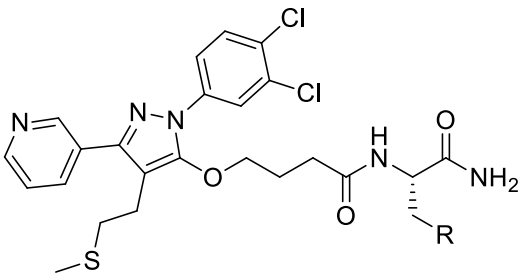

(1) R = Ph (GGTI-DU40)
(2) R = 4-FPh
(3) R = 3-pyridyl
(4) R = 4-pyridyl
(5) R = 4-OMePh

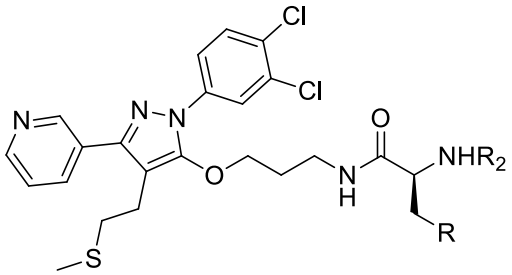

(6) R_1 = Ph; R_2 = $COCH_3$
(**7**) R_1 = Ph; R_2 = SO_2CH_3
(8) R_1 = 4-FPh; R_2 = $COCH_3$
(9) R_1 = 4-FPh; R_2 = SO_2CH_3
(10) R_1 = 4-OMePh; R_2 = $COCH_3$
(11) R_1 = 4-OMePh; R_2 = SO_2CH_3
(12) R_1 = 4-OMePh; R_2 = $COO(CH_3)_3$
(13) R_1 = 3-pyridyl; R_2 = $COCH_3$
(14) R_1 = 3-pyridyl; R_2 = SO_2CH_3
(15) R_1 = 4-pyridyl; R_2 = $COCH_3$
(16) R_1 = 4-pyridy; R_2 = SO_2CH_3

Chemical structures of target compounds 2-16

ملخص الرسالة

الاسم الكامل: محمد منشاء

عنوان الرسالة: تصميم وتوليف وتقييم 1،3-دياريل بيرازولس كمثبطات GGTase-I، وهو هدف للأدوية المضادة للسرطان

التخصص: كيمياء

تاريخ الدرجة العلمية: مايو 2017

تدخل البروتينات راس ورو "Ras and Rho" بالتسبب بأكثر من نصف جميع أشكال السرطان، وتخضع لتعديلات ما بعد متعدية مع لبيد أيزوبرين المحفزة من قبل البروتين فارنيسيلترانزفيراس "farnesyltransferase" (FTase) أو البروتين جيرانيلجيرانييلترانزفيراس-1 "geranylgeranyltransferase-I" (GGTase-I). ويعمل تعديل ما بعد متعدية إلى تحويل البروتينات إلى بروتينات كاره للماء وتدعى "prenylation". وتكون الدهون المرفقة مطلوبة من أجل وظيفة مناسبة للبروتين المعدل، إما كوسيط غشاء الجمعية أو محددا لتفاعلات بروتينبروتين معينة أو كليهما. وبناء على ذلك، طُورت مثبطات لكل من هذه الانزيمات. ومع ذلك فإن مثبطات البروتين فارنيسيلترانزفيراس (FTIs) لم تنفذ بعد ليتوقع أورام صلبة وقشل في الاستجابة في العديد من أنواع السرطان. عندما يثبط الأنزيم فيتس "FTase" فإن المورثة الرومية البشرية للبروتين " K-RasB " الشكل الأيزو للبروتين راس "Ras" يخضع لتعديلات يجعله كاره للماء بواسطة البروتين جي جي تاس -1 "GGTase-I". جي جي تاس-1 "GGTase-I " هو الأنزيم المحفز للتفاعلات التي تجعل البروتين كاره للماء، والتي بدورها مهمة لتوظيف البروتينات رو "Rho " و جي تي باس " GTPases " و العديد من البروتينات التنظيمية الأخرى.

وقد أظهرت الدراسات السابقة أن العديد من هذه البروتينات تسهم في تطور الورم و الورم الخبيث. وهكذا لمنع فعالية مالجة البروتين راس "Ras " يتطلب ذلك تطوير انتقائي للمثبطات من نوع جي جي تاس-1 "GGTase-I ". بلإضافة إلى امكانية تثبيط التفاعلات الكاره للماء لبديلة الناتجة من البروتين ك-راس " K-Ras " وبالتالي التأثير على ك-راس " K-Ras " المعتمدة على تكوين الورم. أُقترح جي جي تاس-1 "" كأدوية لعلاج المضادة للأوعية ولمنع تطور الورم إلى سرطان واضطرابات التهابات وأمراض الجهاز الوعائي والتهاب الكبد C.

في هذه الدراسة، صُنعت سلسلة من بيرازول "pyrazole " ذات أساس بروتيني من جي جي تاس "GGTIs " وكذلك النظائر البنيوية لـ جي جي تي اي – دي يو40 "GGTI-DU40 " **2-16** وقُيمت بيولوجيا مقارنة مع المثبطات جي جي تاس-1 "GGTas-1" وفارنيسيلترانزفيراس "farnesyltransferase". كشفت نتائج الفحص المركب **2** (IC_{50} = 2.4 µM) والمركب **5** (IC_{50} = 3.1 µM) أنها مثبطات أقوى من جي جي تاس-1 "GGTase-I " وتمتلك نشاطا أعلى مقارنة مع المركب **1** (GGTI-DU40, IC_{50} = 3.3 µM). واظهرت نتائج تاثير مضادات التكاثر على الخلايا MDA-MB-231فعالية عالية نسبيا للمركب **2** (IC_{50} = 7.6 µM) مقارنة بالمركب **1** (IC_{50} = 23.0 µM). تم التحقق من كفاءة المركبات المستهدفة من خلال تحليل لطخة غربية في خط الخلية MDA-MB-231 الذي كشف عن فعالية تثبيط عالية جدا للمركبين **2** و**5**، مما يدل على مقدرتهما في تثبيط تحول البروتينات الذاتية إلى كاره للماء. كشفت الدراسة الجزيئية لمعقد إرتباط المركب **2** مع البنية البلورية لجي جي تاس-1 و جيرانيلجيرانيل بيروفوسفات "geranylgeranyl pyrophosphate " (GGPP) وأيضا الساكس (CaaX) (س= سيستين وأ= ألفا أمينو اسيد و أكس= أيَ حمض أميني) جزء من ركيزة الببتيد (KKKSKTKCVIL) العديد من تفاعلات الرابطة هدروجين مع و الرابطة باي –باي (π-π) بين **2** و جيب من جي جي تاس-1. لذك النشاط العالي في المختبر الحيوي لـ **2** يلزمه دراسة واسعة على الجسم الحي.

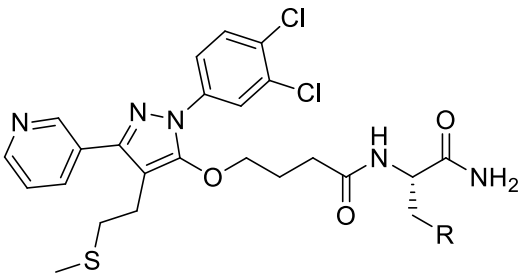

(1) R = Ph (GGTI-DU40)
(2) R = 4-FPh
(3) R = 3-pyridyl
(4) R = 4-pyridyl
(5) R = 4-OMePh

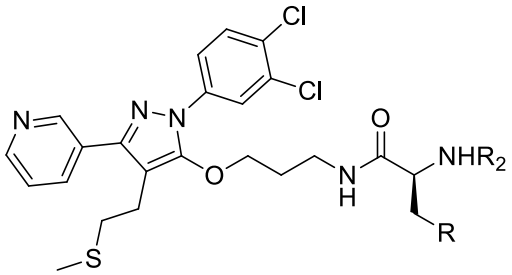

(6) R_1 = Ph; R_2 = $COCH_3$
(**7**) R_1 = Ph; R_2 = SO_2CH_3
(8) R_1 = 4-FPh; R_2 = $COCH_3$
(9) R_1 = 4-FPh; R_2 = SO_2CH_3
(10) R_1 = 4-OMePh; R_2 = $COCH_3$
(11) R_1 = 4-OMePh; R_2 = SO_2CH_3
(12) R_1 = 4-OMePh; R_2 = $COO(CH_3)_3$
(13) R_1 = 3-pyridyl; R_2 = $COCH_3$
(14) R_1 = 3-pyridyl; R_2 = SO_2CH_3
(15) R_1 = 4-pyridyl; R_2 = $COCH_3$
(16) R_1 = 4-pyridy; R_2 = SO_2CH_3

الهياكل الكيميائية من المركبات المستهدفة **2-16**

CHAPTER 1

INTRODUCTION AND LITERATURE REVIEW

1.1 Background

Protein prenylation is one of the crucial post-translational modifications that play an important role in biology. Ras superfamily of small GTPases is the largest protein family that undergoes post-translational prenylation for their biological role [1]. The prenylation of Ras has got immense interest when it is observed that oncogenic Ras are inactive on preventing from membrane attachment [2]. The protein prenylation, a process initiated by covalent attachment of 15-carbon farnesyl or a 20-carbon geranylgeranyl isoprenoids to a conserved cysteine residue, modifies many key regulatory proteins in eukaryotic cells at their C-terminus [3,4].

The majority of these prenylated proteins are termed "CaaX proteins" due to their specific C-terminal motif that directs the lipid modification, which involves covalent addition of either farnesyl (15-carbon) or geranylgeranyl (20-carbon) isoprenoids via thioether linkages to the conserved cysteine fourth in from their C-terminus. The enzymes responsible are termed as protein farnesyltransferase, (FTase, 15-carbon modification) and protein geranylgeranyltransferase-I (GGTase-I, 20-carbon modification). GGTase-I attaches the 20-carbon isoprenoid lipid to CaaX motifs wherein the carboxyl-terminal residue "X" is Leu or Phe) [4–6]. CaaX prenyl proteins, which include most members of the Ras family of GTP-binding proteins (G proteins), play critical roles in a number of

cellular processes, including transmembrane signaling, intracellular membrane trafficking, and mitosis [7,8].

The protein prenylation cascade begins with the addition of a 15-carbon isoprene farnesyl lipid when X residues are Ser, Met, Gln, Cys, and Ala; or a 20-carbon geranylgeranyl lipid is added when the X residue is Leu [9]. The CaaX prenyltransferases include protein farnesyltransferase (FTase) that adds the 15-carbon farnesyl group to the cysteine residue of the CaaX sequence [4] whereas protein geranylgeranyltransferase type I (GGTase-I) transfers the 20-carbon geranylgeranyl group to proteins including critical signaling molecules from many classes, e.g., the Ras superfamily (including K-Ras, Rho, Rap, Cdc42, and Rac), several G-protein γ subunits, protein kinases (rhodopsin kinase, phosphorylase kinase, and GRK7), and protein phosphatases [4,10,11]. In addition to attachment of the isoprenoid, Ras and most other CaaX proteins undergo two subsequent prenylation-dependent processing steps, proteolytic removal of the -aaX tripeptide by the CaaX protease Ras converting enzyme (Rce1) and carboxymethylation of the now C-terminal prenylcysteine residue by an enzyme termed isoprenylcysteine carboxy methyltransfrase (Icmt) [9, 12]. A schematic of the processing pathway for CaaX prenyl proteins is shown in (Fig. 1). The attached lipid imparts significant hydrophobic character to the protein, and can serve as an anchor for membrane association and as a hydrophobic determinant of protein-protein interactions.

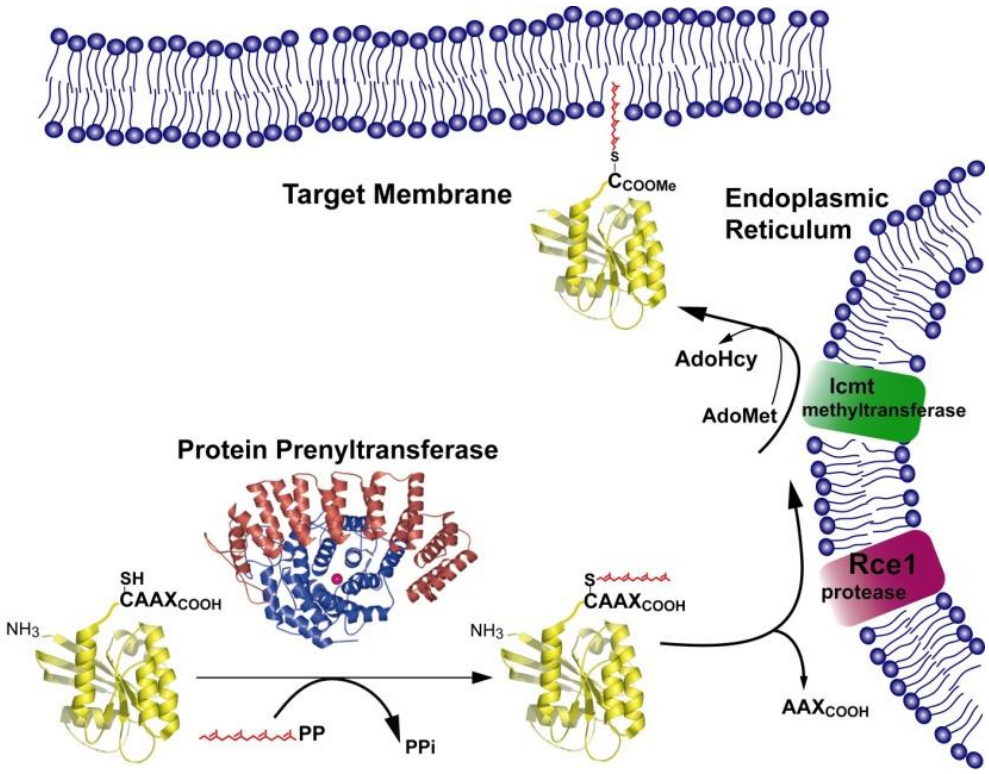

Figure 1: Processing pathway for CaaX proteins

Both Rce1 and Icmt are associated with the endoplasmic reticulum. The product of this 3-steps modification process is to create a mature form of the CaaX protein with increased hydrophobicity that facilitates interaction with membranes; the modified C-terminus can also be viewed as a motif for specific protein-protein recognition events [13].

The Ras proteins, the most thoroughly studied CAAX proteins, are mutated in human cancer more frequently than any other oncogenes. Because of involvement in the pathogenesis of many forms of cancer [14], Ras has been a center of focus for cancer biologist seeking to develop rationally designed anti-cancer drugs. Since isoprenylation is essential for the plasma membrane targeting of the Ras proteins and their ability to

transform cells [15], FTase inhibitors (FTIs) have been developed and tested as anticancer agents [16]. FTIs showed efficacy in preclinical studies of malignancies, including those without Ras mutations [17,18]. However, unfortunately, clinical trials of FTIs in humans have not been particularly successful [16].

1.2 The CaaX Prenyltransferases: FTase and GGTase-I

As noted above, two distinct protein prenyltransferases act on CaaX-type proteins. FTase is a heterodimeric enzyme containing a 48 kDa α subunit and 46 kDa β subunit. GGTase-I is similarly a heterodimer, with the same α subunit as FTase and a distinct 43 kDa β subunit [19,20]. The enzymes use farnesyl diphosphate (FPP) and geranylgeranyl diphosphate (GGPP) as their respective isoprenoid substrates. Proteins modified by FTase include the canonical Ras GTPases (H-, K- and N-), the nuclear protein lamin B, several proteins in the retina involved in phototransduction, and several enzymes controlling protein phosphorylation. Proteins modified by GGTase-I include GTPases in the Rho and Rac families, and many G protein γ subunits. The two CaaX prenyltransferases require the Cys residue fourth from the C-terminus of their protein substrates, with the X residue of the CaaX motif most responsible for which enzyme will act on the protein. When X is Ser, Met, Ala or Gln, FTase will process the protein, while if it is Leu then GGTase-I will handle; Phe seems to be efficiently recognized by both enzymes [11]. The simple tetrapeptide motif is the primary recognition; both enzymes can process CaaX tetrapeptides quite efficiently [14].

The CaaX prenyltransferases are zinc metalloenzymes [21,22]. The kinetic mechanism of FTase has been extensively studied and is functionally ordered, with FPP binding first to

form a complex that reacts with a CaaX protein or peptide [23,24] GGTase-I appears to follow a similar kinetic mechanism [25,26]. The dissociation rate of the product very slow, and in vitro a FTase-product complex can be isolated [27,28]. Considerable structural information is available for both enzymes; FTase being the first to yield to the crystallography [29]. The common α subunit contains seven successive pairs of coiled-coils that wrap around a significant portion of the β subunit, which is primarily helical and folded into an α-α barrel structure. Crystal structures of complexes containing both an isoprenoid analogue and a CaaX peptide bound in the active site revealed the determinants of the active sites both FTase and GGTase-I [30]. The availability of structural information on the CaaX prenyltransferases has allowed incisive structure-function analyses of the enzymes, and allowed structure-aided drug design.

1.3 Structure of FTase and GGTase-I

Including Ras, Rho and lamins more than 30 different types of farnesylated proteins, attachment of a 15-carbon farnesyl group to the cysteine residue of target protein by developing a thioether linkage (Scheme-1) [31], have been identified in the mammalian cells. As this farnesylation is essential for the membrane association and plays a critical role in transformation of normal cells to the cancer cells in mutant form of Ras. This process is catalyzed by a zinc metalloenzyme called as farnesyltransferase (FTase) [32–34]. The studies show that FTase made of two different α and β subunits and for development of high level of FTase both subunits are indispensable. The apparent molecular weight measured by SDS-polyacrylamide gel electrophoresis is of 50 kDa. While by gel filtration chromatography is in range 70-100 kDa and also established the fact that there is one to one ratio of α/β heterodimer [35].

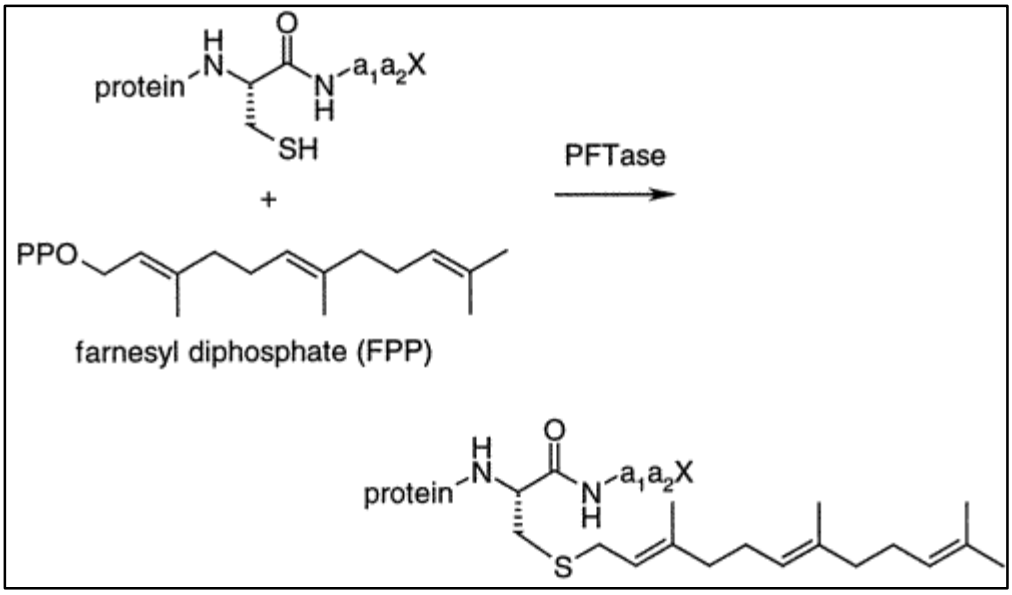

Scheme 1: Farnesylation of Cysteine in CaaX

Hee-Won Park et al. produced FTase from Sf9 cell, purified and determined its crystal structure at 2.25 Å by applying different techniques like multiple isomorphous replacement (MIR) and anomalous scattering with three heavy atom derivatives, phase combination, solvent flattering and crystallographic refinement. The α-helices are the main components in the secondary structure between α and β subunits (Fig. 2 a&b). A series of right handed antiparallel coils formed by folding of 2 to 15 α subunits into seven successive pairs. These helical hairpins are arranged in a double layered, right handed super helix resulting in a crescent shaped subunit that envelops part of the β subunit. It is seen that all helices are parallel in one layer however they are antiparallel to helices in the adjacent neighboring layer. There are about twelve α helices of the β subunits which are folded in the form of α-α barrel. From the figure 3a it is evident that the inner portion of the barrel is formed by a core of six parallel helices (3β, 5β, 7β, 9β, 11β, and 13β). However, the outside of the helical barrel is made up of six helices (2β, 4β, 6β, 8β, 10β, and 12β) that are inter connected

with the inner part. Thus the conclusion can be drawn that peripheral six helices are parallel to each other but antiparallel to other six helices. One ending of the barrel is blocked by a loop formed by residues 399β to 402β while the other end remains open for the solvent and form a cleft in the center where the active sites are present for enzymatic action [29].

The β-subunit of FTase plays its role in binding of the peptide or protein substrate and prenyl donor in the presence of Zn^{2+}. Prenylation product formation efficiently requires enzyme bound Zn^{2+} and high concentration of Mg^{+2} for protein farnesyltransferase [22].

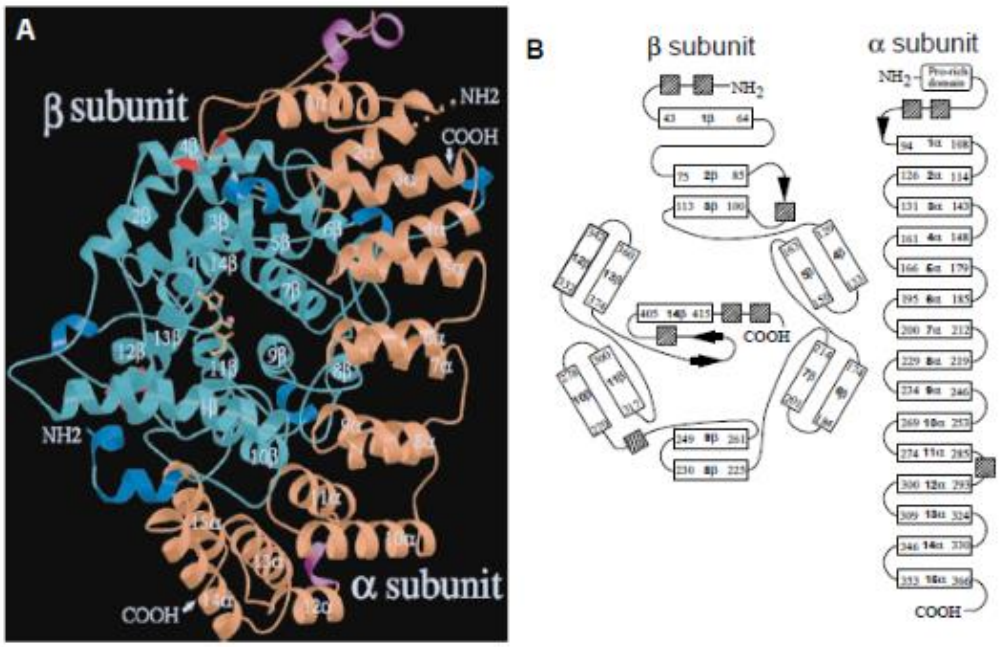

Figure 2a&b: Crystal structure of the rat FTase heterodimer, with resolution of 2.25Å [29].

The crystal structure of FTase shows that zinc ion is located at a junction between hydrophilic surface near the subunit interface and a hydrophobic deep cleft in β-subunit that further lined with aromatic residue. This hydrophobic cleft at the center of α- α barrel is wrinkled with 10 highly conserved aromatic residues ((Trp (102β, 106β, 303β), Phe (253β, 302β), and Tyr (105β, 154β, 205β, 361β, 365β)). Directly opposite of zinc ion, at

the top of the cleft there is Arg202β in helix 7β is positioned in such a manner so that it might have interaction with the phosphate moiety of the substrate. The diphosphate moiety interacts with zinc atom only when the length of farnesyl diphosphate (FPP) is such that its terminal carbon of isoprenoid may bind at bottom of the packet (Fig. 3b). β subunit residues Asp297β and Cys299β residing in NH_2 terminal flanking loop of helix 11β, His362β in helix 13β and water molecule contribute in the coordination of zinc. Where the bidentate ligand is formed by Asp297β and distorted pentacoordinate geometry is formed. Hua-Wen Fu et al. found that the mutation of Cys299β to Ala not only affects the binding of zinc but also leads to abolish catalytic activity [35].

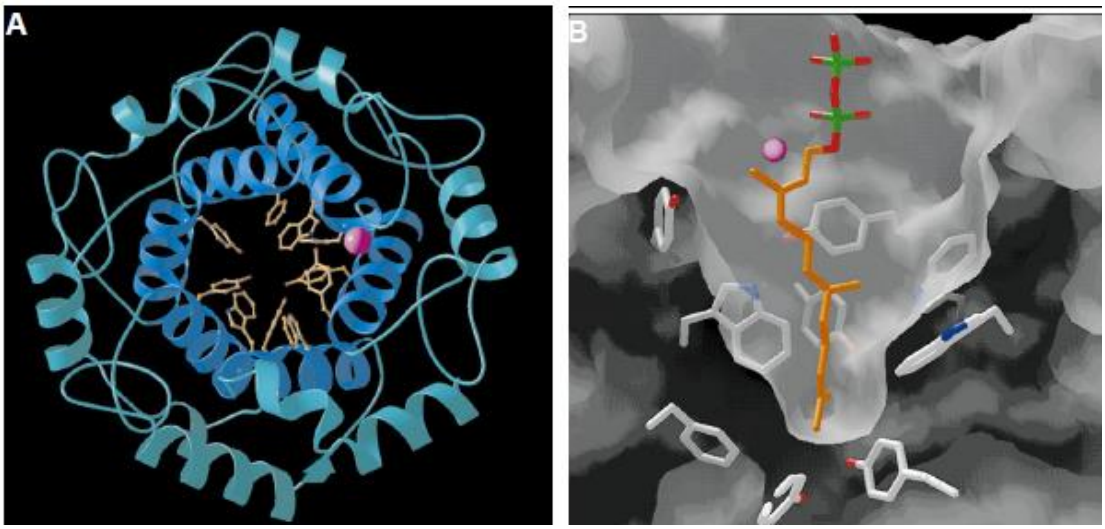

Figure 3 a&b: The β subunit (FT1).
(a) Aromatic pocket in the center of the α-α barrel of the β subunit. Only helices 2β to 13β are shown. (b) A portion of the solvent-accessible surface showing some of the aromatic residues that line the putative FPP binding pocket (PDB: 1FT1) [35].

Cross linking studies revealed that binding sites for the proteins and isoprenoid substrates located on the β subunit. The COOH terminal CaaX peptide and FPP substrates location

can be deduced from two clefts which are entirely different in surface properties and that intersects marked by bound zinc ion. The affinity of a protein substrate for FTase is enhanced by the presence of multiple basic residues just upstream of the CAAX motif (the so-called polybasic region) (Fig. 4a).

Protein geranylgeranyltransferase type I (GGTase-I) is also zinc metalloenzyme where the prenylation leads to an addition of a 20-carbon isoprenoid group to the cysteine residue of CaaX motif. By using the CaaX motif as a substrate, the post translational modifications create lapidated domain that mediate attachment to specific proteins [33,36]. The zinc metalloenzymes (FTase/GGTase-I) are specific for the COOH- terminal residue however the GGTase-I prefer the proteins that have Leucine (Leu.) at terminal. Just like the FTase, GGTase-I is also a heterodimer of α and β subunits having the apparent molecular weight of 50 kDa. GGTase-I recognizes Leu. at the terminal of CaaX shares indistinguishable α subunits as far as FTase but differ entirely in β subunits that is crucial for selectivity of isoprenoid diphosphate substrate.

J.S. Taylor et al. in 2003 presented the structural details for the mammalian GGTase-I along with series of substrate and product complexes that portray the path of chemical reaction. The structure was determined by single isomorphous replacement with anomalous scattering (SIRAS) method [26]. GGTase-I crystals belong to I222 space group, having three complete 91 kDa heterodimers in the asymmetric unit. The overall picture of the structure of GGTase-I is shown in figure 4b. In GGTase-I is found in crescent shape around β subunit of α subunits that are arranged to in α-helical hairpin pairs. The sequence of GGTase-I are identical to FTase α subunit , however, the crescent shaped α subunits of GGTase-I is slightly different by smaller in size (377 residues versus 437). There is an

extensive interface between α and β subunits covering more than 3300 Å. A compact and globular α – α barrel domain having a central funnel shaped cavity is formed by β subunits where the substrate binding site opens. This cavity is lined by the hydrophobic residues. A zinc ion is also bound near the top of active site funnel cavity which is required for the catalytic functions [37]. Zinc ion can be removed by using chelating agents without altering the structure significantly. As α subunits are same in GGTase-I and FTase, so it can be presumed that the functional differences are the results of differences in β subunits having identity of only upto 25%. In GGTase-I a loop is formed by the residues 79β-121β connecting to helix 3β and 11β having an insertion of 26 residues relative to FTase. The loop ending at helix 4β that forms part of CaaX binding site and presents a shift in position to induce CaaX enzyme specificity.

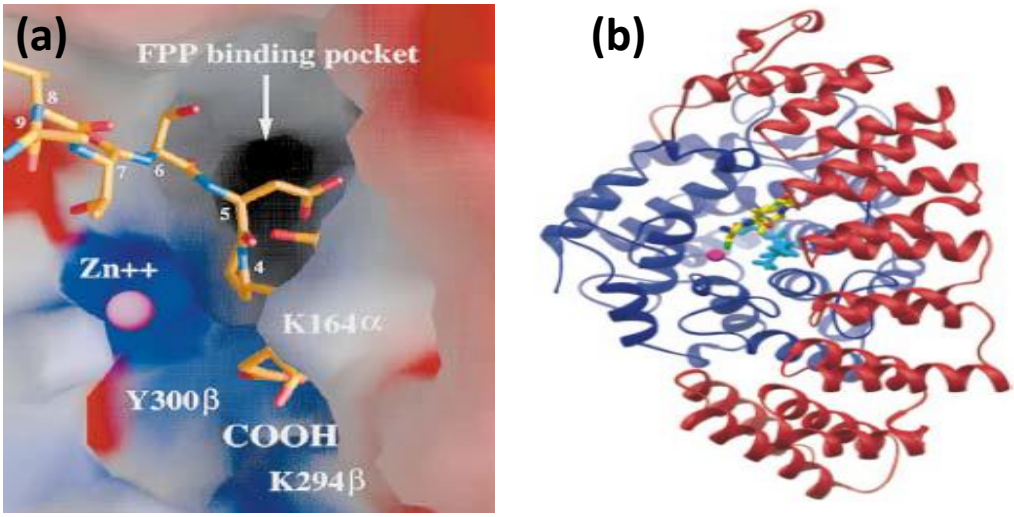

Figure 4: (a) Close-up view of the peptide binding cleft on the interface of the β subunit (PDB: 1FT1) (b) GGTase-I ternary substrate complex (PDB: 1N4P) [37].

Here, the GGTase-I consists of a 48 kD α subunit (red) and a 43 kD β subunit (blue). The non-reactive 3'azaGGPP (cyan) binds similarly to GGPP in the active site. The CaaX

portion of the KKKSKTKCVIL peptide substrate (yellow) binds against the isoprenoid, with the cysteine sulfur coordinating the catalytic zinc ion (magenta).

1.4 Rationale for Targeting GGTase-I in Cancer

The Rho-GTPases act as molecular switch for inactive GDP-bound form and an active GTP-bound state cycle. After activation of GDP-bound undergoes interaction with broad spectrum of diverse effectors to mediate their functions. Similarly another molecular switch for activation of GDP is guanine nucleotide exchange factors (GEFs) by catalyzing exchange of GDP to GTP. The most important investigated members of this group are K-Ras, RhoA, Rac1, and Cdc42. Ras family members, particularly K-Ras, are major contributors to human tumorigenesis through mutational or other types of aberrant activation [38]. It is found that Ras mutations are responsible of ~30% of most cancer types and so far identified it is included in mutated dominant oncogene. The discoveries of tumor suppressor functions for deleted in liver cancer 1 (DLC1) and Rho-GAP has provided evidence Rho GTPase activation is widespread in cancer as shown in figure-5 [37].

Figure 5: Ras GTP - GDP cycle (a significant GAP in the cancer genome).

In cancer progression, most deteriorating change is the switch from locally growing tumor to metastatic that involves numerous alterations to complete complex series of events required for metastasis. RhoC is a major contributor to metastasis of some solid tumors [39,40], and Ral proteins are activated in more than 90% of pancreatic duct adenocarcinoma cases [41]. The realization that many CaaX proteins, most notably Ras family members, are involved in pathologies such as cancer, inflammation and viral infectivity, has spurred efforts to develop inhibitors of CaaX processing as a rational approach to therapeutic development. The first prenyltransferase inhibitors were farnesyltransferase inhibitors (FTIs), which were rapidly developed from early CaaX peptide mimics [42] into the small organic ligands. The first peptidomimetic protein prenyltransferase inhibitors were mixed inhibitors, but highly selective inhibitors were rapidly developed. With the example of one of the canonical oncogenes H-Ras, rationale application of FTIs have shown efficacy in leukemias, gliomas, and breast cancers, providing the impetus for targeting GGTase-I in cancers driven by geranylgeranylated oncogenes [43,44]. However, FTIs have not performed up to expectation in solid tumors and failed to respond in many types of cancer, even those with activated Ras oncogenes [45–47]. The multifactorial nature of human cancers and "alternative prenylation", a process whereby CaaX proteins including some Ras isoforms can be modified by GGTase-I when FTase is inhibited, cause this variability [48,49] (Fig. 6).

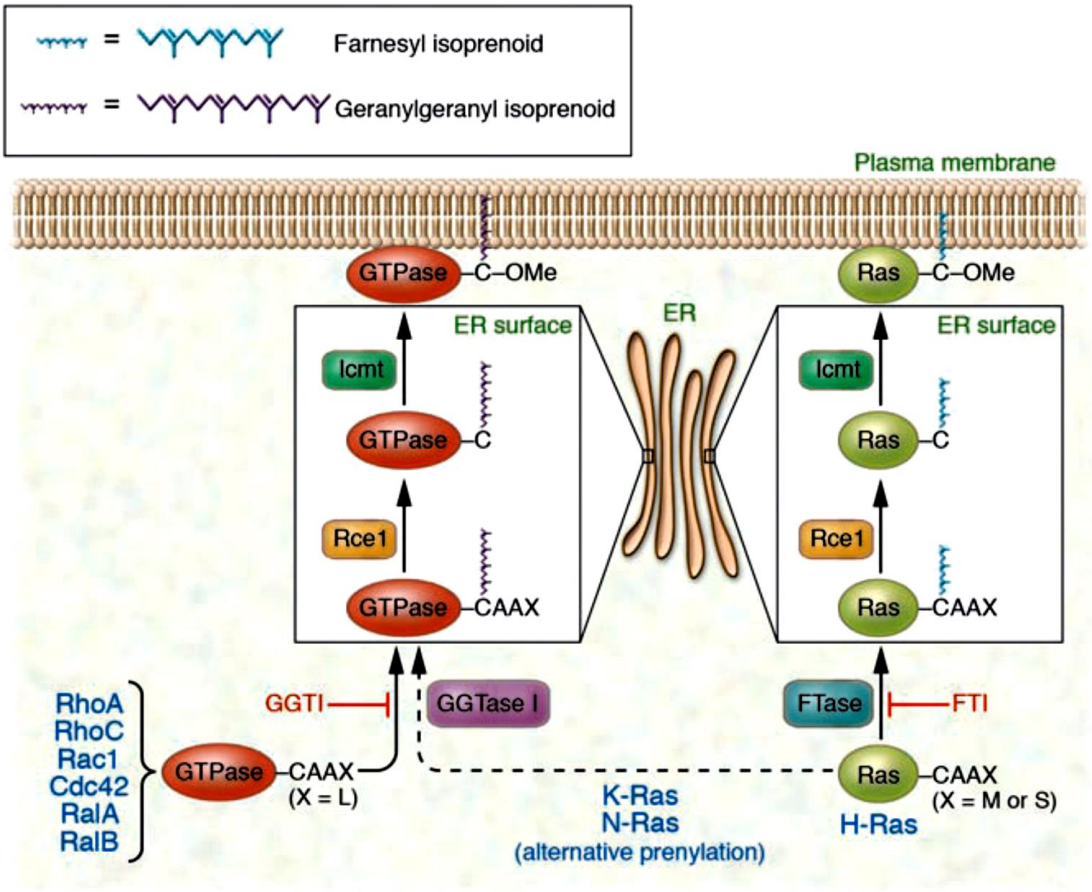

Figure 6: Alternative prenylation by GGTase-I

This cross-prenylation restores at least a portion of the activity [50]. Dual FTase/GGTase inhibitors have received little attention, and this type of treatment would impact a large number of proteins, which make resulting interpretations complicated. As a result several GGTIs have been developed that inhibit C20 lipid modification of GGTase-I substrates. Even though GGTIs have been primarily developed for use as cancer therapeutics, particularly in cancers that have high levels or activating mutations of geranylgeranylated proteins [9,51] they are now receiving broad interest for clinical use. Besides the continuing development as anticancer agents, GGTIs are now postulated to have a potential in treating a wide array of other diseases including inflammation, multiple sclerosis, atherosclerosis,

viral infection (HepC/HIV), apoptosis, angiogenesis, rheumatoid arthritis, psoriasis, glaucoma, and diabetic retinopathy [37,52]. In addition, nonhuman selective GGTIs have been developed as antifungals and antiparasitics since GGTase-I function is a prerequisite in the normal functioning of many parasites and fungi [53,54].

Additionally, a number of CaaX proteins such as Ras, Rho, Rac, and Cdc42 that are substrates for GGTase-I are intimately involved in tumorigenesis [13]. Administration of GGTI to cells has been reported to cause cell cycle arrest at G0/G1 by inactivation of cyclin-dependent kinases that act downstream of Rho [55, 56]. Studies have revealed that GGTIs stimulate apoptosis in multiple cell lines [57–59]. Inhibition of GGTase-I administration resulted in tumor regression in mouse xenograft models of breast cancer with evidence of impact on the afore-mentioned cyclin-dependent kinases [60]. Hence, besides their potential impact on oncogenesis, GGTIs have been proposed as potential drugs for anti-angiogenic therapy and for inhibiting metastatic progression of cancers [13,61]. An impact on Rho proteins, specifically RhoA and RhoC, is most often cited as the way in which GGTIs impact the metastatic phenotype, but recently and "orphan" protein termed C17orf37 has also been implicated. This protein was shown to be modified by GGTase-I, and its ability to increased cellular migration was shown to be dependent on prenylation [62]. Ectopic expression of C17orf37 modulated the dissemination of cancer cells and facilitated formation of metastatic nodules in a mouse model of metastasis.

Glioblastoma multiform represent the most common malignant intracranial tumors, which are characterized by rapid proliferation, poor prognosis, and resistance to traditional therapeutic approaches [63]. In a recent study the expression level and functional significance of GGTase-I in human malignant glioma was investigated [64]. GGTase-I

levels in glioma were found to be significantly elevated compared to normal brain tissue. Knockdown of GGTase-I using siRNAs targeting the β subunit, or treatment with GGTI-2147, markedly decreased the association of RhoA and Rac1 with the plasma membrane and the activation of Rac1; these data were consistent with previous reports in breast cancer and lung cancer cells [65,66]. The glioma study concluded that geranylgeranylation of Rac1 was an important step in glioma cell growth, and that enhanced GGTase-I activity in the cancer may be important in its development.

Genetic targeting of GGTase-I mice has also provided strong evidence supporting GGTase-I as a drug target. Conditional knockout of the enzyme reduced the number and growth of tumors, and increased survival, in mice with lung cancer induced by mutant K-RAS [67]. In sum, these findings have spurred efforts to develop inhibitors of GGTase-I for evaluation as therapeutics, either on their own or in combination with FTIs.

In FTI-treated cells, K-RAS and N-RAS are alternately prenylated by GGTase-I [49] and as a result the research community was prompted to develop GGTase-I inhibitors (GGTIs) [52]. GGTIs have shown promise in preclinical studies [66,68,69] and the rationale for inhibiting GGTase-I is supported by genetic studies in mice: Inactivating the gene for the β-subunit of GGTase-I (Pggt1b) reduced tumor formation and prolonged survival in mice with K-RAS-induced lung cancer [67]. An important role for geranylgeranylated proteins such as Rho in cell regulation, and their aberrant activation diseases, is increasingly being documented [70,71]. Rho proteins stimulate signal transduction pathways that induce cytoskeletal and transcriptional responses through diverse effectors. Dysregulation of the Rho pathway is implicated in multiple pathological conditions including cancer, in particular metastatic progression, cardiovascular disease, hepatic disease, and

developmental disorders. In this light, the interest in targeting these proteins has increased. Rho activity has a clear function in angiogenesis [61], which in turn plays a critical role in the pathogenesis of tumors, rheumatoid arthritis, atherosclerosis, psoriasis, and diabetic retinopathy [72]. In multiple sclerosis, infiltration of leukocytes and monocytes into the central nervous system as part of an inappropriate inflammatory response leads to demyelination of axons and nerve damage, resulting in motor and cognitive impairment. Recent evidence suggests that this migration requires Rho signaling and inhibition of prenylation can lead to decreased disease progression [73,74]. Additionally, the replication of hepatitis C virus in liver cells requires a GGTase-I substrate, and evidence indicates that replication of hepatitis C virus can be attenuated by inhibiting geranylgeranylation, providing a potential new therapeutic prospect for this increasingly prevalent disease [75,76].

1.5 Inhibition of GGTase-I

1.5.1 Inhibitors of GGTase-I

Over the last 20 years a wide variety of GGTIs have been reported in various publications in the relatively short time when the enzyme has been studied. Many of these have been designed rationally on the basis of the substrates of GGTase-I: geranylgeranyl diphosphate (GGPP) or the CaaX peptide. There are also a number of natural compounds that were identified in a screen for inhibition of GGTase-I from Candida sp. A comprehensive review of known GGTIs was published recently [52]. Unfortunately, many of the known binding modes of GGTIs were never characterized and IC_{50} data for the same compounds are often in disagreement when measured by different laboratories. These observations make the large portion of GGTIs less than optimal for quantitative structure-activity relationship

(QSAR) model building. However, there are two known scaffolds that have been well characterized with respect to their binding to the peptide pocket and using similar estimates for IC_{50} values. These include a number of CaaL (L represents leucine) peptidomimetics including aminobenzoic acid derivatives such as GGTI-298 and GGTI-2154 [56,77] and benzoyleneurea-based compounds [78]. More recently three newer classes of GGTIs have been published including one based on a piperazin-2-one backbone [79], dihydropyrole/tetrahydropyridine based small molecules [80], and allenoate compounds [81]. As geranylgeranyltransferase inhibitors (GGTIs) aminobezoic acid derivatives were synthesized following C-terminal CaaL peptidomimetic sequence. Here, 2-aryl-4-aminobenzoic acid moieties were used as mimetics for central two amino acids dipeptide (aa). While the cysteine part was replaced with imidazole and pyridine derivatives at N-terminus. The absence of cysteine in the structure made these molecules non thiol peptidomimetic compounds for exceptional selective inhibition of GGTase-I instead of FTase [77]. Another aminobenzoic acid derivative was GGTI-298 that showed inhibition of GGTase-I led to arrest of G_0/G_1 in fibroblasts [56].

Similarly, the aa part of CaaX tetrapeptide was replaced by benzoyleneurea scaffold by Carrico et.al. These novel compounds were found potent and selective inhibitors of GGTase-I. Further, it was found that compounds having free carboxylic functionality were more potent and compounds having L-configured phenylalanine possess high affinity to bind the hydrophobic X specificity pocket of enzyme [78]. A semi-rigid scaffold of piperazin-2-one were synthesized as mimic the CaaL sequence. The potency of the GGTIs was based on the presence of L-leucine residue having free carboxylic acid as well as the S configuration of the 3-aryl groups. While upon substitution of 5-methyl on imidazole and

fluorine on 3-aryl group attributed for enhanced selectivity [79]. Castellano et al. synthesized dihydropyrrol and tetrahydropyridine heterocyclic compounds via allene phosphine catalysis and used them as GGTIs. From the screening of 4288 analogues, only two compounds showed the IC_{50} in submicromolar [80]. Same kind of heterostructural moieties allenoate derived compounds were synthesized and tested for GGTase-I inhibition. It was observed that derivatization of carboxylic acid originating from the core improved the cellular activity, inhibition of proliferation of human cancer cell lines, induction of $p21^{CIP1/WAF1}$ and G_1 cell cycle arrest [81].

1.5.2 Current Status of GGTase-I Inhibitor Development-literature survey

The results of the detailed studies prompted both pharmaceutical companies and academic laboratories to develop GGTIs [52,55,66,82]. Several GGTIs have been developed, with peptidomimetic-based GGTIs being the largest class to date and include aminobenzoic acid-containing compounds such as GGTI-298 and GGTI-2154 [77,83], and compounds containing benzoyleneurea [78]. In this regard, tetrapeptide-based bivalent inhibitors were developed based on structural data for GGTase-I that simultaneously targeted multiple protein surfaces [84]. All of these bivalent inhibitors exhibited great selectivity for GGTase-I over FTase and the inhibitory ability of these compounds was improved compared to simple tetrapeptide. One compound targeting GGTase-I has advanced to clinical trial [13], although little information is yet available on the results.

In addition to synthetic design of substrate analogues and high-throughput screening to identify compounds, computational design of small molecule inhibitors targeting GGTase-I has begun to bear fruit. Recently, a computation-based 3-D model for human GGTase-I to which a small molecule library was virtually docked using a program termed AutoDock

Vina has revealed that natural compounds camptothecin and curcumin exhibited higher virtual binding affinities to GGTase-I than that of established peptidomimetic GGTIs [85]. Camptothecin is a well-known topoisomerase I inhibitor and anti-cancer drug [86], while curcumin is a pleiotropic molecule that has been shown to impact cancer regression in a number of ways [87]. Based on a number of observations, it was hypothesized that anti-cancer activity of these compounds might in part be due to GGTase-I inhibition, but direct experimental validation of this hypothesis is still lacking. A computational approach involving Quantitative Structure Activity Relationship (QSAR) models of known GGTIs has also led to new scaffolds with inhibitory activity being identified [88], but the activities were rather low and the compounds have not yet been further refined.

A compound termed GGTI-2Z was recently reported to block prenylation process catalyzed by both GGTase-I and RabGGTase (a related enzyme that specifically prenylates most Rab GTPases) [89]. The efficacy of GGTI-2Z was augmented by co-administration of a statin and strongly correlated with the ability to induce autophagy. Another compound, GGTI P61A6, showed strong inhibition of tumor growth in a mouse xenograft of pancreatic cancer [82]. In another discovery effort, small molecule inhibitors of GGTase-I identified in a library of allenoate-derived compounds were reported to inhibit proliferation and trigger cell cycle arrest of a number of cell lines, including leukemic, pancreatic, and breast cancer cell lines [81]. A GGTI termed P61-E7 containing a tetrahydropyridine scaffold has recently been described that inhibited proliferation and impaired cell cycle progression [90]. In addition, P61-E7 impacted processes controlled by cyclin-dependent kinases, and P61-E7 treatment of Panc-1 cells impacted the organization of the actin cytoskeleton and assembly of focal adhesions.

The impact of GGTIs on the prenylation of a number of small GTPases in oral squamous cell carcinoma (SCC) was recently investigated [91]. GGTI-298 treatment resulted in mislocalization of RhoA, leading to increased $p21^{Waf1/Cip1}$ level and G1cell cycle arrest, and affected RalB with subsequent impairment of migration and invasion of SCC cells. The impact of GGTIs on the early events associated with metastasis, specifically the organization of the cytoskeleton and the importance of this process in invasion and migration, has also been investigated [92]. The study revealed that GGTI treatment impaired the migration and invasion of PC-3 cells, consistent with an earlier similar study on human pancreatic cancer cells [93]. A list of recently developed GGTase-I inhibitors is given in table 1. A comprehensive list of previously discovered GGTase-I inhibitors has also been detailed elsewhere [52].

Table 1: Inhibitors of GGTase-I.

		IC_{50} value in vitro		**Ref.**
Entry	**Compound**	**GGTase-I**	**FTase**	
1	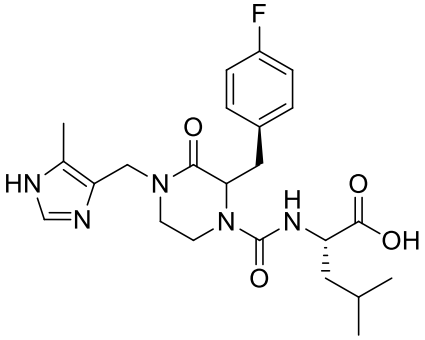	7.1 ± 4.3 nM		[79]

2	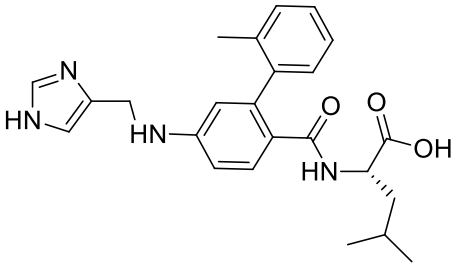	21 nM		[79]
3	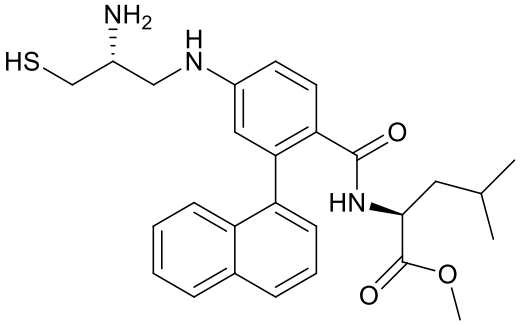	15 μM		[70]
4	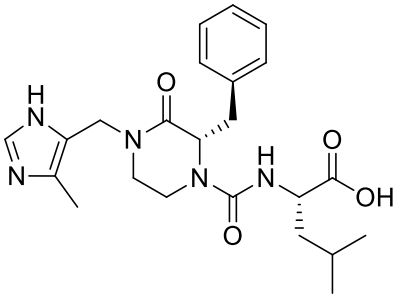	9.5 nM	53,000 nM	[79]
5	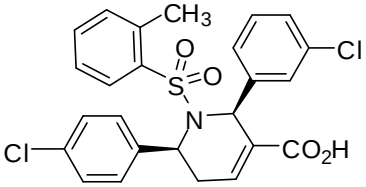	313 nM		[81]
6	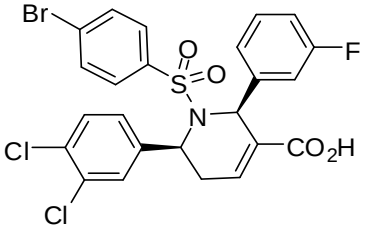	1020 nM		[81]
7	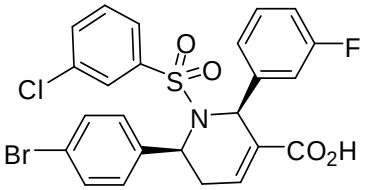	576 nM		[81]

8	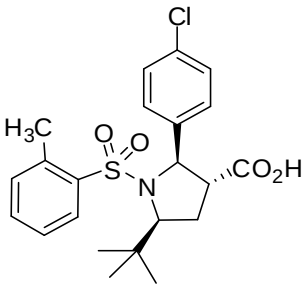	466 nM		[81]
9	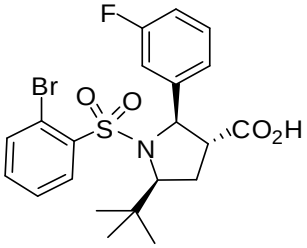	1050 nM		[81]
10	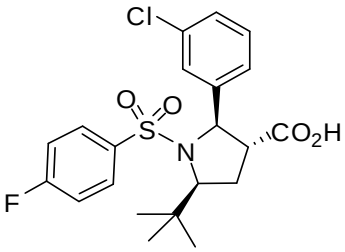	980 nM		[81]
11	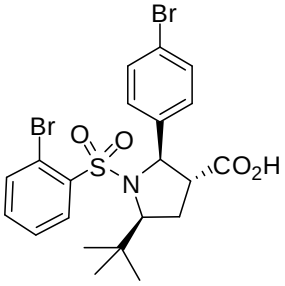	1050 nM		[81]
12	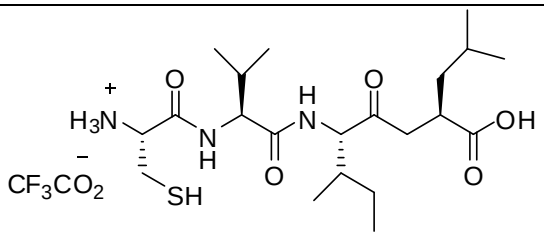	4.8 µM	>100 µM	[84]

13	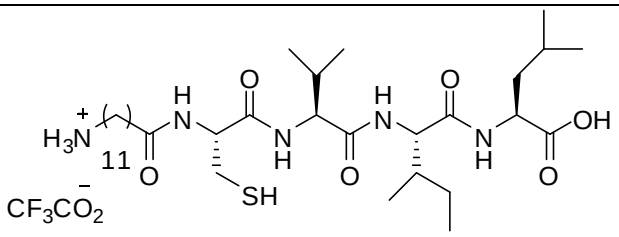	1.4 μM	>100 μM	[84]
14	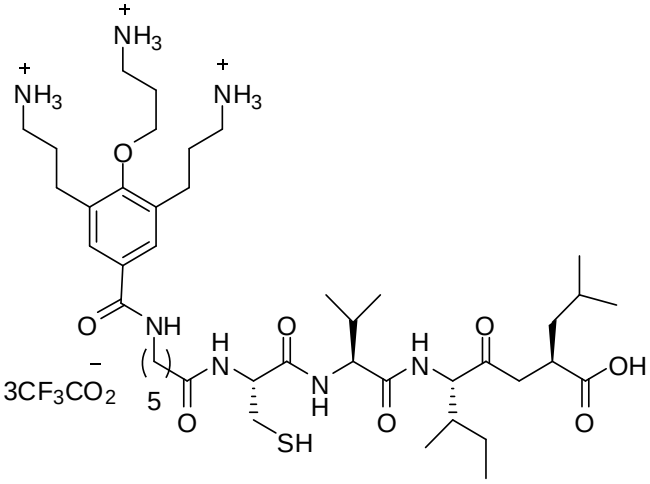	0.62 μM		[84]
15	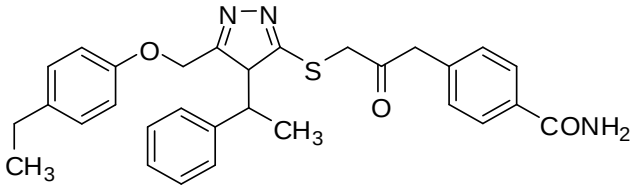	43 μM		[66]
16	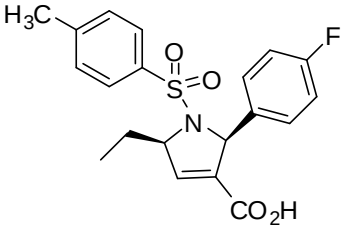	200 μM		[66]
17	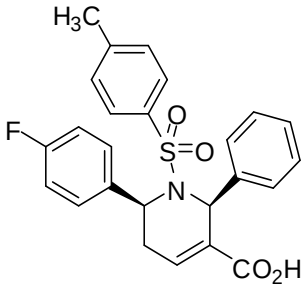	120 μM		[66]

18	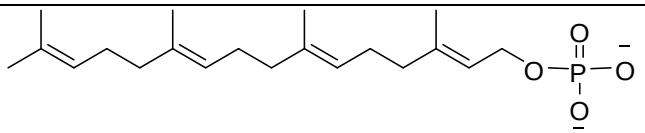	21 nM		[66]
19	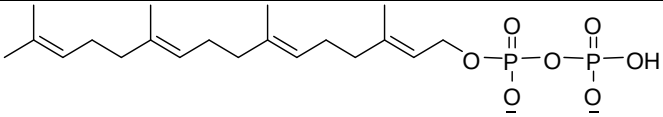	100 nM		[66]
20	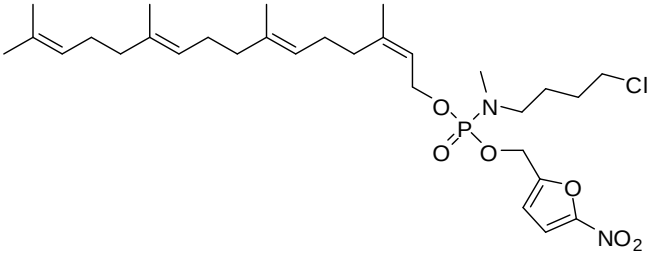	10 µM		[66]
21	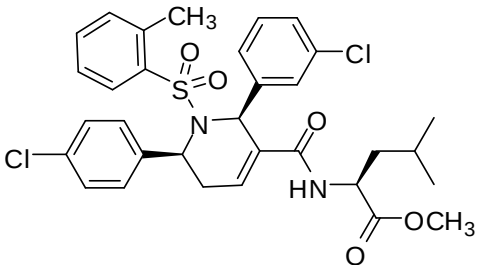	5 µM		[90]
22	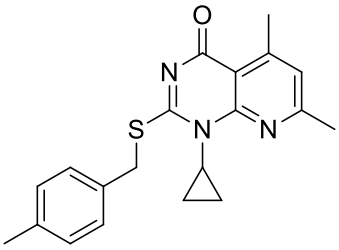	10.9 µM		[94]
23	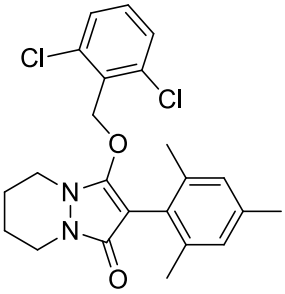	9 µM		[94]

24	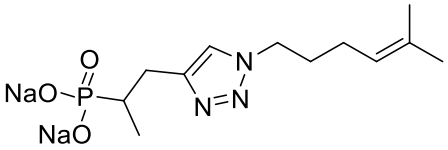	>100 µM	>100 µM	[95]
25	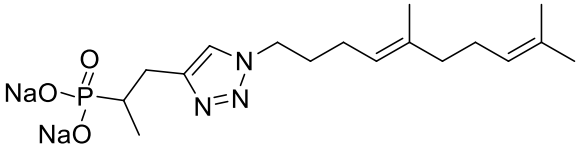	>100 µM	>100 µM	[95]
26	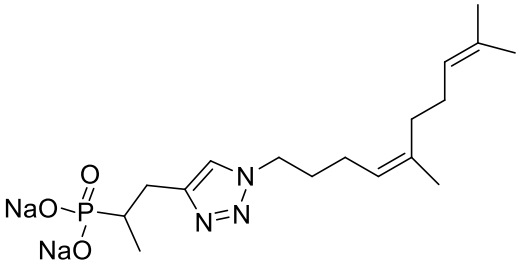	>100 µM	>100 µM	[95]

Despite of good antiproliferative and pro-apoptotic properties FTIs and GGTIs both invitro and in vivo, these compounds became problematic at clinical stage due to toxicity. To avoid the toxicity of these inhibitors, a new strategy for simultaneous inhibition of FTase and GGTase-I (Dual Prenylation Inhibitors, DPIs) was adopted (Table 2) [96]. This approach was evaluated after observing the synergistic inhibition of FTase and GGTase-I simultaneously on various tumor cell lines. More than 70% growth inhibition was seen in myeloid cell lines where apoptosis was induced by GGTI-286, GGTI-298, GGTI-2147 and FTI L-744,832 inhibitors. Thus co-treatment of FTIs and GGTIs led to synergistic cytotoxic effects in primary acute myeloid leukemia (AML) cell lines and myeloid cells [58]. A dual inhibitor of FTase and GGTase-I having geometry of CaaX peptidomimetic sequence, L778,123, was tested. Due to significant inhibitory potential L778,123 was tolerated for phase I and II clinical trials and was able to reduce prenylation of Rap1a and HDJ2 except K-Ras. But QT-prolongation was observed in all trials of L778,123 [58].

Another DPI was AZD3409 also well tolerated for initial phases of trials and showed significant inhibition of tumor growth. The positive aspects demonstrated were no change in heart rate and electrocardiogram recording but the adverse effects of orthostatic hypertension, paranesthesia, nausea diarrhea and dizziness have been noticed [97]. Further studies showed that AZD3409 as DPI inhibits more FTase as compared to GGTase-I and from its radio sensing, it was found that this drug did not inhibit prenylation in case of K-Ras. Similar situation was happened for L778,123 DPI where it inhibited the Rap1A prenylation but not the K-Ras. Thus, even the use of DPI could not resolve or overcome the issues of toxicities and complete inhibition of prenylation process.

Other than DPIs, the problems of toxicities caused by individual treatment of FTase and GGTase were avoided using the following two possible plans; one is the synergistic activity of mevalonate and potent prenyl inhibitors, e.g. the synergistic activity in combinations of FTIs and statins or isoprenoids or bisphosphonates has been studied, and second is the synergistic activity of conventional chemotherapy and radiotherapy. Morgan et al. found that FTI/statin combinations inhibit more effectively the prenylation modifications via decreasing isoprenoid level. The myeloma cells underwent apoptosis and reduced cell migration, where FTIs enhanced the lovastatin ability to inhibit Rho, K-Ras, N-Ras prenylation and activation of MEK/MAPK. The synergistic effect of FTI/statin combinations also led to reduce use of doses as compared to individual implications. While statin/isoprenoid combinations also induced the synergistic inhibition of growth of human DU145, prostate carcinoma, B16 melonoma cells and LNCaP [98,99].

Table 2: Structures of some of the reported DPIs and combinatory drugs (CDs)

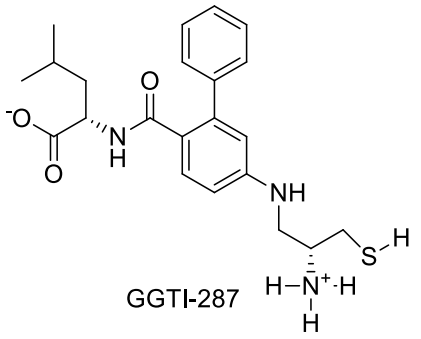 GGTI-287	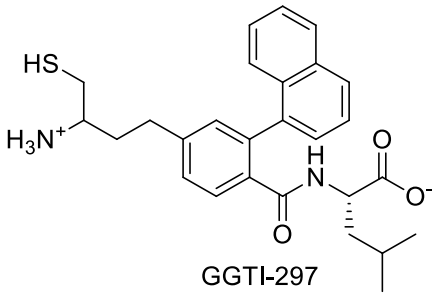 GGTI-297
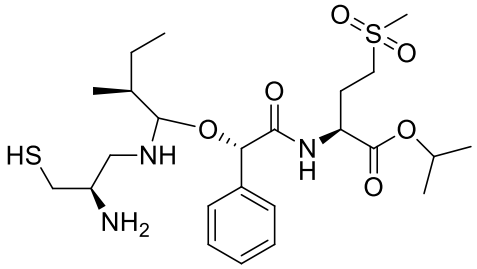 FTI L-744,832	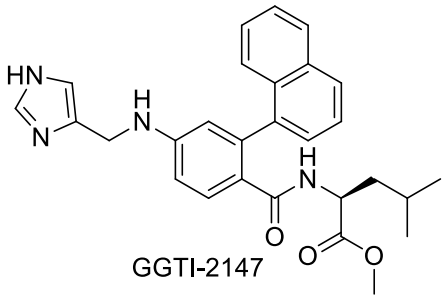 GGTI-2147
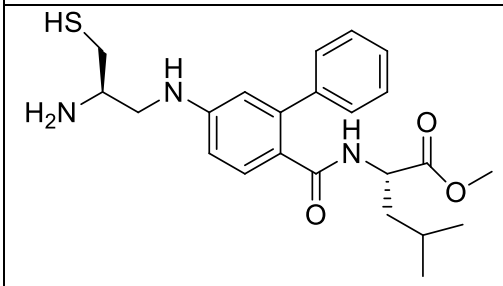 GGTI-286	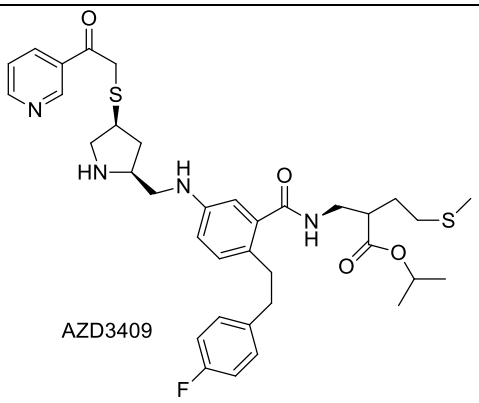 AZD3409
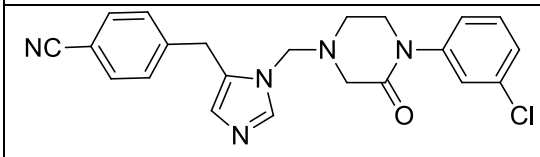 L-778,123	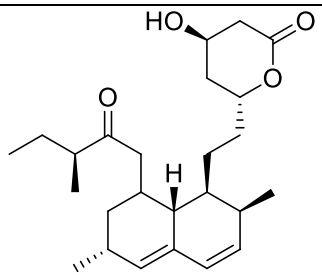 Lovastatin

1.5.3 Future Directions for GGTIs development

The initial emphasis on development of GGTIs was as anticancer agents. However, the activities of Rho proteins, among the major targets of GGTIs, are also important for the ability of macrophages and other inflammatory cells to migrate and to respond to stimuli that trigger an inflammatory response [100]. Given that dysregulation of the Rho pathway is implicated in multiple pathological conditions beyond cancer, for example cardiovascular and hepatic disease, and several developmental disorders, it seems that GGTIs can be considered for applications beyond cancer. In addition, Rho activity has a clear function in angiogenesis [61], which in turn plays a critical role in the pathogenesis of tumors, rheumatoid arthritis, atherosclerosis, psoriasis, and diabetic retinopathy [72]. In multiple sclerosis, infiltration of leukocytes and monocytes into the central nervous system as part of an inappropriate inflammatory response leads to demyelination of axons and nerve damage, resulting in motor and cognitive impairment. Recent evidence suggests that this migration requires Rho signaling and inhibition of prenylation can lead to decreased disease progression [73,74]. Consequently, GGTase-I inhibition presents a viable strategy to impair the pro-inflammatory activities of Rho GTPases and potentially treat of inflammatory disorders, including atherosclerosis and multiple sclerosis [101–103].

There have been many reports on beneficial effects of statins not linked to their lipid-lowering properties, and in many cases these effects have been linked to the inhibition of protein geranylgeranylation [101,104,105]. Statins block the production of mevalonate, and hence also the downstream metabolites FPP and GGPP [9]. However, it has been recently demonstrated that conditional knockout of GGTase-I in macrophages resulted in accumulation of GTP-bound active RhoA, Rac1, and Cdc42 [106], leading to increased

production of pro-inflammatory cytokines and rheumatoid arthritis in mice. These results suggest that geranylgeranylation might restrain, rather than support activity of Rho proteins in macrophages. The study revealed that GGTase-I deficiency in macrophages markedly reduces atherosclerosis despite higher levels of inflammation and development of rheumatoid arthritis. This was a bit surprising, as increased inflammation is generally associated with increased atherosclerosis rather than the opposite. While these results are all quite intriguing, it remains unclear precisely what is happening in the mouse models of GGTase deficiency in lymphoid cells.

A number of fungal and protozoan pathogens express CaaX proteins that are important for virulence and/or survival, and the FTase and GGTase-I have therefore been proposed as targets for treating infectious diseases. The replication of hepatitis C virus in liver cells requires a GGTase-I substrate, and replication of hepatitis C virus can be attenuated by inhibiting geranylgeranylation [75,76]. *Cryptococcus neoformans* (*C. neoformans*), a pathogenic fungus that severely affects immunocompromised people, has become a major health problem because of the prevalence of HIV and the use of immunosuppressive drugs following organ transplant. The function of the *C. neoformans* Ras1 (CnRas1) GTPase requires processing of its C-terminal CaaX motif, and the Ras1 and Ras2 proteins of *C. neoformans* are predicted to be GGTase-I substrates [107]. Further, the *C. neoformans* GGTase-I is required for the prenylation of Cdc42 and Rho10 in the organism [108], and these two proteins are important for the growth of this pathogenic fungus. Knockout of GGTase-I dramatically reduced virulence in an animal model of *C. neoformans* infection, although some compensatory farnesylation was detected that prompted a suggestion that the CaaX motif may not dictate all specificity for prenylation in this organism. The

structure of the GGTase-I from *Candida albicans* (CaGGTase-I) has been solved [109], and close inspection of the active site revealed areas of significant divergence in critical regions from the mammalian orthologue. These unique structural features of the *Candida* GGTase-I could provide opportunities to design selective inhibitors for the development of new anti-fungal therapeutics.

In brief, the physiological significance of protein geranylgeranylation has been highlighted in recent studies. The GGTase-I deficiency has been implicated in proliferation inhibition and accumulation of p21CIP1/WAF1 and reduction of the oncogenic K-Ras-induced lung tumor formation in mice [67]. Moreover, geranylgeranylated proteins such as Rho, Rac and Cdc42 have been linked to tumorigenesis and metastasis [110–112]. In addition, GGTI can cause cell cycle arrest at G0/G1 [55,113], stimulate apoptosis in multiple cell lines [57,59] and geranylgeranylation inhibition was found to regress breast tumor xenografts in vivo [60]. The implications of geranylgeranylated proteins in oncogenesis have highlighted the potential for GGTase-Is as the potential chemotherapies [5,114]. Consequently, different strategies have been explored to develop GGTIs [115], including peptidomimetic and small-molecules inhibitors [81,89].

Peterson et al. described the characteristics of a highly selective and potent GGTase-I inhibitor, GGTI-DU40. The kinetic studies of GGTI-DU40 demonstrated competitive inhibition with the protein substrate but uncompetitive inhibition with isoprenoid substrate where Ki = 0.8 nM. GGTI-DU40 was able to block the prenylation of a number of geranylgeranylated CaaX proteins selectively in vitro as well as in living cells. Further treatment of breast cancer cell lines (MDA-MB-231) by GGTI-DU40 was manifested by inhibition of thrombin-induced cell rounding through a process called Rho proteins

inhibition. Thus, GGTI-DU40 was established as a prime evidence for studying protein geranylgeranylation and a novel class of therapeutics. Driven by the limited bioavailability associated with its hydrophobicity of a potent and selective inhibitor of GGTase-I (GGTI-DU40) both in vitro and in living cells, we were motivated to design a series of substituted pyrazoles **2-16** (Fig. 7) [66]. Herein, we wish to disclose the synthesis and biological evaluation of compounds **2-16** and molecular docking studies of the most active compound **2** in the series.

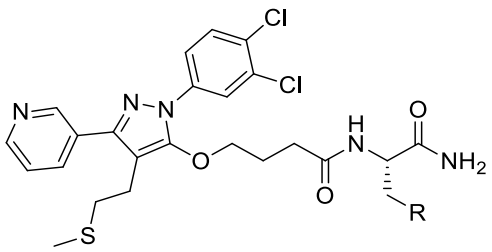

(1) R = Ph (GGTI-DU40)
(2) R = 4-FPh
(3) R = 3-pyridyl
(4) R = 4-pyridyl
(5) R = 4-OMePh

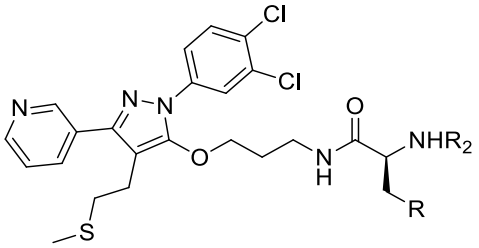

(6) R_1 = Ph; R_2 = $COCH_3$
(**7**) R_1 = Ph; R_2 = SO_2CH_3
(8) R_1 = 4-FPh; R_2 = $COCH_3$
(9) R_1 = 4-FPh; R_2 = SO_2CH_3
(10) R_1 = 4-OMePh; R_2 = $COCH_3$
(11) R_1 = 4-OMePh; R_2 = SO_2CH_3
(12) R_1 = 4-OMePh; R_2 = $COO(CH_3)_3$
(13) R_1 = 3-pyridyl; R_2 = $COCH_3$
(14) R_1 = 3-pyridyl; R_2 = SO_2CH_3
(15) R_1 = 4-pyridyl; R_2 = $COCH_3$
(16) R_1 = 4-pyridy; R_2 = SO_2CH_3

Figure 7: Chemical structures of compounds **1-16**

CHAPTER 2

Research Objectives and Work Plan

2.1 Research Objectives

The objectives of this designed research study are as following;

1. The limited bioavailability and hydrophobicity of highly potent and selective inhibitor of GGTase-I (GGTI-DU40), motivated us to synthesize structural analogues of GGTI-DU40, compounds **2-16** (Fig. 8), in order to improve its drug like profile.
2. *In vitro screening* of **2-16** against the purified enzymes (GGTase-I and FTase).
3. Analysis of cellular activity of **2-16** against cancer cells lines (MDA-MB-231 breast cancer cells).
4. Establishment of structure activity relationship (SAR) studies of compounds **2-16**.

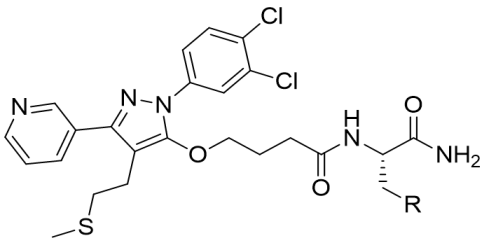

(1) R = Ph (GGTI-DU40)
(2) R = 4-FPh
(3) R = 3-pyridyl
(4) R = 4-pyridyl
(5) R = 4-OMePh

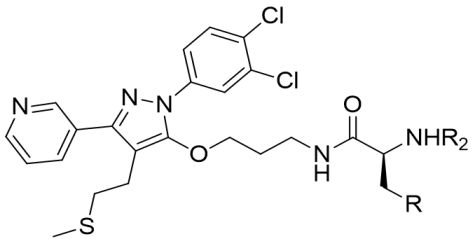

(6) R_1 = Ph; R_2 = $COCH_3$
(**7**) R_1 = Ph; R_2 = SO_2CH_3
(8) R_1 = 4-FPh; R_2 = $COCH_3$
(9) R_1 = 4-FPh; R_2 = SO_2CH_3
(10) R_1 = 4-OMePh; R_2 = $COCH_3$
(11) R_1 = 4-OMePh; R_2 = SO_2CH_3
(12) R_1 = 4-OMePh; R_2 = $COO(CH_3)_3$
(13) R_1 = 3-pyridyl; R_2 = $COCH_3$
(14) R_1 = 3-pyridyl; R_2 = SO_2CH_3
(15) R_1 = 4-pyridyl; R_2 = $COCH_3$
(16) R_1 = 4-pyridy; R_2 = SO_2CH_3

Figure 8: Chemical structures of target compounds **2-16**

2.2 Methodology and Work Plan

2.2.1 Synthesis of Target Compounds (2-5)

The synthesis of target compounds (**2-5**) would necessitate the synthesis of amino acids-derived amides (**25-28**) (Fig. 9), which in turn would be accomplished as outlined in scheme-2.

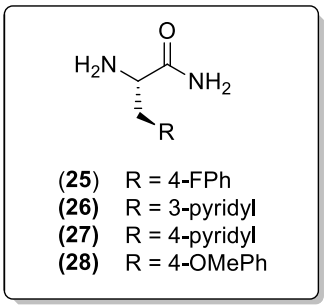

Figure 9: Amino acids-derived amides (**25-28**)

The esterification of amino acids **17-19** would produce the corresponding hydrochloride amino esters **20-22** [116–118]. Similarly, the acid induced deprotection of boc group of ester **23** [119] would generate amino ester **24** [120]. Moreover, condensation of amino esters **20-22** and **24** with ammonium hydroxide in a pressure vessel, would furnish the desired α-amino amides **25-28**, respectively (scheme-2).

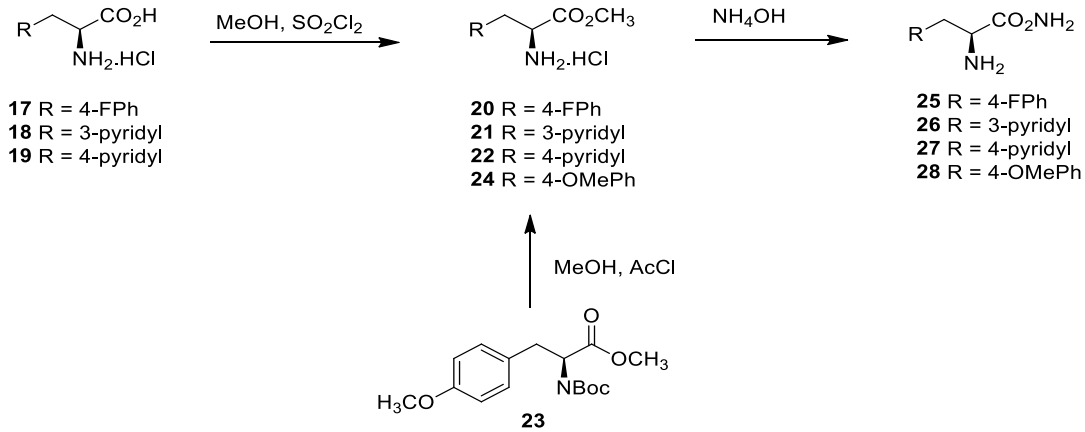

Scheme 2: Synthesis of amino acid derivatives **25-28**

With suitably modified amino acids in hands, we would next move to access the synthesis of **49**, a key intermediate needed to accomplish the synthesis of **2-5** (Scheme-3). To this end, cross Claisen reaction of ethylnicotinate **45** with γ-butyrolactone using sodium ethoxide as base would produce α-ketobutyrolactone **46**, [121] which in turn would be condensed via Knorr pyrazole synthesis reaction with 3,4-dichlorophenylhydrazine hydrochloride in acetic acid to generate pyrazole **47** [122]. Whereas the O-alkylation of **47** with ethyl 4-bromobutanoate in DMF would construct pyrazole ester **48** [122], which will be exposed to basic condition to remove the acetyl protection to produce the desired intermediate **49**. The target compounds **2-5** could be ensued from **49** by the amidation of **49** with amino acid amides **25-28** to generate pyrazole amides **50-53** followed by the mesylation of the resultant intermediates **50-53** and condensation with sodium methanethiolate (Scheme-3).

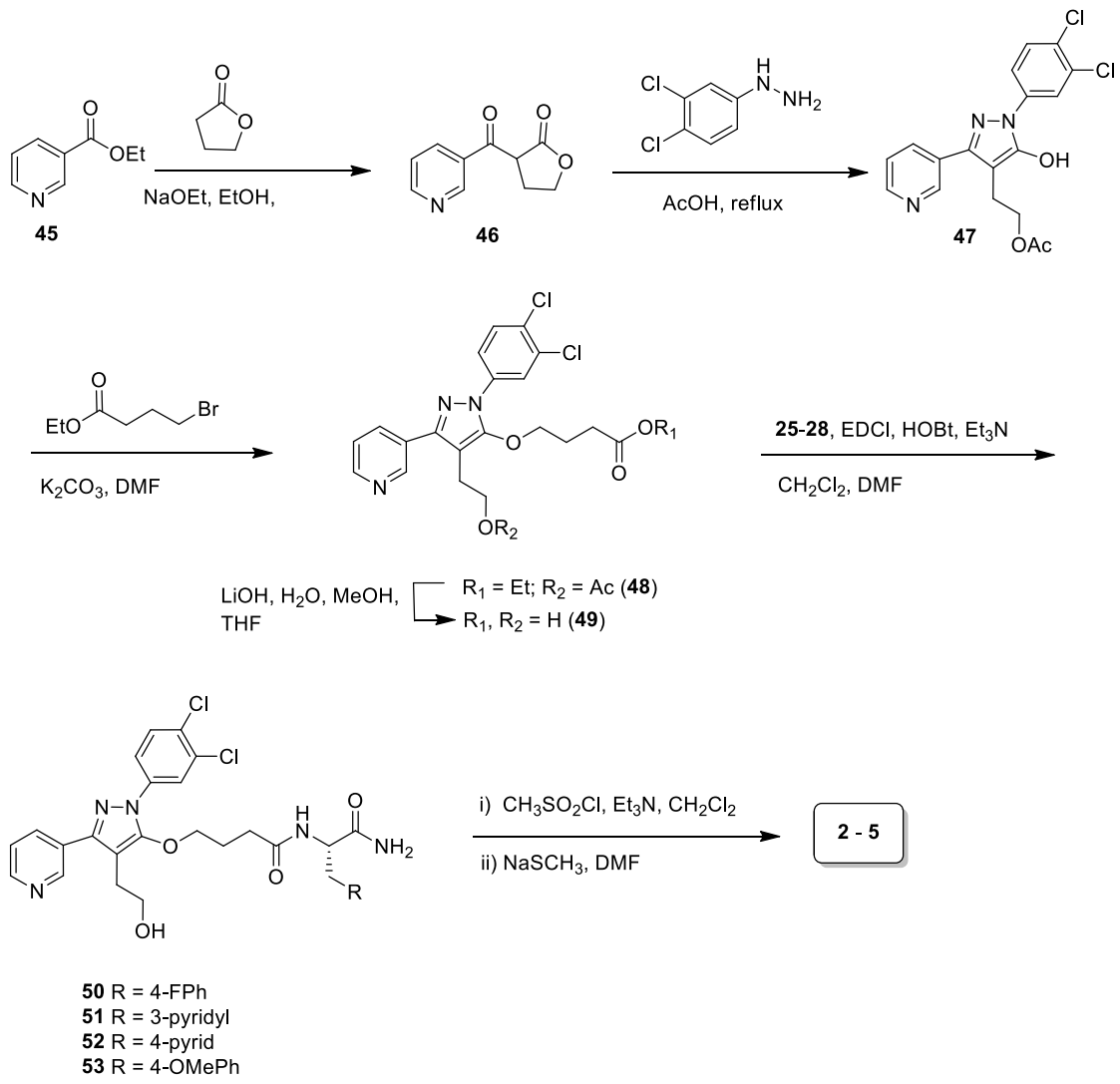

Scheme 3: Synthesis of **2-5**

Alternatively, selective basic hydrolysis of **48** would produce alcohol **49**. The latter can be exposed to the operations of msylation and condensation with sodium methanethiolate to produce the corresponding thioethers. Moreover, the amidation of thioethers with amino acid amides **25-28** would generate the desired target compounds **2-5** (Scheme-4).

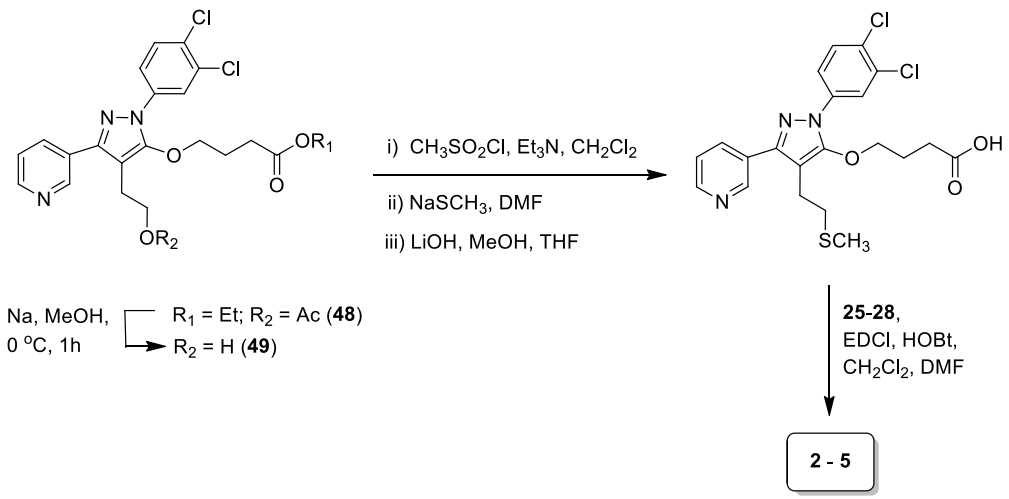

Scheme 4: Alternative way for synthesis of **2-5**

2.2.2 Synthesis of Target Compounds (6-16)

The synthesis of reverse amides **6-16** analogues of GGTI-DU40 would require access to the modified amino acids intermediates **29**-**32** and advanced intermediate **58**. To this end, amino acids **29**-**32** could be converted directly into corresponding N-acetylated amino acids **33**, **35**, **37** and **39** and N-acylated amino acids **34**, **36**, **38** and **40** by the action of acetylation or mesylation, respectively (Scheme-5).

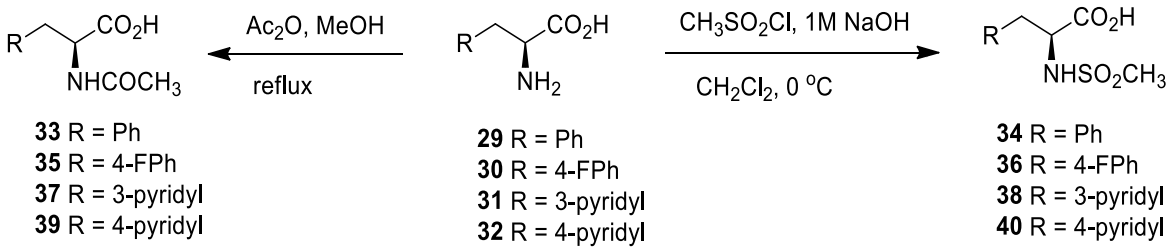

Scheme 5: Synthesis of amino acid derivatives **33-40**

Alternatively, the synthesis of amino acid derivatives **33-40** could be also be ensued from the esterification of amino acids **29-32**, N-acetylation or N-acylation followed by basic hydrolysis (Scheme-6).

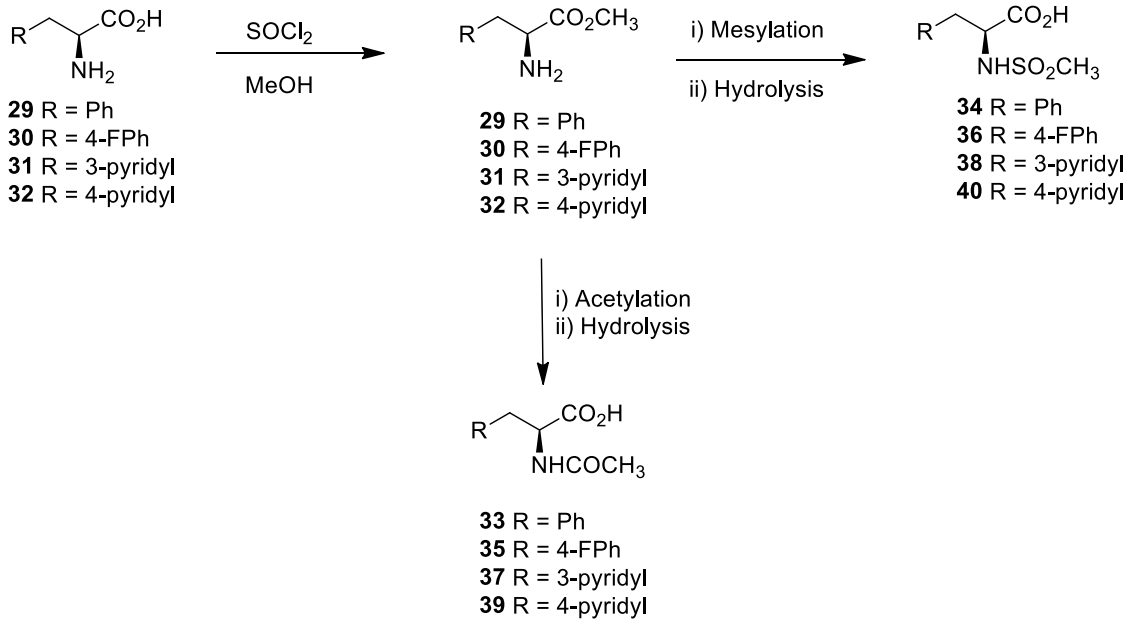

Scheme 6: Alternative way for synthesis of **33-40**

Likewise, L-tyrosine ester hydrochloride **41** would be converted to its corresponding N-acetylated or N-acylated derivatives **42-44** by employing previously-reported procedures (Scheme-7) [123,124].

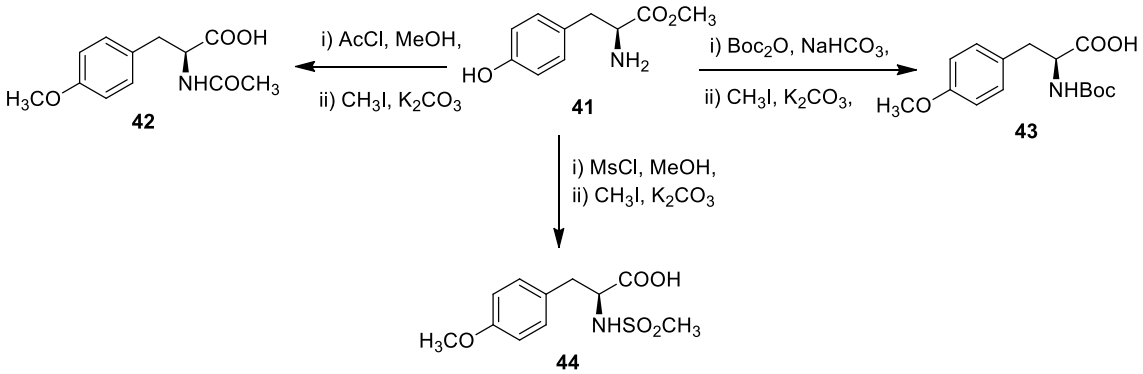

Scheme 7: Synthesis of amino acid derivatives **42-44**

On the other hand, the synthesis of the advanced intermediate **58** and subsequent synthesis of the target compounds **6-16** could be ensued as outlined in scheme-8. The O-alkylation of pyrazole **47** with *tert*-butyl (3-bromopropyl)carbamate would construct the desired intermediate **54**, which in turn would be subjected to basic hydrolysis to produce alcohol **55**. Mesylation of **55** would construct **56**, which upon condensation with sodium methanethiolate would furnish the thioether **57**. The deprotection of Boc with acetyl chloride in MeOH can produce the desired advanced intermediate **58.** The amidation of the latter with **33-40** and **42-44** would finally render access to **6-16** (Scheme-8).

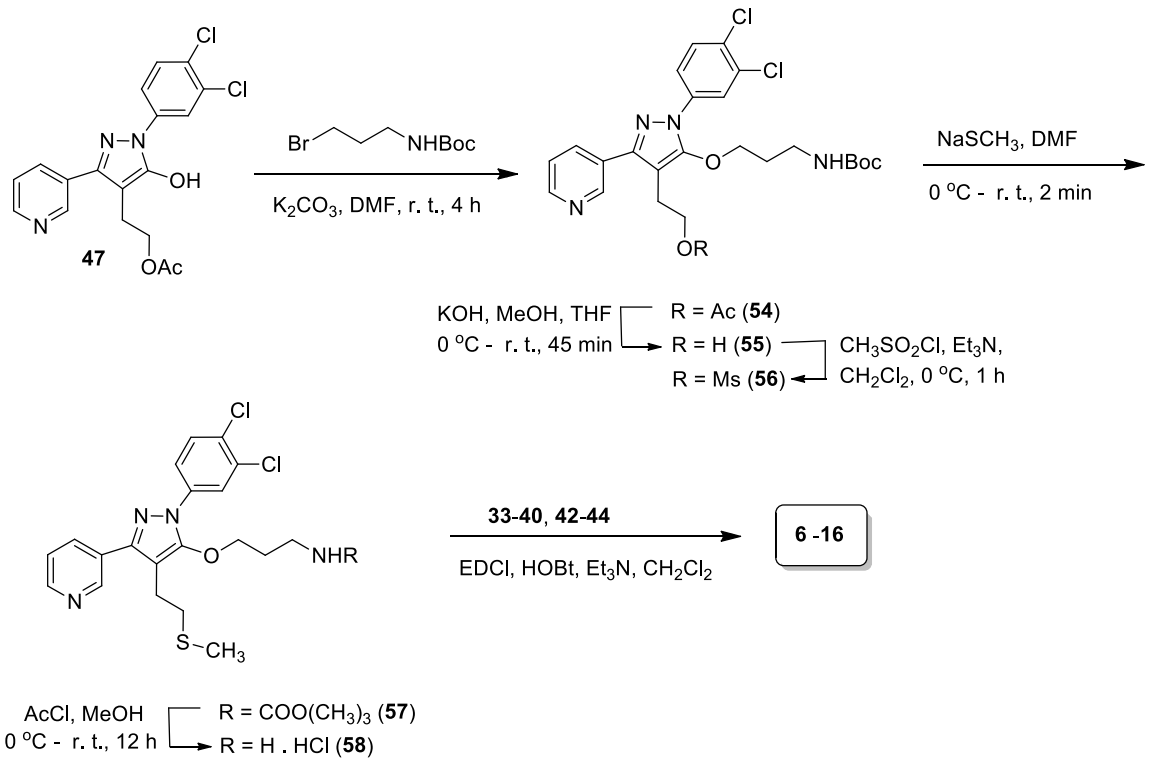

Scheme 8: Synthesis of **6-16**

2.3 Pharmacological screening of synthesized compounds (2-16)

All the synthesized compounds will be tested for their ability to inhibit GGTase-I in *vitro* and in cancer cells to determine IC_{50} values for impact on the signaling pathways controlled

by protein geranylgeranylation. The potential anti-cancer compound will also be tested for antiproliferative activity, which would involve cell proliferation assays, as well as assessment of the activity of key signaling pathways controlling cell growth (MAP kinase, Akt, and apoptotic pathways).

CHAPTER 3

RESULTS and DISCUSSIONS

3.1 Chemistry

The synthesis of compounds **2**-**16** necessitated the preparation of suitably modified amino acid derivatives. As outlined in scheme-9 esterification of amino acids **17**-**19** produced the corresponding amino esters **20**-**22** [116–118]. Likewise, acid induced removal of Boc protection of ester **23** [119] produced the amino ester **24** in 98% yield [120]. Moreover, reaction of amino esters **20**-**22** and **24** with ammonium hydroxide in a pressure vessel heating at 100 ^{o}C overnight furnished the desired α-amino amides **25**-**28** in good to excellent yields (85-95%) [125].

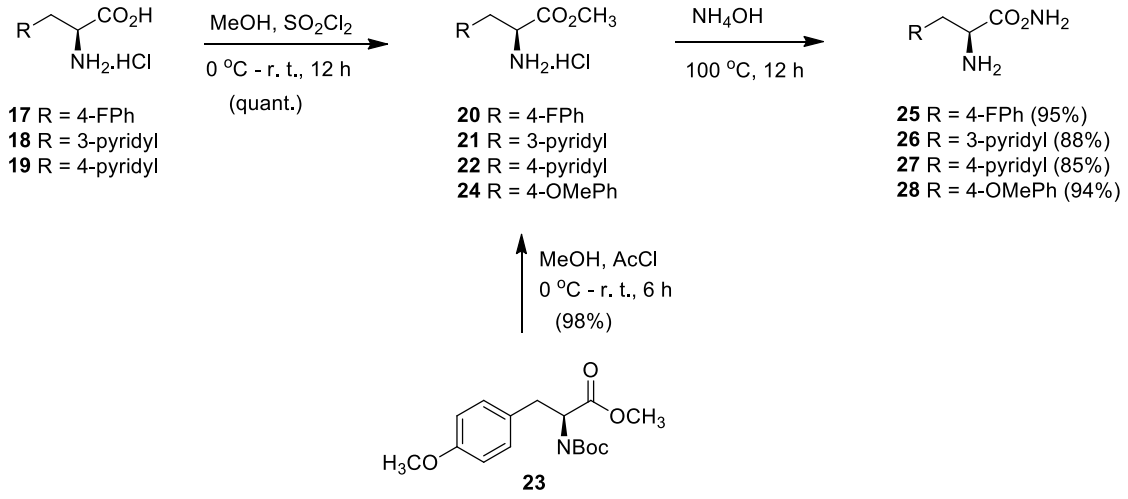

Scheme 9: Synthesis of amino acid derivatives **25**-**28**

Similarly, L-phenylalanine was transformed to the known **33** [126] and **34** [127]. Likewise, amino acids **14-17** were first transformed to their corresponding methyl esters **18-21** by the action of thionyl chloride in methanol. The N-acetylation or N-acylation of **18-21** with acetyl chloride or methane sulfonyl chloride followed by basic hydrolysis with LiOH furnished the desired intermediates **33-40**. Even though this route provided straightforward access to the intermediates **35** and **36** in a moderate overall yield of (64%) and (61%), respectively, the transformation of **20** and **21** to their corresponding **37-40** was low yielding (36-41%). In the latter case, the basic hydrolysis step resulted fewer side products. In addition, the higher water affinity of **37-40**, made their extraction difficult from the aqueous workup (Scheme-10).

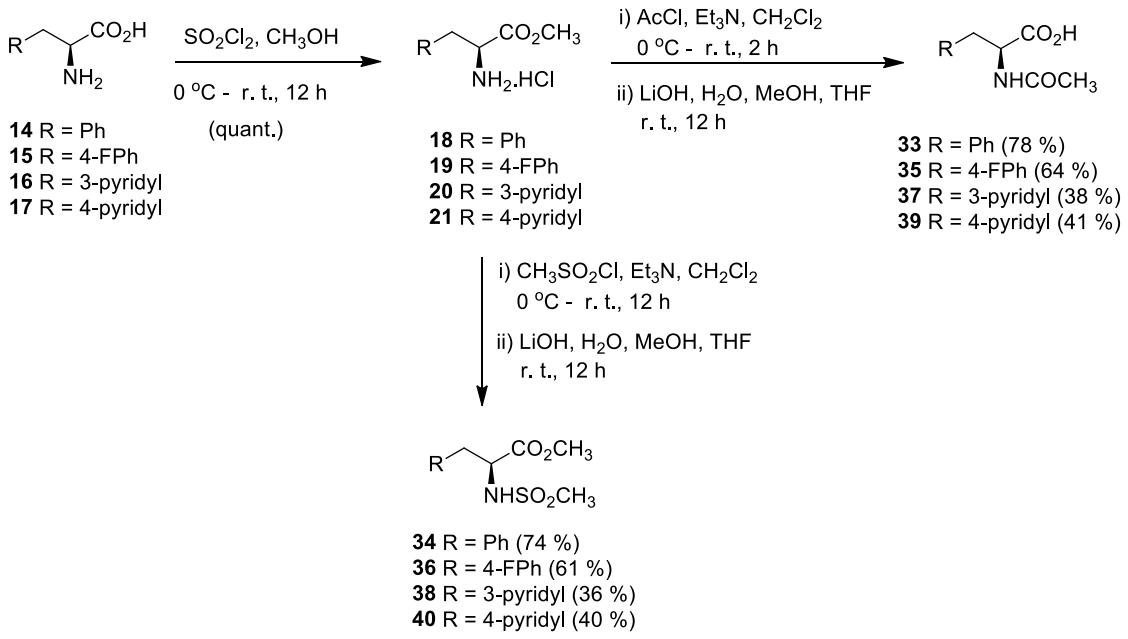

Scheme 10: Synthesis of amino acid derivatives **33-40**.

Consequently, a direct route for the preparation of intermediates **33-40** was envisioned. The acetylation of **18** and **19** with acetic anhydride in MeOH under reflux followed by evaporation of the solvent and aging the obtained residues overnight in a refrigerator

rendered **33** and **35** in excellent yield (81-86%). Under identical conditions, the acetylation of **20** and **21** produced the corresponding **37** (73%) and **39** (75%) in high yields. Similarly, the acylation of **18** and **29** with methane sulfonyl chloride in a mixture of dichloromethane and 1M NaOH furnished **34** and **36** in good yield (80-81%). By adopting similar synthesis strategy, amino acids **20** and **21** were also transformed to the corresponding desired intermediates **38** and **40** in high yields (Scheme-11).

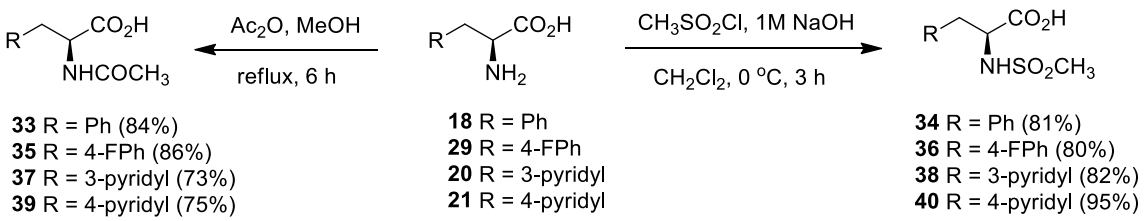

Scheme 11: Alternative synthesis of amino acid derivatives **33-40**

Likewise, an ester intermediate **41** was transformed to the known **42** [118] by the operations of N-acetylation of the amine function with acetic anhydride, O-alkylation of phenolic hydroxyl group with iodomethane and then basic hydrolysis of ester moiety with LiOH [123]. In addition, **43** [119] was produced from **41** from the reactions sequence of N-acylation with di-tert-butyl dicarbonate (boc anhydride) followed by O-alkylation of hydroxyl group with iodomethane and finally basic hydrolysis of ester group [124]. On the other hand, N-acylation of **41** with methane sulfonyl chloride in dichloromethane followed by O-alkylation of phenolic hydroxyl moiety with iodomethane furnished intermediate in a high yield (83% for two steps). The basic hydrolysis of that with LiOH in a mixture of water, methanol and THF finally produced the desired **44** [117] in 68% overall yield from **41** (Scheme-12).

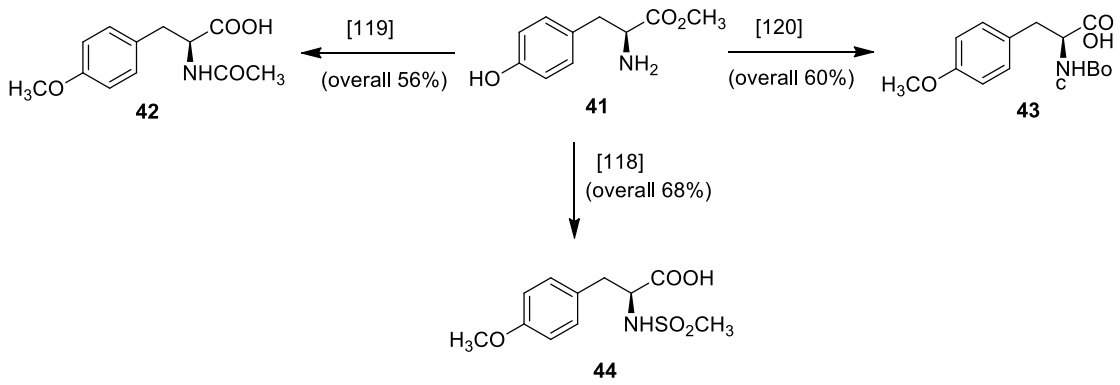

Scheme 12: Synthesis of amino acid derivatives **42-44**

With suitably modified amino acids in hands, we next moved to access the synthesis of target compounds **2-5** (Scheme 13). To this end, ethyl nicotinate **45** was treated via cross Claisen reaction with γ-butyrolactone in ethanol, using sodium ethoxide as a base to produce α-ketobutyrolactone **46** [121]. Knorr pyrazole synthesis condensation of **46** with 3,4-dichlorophenylhydrazine hydrochloride in acetic acid produced the pyrazole **47** [122]. The O-alkylation of **47** with the ethyl 4-bromobutanoate in DMF furnished the pyrazole ester **48** [122], which was subjected to the basic hydrolysis using LiOH in a mixture of H_2O, MeOH and THF to remove both the acetyl and ester moieties, generating intermediate **49** [122] in 42% overall yield from **47**. Next, amidation of intermediate **49** with amino amides **25-28** in a mixture of CH_2Cl_2 and DMF, using N-(3-dimethylaminopropyl)-N′-ethylcarbodiimide hydrochloride and N-hydroxybenzotriazole as coupling agents furnished the corresponding pyrazole amides **50-53** in good yields (Scheme-13). It is worth mentioning that we first attempted to deacetylate **48** by employing milder basic condition (K_2CO_3, MeOH) to produce the corresponding hydroxy ester (R_1 = Et; R_2 = H). The latter was intended to be transformed to the corresponding thiomethyl ether carboxylic acid, a

thioether analogue of **49** (R_1 = H; R_2 = SCH_3), by the sequence of mesylation of alcohol, condensation with sodium methanethiolate and basic hydrolysis of the ester function. However, the deacetylation of **48**, unfortunately, had led us to an undesired side product that had lost the O-acetyl and ester moieties, as evident from the ^{1}H-NMR and IR spectra. Nevertheless, mesylation of intermediates **50**-**53** with MsCl in CH_2Cl_2 followed by condensation of the resultant mesylate with sodium methanethiolate in DMF produced the desired compounds **2**-**5** in good to high yields (67-85%).

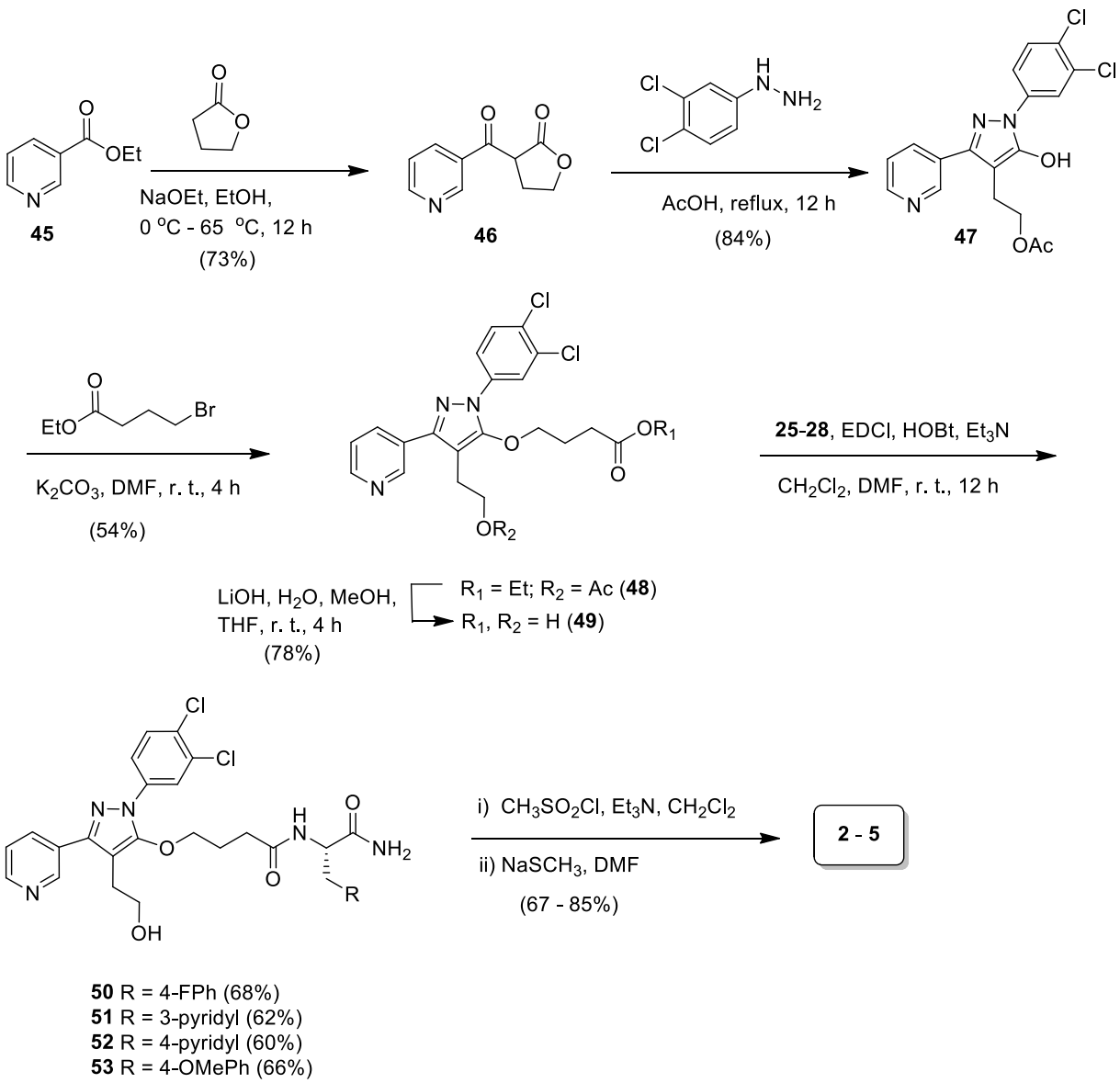

Scheme 13: Synthesis of **2-5**

On the other hand, the synthesis of compounds **6-16** was ensued as outlined in Scheme-14. In brief, the O-alkylation of pyrazole **47** with *tert*-butyl (3-bromopropyl)carbamate in DMF at room temperature constructed the desired intermediate **54** which was in turn subjected to basic hydrolysis to produce alcohol **55**. Mesylation of **55** constructed **56**, which was condensed with sodium methanethiolate in DMF to furnish the thioether **57**. The acid-

induced removal of Boc protection with acetyl chloride in MeOH produced the desired primary amine **58** in 64% overall yield from **54** (Scheme-14). The amidation of the primary amine **58** with **33-40** and **42-44** finally rendered access to **6-16** in moderate to good yields (57-69%).

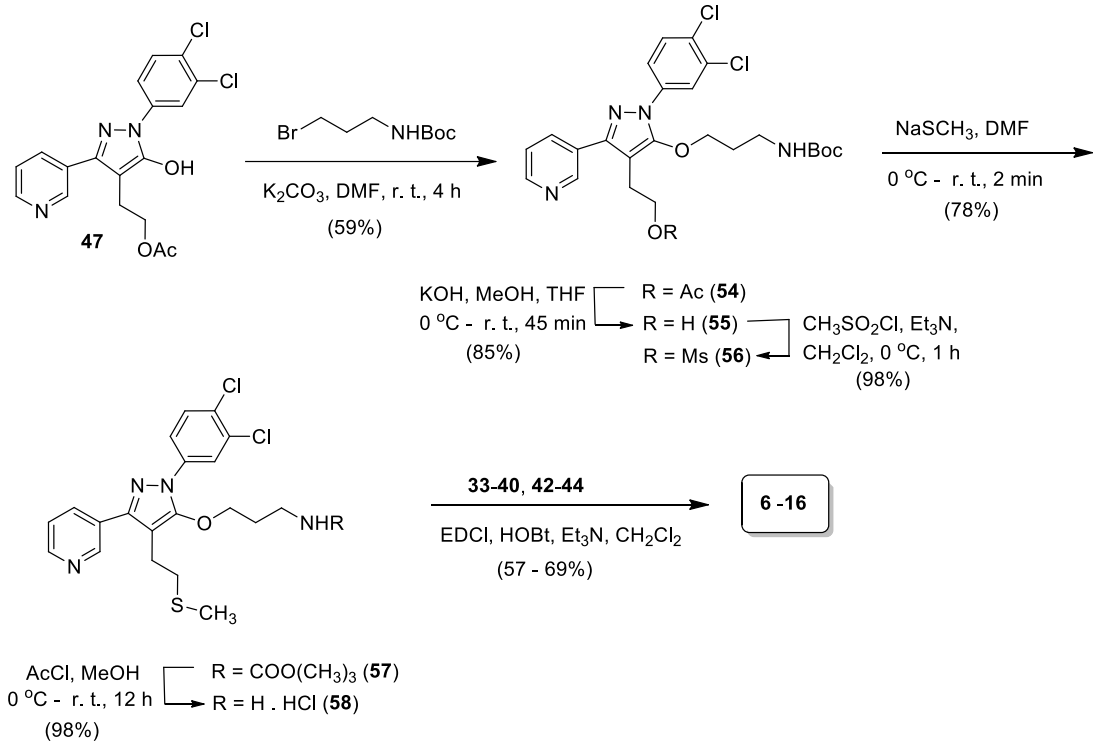

Scheme 14: Synthesis of **6-16**

3.2 Biological results

3.2.1 GGTase-I and FTase assays

All the synthesized compounds (**2**-**16**) were screened for *in vitro* inhibition against recombinant purified GGTase-I (Fig.10) and FTase, using GGTI-DU40 (**1**) and FTI-277 as positive controls, respectively. The screening results are summarized in table 3 and figure 10. In case of GGTase-I inhibition, a clear trend of decreased inhibitory activity for propanamides (**6**-**16**), derived from the coupling of propanoxypyrazole propanamine with suitably modified amino acid derivatives, compared to butanamides (**2**-**5**), originated from the reaction of propanoxypyrazole butanoic acid with α-amino amides, was clearly observed. Compound **11** (IC_{50} = 9.9 μM) that bears 4-methoxyphenyl ring on the amino acid turned out to be the most active in the propanamide series. However, the activity was diminished to more than three-fold when the N-methylsulfonamido moiety of **11** was substituted with an acetamido moiety, producing **10** (IC_{50} = 34.8 μM). The influence of N-methylsulfonamido group in the enhanced activity of the propanamide series was further evident when the activity of **9** (IC_{50} = 19.7 μM), possessing 4-fluorophenyl ring on the amino acid, was slightly reduced compared to its acetamido counterpart **8** (IC_{50} = 26.3 μM). Moreover, comparison of inhibitory activities of **9** with **11** revealed that the 4-methoxyphenyl on amino acid is more crucial compared to the corresponding 4-methoxyphenyl moiety. In fact the activities of propanamides were totally lost or diminished significantly when the combination of either 4-methoxyphenyl or 4-fluorophenyl on amino acid and the N- methylsulfonamido group was absent. For instance, whereas compounds **6** (IC_{50} = 22.9 μM), **7** (IC_{50} = 31.9 μM), **15** (IC_{50} = 26.9 μM) and **16**

(IC_{50} = 19.0 µM) had moderate activities, compounds **12-14** turned out to be completely inactive (Table-3).

It is apparent that, in general, the nature of linker between the pyrazole moiety and the amino acid played a significant role in the activities of **2-5** compared to **6-16**. Compound **2** (IC_{50} = 2.4 µM) that was produced by incorporating the fluoro group at C-4 of phenyl ring of amino acid of **1** turned out to be the most active in the series, showing higher activity than **1** (IC_{50} = 3.3 µM). An earlier report has suggested that placing fluorine at C-4 of phenyl ring has significantly enhanced the activity of a thrombin inhibitor compared to when it was present at other positions of phenyl ring. This high potency was attributed to the dipolar C–F…H–C_{α} and C–F…C=O interactions between the 4-fluorophenyl ring and the enzyme's active site [128]. The role of 4-fluorophenyl ring in the high potency of compound **2** was evident with the observation that when it was replaced with pyridyine-3-yl or pyridyine-4-yl group to produce **3** (IC_{50} = 11.6 µM) and **4** (IC_{50} = 7.8 µM), respectively, the activity was diminished to 5 and 3-fold, respectively. In contrast to our observation in propanamide series, where the 4-methoxyphenyl ring on the amino acid was more effective compared to the 4-fluorophenyl ring (**11** vs **9**), comparison in the butanamide series revealed that compounds with 4-fluorophenyl ring was relatively more active compared to its 4-methoxyphenyl counterpart (**2** (IC_{50} = 2.4 µM) vs **5** (IC_{50} = 3.1 µM)). This suggested that electronegative fluoro or methoxy groups attached to C-4 of phenyl ring of amino acid may play an important role in the interaction with the active site of enzyme. All target compounds **2-16** were also tested for *in vitro* inhibition against recombinant purified FTase enzyme, using inhibitor FTase-277 as control. The screening results, summarized in table 3, revealed that compounds **2-16** do not show any activity at

100 µM concentration which suggested that these compounds are selective inhibitors of GGTase-I.

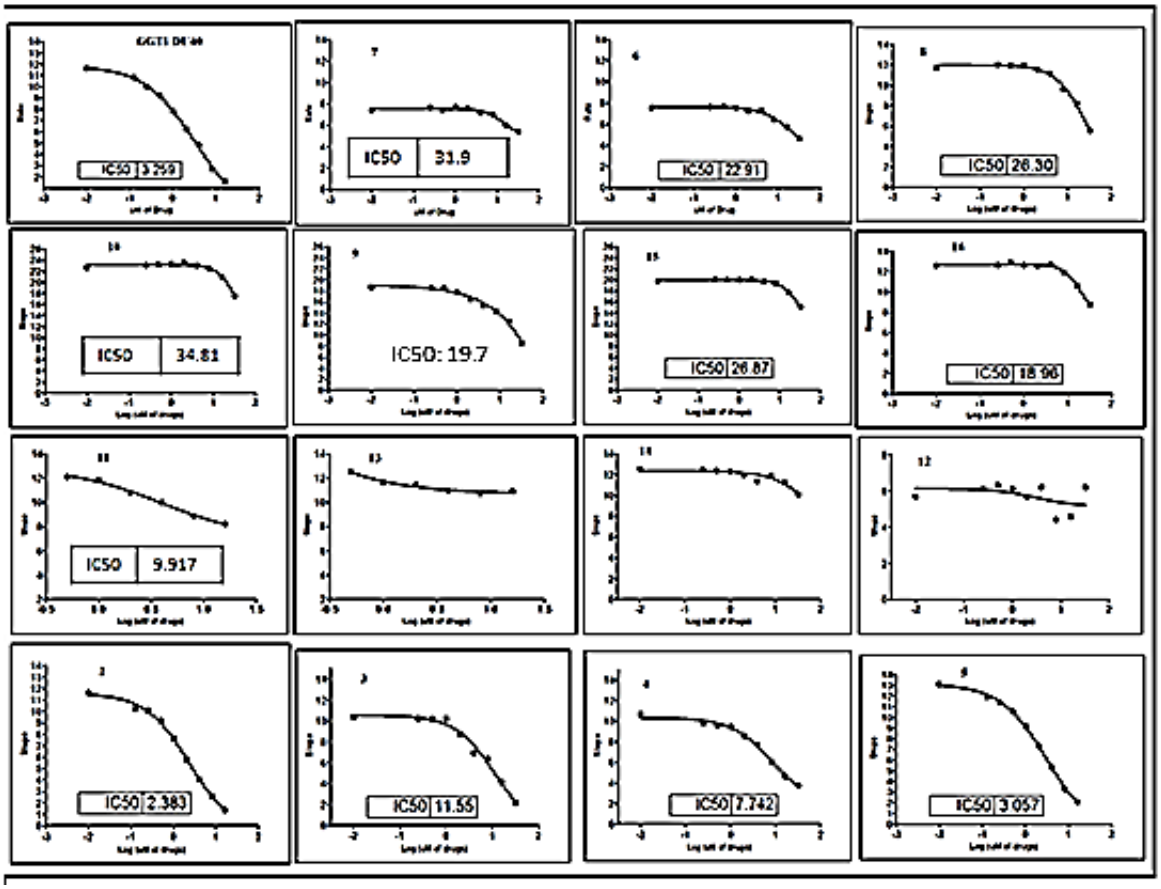

Figure 10: GGTase-1 assay with GGTI-DU40 as the positive control inhibitor

Table 3: *In vitro* GGTase-1 and FTase activity, impact on GTPase Rap1A and MTT assay of compounds **2-16**

Compd	GGTase-1 (IC_{50}, μM)[a]	FTase (IC_{50}, μM)[a]	Rap1A[c]	MTT Assay (IC_{50}, μM)[d]
1 (DU40)	3.3	1.1[b]	+++++	23.0 ± 1.22
2	2.4	> 100	+++++	7.6 ± 1.08
3	11.6	> 100	++	29.4 ± 1.01
4	7.8	> 100	+++	> 50
5	3.1	> 100	+++++	33.2 ± 1.29
6	22.9	> 100	+	15.4 ± 1.03
7	31.9	> 100	++	> 50
8	26.3	> 100	+++	13.2 ± 1.06
9	19.7	> 100	++	> 50
10	34.8	> 100	+	14.8 ± 1.08
11	9.9	> 100	++	> 50
12	> 50	> 100	-	> 50
13	> 50	> 100	-	> 50
14	> 50	> 100	-	> 50
15	26.9	> 100	-	34.9 ± 1.06
16	19.0	> 100	-	26.5 ± 1.10

[a] Each measurement was performed as triplicate. [b] Inhibitor FTI-277 as control. [c] Impact on GTPase Rap1A in cells (5 μM, 48 h). [d]Assay in MDAMB231 cells, repeated 3 times individual experiments) with 2 different time points of 48 hours and 72 hours. Data presented by one set of experiment with one time point (72 hours). +represents fold difference after normalization with internal control tubulin.

3.2.2 Western blot analysis

Rap1A is normally isoprenylated by GGTase-I and is used as an indicator for protein geranylgeranylation. In the Western blot analysis, the impairment of prenylation is noted by the use of anti-Rap1A antibody that selectively recognizes the unprenylated form of the Rap1A, a band indicating an alteration in Rap1A geranylgeranylation. This cellular assay was used to examine the capacity of the compounds to inhibit GGTase-I in an intact cell, namely the breast cancer cell line MDA-MB-231. ImageJ software was used to quantitate the Rap1A expression and normalized with internal control tubulin (Table-1). In normal growing cells treated with the DMSO control (10 µL of DMSO (0.5%)), all the Rap1A was geranylgeranylated and the lane was fairly blank. When GGTase-I was inhibited by GGTI DU40 (control), the accumulation of unprenylated Rap1A was readily observed (Fig. 11). Compounds **2** and **5** have shown the highest level of Rap1A expression which is in line with their highest GGTase-I inhibitory activity. These data indicated the capacity of **2** and **5** to inhibit prenylation of endogenous proteins. Moreover, compounds that showed similar GGTase-I inhibitory activity have shown almost similar alteration in Rap1A geranylgeranylation. For instance, compounds **4** (IC_{50} = 7.8 µM) and **11** (IC_{50} = 9.9 µM) have exhibited similar levels of Rap1A expression so was the case with compounds **6** (IC_{50} = 22.9 µM) and **10** (IC_{50} = 34.8 µM). Likewise, compounds **12**-**14** that were inactive in the GGTase-I inhibition did not alter Rap1A geranylgeranylation. The lower cellular activities of compounds **3**, **15** and **16** suggest that they are less capable of permeating the cells (Fig. 11).

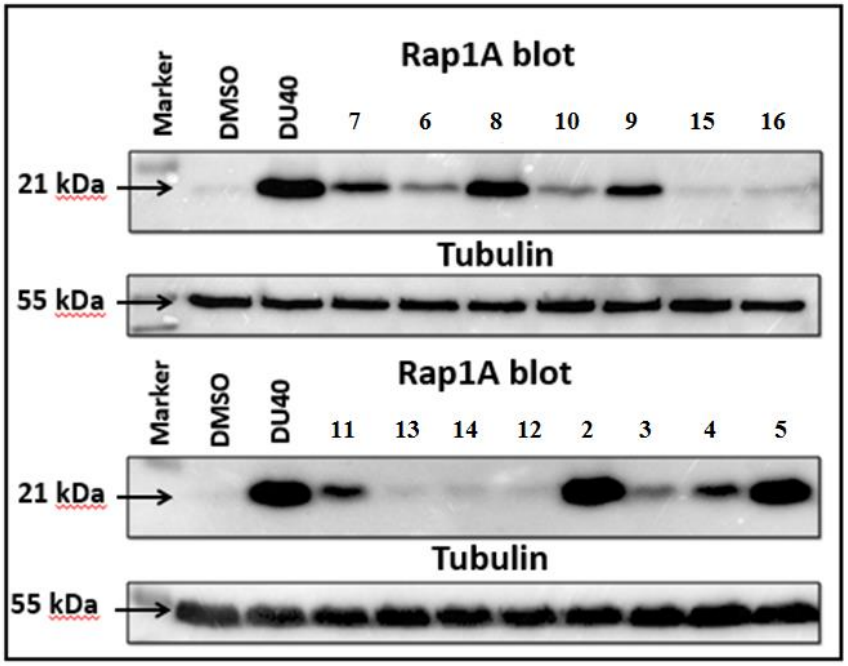

Figure 11: Inhibition of geranylgeranylation of Rap1A in MDA-MB-231 cells by **2-16**. Western blots of Rap1A following 48 hours treatments with the indicated inhibitors at a concentration (5 µM). Tubulin was used as the loading control for the immunoblot and GGTI- DU40 as the positive control inhibitor. The anti-Rap1A antibody detects the unprenylated form of Rap1A, a band indicating a reduction in Rap1A geranylgeranylation.

3.2.3 Cell proliferation assay

To determine the *in vitro* dose-dependent cytotoxicity effect of compounds **2-16**, the ability of **2-16** to inhibit growth of breast cancer cells MDA-MB-231 were assessed using the MTT assay (Fig. 12). This colorimetric assay is based on the ability of mitochondrial enzymes of live cells to reduce MTT to formazan salt. The cultured cells were treated with compounds at various concentration (2 - 32 µM) followed by the determination of cell growth by CellTiter 96® Aqueous one (Promega) cell proliferation assay solution after 48 hours. The cytotoxic effects of the extracts were estimated in terms of growth inhibition percentage with reference to the control (DMSO treated cells) and expressed as IC_{50} values

(Table-3). Whereas compounds **12-14** were found to be inactive in both GGTase-I inhibition as well as MTT assay, the activities of compounds **6**, **8**, **15** and **16** were almost comparable i.e. showing moderate GGTase-I inhibition and cytotoxicity in MTT assay. In addition, **2** (IC_{50} = 7.6 µM) turned out to be the most active compound which has shown significantly higher activity compared to **1** (IC_{50} = 23.0 µM). There is a general, but not perfect, correlation with impact on Rap1A prenylation and IC_{50} in the MTT assay, both of which read out cellular activity. The GGTase IC_{50} may not correlate for reasons of cell permeability as noted above.

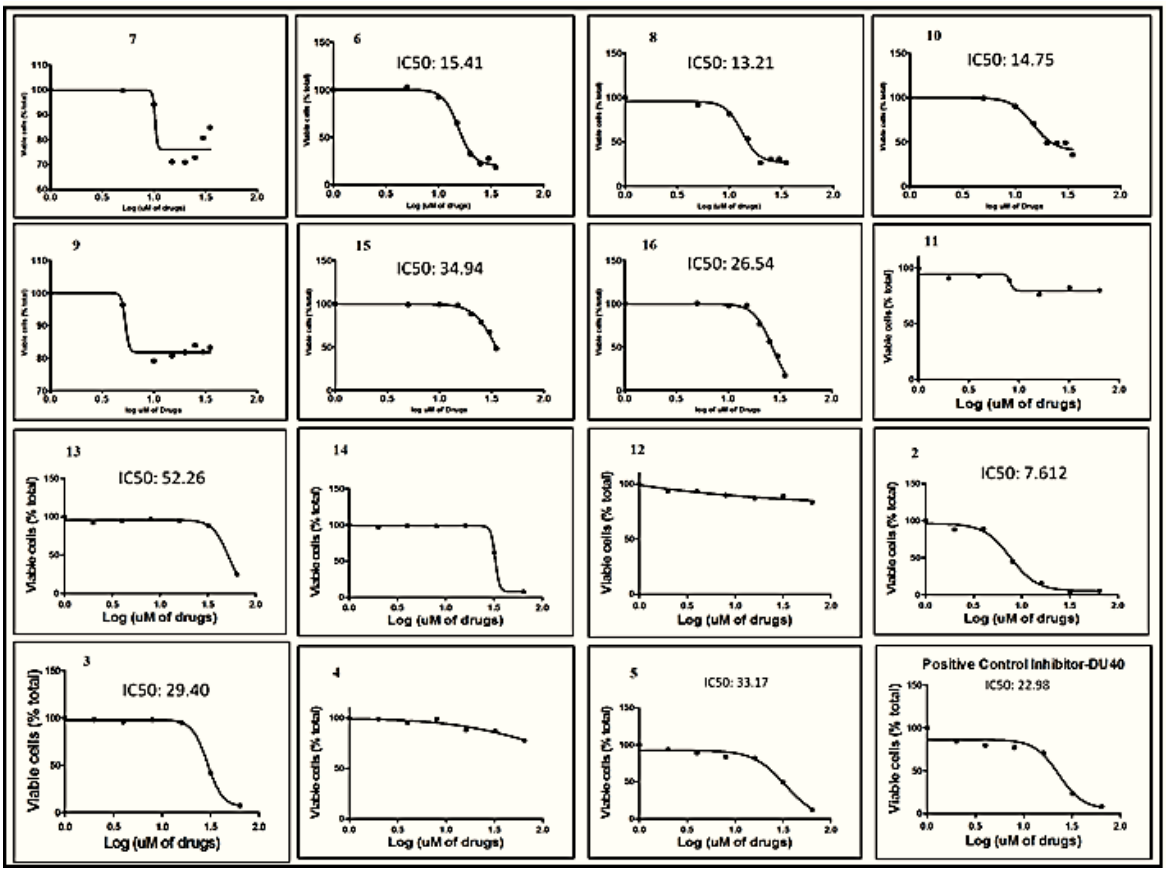

Figure 12: Cell proliferation assay against MDA-MB-231 cell line using the MTT assay

3.3 Molecular docking studies

In order to probe the possible binding mode of **2-16**, compound **2** was docked into GGTase-I binding pocket based on the co-crystal structure of GGTase-I complexed with a GGPP Analog and a KKKSKTKCVIL peptide (PDB ID: 1N4Q) using Glide (Glide, Schrodinger Inc.) [26]. The GGTase-I binding pocket is lined by mainly hydrophobic residues that bind the methyl-5-geranyl-4-methyl-pent-3-enyl moiety. At the entrance of the binding pocket, the positively charged residues Arg172, Lys266, Arg263, and His219 bind to the phosphate group of the co- crystallized ligand (Fig. 13).

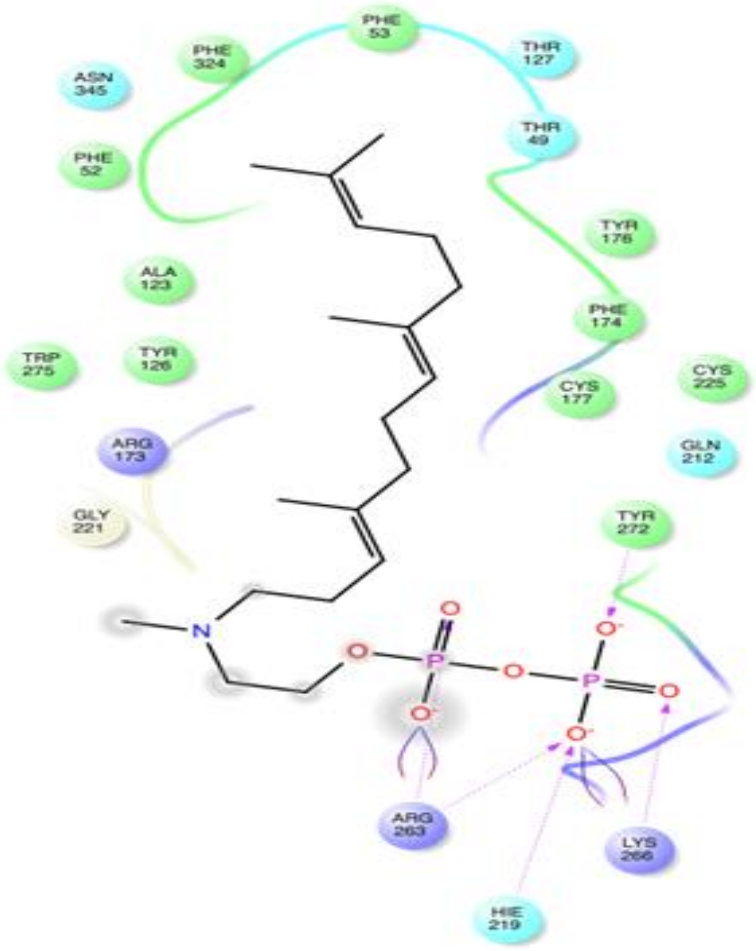

Figure 13: Binding of the native ligand

Computationally removing the KKKSKTKCVIL peptide substrate from enzyme exposed a large volume of the active site, which in turn resulted in different docking poses of **2** using the two scoring function of Glide, SP and XP [129,130]. Based on Figures 14a and 14b, Thr45 and Arg173 serve as hydrogen bond donors for the primary amide oxygen and oxygen at C-5 of the pyrazole moiety, respectively. Similarly, Ser46 and Thr49 are hydrogen bond acceptors for the primary amide hydrogens of **2** (Fig. 14b). In addition, **2** is engaged in π-π contacts through the 4-fluorophenyl (Fig. 14a) and 3,4-dichlorophenyl moieties (Fig. 14b) to the imidazole moiety of His121 and via pyridyl ring to the phenyl moiety of Tyr126 (Fig. 14b). However, when the KKKSKTKCVIL peptide was kept in the binding pocket, the obtained poses using the SP and XP scoring functions of Glide are very similar. The central pyrimidine phenyl diazole is kept inside the hydrophobic pocket, while the peptidic part orients itself towards the solvent and assumes different conformations between the SP and XP modes. By keeping the KKKSKTKCVIL peptide in the pocket, Glu 169 and Leu 511 acted as hydrogen bond acceptors for the primary amide hydrogens of **2** (Fig. 14c) and so was the case for Asp 269 (Fig. 14d). Additional H-bond interactions were evident between the nitrogen (N-2) of pyrazole moiety of 2 with Gln 212 (Fig. 14c & 14d) as well as between the Arg 263 and Tyr 272 with the secondary and primary amide oxygens, respectively (Fig. 14d). Additional π-π contact of **2** was observed through the 3,4-dichlorophenyl, pyridyl, pyrazole and 4-fluorophenyl moieties with Hie 219, Trp 272, Arg 263 and Lys 311 (Fig. 14c & 14d).

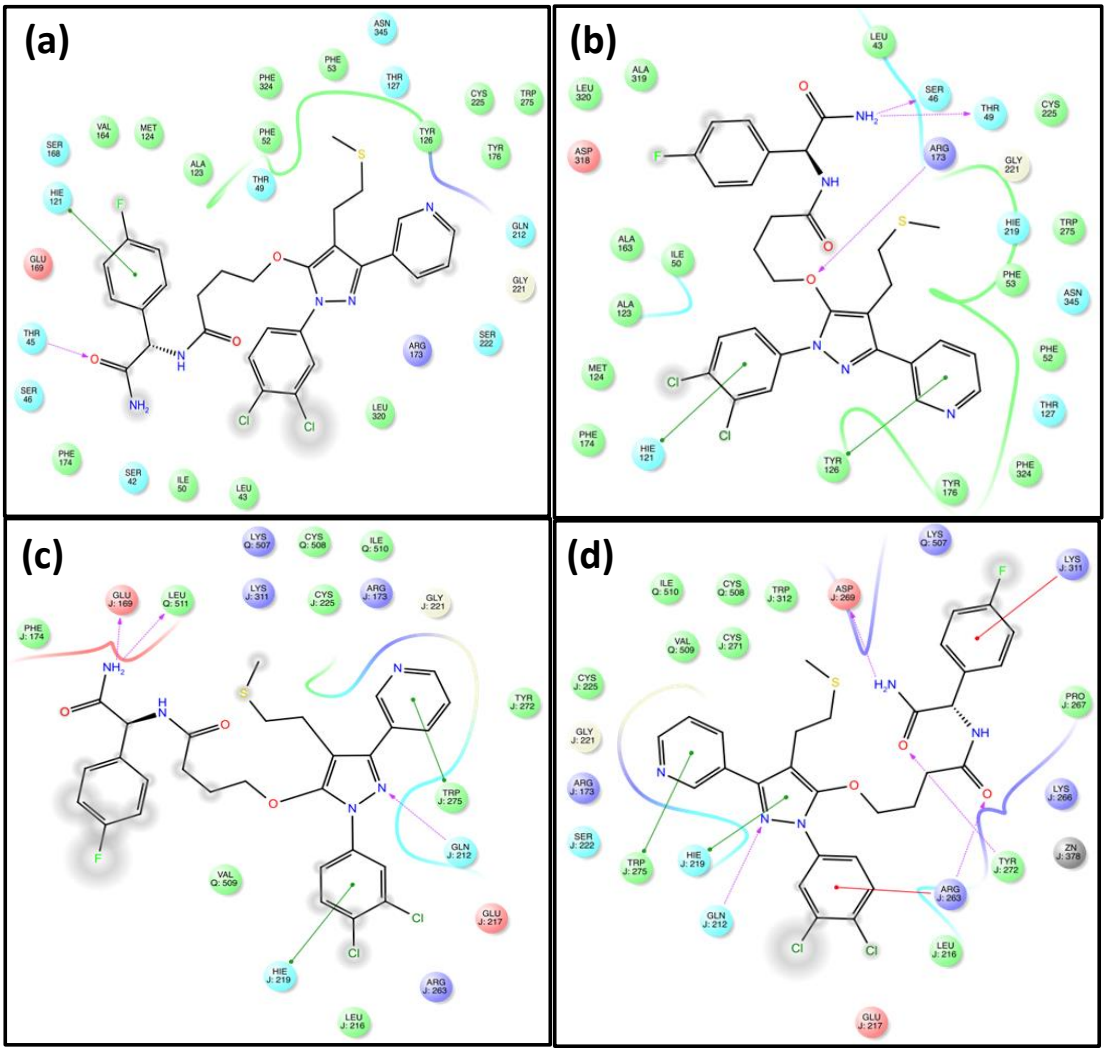

Figure 14: Molecular docking of 2 into GGTase-1 binding pocket without the KKKSKTKCVIL peptide.

(**a**) Using the Glide SP mode and (**b**) using the Glide XP mode. Molecular Docking of **2** into GGTase-1 binding pocket in presence of the KKKSKTKCVIL peptide (**c)** using the Glide SP mode and (**d**) using the Glide XP mode.

CHAPTER 4

Experimental Work

4.1 Instruments and chemicals

General: Melting Points were determined on a Büchi apparatus (Büchi Labortechnik AG, Switzerland) and are uncorrected. Elemental analysis was carried out on a Perkin Elmer Elemental Analyzer Series 11 Model 2400 (PerkinElmer Inc. USA). IR spectra were recorded on a Perkin Elmer 16F PC FTIR spectrophotometer (PerkinElmer Inc. USA) and reported in wavenumber (cm^{-1}). ^{1}H and ^{13}C NMR spectra were measured in $CDCl_3$ and d_6-DMSO using TMS as internal standard on a JEOL JNM-LA 500 MHz spectrometer (JEOL USA Inc.). Chemical shifts were reported in ppm (δ) relative to tetramethyl silane (TMS) by using CDCl3, DMSO or d_4-methanol as deuterated solvents. Multiplicities in signals of ^{1}H-NMR were recorded and reported as singlet (s), doublet (d), triplet (t), quartet (q) or multiplet (m) and coupling constant (J) were measured and reported in Hz.

Analytical TLC was carried out on silica gel 60 F_{254} plates (E. Merck) for monitoring of reactions as well as qualitative determination of sample purity by analyzing the spots under spectroline UV lamp operating at short and long wavelength ranges. For UV insensitive samples the visualization was improved by using solution of phosphomolybdic acid (PMA) and iodine chamber. Column chromatography was carried out on silica gel (200-400 mesh, E. Merck) for purification of the products.

Chemical were purchased from the most credible manufacturers like Sigma Aldrich, Fluka, Merck Chemicals, and BDH etc. and used without further purification unless otherwise

specified. All solvents used were of reagent or analytical grade and anhydrous solvents were used wherever necessary. Glassware was dried in an oven (Precision, Winchester, Virginia) at 120-140 ^{o}C for 3-4 hours and cooled in silica gel containing desiccators prior to use in case of moisture sensitive reactions. Similarly, reaction requiring inert conditions were performed under nitrogen or helium atmosphere.

4.2 Synthesis of target compounds 2-5

The synthesis of target compounds **2-5** was accomplished from intermediates **50-53** by the operations of mesylation that followed condensation of the resultant mesylates with sodium methanethiolate. The intermediates **50-53**, in turn, were synthesized from the amidation reaction of amino acid derivatives **25-28** and the key intermediate **49**. The detailed description about the syntheses procedures and spectroscopic analysis including ^{1}H-NMR, ^{13}C-NMR, FTIR, elemental analysis, melting points and specific rotation (if necessary) for all the intermediates and final target compounds is given below;

4.2.1 Synthesis of (S)-Methyl 2-amino-3-(4-fluorophenyl)propanoate hydrochloride (20)

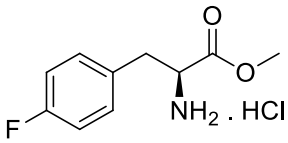

20

To a solution of L-4-fluorophenylalanine (3.0 g, 16.37 mmol) in anhydrous methanol (50 mL), thionyl chloride (9 mL) was added dropwise in about 30 minutes at 0°C and the mixture was stirred overnight at room temperature. The solvent was removed under reduced pressure and the crude product was purified by recrystallization with diethyl ether to obtain the title compound **20** as a colorless solid in quantitative yield [116]. ^{1}H NMR

(500 MHz, DMSO): δ 3.23-3.35 (dd, J=5.8, 7.5 Hz, 1H, CH-*CH*$_2$), 3.42-3.45 (dd, J=5.8, 6.7 Hz, 1H, CH-*CH*$_2$), 3.74 (s, 3H, CH_3), 4.33 (m, 1H, *CH*-CH_2), 7.23 (d, J= 10.1 Hz, 2H, Ar-H), 7.35 (d, J = 6.1Hz, 2H, Ar-H). ^{13}C-NMR (125.7 MHz, DMSO): δ 28.25 (*CH*-CH_2), 55.28 (*CH*-CH_2), 57.48 (OCH_3), 114.18 (C_{arom}), 127.74 (C_{arom}), 130.66 (C_{arom}), 158.85 (F-C), 158.88 (F-C), 175.10 ($COOCH_3$). Anal. Calcd for $C_{10}H_{13}ClFNO_2$ (233.06): C 51.40, H 5.61, N 5.99; Found: C 50.80, H 6.01, N 5.89.

4.2.2 Synthesis of (S)-methyl 2-amino-3-(pyridin-3-yl)propanoate hydrochloride (21)

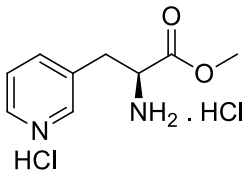

21

Following the procedure adopted for the synthesis of **20**, the reaction of L-3-pyridylalanine with NH_4OH yielded compound **21** as a light yellow solid (yield 95%) [117]. IR (neat): 3472.3, 3173.6, 1743.9, 1615.0, 1556.1, 1470.0, 1374.7, 1289.5, 1219.5, 1069.1, 805.6, 678.7 cm^{-1}. ^{1}H-NMR (500 MHz, CD_3OD): δ 3.39-3.34 (dd, J=7.3, 6.7 Hz, 1H, CH-*CH*$_2$), 3.5-3.45 (dd, J=7.3, 9.5 Hz, 1H, CH-*CH*$_2$), 3.72 (s; 3H, CH_3), 4.49 (m; 1H, *CH*-CH_2), 7.93 (t; J= 7.3 Hz, 1H, Ar-H), 8.39 (d, J= 7.95 Hz, 1H, Ar-H), 8.58 (s, 1H, Ar-H), 8.80 (d, J=5.45 Hz, 1H, Ar-H). ^{13}C-NMR (125.7 MHz, DMSO): δ 32.37 (CH-*CH*$_2$), 52.35 (*CH*-CH_2), 53.10 (OCH_3), 126.49 (C_{arom}), 134.44 (C_{arom}), 142.09 (C_{arom}), 144.07 (C_{arom}), 145.45 (C_{arom}), 168.85 ($COOCH_3$). Anal. Calcd for $C_9H_{14}C_{l2}N_2O_2$ (252.04): C 42.70, H 5.57, N 11.07; Found: C 41.60, H 5.25, N 12.17.

4.2.3 Synthesis of (S)-methyl 2-amino-3-(pyridin-4-yl)propanoate hydrochloride (22)

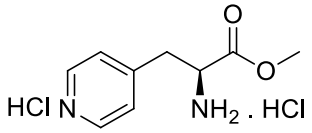

22

Following the procedure adopted for the synthesis of **20**, the reaction of L-4-pyridylalanine with NH_4OH yielded compound **22** as a light yellow solid (yield 92%). IR (neat): 3510.0, 3223.5, 1737.4, 1635.4, 1500.2, 1430.1, 1376.6, 1285.9, 1217.3, 1133.6, 970.4, 807.5, 573.7 cm^{-1}. ^{1}H-NMR (500 MHz, CD_3OD): δ 3.56-3.53 (dd, J=6.1, 7.95 Hz, 1H, CH-*CH_2*), 3.62-3.60 (dd, J=7.95, 4.6 Hz, 1H, CH-*CH_2*), 3.81 (s; 3H, *CH_3*), 4.65 (m, J= 7.0 Hz, 1H, *CH*-CH_2), 8.13 (d, J= 6.1 Hz, 2H, Ar-H), 8.86 (d, J= 5.45 Hz, 2H, Ar-H). ^{13}C-NMR (125.7 MHz, DMSO): δ 37.12 (*CH*-CH_2), 53.49 (*CH*-CH_2), 54.02 (OCH_3), 129.68 (C_{arom}), 142.81 (C_{arom}), 142.90 (C_{arom}), 158.31 (C_{arom}), 169.36 ($COOCH_3$). Anal. Calcd for $C_9H_{14}Cl_2N_2O_2$ (252.04): C 42.70, H 5.57, N 11.07; Found: C 42.60, H 6.25, N 12.47.

4.2.4 Synthesis of (S)-methyl 2-amino-3-(4-methoxyphenyl)propanoate hydrochloride (24)

The synthesis of **24** was achieved by esterification of L-tyrosine to get **24a**, which was condensed with di-tert-butyl dicarbonate (Boc anhydride) to produce intermediate **24b**. The O-alkylation of **24b** with iodomethane furnished **24c** and the exposure of the latter to acid conditions rendered the desired **24**.

4.2.5 Synthesis of (S)-methyl 2-amino-3-(4-hydroxyphenyl)propanoate (24a)

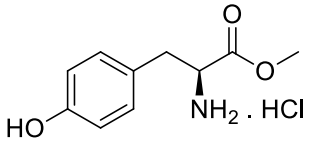

24a

To a solution of L-Tyrosine (5.0 g, 47.5 mmol) in methanol (25 mL), thionyl chloride (10 mL) was added at 0°C and the mixture was then stirred overnight at room temperature. After concentration under reduced pressure, the recrystallization of the crude product with diethyl ether gave the tittle compound **24a** as a colorless solid (yield, 99%) [131]. IR (neat): 3342.0, 2883.2, 1743.7, 1613.6, 1514.7, 1449.6, 1396.4, 1105.6, 1057.6, 839.9, 732.0 cm^{-1}. ^{1}H-NMR (500 MHz, CD_3OD): δ 3.20-3.10 (dd, J= 5.1, 6.5 Hz, 1H, CH-*CH_2*), 3.37-3.25 (dd, J=6.1, 7.95 Hz, 1H, CH-*CH_2*), 3.82 (s, 3H, CH_3), 4.28 (m, 1H, *CH*-CH_2), 6.81 (d, J=8.5 Hz, 2H, Ar-H), 7.10 (d, J= 8.5 Hz, 2H, Ar-H). ^{13}C-NMR (125.7 MHz, DMSO): δ 36.7 (CH-*CH_2*), 53.7 (*CH*-CH_2), 55.6 (0CH_3), 117.0 (C_{arom}), 131.7 (C_{arom}), 125.8 (C_{arom}), 158.4 (C_{arom}), 170.6 (C=O). Anal. Calcd for $C_{10}H_{14}ClNO_3$ (231.07): C 51.84, H 6.09, N 6.05; Found: C 50.96, H 5.97, N 7.05.

4.2.6 Synthesis of (S)-methyl 2-(tert-butoxycarbonylamino)-3-(4-hydroxyphenyl)propanoate (24b)

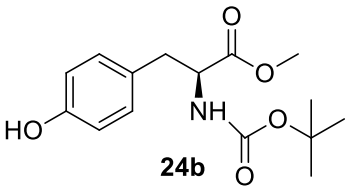

24b

To a solution of mixture of **24a** (2.50 g, 10.84 mmol) and K_2CO_3 (1.82 g, 21.68 mmol) in THF/methanol (50 ml/15 ml) was added di-tert-butyl dicarbonate (2.366 g, 10.84 mmol) dissolved in THF (20 ml). The solution was stirred for 22 h at room temperature and the

solvents were then removed in vacuo. The residue was dissolved in CH_2Cl_2, washed with water and the organic layer was dried over $MgSO_4$. The filtrate was concentrated under reduced pressure. Recrystallization of the residue from CH_2Cl_2 yielded **24b** as white crystalline solid (yield, 84%) [132]. IR (neat): 3389.7, 3002.6, 2978.3, 2952.0, 1717.2, 1688.9, 1617.0, 1446.1, 1396.1, 1159.3, 994.0, 830.1 cm^{-1}. ^{1}H-NMR (500 MHz, $CDCl_3$): δ 1.42 (s, 9H, $(CH_3)_3$), 2.98-2.95 (dd: J=7.05, 6.4 Hz, 1H, CH), 3.05-3.02 (dd, J=5.5, 6.4 Hz, 1H, CH), 3.71 (s, 3H, CH_3), 4.54 (m, 1H, *CH*-CH_2), 5.01 (d, J= 9.45Hz, 1H, NH), 5.62 (s: 1H, OH), 6.74 (d, J=7.65 Hz, 2H, Ar-H), 6.97 (d, J=8.25 Hz, 2H, Ar-H). ^{13}C-NMR (500 MHz, $CDCl_3$): δ 28.5 ($(CH_3)_3$), 37.7 (CH-*CH_2*), 52.4 (OCH_3), 54.8 (C*H*-CH_2), 80.4 ($OC(CH_3)_3$), 115.7 (C_{arom}), 127.7 (C_{arom}), 130.5 (C_{arom}), 155.3 (C_{arom}), 155.5 ($COOCH_3$), 172.8 (CONH). Anal. calcd. for $C_{15}H_{21}NO_5$ (295.14): C 61.00, H 7.17, N 4.74; Found C 61.50, H 5.55, N 6.87.

4.2.7 Synthesis of (S)-methyl 2-(tert-butoxycarbonylamino)-3-(4-methoxyphenyl)propanoate (24c)

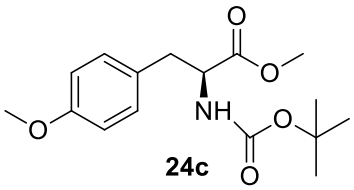

24c

To a solution of **24b** (0.323g, 1.0936 mmol) in DMF (40 mL) was added $NaHCO_3$ (0.226g, 1.604 mmol) and after being stirred 10 minutes, MeI (0.1709 mL, 2.74 mmol) was added to the mixture dropwise. The reaction was stirred overnight at room temperature and then quenched with 1N HCl (40 mL). The mixture was transferred in a separating funnel and extracted with ethyl acetate (20 mL × 3) and the organic layer was washed with 1N HCl (20 mL x 3), H_2O (20 mL) and brine (15 mL). The organic layer was dried over Na_2SO_4

and evaporated under reduced pressure to get the title compound **24c** as pale yellow sticky solid (yield, 78%) [132]. IR (neat): 3445.9, 3347.9, 2978.7, 2929.8, 1717.7, 1513.9, 1513.9, 1397.4, 1368.8, 1249.4, 1167.1, 1032.1, 829.7 cm^{-1}. ^{1}H-NMR (500 MHz, $CDCl_3$): δ 1.42 (s, 9H, $(CH_3)_3$), 3.01-2.98 (dd, J=7.65, 6.45 Hz, 1H, CH-*CH_2*), 3.07-3.03 (dd, J=6.75, 7.52 Hz, 1H, CH-*CH_2*), 3.71(s, 3H), 3.78 (s, 3H), 4.53 (m, 1H, *CH*-CH_2), 4.97 (d: 1H, NH), 6.83 (d: J=8.5 Hz, 2H, Ar-H), 7.04 (d, J=8.2 Hz, 2H, Ar-H). ^{13}C-NMR (125.7 MHz, CDCl3): δ 28.20 ($(CH_3)3$), 37.34 (CH-*CH_2*), 52.05 (OCH_3), 54.47 (*CH*-CH_2), 55.10 (OCH_3), 79.75 ($OC(CH_3)3$), 113.88 (C_{arom}), 127.86 (C_{arom}), 130.18 (C_{arom}),155.03 (C_{arom}), 158.56 (C_{arom}), 172.34 ($COOCH_3$), 192.45 ($COOC(CH_3)3$). Anal. Calcd for $C_{16}H_{23}NO_5$ (309.16): C 62.12, H 7.49, N 4.53; Found: C 61.42, H 6.49, N 5.20.

4.2.8 Synthesis of (S)-methyl 2-amino-3-(4-methoxyphenyl)propanoate hydrochloride (24)

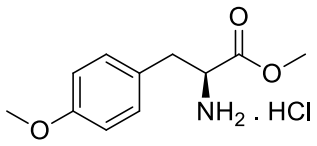

24

Following the same procedure adopted for the synthesis of **20**, the reaction of (**24c**) with acetyl chloride in methanol yielded compound **24** as a white solid (yield, 85%) [120]. IR (neat): 3411.6, 3032.2, 2834.6, 1740.4, 1615.7, 1516.1, 1489.5, 1305.1, 1250.2, 1053.1, 837.7 cm^{-1}. ^{1}H-NMR (500 MHz, CD_3OD): δ 3.01-2.98 (dd, J=6.8, 7.65 Hz, 1H, CH-*CH_2*), 3.07-3.03 (dd, J=6.75, 7.9 Hz, 1H, CH-*CH_2*), 3.77 (s, 3H, CH_3), 3.80 (s, 3H, CH_3), 4.25 (m, 1H, *CH*-CH_2), 6.92 (d: J=8.5 Hz, 2H, Ar-H), 7.15 (d, J=8.5 Hz, 2H, Ar-H). ^{13}C-NMR (125.7 MHz, CDCl3): δ 36.59 (CH-*CH_2*), 52.05 (OCH_3), 54.47 (*CH*-CH_2), 55.72 (OCH_3), 113.88 (C_{arom}), 115.56 (C_{arom}), 126.89 (C_{arom}), 131.51 (C_{arom}), 160.93 (C_{arom}), 170.51

($COOCH_3$). Anal. Calcd for $C_{11}H_{16}ClNO_3$ (245.08): C 53.77, H 6.56, N 5.70; Found: C 52.87, H 6.96, N 6.30.

4.2.9 Synthesis of (S)-2-amino-3-(4-fluorophenyl)propanamide (25)

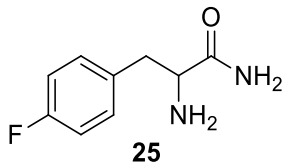

25

In a pressure vessel, a solution of compound **20** (0.50 g, 2.54 mmol) in NH_4OH (2 mL) was heated overnight at 100 ºC. After cooling to room temperature, the reaction was added CH_2Cl_2 (10 mL) and the organic layer was separated and dried over Na_2SO_4 and evaporated to get the title compound **25** as a light yellow solid (yield 95%) [116]. M. p. 153-154 ºC. IR (neat): 3377, 3329, 2958, 2926, 2834, 1667, 1613, 1512, 1448, 1299, 1249, 1035 cm^{-1}. ^{1}H-NMR (500 MHz, CD_3OD): δ 3.04 (dd, *J* = 7.65, 13.9 Hz, 1H, *CH*$_2$CH), 3.20 (dd, *J* = 5.8, 13.9 Hz, 1H, *CH*$_2$CH), 4.06 (m, 1H, CH$_2$*CH*), 7.08 (m, 2H, 3'-H, 5'-H), 7.31 (m, 2H, 2'-H, 6'-H). ^{13}C-NMR (125.7 MHz, CD_3OD): δ 37.82 (*CH*$_2$CH), 55.60 (CH$_2$*CH*), 116.76 (d, *J* = 21.8 Hz, C-3', C-5'), 132.40 (d, *J* = 8.3 Hz, C-2', C-6'), 134.40 (C-1') 163.70 (d, *J* = 247.0 Hz, C-4'), 171.82 (C=O). Anal. Calcd for $C_9H_{11}FN_2O$ (198.19): C 59.33 H 6.09, N 15.38. Found: C 59.29, H 6.13, N 15.31.

4.2.10 Synthesis of (S)-2-amino-3-(pyridin-3-yl)propanamide (26)

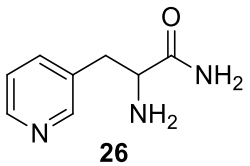

26

Following the same procedure adopted for the synthesis of **25**, the reaction of **21** with NH_4OH yielded compound **26** as a light yellow solid (yield 88%) [117]. M. p. 114-115 ºC.

IR (neat): 3366, 2977, 2936, 1703, 1519, 1429, 1346, 1168, 1036 cm^{-1}. ^{1}H-NMR (500 MHz, CD_3OD): δ 2.88 (dd, *J* = 7.3, 13.7 Hz, 1H, *CH*$_2$CH), 3.04 (dd, *J* = 6.4, 13.7 Hz, 1H, *CH*$_2$CH), 3.62 (t, *J* = 7.0 Hz, 1H, CH$_2$*CH*), 7.37 (m, 1H, 5'-H), 7.75 (m, 1H, 6'-H), 8.40 (d, *J* = 6.5 Hz, 1H, 4'-H), 8.42 (d, *J* = 1.3 Hz, 1H, 2'-H). ^{13}C-NMR (125.7 MHz, CD_3OD): δ 34.85 (*CH*$_2$CH), 54.48 (CH$_2$*CH*), 125.22, 131.34, 139.39, 148.59, 149.70 (all C_{arom}), 172.23 (C=O). Anal. Calcd for $C_8H_{11}N_3O$ (181.19): C 58.17, H 6.71, N 25.44. Found: C 58.13, H 6.76, N 25.37.

4.2.11 Synthesis of (S)-2-amino-3-(pyridin-4-yl)propanamide (27)

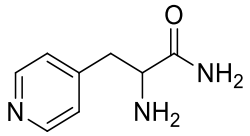

27

Following the same procedure adopted for the synthesis of **25**, the reaction of compound **22** with NH_4OH gave compound **27** as a light yellow solid (yield 85%). M. p. 158-159 ºC. IR (neat): 3364, 3250, 3035, 2939, 1695, 1607, 1539, 1420, 1398, 1038 cm^{-1}. ^{1}H-NMR (500 MHz, CD_3OD): δ 3.05 (dd, *J* = 7.9, 14.0 Hz, 1H, *CH*$_2$CH), 3.22 (dd, *J* = 5.4, 14.0 Hz, 1H, *CH*$_2$CH), 4.02 (m, 1H, CH$_2$*CH*), 7.38 (d, *J* = 6.1 Hz, 2H, 2'-H, 6'-H), 8.50 (d, *J* = 6.1 Hz, 2H, 3'-H, 5'-H). ^{13}C-NMR (125.7 MHz, CD_3OD): δ 37.50 (*CH*$_2$CH), 56.48 (CH$_2$*CH*), 126.53 (C-2', C-6'), 146.97 (C-1'), 150.47 (C-3', C-5'), 172.60 (C=O). Anal. Calcd for $C_8H_{11}N_3O_2$ (181.19): C 58.17, H 6.71, N 25.44. Found: C 58.14, H 6.75, N 25.37.

4.2.12 Synthsis of (S)-2-amino-3-(4-methoxyphenyl)propanamide (28)

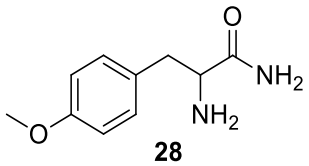

28

Following the same procedure adopted for the synthesis of **25**, the reaction of compound **24** with NH_4OH gave the title compound **28** [120] as a light yellow solid (yield 94%). M. p. 177-178 ^oC. IR (neat): 3376, 3056, 2958, 1667, 1613, 1511, 1449, 1299, 1250, 1035 cm^{-1}. ^1H-NMR (500 MHz, CD_3OD): δ 2.75 (dd, *J* = 7.6, 13.9 Hz, 1H, CH_2), 2.91 (dd, *J* = 6.1, 13.9 Hz, 1H, CH_2), 3.53 (m, 1H, CH), 3.75 (s, 3H, OCH_3), 6.85 (d, *J* = 8.5 Hz, 2H, 3'-H, 5'-H), 7.15 (d, *J* = 8.3 Hz, 2H, 2'-H, 6'-H). ^{13}C NMR (125.7 MHz, CD_3OD): δ 41.42 (*CH_2*CH), 55.65 (OCH_3), 57.37 (CH_2*CH*), 114.17 (C-3', C-5'), 130.51 (C-1'), 131.41 (C-2', C-6'), 160.12 (C-4'), 179.19 (C=O). Anal. Calcd for $C_{10}H_{14}N_2O_2$ (210.23): C 61.84, H 7.27, N 14.42. Found: C 61.79, H 7.33, N, 14.35.

4.2.13 Synthesis of 3-nicotinoyldihydrofuran-2(3H)-one (46)

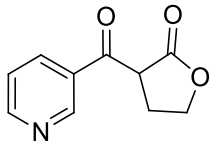

46

A solution of NaOEt (8.16g, 120 mmol) in EtOH (38.8), making a concentration of 21% w/v, was added to a dry flask under N_2. The mixture was cooled to 0^oC followed by the addition of ethylnicotinate (16.4 mL, 120 mmol) in one portion. ϒ-Butyrolactone (8 mL, 120 mmol) was then added drop wise to mixture in 1 hr and the reaction was stirred first at 0^oC for 1 h followed by heating to 65 ^0C overnight. The ethanol was removed in vacuo and the residue was diluted with H_2O (50 mL) and the unreacted materials were removed by

extraction with diethyl ether. The pH of aqueous phase was adjusted to 4-5 with 3N HCl and then extracted with CH_2Cl_2 (20 mL x 3). After washing with water and brine, the organic layer was dried over Na_2SO_4 and evaporated to yield **46** as a brown oil (Yield 73%). IR (neat): 3411.2, 3058.01, 2918.1, 29.22.6, 1759.3, 1689.5, 1586.9, 1377.1, 1346.9, 1021.9 cm^{-1}. ^{1}H-NMR (500 MHz, CDCl3): δ 2.52 (m,1H), 2.92 (m, 0.98H), 3.22 (t, J=7.5Hz, 0.35H), 4.5-4.3 (m, 3.34H), 7.42-7.41 (dd, J= 4.8 Hz, 1H), 8.32-8.30 (d, J= 3.9 Hz; 1H), 8.7710-8.7582 (dd, J=1.5 Hz, 1H), 9.2 (d, J=2.15 Hz;1H). ^{13}C-NMR (500 MHz, CDCl3): δ 22.07, 25.11, 48.41, 67.77, 68.47, 123.41, 123.75, 137.14, 137.39, 150.30, 150.44, 152.71, 153.68, 177.77, 191.9. Anal. Calcd for $C_{10}H_9NO_3$ (191.06): C 62.82, H 4.74, N 7.33; Found: C 61.70, H 4.67, N 7.44.

4.2.14 Synthesis of 2-(1-(3,4-Dichlorophenyl)-5-hydroxy-3-(pyridin-3-yl)-1H-pyrazol-4-yl)ethyl acetate (47)

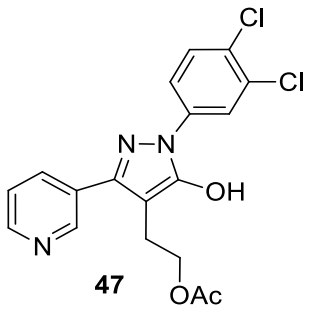

47

A slightly modified procedure was followed [122]. To the solution of α-ketobutyrolactone **46** (4.78 g, 25.03 mmol) in acetic acid (20 mL) was added 3,4-dichlorophenylhydrazine hydrochloride (5.86 g, 27.5 mmol) in one portion. The mixture was heated at reflux overnight and then cooled to room temperature. The mixture was diluted with H_2O (20 mL) and then extracted with EtOAc (2 x 30 mL). The combined organic layers was washed with saturated aqueous solution of $NaHCO_3$ (2 x 15 mL), dried over Na_2SO_4 and evaporated under reduced pressure. Column chromatography of the light oily material eluting with

EtOAc-hexane (1:1) afforded the title compound **47** as a yellow solid (8.22 g, 84%). M. p. 176-177 ^{o}C. IR (neat): 3426, 3099, 3076, 2993, 2984, 1725, 1589, 1475, 1409, 1250, 1025 cm^{-1}. ^{1}H-NMR (500 MHz, d_6-DMSO): δ 1.78 (s, 3H, $COCH_3$), 2.84 (t, *J* = 6.4 Hz, 2H, Ar*CH*$_2$), 4.03 (t, *J* = 6.5 Hz, 2H, OCH_2), 7.49 (dd, *J* = 2.1, 8.7 Hz, 1H, Ar-H), 7.73 (d, *J* = 8.8 Hz, 1H, Ar-H), 7.84 (dd, *J* = 2.1, 6.8 Hz, 1H, Ar-H), 8.06 (m, 2H, Ar-H), 8.58 (d, J = 1.8 Hz, 1H, Ar-H), 8.86 (s, 1H, Ar-H). ^{13}C-NMR (125.7 MHz, d_6-DMSO): δ 20.55 (CO*CH*$_3$), 21.63 (Ar-*CH*$_2$), 63.13 (OCH_2), 120.65, 122.04, 123.84, 127.87, 131.09, 131.49, 135.01, 138.18, 147.79, 148.01, 149.17 (all C_{arom}), 170.31 (C=O). Anal. Calcd for $C_{18}H_{15}Cl_2N_3O_3$ (391.05): C 55.12, H 3.85, N 10.71; Found: C 55.08, H 3.89, N 10.65.

4.2.15 Synthesis of Ethyl 4-((4-(2-acetoxyethyl)-1-(3,4-dichlorophenyl)-3-(pyridin-3-yl)-1H-pyrazol-5-yl)oxy)buta-noate (48)

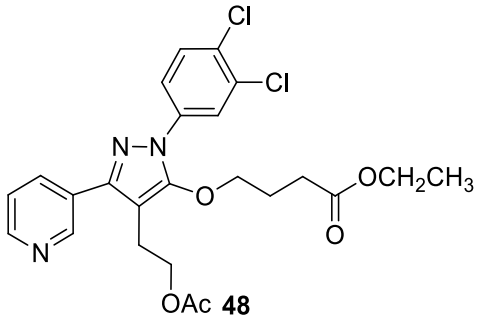

48

To a solution of **47** (2.0 g, 5.10 mmol) in anhydrous DMF (20 mL) was added K_2CO_3 (1.06 g, 7.65 mmol) followed by the addition of ethyl 4-bromobutanoate (0.88 mL, 6.12 mmol) and the mixture was stirred for 4 hours at room temperature until the completion of the reaction (TLC analysis). The reaction was diluted with EtOAc (30 mL) and then washed successively with 1M aqueous HCl (10 mL), H_2O (10 mL) and brine (10 mL). The organic layer was dried over anhydrous Na_2SO_4 and evaporated under reduced pressure. Column chromatography of the light orange oily material, eluting with EtOAc-hexane (8:2)

afforded the title compound **48** as a yellow thick oil (1.42 g, 54%). IR (neat): 3034, 2954, 1740, 1592, 1484, 1415, 1366, 1230, 1029 cm^{-1}. ^{1}H-NMR (500 MHz, CD_3OD): δ 1.26 (t, *J* = 7.0 Hz, 2H, *CH*$_3$$CH_2O$), 1.96 (s, 3H, $COCH_3$), 2.07 (quint, 2H, *J* = 6.7 Hz, 2H, -CH_2*CH*$_2$$CH_2$-), 2.48 (t, *J* = 7.3 Hz, 2H, *CH*$_2$$CO_2Et$), 2.96 (t, *J* = 7.0 Hz, 2H, Ar*CH*$_2$), 4.04 (t, *J* = 6.4 Hz, 2H, OCH_2), 4.14 (q, *J* = 7.0 Hz, 2H, CH_3*CH*$_2$O), 4.19 (t, *J* = 7.0 Hz, 2H, OCH_2), 7.57 (d, *J* = 8.8 Hz, 1H, Ar-H), 7.61-7.66 (m, 2H, Ar-H), 7.93 (d, *J* = 2.4 Hz, 1H, Ar-H), 8.36 (d, *J* = 7.9 Hz, 1H, Ar-H), 8.67 (d, *J* = 4.5 Hz, 1H, Ar-H), 9.06 (br. s, 1H, Ar-H). ^{13}C-NMR (125.7 MHz, CD_3OD): δ 14.16 (*CH*$_3$$CH_2O$), 20.08 ($COCH_3$), 22.41 (Ar-*CH*$_2$), 25.03 (-$CH_2$*CH*$_2$$CH_2$-), 30.17 (*CH*$_2$$CO_2Et$), 60.68 ($CH_3$*CH*$_2$O), 63.30 ($OCH_2$), 74.67 ($OCH_2$), 103.13, 121.05, 123.83, 124.79, 130.65, 130.89, 131.25, 133.32, 137.30, 137.98, 144.95, 145.36, 146.39, 152.43 (all C_{arom}), 170.83 (C=O), 172.44 (C=O). Anal. Calcd for $C_{24}H_{25}Cl_2N_3O_5$ (505.12): C 56.93, H 4.98, N 8.30; Found: C 56.85, H 5.03, N 8.25.

4.2.16 Synthesis of 4-((1-(3,4-Dichlorophenyl)-4-(2-hydroxyethyl)-3-(pyridin-3-yl)-1H-pyrazol-5-yl)oxy)butanoic acid (49)

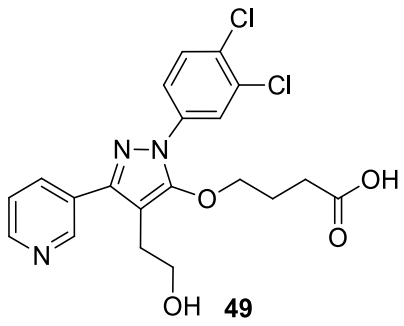

49

To a solution of **48** (1.64 g, 3.24 mmol) in a mixture of MeOH-H_2O-THF (25 mL, 1:1:3) was added LiOH.H_2O (0.68 g, 16.2 mmol) and the mixture was stirred for 4 hours at room temperature until the completion of the reaction (TLC analysis). The volatiles were evaporated under reduced pressure to get the title compound **49** as a white crystalline solid

(1.10 g, 78%). M. p. 119-120 ^{o}C. IR (neat): 3388, 2954, 2922, 1677, 1594, 1489, 1452, 1368, 1146, 1024 cm^{-1}. ^{1}H-NMR (500 MHz, CD_3OD): δ 2.00 (quint, *J* = 7.3 Hz, 2H, -CH_2*CH_2*CH_2-), 2.28 (t, *J* = 7.3 Hz, 2H, *CH_2*CO_2H), 2.86 (t, *J* = 7.3 Hz, 2H, Ar*CH_2*), 3.66 (t, *J* = 7.0 Hz, 2H, OCH_2), 4.08 (t, *J* = 6.7 Hz, 2H, OCH_2), 7.53 (dd, *J* = 4.8, 7.9 Hz, 1H, Ar-H), 7.68 (d, *J* = 8.5 Hz, 1H, Ar-H), 7.75 (dd, *J* = 2.4, 8.8 Hz, 1H, Ar-H), 7.97 (d, *J* = 2.4 Hz, 1H, Ar-H), 8.18 (m, 1H, Ar-H), 8.55 (dd, *J* = 1.5, 4.8 Hz, 1H, Ar-H), 8.89 (d, *J* = 1.4 Hz, 1H, Ar-H). ^{13}C-NMR (125.7 MHz, CD_3OD): δ 26.36 (Ar*CH_2*), 27.22 (CH_2*CH_2*CH_2), 31.22 (*CH_2*CO_2H), 62.19 (OCH_2), 75.86 (OCH_2), 105.20, 123.06, 125.26, 131.71, 131.91, 132.26, 134.01, 137.33, 139.17, 149.08, 149.55, 153.89 (all C_{arom}), 176.75 (C=O). Anal. Calcd for $C_{20}H_{19}Cl_2N_3O_4$ (435.08): C 55.06, H 4.39, N 9.63; Found: C 55.0, H 4.45, N 9.55.

4.2.17 Synthesis of (S)-N-(1-Amino-3-(4-fluorophenyl)-1-oxopropan-2-yl)-4-((1-(3,4-dichlorophenyl)-4-(2-hydroxyethyl)-3-(pyridin-3-yl)-1H-pyrazol-5-yl)oxy)butanamide (50)

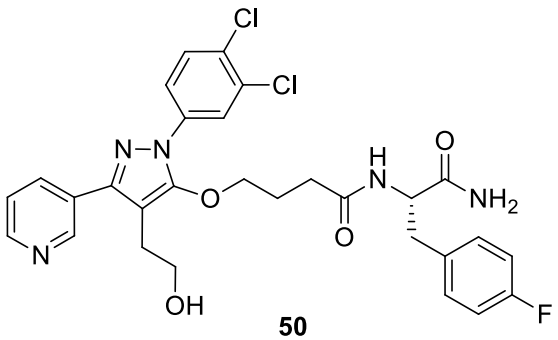

50

To a solution of mixture of compound **25** (0.089 g, 0.49 mmol) and **49** (0.32 g, 0.73 mmol) in anhydrous CH_2Cl_2 (15 mL) was sequentially added hydroxybenzotriazole (0.17 g, 1.1 mmol), N-(3-dimethylaminopropyl)-N′-ethylcarbodiimide hydrochloride (0.28 g, 1.46 mmol) and Et_3N (0.51 mL, 3.65 mmol) and the reaction was stirred overnight at room

temperature. The mixture was diluted with ethyl acetate (30 mL) and washed with H_2O (10 mL) and brine (10 mL). The organic layer was dried over Na_2SO_4 and evaporated under reduced pressure. Column chromatography of thick oily material, eluting with the EtOAc-hexane (8:2) gave the desired product **50** as a white solid (yield 68%). M. p. 182-183 ^oC. IR (neat): 3356, 3292, 3051, 2956, 1632, 1593, 1481, 1418, 1222, 1028 cm^{-1}. ^1H-NMR (500 MHz, CD_3OD): δ 1.92 (t, *J* = 6.7 Hz, 2H, $COCH_2$), 2.30 (pent, 2H, $CH_2CH_2CH_2$), 2.83 (m, 3H, $ArCH_2$, CH_2CH), 3.12 (dd, *J* = 4.9, 11.6 Hz, 1H, CH_2CH), 3.66 (t, *J* = 7.0 Hz, 2H, OCH_2), 3.96 (t, *J* = 6.7 Hz, 2H, OCH_2), 4.58 (m, 1H, CH_2CH), 6.93 (m, 2H, Ar-H), 7.21 (m, 2H, Ar-H), 7.53 (dd, *J* = 2.4, 8.1 Hz, 1H, Ar-H), 7.65-7.71 (m, 2H, Ar-H), 7.93 (d, *J* = 2.1 Hz, 1H, Ar-H), 8.17 (dd, *J* = 2.3, 8.1 Hz, 1H, Ar-H), 8.55 (d, *J* = 8.3 Hz, 1H, Ar-H), 8.88 (d, *J* = 2.3 Hz, 1H, Ar-H). ^{13}C-NMR (125.7 MHz, CD_3OD): δ 26.81 ($ArCH_2$), 27.21 ($CH_2CH_2CH_2$), 32.77 ($COCH_2$), 38.26 (CH_2CH), 55.52 (OCH_2), 62.21 (CH_2CH), 75.81 (OCH_2), 105.19, 115.98 (d, *J* = 21.8 Hz), 122.94, 125.13, 125.27, 131.70, 131.81, 131.95, 132.27, 133.97, 134.57, 137.32, 139.18, 149.05, 149.56, 153.81, 163.56 (d, *J* = 248.0 Hz) (all C_{arom}), 174.65 (C=O), 176.05 (C=O). Anal. Calcd for $C_{29}H_{28}Cl_2FN_5O_4$ (600.47): C 58.01, H 4.70, N 11.66; Found: C 57.94, H 4.76, N 11.60.

4.2.18 Synthesis of (S)-N-(1-amino-1-oxo-3-(pyridin-3-yl)propan-2-yl)-4-((1-(3,4-dichlorophenyl)-4-(2-hydroxyethyl)-3-(pyridin-3-yl)-1H-pyrazol-5-yl)oxy)butanamide (51)

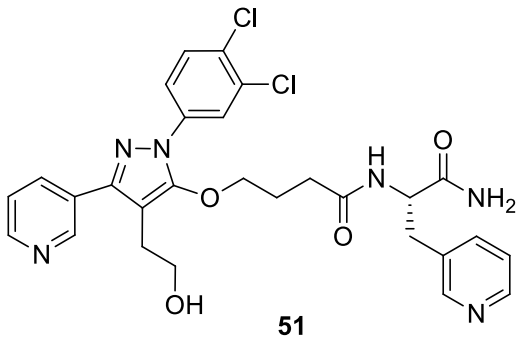

51

Following the procedure adopted for the synthesis of **50**, the reaction of **49** with **26** gave compound **51** as a yellowish gum (yield 62%). IR (neat): 3417, 2925, 1668, 1593, 1482, 1368, 1024 cm^{-1}. ^{1}H-NMR (500 MHz, CD_3OD): δ 1.90 (t, *J* = 6.7 Hz, 2H, $COCH_2$), 2.31 (pent, 2H, $CH_2CH_2CH_2$), 2.83 (t, *J* = 6.7 Hz, 2H, $ArCH_2$), 2.89 (dd, *J* = 9.1, 13.7 Hz, 1H, CH_2CH), 3.19 (dd, *J* = 5.5, 13.7 Hz, 1H, CH_2CH), 3.65 (t, *J* = 7 Hz, 2H, OCH_2), 3.95 (t, *J* = 6.7 Hz, 2H, OCH_2), 4.60 (m, 1H, CH_2CH), 7.31 (dd, *J* = 4.8, 8.5 Hz, 1H, Ar-H), 7.53 (dd, *J* = 4.9, 8.2 Hz, 1H, Ar-H), 7.67 (d, *J* = 8.7 Hz, 1H, Ar-H), 7.70 (dd, *J* = 2.45 Hz, 1H, Ar-H), 7.73 (m, 1H, Ar-H), 7.94 (d, *J* = 2.4 Hz, 1H, Ar-H), 8.20 (dd, *J* = 2.15, 8.0 Hz, 1H, Ar-H), 8.33 (dd, *J* = 1.5, 4.9 Hz, 1H, Ar-H), 8.41 (d, *J* = 1.5 Hz, 1H, Ar-H), 8.56 (dd, *J* = 1.5, 4.9 Hz, 1H, Ar-H), 8.89 (d, *J* = 1.5 Hz, 1H, Ar-H). ^{13}C-NMR (125.7 MHz, CD_3OD): δ 26.79 ($ArCH_2$), 27.23 ($CH_2CH_2CH_2$), 32.73 ($COCH_2$), 36.23 (CH_2CH), 54.89 (OCH_2), 62.19 (CH_2CH), 75.84 (OCH_2), 105.25, 122.92, 125.08, 125.11, 125.29, 131.68, 131.80, 132.28, 133.97, 135.29, 137.32, 139.06, 139.17, 148.34, 149.03, 149.47, 149.57, 150.79, 153.82 (all C_{arom}), 174.67 (C=O), 175.51 (C=O). Anal. Calcd for $C_{28}H_{28}Cl_2N_6O_4$ (543.47): C 57.64, H 4.84, N 14.40; Found: C 57.57, H 4.89, N 14.33.

4.2.19 Synthesis of (S)-N-(1-amino-1-oxo-3-(pyridin-4-yl)propan-2-yl)-4-((1-(3,4-dichlorophenyl)-4-(2-hydroxy-ethyl)-3-(pyridin-3-yl)-1H-pyrazol-5-yl)oxy)butanamide (52)

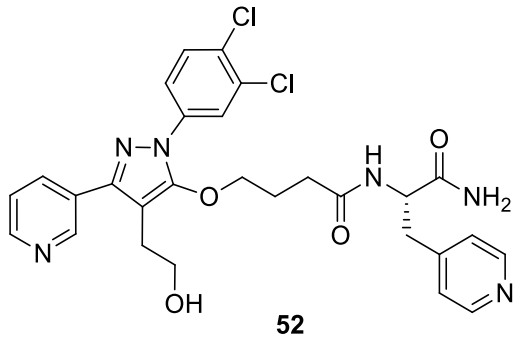

52

Following the procedure adopted for the synthesis of **50**, the reaction of **49** with **27** gave compound **52** as a white solid (yield 60%). M. p. 159-160 ^{o}C. IR (neat): 3402, 2924, 1689, 1592, 1482, 1367, 1134, 1029 cm^{-1}. ^{1}H-NMR (500 MHz, CD_3OD): δ 1.91 (t, *J* = 6.7 Hz, 2H, $COCH_2$), 2.32 (pent, 2H, $CH_2CH_2CH_2$), 2.83 (t, *J* = 6.7 Hz, 2H, $ArCH_2$), 2.91 (dd, *J* = 9.7, 13.7 Hz, 1H, CH_2CH), 3.20 (dd, *J* = 5.5, 13.7 Hz, 1H, CH_2CH), 3.64 (t, *J* = 7 Hz, 2H, OCH_2), 3.97 (t, *J* = 6.4 Hz, 2H, OCH_2), 4.71 (m, 1H, CH_2CH), 7.32 (d, *J* = 6.1 Hz, 2H, Ar-H), 7.54 (m, 1H, Ar-H), 7.67 (d, *J* = 8.8 Hz, 1H, Ar-H), 7.71 (d, *J* = 8.8 Hz, 1H, Ar-H), 7.94 (d, *J* = 2.4 Hz, 1H, Ar-H), 8.19 (d, *J* = 8.5 Hz, 1H, Ar-H), 8.40 (dd, *J* = 1.5, 4.9 Hz, 1H, Ar-H), 8.56 (dd, *J* = 1.7, 4.9 Hz, 1H, Ar-H), 8.89 (d, *J* =1.5 Hz, 1H, Ar-H). ^{13}C-NMR (125.7 MHz, CD_3OD): δ 26.81 ($ArCH_2$), 27.23 ($CH_2CH_2CH_2$), 32.74 ($COCH_2$), 38.34 (CH_2CH), 54.37 (OCH_2), 62.21 (CH_2CH), 75.86 (OCH_2), 105.22, 125.96, 125.14, 125.29, 126.34, 131.70, 131.81, 132.27, 133.97, 137.32, 139.18, 149.04, 149.49, 149.57, 149.92, 153.82 (all C_{arom}), 174.74 (C=O), 175.43 (C=O). Anal. Calcd for $C_{28}H_{28}Cl_2N_6O_4$ (583.47): C 57.64, H 4.84, N 14.40; Found: C 57.56, H 4.88, N 14.33.

4.2.20 Synthesis of (S)-N-(1-amino-3-(4-methoxyphenyl)-1-oxopropan-2-yl)-4-((1-(3,4-dichlorophenyl)-4-(2-hydroxyethyl)-3-(pyridin-3-yl)-1H-pyrazol-5-yl)oxy)butanamide (53)

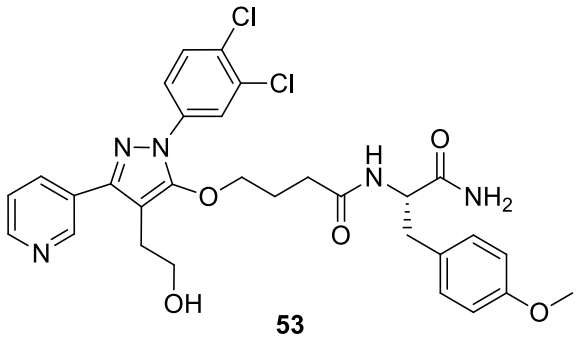

53

Following the procedure adopted for the synthesis of **50**, the reaction of **49** with **28** gave compound **53** as a white solid (yield 66%). M. p. 175-176 ^{o}C. IR (neat): 3350, 3274, 3189, 2925, 1676, 1641, 1593, 1482, 1248, 1049 cm^{-1}. ^{1}H NMR (500 MHz, CD_3OD): δ 1.91 (t, *J* = 6.7 Hz, 2H, $COCH_2$), 2.30 (pent, 2H, $CH_2CH_2CH_2$), 2.75 (dd, *J* = 9.1, 13.7 Hz, 1H, CH_2CH), 2.82 (t, *J* = 6.7 Hz, 2H, $ArCH_2$), 3.06 (dd, *J* = 5.5, 13.7 Hz, 1H, CH_2CH), 3.64 (t, *J* = 7.3 Hz, 2H, OCH_2), 3.97 (t, *J* = 7.0 Hz, 2H, OCH_2), 4.58 (m, 1H, CH_2CH), 6.76 (d, *J* = 8.5 Hz, 2H, Ar-H), 7.14 (d, *J* = 8.5 Hz, 2H, Ar-H), 7.53 (m, 1H, Ar-H), 7.65 (d, *J* = 8.8 Hz, 1H, Ar-H), 7.69 (dd, *J* = 2.1, 8.5 Hz, 1H, Ar-H), 7.94 (d, *J* = 2.1 Hz, 1H, Ar-H), 8.56 (dd, *J* = 1.7, 4.9 Hz, 1H, Ar-H), 8.89 (d, *J* =1.5 Hz, 1H, Ar-H). ^{13}C-NMR (125.7 MHz, $CDCl_3$): δ 26.83 ($ArCH_2$), 27.25 ($CH_2CH_2CH_2$), 32.70 ($COCH_2$), 38.30 (CH_2CH), 54.39 (OCH_2), 62.20 (CH_2CH), 75.82 (OCH_2), 107.12, 115.22, 115.75, 122.39, 124.92, 125.07, 129.47, 131.24, 131.26, 131.65, 132.27, 134.58, 136.36, 139.09, 149.31, 149.85, 150.70, 153.44, 159.10 (all C_{arom}), 172.80 (C=O), 174.30 (C=O). Anal. Calcd for $C_{30}H_{31}Cl_2N_5O_5$ (612.50): C 58.83, H 5.10, N 11.43; Found: C 58.77, H 5.16, N 11.35.

4.2.21 Synthesis of (S)-N-(1-amino-3-(4-fluorophenyl)-1-oxopropan-2-yl)-4-((1-(3,4-dichlorophenyl)-4-(2-(methylthio)ethyl)-3-(pyridin-3-yl)-1H-pyrazol-5-yl)oxy)butanamide (2)

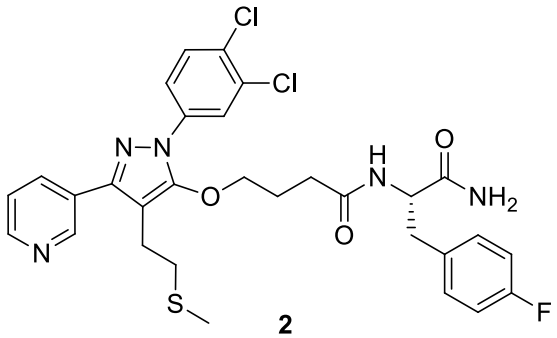

2

To a solution of compound **50** (0.15 g, 0.25 mmol) in THF (5 mL) at 0 ^{o}C was added Et_3N (0.1 mL, 0.75 mmol) and after being stirred for 10 minutes, a solution of MsCl (0.03 mL, 0.37 mmol) in THF (1 mL) was added dropwise. The reaction mixture was stirred for 2 hours and then diluted with ethyl acetate (15 mL) and successively washed with H_2O (5 mL) and brine (2 x 5 mL). The organic layer was dried over Na_2SO_4 and evaporated under reduced pressure to get the mesylated product as light yellow thick oil, which was dissolved in DMF (7 mL) followed by the addition of sodium methane thiolate (0.04 g, 0.5 mmol) at 0 ^{o}C. The stirring was continued for 2 hours until the completion of reaction (TLC analysis) and the mixture was then diluted with ethyl acetate (15 mL) and successively washed with H_2O (5 mL) and brine (2 x 5 mL). The organic layer was dried over Na_2SO_4 and evaporated under reduced pressure. Column chromatography of the light yellow oily material, eluting with EtOAc-hexane (8:2) gave the title compound **2** as a colorless solid (yield 85%). M. p. 140-141 ^{o}C. $-[\alpha]_D^{20}$ = –29.15 (c = 0.0029, EtOH). IR (neat): 3398, 3309, 3205, 3072, 2919, 1661, 1592, 1482, 1366, 1221, 1025 cm^{-1}. ^{1}H-NMR (500 MHz, $CDCl_3$): δ 2.03-2.08 (m, 5H, SCH_3, $COCH_2$), 2.36 (pent, 2H, $CH_2CH_2CH_2$), 2.63 (t, *J* = 7.6 Hz, 2H, SCH_2), 2.87 (t, *J* = 7.5 Hz, 2H, ArCH_2), 3.03 (m, 2H, CH_2CH), 3.99 (t, *J* = 7.1 Hz, 2H, OCH_2), 4.62 (m,

1H, CH_2CH), 6.25 (d, *J* = 7.3 Hz, 1H, NH), 6.97 (m, 2H, Ar-H), 7.21 (m, 2H, Ar-H), 7.39 (m, 1H, Ar-H), 7.54 (d, *J* = 8.8 Hz, 1H, Ar-H), 7.65 (dd, *J* = 2.4, 8.8 Hz, 1H, Ar-H), 7.93 (d, *J* = 2.4 Hz, 1H, Ar-H), 8.00 (dd, *J* = 2.3, 8.5 Hz, 1H, Ar-H), 8.63 (d, *J* = 2.4 Hz, 1H, Ar-H), 8.89 (s, 1H, Ar-H). ^{13}C-NMR (125.7 MHz, $CDCl_3$): δ 15.62 (SCH_3), 23.12 (Ar-CH_2), 25.37 ($CH_2CH_2CH_2$), 32.11 ($COCH_2$), 34.04 (SCH_2), 37.58 (CH_2CH), 54.12 (CH_2CH), 74.57 (OCH_2), 105.74, 115.65 (d, *J* = 21.8 Hz), 115.73, 121.01, 123.63, 130.72, 130.73, 130.76, 130.79, 130.86, 131.98, 132.0 (*d*, *J* = 3.1 Hz), 133.09, 134.95, 137.65, 148.54, 149.35, 163.59 (d, *J* = 247 Hz) (all C_{arom}), 171.42 (C=O), 172.36 (C=O). Anal. Calcd for $C_{30}H_{30}Cl_2FN_5O_3S$ (630.56): C 57.14, H 4.80, N 11.11; Found C 57.08, H 4.87, N 11.04.

4.2.22 Synthesis of (S)-N-(1-amino-1-oxo-3-(pyridin-3-yl)propan-2-yl)-4-((1-(3,4-dichlorophenyl)-4-(2-(methyl-thio)ethyl)-3-(pyridin-3-yl)-1H-pyrazol-5-yl)oxy)butanamide (3)

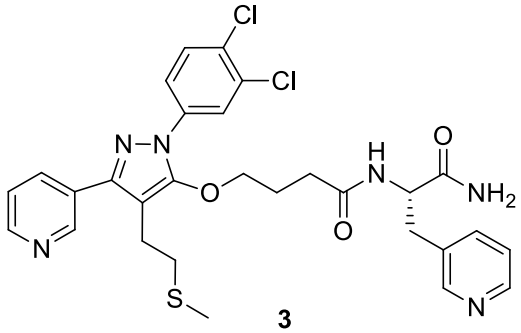

3

Following the procedure adopted for the synthesis of **2**, acylation of **51** with MsCl followed by condensing the resultant mesylate with sodium methane thiolate yielded compound **3** as an off white gum (yield 75%). $-[\alpha]_D^{20}$ = –44.1 (c = 0.0015, EtOH). IR (neat): 3393, 3186, 3047, 2958, 2857, 1738, 1673, 1592, 1481, 1366, 1026 cm^{-1}. ^{1}H-NMR (500 MHz, $CDCl_3$): δ 1.92 (t, *J* = 6.7 Hz, 2H, $COCH_2$), 1.99 (s, 3H, SCH_3), 2.32 (pent, 2H, $CH_2CH_2CH_2$), 2.55

(t, *J* = 7.6 Hz, 2H, SCH_2), 2.81 (t, *J* = 6.7 Hz, 2H, Ar*CH_2*), 3.12 (dd, *J* = 7.6, 14.3 Hz, 1H, *CH_2*CH), 3.24 (dd, *J* = 5.8, 14.3 Hz, 1H, *CH_2*CH), 3.91 (t, *J* = 6.1 Hz, 2H, OCH_2), 4.82 (m, 1H, CH_2*CH*), 7.12 (d, *J* = 8.1 Hz, 1H, NH), 7.36 (m, 1H, Ar-H), 7.44-7.49 (m, 2H, Ar-H), 7.58 (dd, *J* = 2.4, 8.8 Hz, 1H, Ar-H), 7.85 (d, *J* = 2.4 Hz, 1H, Ar-H), 7.88 (m, 1H, Ar-H), 7.99 (m, 1H, Ar-H), 8.45 (d, *J* = 5.2 Hz, 1H, Ar-H), 8.56 (d, *J* = 5.2 Hz, 1H, Ar-H), 8.76 (d, *J* = 1.7 Hz, 1H, Ar-H), 8.87 (d, *J* = 1.7 Hz, 1H, Ar-H). ^{13}C-NMR (125.7 MHz, $CDCl_3$): δ 15.64 (SCH_3), 23.15 (Ar-*CH_2*), 25.38 (CH_2*CH_2*CH_2), 32.10 (CO*CH_2*), 34.03 (SCH_2), 35.43 (*CH_2*CH), 53.68 (CH_2*CH*), 74.57 (OCH_2), 105.77, 121.10, 123.64, 123.60, 129.60, 130.72, 130.88, 132.04, 133.10, 134.96, 136.92, 137.66, 147.92, 148.51, 149.34, 150.40, 151.79 (all C_{arom}), 171.60 (C=O), 172.07 (C=O). Anal. Calcd for $C_{29}H_{30}Cl_2N_6O_3S$ (613.56): C 56.77, H 4.93, N 13.70; Found: C 56.72, H 4.98, N 13.63.

4.2.23 Synthesis of (S)-N-(1-amino-1-oxo-3-(pyridin-4-yl)propan-2-yl)-4-((1-(3,4-dichlorophenyl)-4-(2-(methyl-thio)ethyl)-3-(pyridin-3-yl)-1H-pyrazol-5-yl)oxy)butanamide (4)

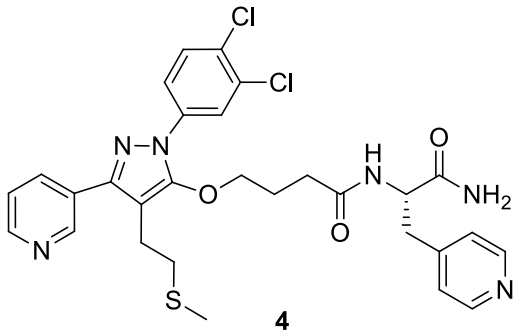

4

Following the procedure adopted for the synthesis of **2**, acylation of **52** with MsCl followed by condensing the resultant mesylate with sodium methane thiolate yielded compound **4** as a white solid (yield 67%). M. p. 183-184 °C. $-[\alpha]_D^{20}$ = –96.60 (c = 0.0012, EtOH). IR (neat): 3342, 3279, 3050, 2935, 1681, 1645, 1480, 1420, 1131, 1024 cm^{-1}. ^{1}H-NMR (500 MHz,

CD_3OD): δ 2.0 (t, *J* = 6.7 Hz, 2H, $COCH_2$), 2.07 (s, 3H, SCH_3), 2.38 (pent, 2H, $CH_2CH_2CH_2$), 2.63 (t, *J* = 7.3 Hz, 2H, SCH_2), 2.87 (t, *J* = 6.7 Hz, 2H, $ArCH_2$), 3.10 (dd, *J* = 9.3, 13.9 Hz, 1H, CH_2CH), 3.18 (dd, *J* = 5.6, 13.9 Hz, 1H, CH_2CH), 3.99 (t, *J* = 6.7 Hz, 2H, OCH_2), 4.78 (m, 1H, CH_2CH), 7.30 (d, *J* = 6.8 Hz, 2H, Ar-H), 7.41 (m, 1H, Ar-H), 7.55 (d, *J* = 8.5 Hz, 1H, Ar-H), 7.65 (dd, *J* = 2.7, 8.5 Hz, 1H, Ar-H), 7.93 (d, *J* = 2.7 Hz, 1H, Ar-H), 8.03 (m, 1H, Ar-H), 8.53 (d, *J* = 6.9 Hz, 2H, Ar-H), 8.62 (m, 1H, Ar-H), 8.91 (d, *J* =1.7 Hz, 1H, Ar-H). ^{13}C-NMR (125.7 MHz, $CDCl_3$): δ 15.67 (SCH_3), 23.17 (Ar-CH_2), 25.39 ($CH_2CH_2CH_2$), 32.08 ($COCH_2$), 34.05 (SCH_2), 37.67 (CH_2CH), 53.12 (CH_2CH), 74.61 (OCH_2), 105.80, 121.07, 123.66, 123.72, 125.21, 130.92, 135.29, 148.19, 148.29, 148.97, 153.80 (all C_{arom}), 171.78 (C=O), 172.07 (C=O). Anal. Calcd for $C_{29}H_{30}Cl_2N_6O_3S$ (613.56): C 56.77, H 4.93, N 13.70; Found: C 56.73, H 4.98, N 13.64.

4.2.24 Synthesis of (S)-N-(1-amino-3-(4-methoxyphenyl)-1-oxopropan-2-yl)-4-((1-(3,4-dichlorophenyl)-4-(2-(methylthio)ethyl)-3-(pyridin-3-yl)-1H-pyrazol-5-yl)oxy)butanamide (5)

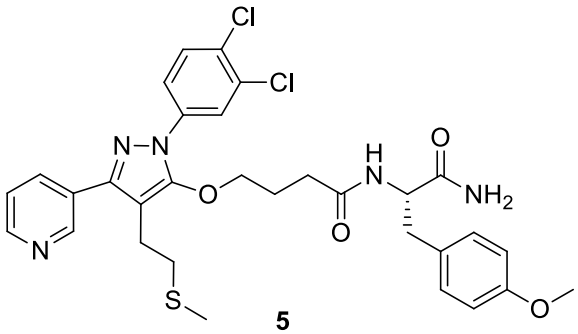

5

Following the procedure adopted for the synthesis of **2**, acylation of **53** with MsCl followed by condensing the resultant mesylate with sodium methane thiolate yielded compound **5** as a colorless solid (yield 70%). M. p. 154-155 ºC. $-[\alpha]_D^{20}$= –79.13 (c = 0.0007, EtOH). IR (neat): 3341, 3300, 3040, 2922, 1677, 1592, 1512, 1481, 1245, 1028 cm^{-1}. ^{1}H-NMR (500

MHz, CD_3OD): δ 2.05 (t, *J* = 7.6 Hz, 2H, $COCH_2$), 2.07 (s, 3H, SCH_3), 2.36 (pent, 2H, $CH_2CH_2CH_2$), 2.63 (t, *J* = 7.3 Hz, 2H, SCH_2), 2.87 (t, *J* = 7.6 Hz, 2H, $ArCH_2$), 2.99 (dd, *J* = 6.1, 13.7 Hz, 1H, CH_2CH), 3.03 (dd, *J* = 4.9, 13.7 Hz, 1H, CH_2CH), 3.77 (s, 3H, OCH_3), 3.99 (t, *J* = 6.7 Hz, 2H, OCH_2), 4.61 (m, 1H, CH_2CH), 6.82 (d, *J* = 8.2 Hz, 2H, Ar-H), 7.14 (d, *J* = 8.2 Hz, 2H, Ar-H), 7.38 (m, 1H, Ar-H), 7.52 (d, *J* = 8.5 Hz, 1H, Ar-H), 7.64 (dd, *J* = 2.1, 8.5 Hz, 1H, Ar-H), 7.92 (d, *J* = 2.1 Hz, 1H, Ar-H), 8.00 (m, 1H, Ar-H), 8.62 (dd, *J* = 1.6, 6.1 Hz, 1H, Ar-H), 8.90 (d, *J* = 1.5 Hz, 1H, Ar-H). ^{13}C-NMR (125.7 MHz, $CDCl_3$): δ 17.04 (SCH_3), 24.54 (Ar-CH_2), 26.84 ($CH_2CH_2CH_2$), 32.47 ($COCH_2$), 34.06 (SCH_2), 35.43 (CH_2CH), 56.64 (OCH_3), 57.82 (CH_2CH), 76.06 (OCH_2), 107.17, 115.42, 115.55, 122.39, 124.99, 125.04, 129.67, 131.04, 131.21, 131.69, 132.27, 134.52, 136.37, 139.06, 149.33, 149.95, 150.75, 153.24, 160.12 (all C_{arom}), 172.86 (C=O), 174.33 (C=O). Anal. Calcd for $C_{31}H_{33}Cl_2N_5O_4S$ (642.60): C 57.94, H 5.18, N 10.90; Found: C 57.90, H 5.24, N 10.83.

4.3 Synthesis of target compounds 6-16

Similarly the synthesis of **6-16** target compounds need the amino acid derivatives **33-40**, **42-44** and main intermediate **58** for amidation reaction. The detailed description comprising of procedures, ^{1}H-NMR, ^{13}C-NMR, FTIR, elemental analysis, melting points and specific rotation (if necessary) for all the step wise synthesis of intermediates and final target compounds is given below;

4.3.1 Synthesis of (S)-2-acetamido-3-phenylpropanoic acid (33)

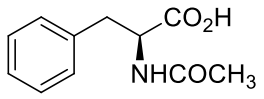

33

To a 1.2 M solution phenylalanine in methanol was added acetic anhydride and the mixture was reflux for 6 hours. After cooling to room temperature, all the volatiles were removed at reduced pressure and the resultant colorless oil was kept overnight at -18 ^{o}C and resultant solid was filtered to obtained **33** as a colorless crystalline solid (Yield: 95 %) [126]. IR (neat): 3329.9, 3088.1, 3034.3, 2936.1, 2913.1, 1701.3, 1554.6, 1437.0, 1277.3, 1246.6, 1115.7, 976.8, 706.1 cm^{-1}. ^{1}H-NMR (500 MHz, DMSO): δ 1.76 (s; 3H; *CH$_3$*), 2.83-2.79 (dd; J= 9.45 Hz, 1H, *CH$_2$*-CH), 3.05-3.01 (dd, J=4.8 Hz, 1H, CH-*CH$_2$*), 4.50 (m, 1H, *CH*-CH$_2$), 7.19-7.10 (m, 5H, Ar-H). ^{13}C-NMR (500 MHz, DMSO): δ 22.34 (*CH$_2$*-CH), 36.82 (COCH$_3$), 53.59 (*CH*-CH$_2$), 126.36 (C$_{arom}$), 128.15 (C$_{arom}$), 129.05 (C$_{arom}$), 137.80 (C$_{arom}$), 169.19 (CONH), 173.21 (COOH). Anal. Calcd for $C_{11}H_{13}NO_3$ (207.09): C 63.76, H 6.32, N 6.76; Found: C 62.96, H 5.02, N 7.56.

4.3.2 Synthesis of (S)-2-(methylsulfonamido)-3-phenylpropanoic acid (34)

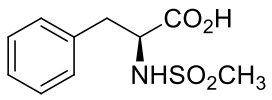

34

To a solution of L-phenylalanine (2.0 g, 12.12 mmol) in 1N NaOH (15 mL) at 0 ^{o}C was added CH_2Cl_2 (5 mL) followed by the addition of methane sulphonyl chloride (1.130 mL) dropwise and mixture was stirred for 3 hours at 0 ^{o}C. The reaction was acidified to pH-3 with 1N HCl and then extracted with EtOAc (30 mL). The organic layer was separated and dried over Na_2SO_4 and evaporated under vacuum to obtain the title compound **34** as a white solid (Yield: 70%) **[**127**]**. IR (neat): 3256.9, 3028.0, 2931.5, 1748.6, 1720.3, 1311.7, 1028.7, 765.9 cm^{-1}. ^{1}H-NMR (500 MHz, $CDCl_3$): δ 2.61 (s, 3H, CH_3), 3.02-2.97 (dd, J= 8.25 Hz, 1H, *CH_2*-CH), 3.25-3.3.21(dd, J=4.85 Hz, 1H, CH-*CH_2*), 4.41 (m, 1H, *CH*-CH_2), 5.08 (d, J=9.15 Hz, 1H, *NH*), 7.34-7.22 (m, 5H, Ar-H). ^{13}C-NMR (500 MHz, $CDCl_3$): δ 38.99 (CH-*CH_2*), 41.31 (*CH*-CH_2), 57.03 (CH_3), 127.56 (C_{arom}), 128.84 (C_{arom}), 129.56 (C_{arom}), 135.38 (C_{arom}), 175.26 (COOH). Anal. Calcd for $C_{10}H_{13}NO_4S$ (243.06): C 49.37, H 5.39, N 5.76; Found: C 48.37, H 5.30, N 6.82.

4.3.3 Synthesis of (S)-2-Acetamido-3-(4-fluorophenyl)propanoic acid (35)

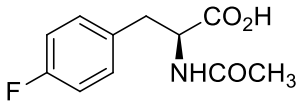

35

To a solution of compound **30** (1 g, 5.46 mmol) in MeOH (7 mL) was added acetic anhydride (1.40 mL, 14.75 mmol) and the mixture was refluxed for 6 hours. The reaction was cooled to room temperature and all the volatiles were removed at reduced pressure. The residue was kept overnight in a refrigerator and then warmed up to the room

temperature to allow the recrystallization of the title compound as a colorless crystalline solid (yield 86%). M. p. 139-140 ^{o}C. IR (neat): 3367, 3025, 2953, 1720, 1625, 1581, 1451, 1360, 1028 cm^{-1}. ^{1}H NMR (500 MHz, $CDCl_3$): δ 1.89 (s, 3 H, $COCH_3$), 2.92 (dd, J = 9.1, 14.0 Hz, 1 H, CH_2CH), 3.16 (dd, J = 5.5, 14.1 Hz, 1 H, CH_2CH), 4.61 (m, 1 H, CH_2CH), 6.98 (t, J = 8.5 Hz, 2 H, 3'-H, 5'-H), 7.22 (m, 2 H, 2'-H, 6'-H), 8.09 (d, J = 6.2 Hz, 1 H, NH). ^{13}C NMR (125.7 MHz, $CDCl_3$): δ 22.27 ($COCH_3$), 37.63 (CH_2CH), 55.10 (CH_2CH), 115.99 (C-3', C-5'), 131.95 (C-2', C-6'), 134.45 (C-1'), 162.60 (C-4'), 173.10 (C=O), 174.54 (C=O). Anal. Calcd. $C_{11}H_{12}FNO_3$: (225.22): C 58.66, H 5.37, N 6.22; Found C 58.61, H 5.41, N 6.14.

4.3.4 Synthesis of (S)-3-(4-Fluorophenyl)-2-(methylsulfonamido)propanoic acid (36)

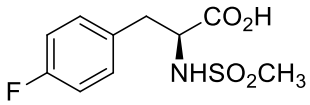

36

To a cold solution of compound **30** (0.5 g, 2.73 mmol) in 1M NaOH (10 mL) at 0 ^{o}C was added CH_2Cl_2 (2 mL) followed by the dropwise addition of methane sulphonyl chloride (0.25 mL, 3.28 mmol). The reaction mixture was stirred for 3 hours at 0 ^{o}C, transferred into a separatory funnel, and washed with diethyl ether (10 mL). The aqueous layer was acidified to pH 3 with 1N HCl and extracted with EtOAc (10 mL x 2). The organic layer was dried over Na_2SO_4 and evaporated to get compound **36** as a colourless gummy solid (yield 80%). IR (neat): 3538, 3034, 2930, 1733, 1605, 1512, 1412, 1225 cm^{-1}. ^{1}H NMR (500 MHz, CD_3OD): δ 2.70 (s, 3 H, SO_2CH_3), 2.91 (dd, J = 8.5, 13.7 Hz, 1 H, CH_2CH), 3.13 (dd, J = 5.2, 13.7 Hz, 1 H, CH_2CH), 4.20 (m, 1 H, CH_2CH), 7.01 (m, 2 H, 3'-H, 5'-H),

7.28 (m, 2 H, 2'-H, 6'-H). ^{13}C NMR (125.7 MHz, CD_3OD): δ = 39.11 (SO_2CH_3), 41.28 (*CH_2*CH), 58.90 (CH_2*CH*), 116.03 (C-3', C-5'), 132.40 (C-2', C-6'), 134.27 (C-1'), 162.60 (C-4'), 174.59 (C=O). Anal. Calcd. $C_{10}H_{12}FNO_4S$ (261.27): C 45.97, H 4.63, N 5.36; Found C 45.92, H 4.67, N 5.30.

4.3.5 Synthesis of (S)-2-Acetamido-3-(pyridin-3-yl)propanoic acid (37)

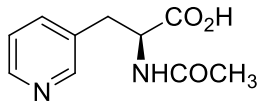

37

Following the same procedure adopted for the synthesis of **35**, acetylation of compound **31** gave compound **37** as a colourless sticky solid (yield 73%). IR (neat): 3428, 3050, 2946, 1732, 1668, 1606, 1512, 1370, 1226, 1060 cm^{-1}. ^{1}H NMR (500 MHz, $CDCl_3$): δ 1.82 (s, 3 H, $COCH_3$), 2.90 (dd, *J* = 8.5, 14.0 Hz, 1 H, *CH_2*CH), 3.17 (dd, *J* = 5.2, 14.0 Hz, 1 H, *CH_2*CH), 4.54 (m, 1 H, CH_2*CH*), 7.29 (m, 1 H, 5'-H), 7.67 (m, 1 H, 6'-H), 8.30 (m, 1 H, 4'-H), 8.41 (d, *J* = 1.1 Hz, 1 H, 2'-H). ^{13}C NMR (125.7 MHz, $CDCl_3$): δ 22.39 (CO*CH_3*), 35.91 (*CH_2*CH), 55.34 (CH_2*CH*), 125.10 (C-5'), 135.67 (C-6'), 139.26 (C-1'), 148.12 (C-4'), 150.68 (C-2'), 172.92 (C=O). Anal. Calcd. $C_{10}H_{12}N_2O_3$ (208.21): C 57.68, H 5.81, N 13.45; Found C 57.62, H 5.86, N 13.38.

4.3.6 Synthesis of (S)-2-(Methylsulfonamido)-3-(pyridin-3-yl)propanoic acid (38)

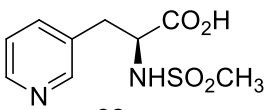

38

Following the same procedure adopted for the synthesis of **35**, acylation of **31** produced compound **38** as a light yellow gum (yield 82%). IR (neat): 3475, 3427, 3062, 2955, 1750,

1582, 1435, 1322, 1150 cm^{-1}. ^{1}H NMR (500 MHz, $CDCl_3$): δ 2.69 (s, 3 H, SO_2CH_3), 2.85 (dd, J = 7.3, 13.7 Hz, 1 H, CH_2CH), 3.05 (dd, J = 5.2, 13.7 Hz, 1 H, CH_2CH), 3.46 (m, 1 H, CH_2CH), 7.34 (m, 1 H, 5'-H), 7.76 (m, 1 H, 6'-H), 8.36 (m, 1 H, 4'-H), 8.43 (d, J = 1.3 Hz, 1 H, 2'-H). ^{13}C NMR (125.7 MHz, $CDCl_3$): δ 39.42 (SO_2CH_3), 39.75 (CH_2CH), 58.71 (CH_2CH), 125.04 (C-5'), 136.77 (C-6'), 139.26 (C-1'), 147.86 (C-4'), 150.89 (C-2'), 181.15 (C=O). Anal. Calcd. $C_9H_{12}N_2O_4S$ (244.27): C 44.25, H 4.95, N 11.47; Found C 44.20, H 4.99, N 11.40.

4.3.7 Synthesis of (S)-2-Acetamido-3-(pyridin-4-yl)propanoic acid (39)

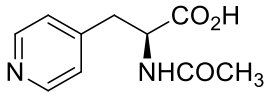

39

Following the same procedure adopted for the synthesis of **35**, acetylation of **32** gave compound **39** as a brown gum (yield 75%). IR (neat): 3441, 3054, 2926, 1738, 1664, 1609, 1508, 1378, 1223, 1066 cm^{-1}. ^{1}H NMR (500 MHz, CD_3OD): δ 1.85 (s, 3 H, $COCH_3$), 3.01 (dd, J = 8.8, 13.7 Hz, 1 H, CH_2CH), 3.26 (dd, J = 5.5, 13.7 Hz, 1 H, CH_2CH), 4.72 (m, 1 H, CH_2CH), 7.35 (d, J = 6.1 Hz, 2 H, 2'-H, 6'-H), 8.44 (d, J = 6.1 Hz, 2 H, 3'-H, 5'-H). ^{13}C NMR (125.7 MHz, CD_3OD): δ 22.29 ($COCH_3$), 37.92 (CH_2CH), 54.21 (CH_2CH), 126.50 (C-2', C-6'), 149.38 (C-1'), 150.29 (C-3', C-5'), 173.11 (C=O), 175.27 (C=O). Anal. Calcd. $C_{10}H_{12}N_2O_3$ (208.21): C 57.68, H 5.81, N 13.45; Found C 57.63, H 5.86, N 13.39.

4.3.8 Synthesis of (S)-2-(Methylsulfonamido)-3-(pyridin-4-yl)propanoic acid (40)

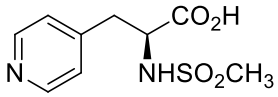

40

Following the same procedure adopted for the synthesis of **35**, acylation of **32** rendered compound **40** as a light yellow gum (yield, 85%). IR (neat): 3500, 3073, 2923, 1702, 1607, 1393, 1297, 1153 cm^{-1}. ^{1}H NMR (500 MHz, CD_3OD): δ 2.85 (s, 3 H, SO_2CH_3), 2.98 (dd, J = 8.2, 13.7 Hz, 1 H, CH_2CH), 3.15 (dd, J = 5.2, 13.7 Hz, 1 H, CH_2CH), 4.02 (m, 1 H, CH_2CH), 7.36 (d, J = 6.8 Hz, 2 H, 2'-H, 6'-H), 8.43 (d, J = 6.8 Hz, 2 H, 3'-H, 5'-H). ^{13}C NMR (125.7 MHz, CD_3OD): δ 37.35 (CH_2CH), 40.29 (SO_2CH_3), 60.32 (CH_2CH), 126.96 (C-2', C-6'), 149.47 (C-1'), 150.49 (C-3', C-5'), 176.85 (C=O). Anal. Calcd. $C_9H_{12}N_2O_4S$ (244.27): C 44.25, H 4.95, N 11.47; Found C 44.19, H 5.00, N 11.41.

4.3.9 (S)-2-acetamido-3-(4-methoxyphenyl)propanoic acid (42)

The synthesis of (S)-2-acetamido-3-(4-methoxyphenyl)propanoic acid (**42**) started from the L-tyrosine and converted into a methyl ester of L-tyrosine hydrochloride. Further, this ester was modified into an N-acetylated product **42a** and then to O-alkylated **42b** followed by hydrolysis to accomplish the final intermediate **42**.

4.3.10 Synthesis of (S)-methyl 2-acetamido-3-(4-hydroxyphenyl)propanoate (42a)

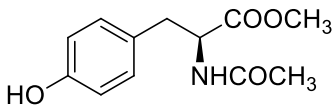

42a

To a solution of pyridine (10 mL) and acetic anhydride (11 mL, 120 mmol) at 0 ^{o}C was added L-tyrosine-methyl ester HCl (5.0 g, 23 mmol) portion wise. The reaction was then allowed to run overnight at room temperature. The reaction was quenched by adding ice-water (100 mL) and then extracted CH_2Cl_2 (15 mL x 4) and the organic layer was sequentially washed with sat. $NaHCO_3$ (20 mL), 0.1 M HCl (20 mL) and H_2O (20 mL). The organic layer was dried over $MgSO_4$ and evaporated under vacuum to get the title compound **42a** as white solid (yield, 87%) [133, 134]. IR (neat): 3551.3, 3363.6, 3157.5, 3015.3, 2958.3, 1730.9, 1663.9, 1548.8, 1443.8, 1378.3, 1048.1, 833.1 cm^{-1}. ^{1}H NMR (500 MHz, $CDCl_3$): δ 1.97 (s, 3H, *CH*$_3$), 3.01-2.97 (dd, J=5.5Hz, J= 7.6 Hz, CH-*CH*$_2$), 3.08-3.04 (dd, J=5.8 Hz, J= 7.6Hz, CH-*CH*$_2$), 4.84 (m, 1H, *CH*-CH_2), 6.73 (d, J=8.5 Hz, Ar-H), 6.93 (d, J=8.5 Hz, Ar-H). ^{13}C-NMR (500 MHz, $CDCl_3$): δ 22.90 (CH-*CH*$_2$), 37.0 ($COCH_3$), 52.14 (OCH_3), 53.19 (*CH*-CH_2), 115.50 (C_{arom}), 126.70 (C_{arom}), 130.01 (C_{arom}), 155.52 (C_{arom}), 170.70 (CONH), 172.3 (COOH). Anal. Calcd. $C_{12}H_{15}NO_4$ (237.10): C 60.75, H 6.37, N5.90; Found C 61.75, H 5.87, N 6.50.

4.3.11 Synthesis of (S)-methyl 2-acetamido-3-(4-methoxyphenyl)propanoate (42b)

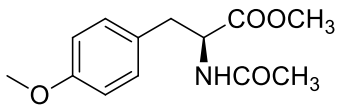

42b

To a solution of **42a** (3.23 g, 10.93 mmol) in DMF (40 mL) was added K_2CO_3 (2.26 g, 16.39 mmol) and after the reaction being stirred for 10 minutes, iodomethane (1.71 mL, 27.32 mmol) was added and the reaction was then allowed to run overnight at room temperature. After completion of the reaction (TLC), the reaction was quenched with cold 1N HCl (25 mL) and extracted with ethyl acetate (15 mL x 3). The organic layer was washed with brine (15 mL x 2), dried over anhydrous Na_2SO_4 and evaporated under vaccuo to obtain the title compound **42b** as a colourless sticky solid. IR (neat): 3273.5, 3079.4, 3013.0, 2960.0, 2842.3, 1759.4, 1646.8, 1560.9, 1453.9, 1375.5, 1184.3, 1027.3, 826.7 cm^{-1}. ^1H NMR (500 MHz, $CDCl_3$): δ 1.90 (s, 3H, CH_3), 2.96-2.93 (dd: J= 5.8 Hz, 1H, CH-CH_2), 3.02-2.98 (dd, J=6.7 Hz, J=6.7 Hz, 1H, CH-CH_2), 3.64 (s, 3H, CH_3), 3.70 (s, 3H, CH_3), 4.75 (m, 1H, CH-CH_2), 6.78 (d, J=8.5, 6.5 Hz, 2H, Ar-H), 6.98 (d, J=8.5, 9.4Hz, 2H, Ar-H). ^{13}C-NMR (500 MHz, $CDCl_3$): δ 22.90 (CH-CH_2), 31.30 -$COCH_3$), 52.14 (OCH_3), 53.19 (CH-CH_2), 55.062 (OCH_3), 113.82 (C_{arom}), 127.70 (C_{arom}), 130.08 (C_{arom}), 158.52 (C_{arom}), 169.70 (CONH), 172.13 (COOH). Anal. Calcd. $C_{13}H_{17}NO_4$ (251.12): C 62.14, H 6.82, N 5.57, O 25.47; found C 61.75, H 5.87, N 6.50, O 25.97.

4.3.12 (S)-2-acetamido-3-(4-methoxyphenyl)propanoic acid (42)

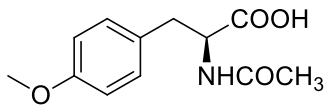

42

To a solution of compound **42b** (0.88 g, 4 mmol) in a mixture of THF: MeOH: H_2O (6:2:1, 15 mL) was added LiOH (0.1 g, 8 mmol) and the mixture was stirred for overnight at room temperature. The pH of mixture was adjusted to 5-6 with 1M HCl and was portioned between ethyl acetate and water. Then separated the organic layer and washed with brine, dried over Na_2SO_4 and evaporated to dryness under reduced pressure. Column chromatography on silica gel eluting with ethyl acetate: hexanes (1:1) and then changing to (2:1) gave the titled compound **42** (Yield, 86%). IR (neat): 3322.7, 3075.5, 3013.1, 2927.4, 2831.7, 1706.8, 1617.0, 1555.3, 1512.6, 1452.7, 1327.7, 1035.5, 843.3 cm^{-1}. ^1H NMR (500 MHz, $CDCl_3$): δ 2.00 (s, 3H, CH_3), 3.10-3.06 (dd, J=5.75Hz, 1H, CH-CH_2), 3.18-3.14 (dd, J=5.5 Hz, 1H, CH-CH_2), 3.78 (s, 3H, CH_3), 4.80 (m, 1H, CH-CH_2), 5.98 (d, J= 7.35 Hz, NH), 6.84 (d, J=8.25 Hz, 2H, Ar-H), 7.08 (d, J=8.25 Hz, 2H, Ar-H). ^{13}C-NMR (500 MHz, $CDCl_3$): δ 23.09 (CH-CH_2), 36.29 (OCH_3), 53.38 (CH-CH_2), 55.21 (OCH_3), 114.09 (C_{arom}), 127.46 (C_{arom}), 130.31 (C_{arom}), 158.87 (C_{arom}), 170.75 (CONH), 173.97 (COOH). Anal. Calcd. $C_{12}H_{15}NO_4$ (237.10): C 60.75, H 6.37, N 5.90, O 26.97; Found C 62.25, H 5.50, N 6.87, O 25.47.

4.3.13 (S)-2-((tert-butoxycarbonyl)amino)-3-(4-methoxyphenyl)propanoic acid (43)

The synthesis of (S)-2-((tert-butoxycarbonyl)amino)-3-(4-methoxyphenyl)propanoic acid (**43**) was accomplished from methyl ester of L-tyrosine hydrochloride by the operations of

N-acetylation with boc anhydride to obtain **43a**, which in turn was subjected to O-alkylation to furnish the desired intermediate **43**.

4.3.14 Synthesis of (S)-methyl 2-(tert-butoxycarbonylamino)-3-(4-hydroxyphenyl)propanoate (43a)

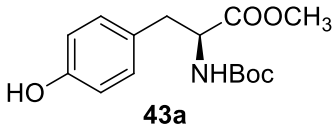

43a

To a solution of (S)-tyrosine methyl ester hydrochloride (**41**) (2.51 g, 10.84 mmol) in a mixture of THF/methanol (50 ml/15 ml) was added $NaHCO_3$ (1.82 g, 21.68 mmol) followed by the addition of solution of di-tert-butyl dicarbonate (2.366 g, 10.84 mmol) dissolved in THF (20 ml). The reaction mixture was stirred at room temperature for 22 h and the solvents were evaporated under vacuo. The residue was dissolved in CH_2Cl_2, washed with water and dried over $MgSO_4$. The filtrate was concentrated under reduced pressure and recrystallization from CH_2Cl_2 provided the title compound **43a** as white crystalline solid (yield, 98%) [135, 136]. IR (neat): 3389.7, 3002.6, 2978.3, 2952.0, 1717.2, 1688.9, 1617.0, 1446.1, 1396.1, 1159.3, 994.0, 830.1 cm^{-1}. ^{1}H-NMR (500 MHz, $CDCl_3$): δ 1.42 (s, 9H, $(CH_3)_3$), 2.98-2.95 (dd, J=7.05, 3.05-3.02 (dd, J=5.5, 9.5 Hz, 1H, CH-*CH_2*), 3.71 (s, 3H, CH_3), 4.05 Hz, 1H, CH-*CH_2*), 4.54 (m, 1H, C*H*-CH_2), 5.01 (d: J= 9.45Hz, 1H, NH), 5.62 (s, 1H, OH), 6.74 (d, J=7.65 Hz, 2H, Ar-H), 6.97 (d, J=8.25 Hz, 2H, Ar-H). ^{13}C-NMR (500 MHz, $CDCl_3$): δ 28.5 ($(CH_3)_3$), 37.7 (CH-*CH_2*), 52.4 (OCH_3), 54.8 (C*H*-CH_2), 80.4 ($OC(CH_3)_3$), 115.7 (C_{arom}), 127.7 (C_{arom}), 130.5 (C_{arom}),155.3 (C_{arom}), 155.5 ($COOCH_3$), 172.8 (CONH). Anal. Calcd. $C_{15}H_{21}NO_5$ (295.14): C 61.00, H 7.17, N 4.74.09; Found C 61.50, H 5.55, N 6.87.

4.3.15 Synthesis of (S)-methyl 2-(tert-butoxycarbonylamino)-3-(4-methoxyphenyl)propanoate (43b)

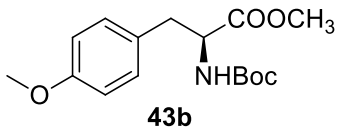

43b

To a solution of **43a** (1.62 g, 5.45 mmol) in DMF (30 mL) was added K_2CO_3 (1.13 g, 8.202 mmol) and after the reaction being stirred for 10 minutes, iodomethane (0.86 mL, 12.65 mmol) was added to the mixture. The reaction was stirred overnight at room temperature and then transferred in separating funnel and extracted ethyl acetate (15 mL × 3) and the organic layer was washed with brine (15 mL). The organic layer was dried over anhydrous Na_2SO_4 and evaporated under reduced pressure to get the title compound **43b** as colourless sticky solid. IR (neat): 3445.9, 3347.9, 2978.7, 2929.8, 1717.7, 1513.9, 1513.9, 1397.4, 1368.8, 1249.4, 1167.1, 1032.1, 829.7 cm^{-1}. ^{1}H-NMR (500 MHz, $CDCl_3$): δ 1.42 (s, 9H, $(CH_3)_3$), 3.01-2.98 (dd, J=7.65 Hz, J=5.72 Hz, 1H, CH-*CH_2*), 3.07-3.03 (dd, J=6.75 Hz, J=7.05 Hz, 1H, CH-*CH_2*), 3.71(s, 3H, CH_3), 3.78 (s, 3H, CH_3), 4.53 (m, 1H, *CH*-CH_2), 4.97(d, 1H, NH), 6.83 (d, J=8.5 Hz, 2H, Ar-H), 7.04 (d, J=8.2 Hz, 2H, Ar-H). ^{13}C-NMR (125.7 MHz, CDCl3): δ 28.20 ($(CH_3)3$), 37.34 (CH-*CH_2*), 52.05 (OCH_3), 54.47 (*CH*-CH_2), 55.10 (OCH_3), 79.75 ($OC(CH_3)3$), 113.88 (C_{arom}), 127.86 (C_{arom}), 130.18 (C_{arom}), 155.03 (C_{arom}), 158.56 (C_{arom}), 172.34 ($COOCH_3$), 192.45 (CONH). Anal. Calcd. $C_{16}H_{23}NO_5$ (309.16): C 62.12, H 7.49, N 4.53; Found C 61.70, H 5.35, N 6.37.

4.3.16 (S)-2-((tert-butoxycarbonyl)amino)-3-(4-methoxyphenyl)propanoic acid (43)

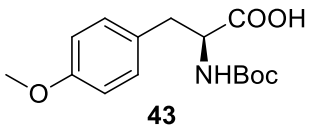

43

To a solution of **42b** (0.450 g, 1.464 mmol) in a mixture of THF: MeOH: H_2O (3:1:1, 15 mL) was added LiOH (0.307 g, 27.34 mmol) and the mixture was stirred overnight at room temperature. The mixture was carefully acidified with 1M HCl to pH and then ethyl acetate (15 mL × 3). The organic layer was washed with brine (10 mL), dried over Na_2SO_4 and evaporated under reduced pressure. Column chromatography on silica gel eluting with ethyl acetate: hexanes (1:1) and then changing to (2:1) gave the titled compound **43** as sticky white solid (yield, 86%). IR (neat): 3439.6, 3346.5, 2979.2, 2933.0, 1719.4, 1614.2, 1513.9, 1397.6, 1368.7, 1164.1, 1032.7, 829.7 cm^{-1}. ^1H NMR (500 MHz, $CDCl_3$): δ 1.42 (s, 9H, $(CH_3)_3$)), 3.04-3.00 (dd, J=7.65, 9.75 Hz, 1H, CH-CH_2), 3.15-3.10 (dd, J=6.75, 9.75 Hz, 3.78 (s, 3H, CH_3), 1H, CH-CH_2), 4.53 (m, 1H, CH-CH_2), 4.92 (d, 1H, NH), 6.85 (d, J=8.2 Hz, 2H, Ar-H), 7.10 (d J=8.25 Hz,2H, Ar-H). ^{13}C-NMR (500 MHz, $CDCl_3$): δ 1.39 ($(CH_3)3$), 27.00 (CH-CH_2), 55.85 (CH-CH_2), 56.65 (OCH_3), 81.77 (OC (CH_3)3), 115.50 (C_{arom}), 131.78 (C_{arom}), 156.92 (C_{arom}), 160.17 (C_{arom}), 176.80 (COOH), 190.10 (CO). Anal. Calcd. $C_{15}H_{21}NO_5$ (295.14): C 61.00, H 7.17, N 4.74; Found C 61.40, H 6.35, N 5.67.

4.3.17 (S)-3-(4-Methoxyphenyl)-2-(methylsulfonamido)propanoic acid *(44)*

The synthesis of (S)-3-(4-Methoxyphenyl)-2-(methylsulfonamido)propanoic acid (**44**) was achieved from the acylation of methyl ester of L-tyrosine hydrochloride (**41**) with

methanesulfonyl chloride to produce **44a**, which was subjected to the operations of O-alkylation followed by basic hydrolysis of ester function.

4.3.18 Synthesis of (S)-Methyl 3-(4-hydroxyphenyl)-2-(methylsulfonamido)propanoate (44a)

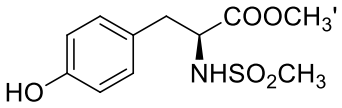

44a

To a cold suspension of methyl ester of L-tyrosine hydrochloride (**41**) (0.5 g, 2.16 mmol) in CH_2Cl_2 (15 mL) was added trimethylamine (1.20 mL, 8.6 mmol) followed by the dropwise addition of a solution of methane sulphonyl chloride (0.25 mL, 3.24 mmol) in CH_2Cl_2 (2 mL). The reaction mixture was stirred overnight at room temperature and quenched with water (10 mL) followed by the pH of the mixture was adjusted to 4-5 with dilute HCl. The organic layer was separated, dried over Na_2SO_4 and evaporated under reduced pressure to get the title compound **44a** as a white solid (yield 90%). M. p. 102-103 ^oC. IR (neat): 3310, 3022, 2941, 1738, 1506, 1451, 1367, 973 cm^{-1}. ^1H NMR (500 MHz, $CDCl_3$): δ 2.76 (s, 3 H, SO_2CH_3), 3.06 (dd, J = 7.0, 14.0 Hz, 1 H, CH_2CH), 3.18 (dd, J = 5.5, 14.0 Hz, 1 H, CH_2CH), 3.79 (s, 3 H, OCH_3), 4.41 (m, 1 H, CH_2CH), 4.93 (d, J = 9.15 Hz, 1 H, NH), 6.70 (d, J = 8.5 Hz, 2 H, 3'-H, 5'-H), 6.96 (d, J = 8.5 Hz, 2 H, 2'-H, 6'-H). ^{13}C NMR (125.7 MHz, $CDCl_3$): δ 38.80 (SO_2CH_3), 41.31 (CH_2CH), 52.95 (OCH_3), 56.84 (CH_2CH), 122.37 (C-3', C-5'), 131.14 (C-1'), 134.80 (C-2', C-6'), 148.40 (C-4'), 171.53 (C=O). Anal. Calcd. $C_{11}H_{15}NO_5S$ (271.31):: C 48.34, H 5.53, N 5.12; Found C 48.28, H 5.47, N 5.05.

4.3.19 Synthesis of (S)-Methyl 3-(4-methoxyphenyl)-2-(methylsulfonamido)propanoate (44b)

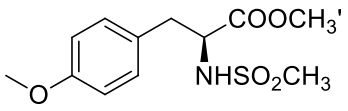

44b

To a solution of compound **44a** (0.7 g, 2.56 mmol) in DMF (15 mL) was added $NaHCO_3$ (0.43 g, 5.12 mmol) was added at room temperature and after the mixture being stirred for 10 minutes, CH_3I (0.32 mL, 5.12 mmol) was added. The reaction mixture was stirred overnight at room temperature followed by the addition of H_2O (10 mL) and 1M HCl (10 mL) and extracted with EtOAc (10 mL x 3). The organic layer was washed with brine, dried over Na_2SO_4 and evaporated under reduced pressure to obtain the title compound **44b** as a colorless thick gum (yield 92%). IR (neat): 3033, 2971, 2936, 1738, 1660, 1506, 1362, 1146 cm^{-1}. ^1H NMR (500 MHz, $CDCl_3$): δ 2.72 (s, 3 H, SO_2CH_3), 3.00 (dd, J = 7.3, 13.9 Hz, 1 H, CH_2CH), 3.10 (dd, J = 5.8, 13.9 Hz, 1 H, CH_2CH), 3.78 (s, 3 H, OCH_3), 3.79 (s, 3 H, OCH_3), 4.37 (m, 1 H, CH_2CH), 6.85 (d, J = 8.5 Hz, 2 H, 3'-H, 5'-H), 7.10 (d, J = 8.5 Hz, 2 H, 2'-H, 6'-H). ^{13}C NMR (125.7 MHz, $CDCl_3$): δ 38.57 (SO_2CH_3), 41.35 (CH_2CH), 52.72 (OCH_3), 55.23 (OCH_3), 57.15 (CH_2CH), 114.17 (C-3', C-5'), 127.09 (C-1'), 130.49 (C-2', C-6'), 158.94 (C-4'), 171.9 (C=O). Anal. Calcd. $C_{12}H_{17}NO_5S$ (287.33): C 50.16, H 5.96, N 4.87; found C 50.12, H 6.03, N 4.81.

4.3.20 Synthesis of (S)-3-(4-Methoxyphenyl)-2-(methylsulfonamido) propanoic acid *(44)*

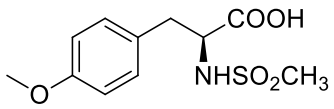

44

To a solution of **44b** (0.86 g, 3 mmol) in a mixture of THF:MeOH:H_2O (6:2:1, 15 mL) was added LiOH.H_2O (0.38 g, 9 mmol) and the mixture was stirred overnight at room temperature followed by the addition of 1M HCl to adjust the pH of the reaction to 6. The mixture was extracted with EtOAc (20 mL) and the organic layer was washed with brine, dried over Na_2SO_4 and evaporated. Column chromatography on silica gel eluting with ethyl acetate:hexanes (1:1) and then changing to (2:1) gave the titled compound **44** as a thick brown gum (yield 86%). IR (neat): 3541, 3281, 3025, 2936, 1735, 1609, 1513, 1307, 1149 cm^{-1}. ^1H NMR (500 MHz, $CDCl_3$): δ 2.67 (s, 3 H, SO_2CH_3), 2.96 (dd, J = 7.6, 14.0 Hz, 1 H, CH_2), 3.16 (dd, J = 4.5, 14.0 Hz, 1 H, CH_2), 3.78 (s, 3 H, OCH_3), 4.35 (m, 1 H, CH), 5.10 (br. s, 1 H, NH), 6.86 (d, J = 8.5 Hz, 2 H, aromatic H), 7.16 (d, J = 8.5 Hz, 2 H, aromatic H). ^{13}C NMR (125.7 MHz, $CDCl_3$): δ 38.07 (SO_2CH_3), 41.23 (CH_2CH), 55.28 (OCH_3), 57.48 (CH_2CH), 114.18, 127.74, 130.66, 158.85 (C_{arom}), 175.10 (C=O). Anal. Calcd. $C_{11}H_{15}NO_5S$ (273.31): C 48.34, H 5.53, N 5.12; Found C 48.29, H 5.59, N 5.05.

4.3.21 Synthesis of 2-(5-(3-((tert-Butoxycarbonyl)amino)propoxy)-1-(3,4-dichlorophenyl)-3-(pyridin-3-yl)-1H-pyrazol-4-yl)ethyl acetate (54)

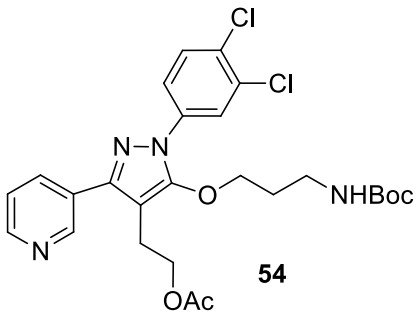

54

To a solution of **47** (2.0 g, 5.11 mmol) in DMF (20 mL) was sequentially added K_2CO_3 (0.92 g, 6.66 mmol) followed by tert-butyl-(3-bromoropropyl)carbamate (1.45 g, 6.12 mmol) and the mixture was further stirred for 8 hours at room temperature. The reaction was diluted with H_2O (15 mL) and extracted with EtOAc (50 mL). The organic layer was washed with H_2O (10 mL), brine (10 mL), dried over Na_2SO_4 and concentrated under reduced pressure. Column chromatography of the dark orange oily material, eluting with EtOAc-hexane (3:1) yielded compound **54** as a light yellow oil (yield 59%). IR (neat): 3361, 3040, 2973, 1740, 1710, 1675, 1592, 1481, 1386, 1234, 1029 cm^{-1}. ^1H NMR (500 MHz, $CDCl_3$): δ 1.44 (s, 9 H, OC(CH_3)$_3$), 1.96 (s, 3 H, $COCH_3$), 2.27 (pent, 2H, $CH_2CH_2CH_2$), 2.98 (t, J = 7.3 Hz, 2 H, ArCH_2), 3.29 (m, 2 H, NCH_2), 4.04 (t, J = 6.1 Hz, 2 H, OCH_2), 4.22 (t, J = 7.0 Hz, 2 H, OCH_2), 7.39 (dd, J = 4.85, 7.9 Hz, 1 H, aromatic H), 7.66 (dd, J = 2.4, 8.5 Hz, 1 H, aromatic H), 7.94 (d, J = 2.4 Hz, 1 H, aromatic H), 8.00-8.03 (m, 2 H, aromatic H), 8.64 (dd, J = 2.1, 6.5 Hz, 1 H, aromatic H), 8.93 (*d*, J =1.8 Hz, 1 H, aromatic H). ^{13}C NMR (125.7 MHz, $CDCl_3$): δ 20.84 (COCH_3), 21.25 (Ar-CH_2), 28.38 (OC$(CH_3)_3$), 30.30 ($CH_2CH_2CH_2$), 36.50 (NCH_2), 65.39 (OCH_2), 73.34 (OCH_2), 79.44 (OC(CH_3)$_3$), 103.27, 120.47, 123.62, 123.70, 129.58, 130.86, 133.23, 135.12, 137.62, 148.19, 148.46, 149.10, 152.06 (all C_{arom}), 155.97 (C=O), 170.97 (C=O). Anal. Calcd. $C_{26}H_{30}Cl_2N_4O_5$ (549.45): C 56.84, H 5.50, N 10.20; Found C 56.78, H 5.55, N, 10.14.

4.3.22 Synthesis of tert-Butyl (3-((1-(3,4-dichlorophenyl)-4-(2-hydroxyethyl)-3-(pyridin-3-yl)-1H-pyrazol-5-yl)-oxy)propyl)carbamate (55)

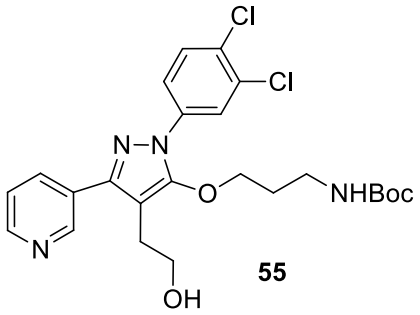

55

To a cold solution of compound **54** (0.83 g, 1.64 mmol) in a mixture of THF (10 mL) and MeOH (5 mL) at 0 ^{o}C was added a solution of KOH (0.34 g, 6.06 mmol) in H_2O (5 mL). After being stirred for 15 minutes at 0 ^{o}C, the reaction was further stirred for 45 minutes at room temperature. Upon completion of the reaction (TLC), the mixture was concentrated under reduced pressure and diluted with EtOAc (30 mL) and successively washed with H_2O (10 mL) and brine (10 mL). The organic layer was dried over Na_2SO_4 and evaporated to dryness under reduced pressure. Column chromatography of the light orange oil material, eluting with EtOAc:hexan (6:4) gave the title compound **55** as a light yellow gum (yield 85%). IR (neat): 3345, 3055, 2974, 1691, 1593, 1482, 1366, 1169 cm^{-1}. ^{1}H NMR (500 MHz, $CDCl_3$): δ 1.44 (s, 9 H, OC(CH_3)$_3$), 1.91 (pent, 2 H, $CH_2CH_2CH_2$), 2.86 (t, J = 6.7 Hz, 2 H, Ar-CH_2), 3.36 (m, 2 H, NCH_2), 3.77 (t, J = 5.8 Hz, 2 H, OCH_2), 4.02 (t, J = 5.8 Hz, 2 H, OCH_2), 4.81 (br. s, 1 H, NH/OH), 7.36 (dd, J = 4.8, 7.9 Hz, 1 H, aromatic H), 7.54 (d, J = 8.5 Hz, 1 H, aromatic H), 7.67 (dd, J = 2.4, 8.5 Hz, 1 H, aromatic H), 7.96 (d, J = 2.4 Hz, 1 H, aromatic H), 8.00 (dd, J = 5.8, 7.9 Hz, 1 H, aromatic H), 8.61 (dd, J = 1.5, 4.9 Hz, 1 H, aromatic H), 8.91 (d, J = 2.1 Hz, 1 H, aromatic H). ^{13}C NMR (125.7 MHz, $CDCl_3$): δ 23.30 (Ar-CH_2), 28.36 (OC(CH_3)$_3$), 30.28 ($CH_2CH_2CH_2$), 37.25 (NCH_2), 63.37

(OCH_2), 73.30 (OCH_2), 79.44 ($OC(CH_3)_3$), 102.68, 120.94, 123.54, 123.68, 129.46, 130.83, 133.21, 134.98, 137.58, 148.26, 148.59, 149.35, 152.26 (all C_{arom}), 155.97 (C=O). Anal. Calcd. $C_{24}H_{28}Cl_2N_4O_4$ (507.41): C 56.81, H 5.56, N 11.04; found C 56.76, H 5.50, N 11.97.

4.3.23 Synthesis of 2-(5-(3-((tert-Butoxycarbonyl)amino)propoxy)-1-(3,4-dichlorophenyl)-3-(pyridin-3-yl)-1H-pyrazol-4-yl)ethyl methanesulfonate (56)

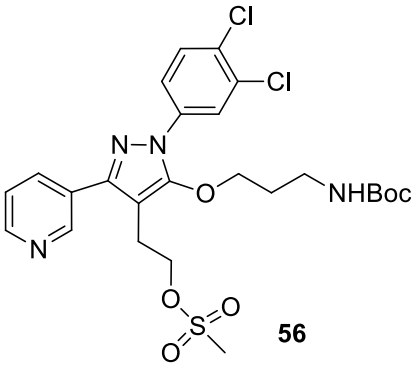

56

To an ice-cold solution of compound **55** (0.41 g, 0.81 mmol) in anhydrous CH_2Cl_2 (10 mL) was added Et_3N (0.34 mL, 2.44 mmol) and after being stirred for 15 minutes, methane sulphonyl chloride (0.094 mL, 1.212 mmol) was added to the mixture. The stirring was continued for 1 hour at 0 ^{0}C and the mixture then diluted with H_2O (5 mL) followed by the addition of 1M HCl (5 mL). The organic layer was separated, dried over Na_2SO_4 and evaporated under reduced pressure to obtain the target compound **56** as a crystalline white solid (yield 98%). M. p. 94-95 ^{o}C. IR (neat): 3356, 3038, 3015, 2986, 1682, 1590, 1483, 1384, 1172 cm^{-1}. ^{1}H NMR (500 MHz, $CDCl_3$): δ 1.44 (s, 9 H, OC(CH_3)$_3$), 1.93 (pent, 2 H, $CH_2CH_2CH_2$), 3.00 (s, 3 H, SO_2CH_3), 3.14 (t, J = 6.4 Hz, 2 H, Ar-CH_2), 3.29 (m, 2 H, NCH_2), 4.02 (t, J = 6.1 Hz, 2 H, OCH_2), 4.37 (t, J = 6.7 Hz, 2 H, OCH_2), 4.72 (br. s, 1 H,

NH), 7.59 (d, *J* = 8.5 Hz, 1 H, aromatic H), 7.65 (dd, *J* = 2.4, 8.8 Hz, 1 H, aromatic H), 7.86 (m, 1 H, aromatic H), 7.92 (d, *J* = 2.4 Hz 1 H, aromatic H), 8.63 (m, 1 H, aromatic H), 8.70 (d, *J* = 5.2 Hz, 1 H, aromatic H), 9.09 (d, *J* = 1.2 Hz, 1 H, aromatic H). ^{13}C NMR (125.7 MHz, $CDCl_3$): δ 23.32 (Ar-*CH_2*), 28.38 (OC*$(CH_3)_3$*), 30.46 (CH_2*CH_2*CH_2), 37.70 (SCH_3), 38.35 (NCH_2), 68.43 (OCH_2), 73.78 (OCH_2), 79.59 (O*C*$(CH_3)_3$), 102.56, 121.15, 123.91, 126.23, 131.10, 131.89, 132.99, 133.52, 137.00, 141.11, 141.26, 141.55, 144.57, 152.92 (all C_{arom}), 156.03 (C=O). Anal. Calcd. $C_{25}H_{30}Cl_2N_4O_6S$ (584.13): C 51.28, H 5.16, N 9.57; Found: C 51.22, H 5.09, N 9.63.

4.3.24 Synthesis of tert-Butyl (3-((1-(3,4-dichlorophenyl)-4-(2-(methylthio)ethyl)-3-(pyridin-3-yl)-1H-pyrazol-5-yl)oxy)propyl)carbamate (57)

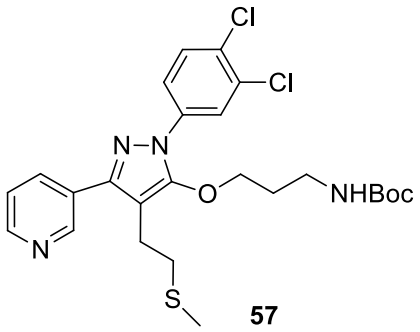

57

To a solution of compound **56** (1.25 g, 2.14 mmol) in DMF (15 mL) at 0 ^{o}C was added $NaSCH_3$ (0.6 g, 8.57 mmol) and the mixture was stirred for 2 hours at room temperature. The reaction was diluted with EtOAc (30 mL) and washed with H_2O (10 mL) and brine (10 mL x 2). The light yellow residue was resolved over column chromatography, eluting with EtOAc: hexane (6:4) to produce the title compound **57** as a light brown gum (yield 78%). IR (neat): 3402, 3092, 2975, 1696, 1590, 1483, 1386, 1171 cm^{-1}. ^{1}H NMR (500 MHz, $CDCl_3$): δ 1.43 (s, 9 H, OC(*CH_3*)$_3$), 1.95 (pent, 2 H, CH_2*CH_2*CH_2), 2.10 (s, 3 H,

SCH_3), 2.71 (t, *J* = 7.3 Hz, 2 H, SCH_2), 2.95 (t, *J* = 7.3 Hz, 2 H, Ar-*CH_2*), 3.28 (m, 2 H, NCH_2), 4.04 (t, *J* = 6.1 Hz, 2 H, OCH_2), 7.59 (d, *J* = 8.8 Hz, 1 H, aromatic H), 7.65 (dd, *J* = 2.4, 8.8 Hz, 1 H, aromatic H), 7.89 (m, 1 H, aromatic H), 7.93 (d, *J* = 2.4 Hz, 1 H, aromatic H), 8.65 (d, *J* = 7.9 Hz, 1 H, aromatic H), 8.71 (d, *J* = 4.6 Hz, 1 H, aromatic H), 9.12 (d, *J* = 2.4 Hz, 1 H, aromatic H). ^{13}C NMR (125.7 MHz, $CDCl_3$): δ 15.90 (SCH_3), 23.21 (Ar-*CH_2*), 28.44 (OC(*CH_3*)$_3$), 30.96 (CH_2*CH_2*CH_2), 34.15 (SCH_2), 36.97 ((*CH_2*CH)), 38.49 (NCH_2), 73.54 (OCH_2), 79.33 ($OC(CH_3)_3$), 104.85, 120.89, 123.67, 125.66, 131.06, 131.61, 133.50, 137.17, 139.68, 142.50, 143.50, 144.82, 152.60 (all C_{arom}), 156.20 (C=O). Anal. Calcd. $C_{25}H_{30}Cl_2N_4O_3S$ (537.50): C 55.86, H 5.63, N 10.42; found C 55.80, H 5.68, N 10.36.

4.3.25 Synthesis of 3-((1-(3,4-Dichlorophenyl)-4-(2-(methylthio)ethyl)-3-(pyridin-3-yl)-1H-pyrazol-5-yl)oxy)-propan-1-amine hydrochloride (58)

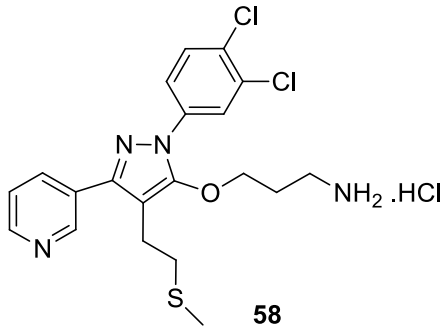

58

To a solution of compound **57** (0.37 g, 0.69 mmol) in anhydrous CH_3OH (10 mL) at 0 ^oC was added acetyl chloride (1 mL) and the reaction mixture was stirred overnight at room temperature. The volatiles were evaporated under reduced pressure and then triturated with diethyl ether to get a compound **58** as a very hygroscopic light yellow solid (yield 98%). IR (neat): 3419, 2962, 1624, 1586, 1481, 1140 cm^{-1}. ^{1}H NMR (500 MHz, CD_3OD): δ 1.98

(s, 3 H, SCH_3), 2.00 (m, 2 H, $CH_2CH_2CH_2$), 2.64 (t, *J* = 7.3 Hz 2 H, SCH_2), 2.95-3.00 (m, 4H, Ar-CH_2, NCH_2), 4.09 (t, *J* = 6.15 Hz, 2 H, OCH_2), 7.65 (m, 2 H, aromatic H), 7.90 (d, *J* = 2.2 Hz, 1 H, aromatic H), 8.07 (m, 1 H, aromatic H), 8.77 (d, *J* = 5.8 Hz, 1 H, aromatic H), 8.85 (d, *J* = 8.2 Hz, 1 H, aromatic H), 9.12 (*d*, J = 2.4 Hz, 1 H, aromatic H). ^{13}C NMR (125.7 MHz, CD_3OD): δ 15.66 (SCH_3), 23.65 (Ar-CH_2), 29.02 ($CH_2CH_2CH_2$), 35.05 (SCH_2), 38.01 (NCH_2), 74.02 (OCH_2), 108.02, 123.38, 125.60, 128.63, 131.18, 132.50, 132.78, 137.10, 141.73, 142.43, 145.02, 153.56, 156.13 (all C_{arom}). Anal. Calcd. $C_{20}H_{23}Cl_3N_4OS$ (473.85): C 50.69, H 4.89, N 11.82; Found C 50.63, H 4.95, N 11.74.

4.3.26 Synthesis of (S)-2-Acetamido-N-(3-((1-(3,4-dichlorophenyl)-4-(2-(methylthio)ethyl)-3-(pyridin-3-yl)-1H-pyrazol-5-yl)oxy)propyl)-3-phenylpropanamide (6)

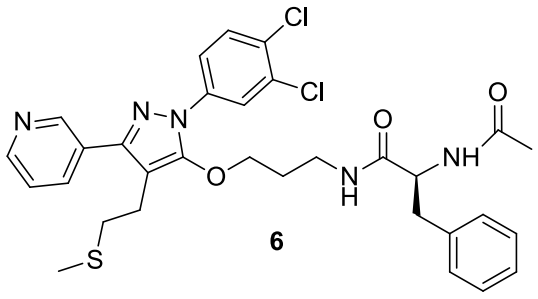

6

To a solution of mixture of compounds **58** (0.15 g, 0.32 mmol) and **33** (0.068 g, 0.33 mmol) in CH_2Cl_2 (10 mL) was sequentially added hydroxybenzotriazole (0.050 g, 0.33 mmol), N-(3-dimethylaminopropyl)-N′-ethylcarbodiimide hydrochloride (0.084 g, 0.44 mmol) and Et_3N (0.15 mL, 1.1 mmol) and the mixture was stirred overnight at room temperature. The reaction was diluted with ethyl acetate (20 mL) and washed with sat. $NaHCO_3$ (10 mL), H_2O (10 mL) and brine (10 mL). The organic layer was dried over Na_2SO_4 and evaporated under reduce pressure. Column chromatography purifications of light yellow oily material,

eluting with EtOAc: hexane (8:2) gave the product as a light green solid (yield 69%). M. p. 125-126 °C. $-[\alpha]_D^{20}$ = –3.1 (c = 0.0051, EtOH). IR (neat): 3255, 3072, 2952, 1670, 1639, 1592, 1563, 1480.7, 1368, 1139, 1082 cm^{-1}. ^1H NMR (500 MHz, $CDCl_3$): δ 1.83 (pent, 2 H, $CH_2CH_2CH_2$), 1.97 (s, 3 H, $COCH_3$), 2.08 (s, 3 H, SCH_3), 2.67 (t, *J* = 7.1 Hz, 2 H, SCH_2), 2.91 (t, *J* = 7.9 Hz, 2H, $ArCH_2$), 3.10 (dd, *J* = 8.2, 13.7 Hz, 1 H, CH_2CH), 3.11 (dd, *J* = 5.8, 13.7 Hz, 1 H, CH_2CH), 3.31 (m, 2 H, NCH_2), 3.87 (t, *J* = 6.2 Hz, 2 H, OCH_2), 4.58 (m, 1 H, CH_2CH), 6.23-6.29 (br. s, 2 H, 2NH), 7.18-7.22 (m, 2 H, aromatic H), 7.25-7.29 (m, 3 H, aromatic H), 7.57 (d, *J* = 8.8 Hz, 1 H, aromatic H), 7.63 (dd, *J* = 2.4, 8.8 Hz, 1 H, aromatic H), 7.76 (m, 1 H, aromatic H), 7.90 (d, *J* = 2.4 Hz, 1 H, aromatic H), 8.49 (d, *J* = 8.0 Hz, 1 H, aromatic H), 8.73 (d, *J* = 6.5 Hz, 1 H, aromatic H), 9.10 (s, 1 H, aromatic H). ^{13}C NMR (125.7 MHz, $CDCl_3$): δ 15.89 (SCH_3), 23.05 ($COCH_3$), 23.21 ($Ar\text{-}CH_2$), 30.93 ($CH_2CH_2CH_2$), 34.19 (SCH_2), 36.15 (CH_2CH), 38.38 (NCH_2), 54.46 (CH_2CH), 73.21 (OCH_2), 106.19, 121.06, 123.72, 127.06, 128.68, 129.21, 129.42, 131.00, 131.33, 133.32, 136.62, 137.31, 152.12 (all C_{arom}), 170.10 (C=O), 171.10 (C=O). Anal. Calcd. $C_{31}H_{33}Cl_2N_5O_3S$ (626.60): C 59.42, H 5.31, N 11.18; Found C 59.36, H 5.37, N 11.10.

4.3.27 Synthesis of (S)-N-(3-((1-(3,4-Dichlorophenyl)-4-(2-(methylthio)ethyl)-3-(pyridin-3-yl)-1H-pyrazol-5-yl)oxy)propyl)-2-(methylsulfonamido)-3-phenylpropanamide (7)

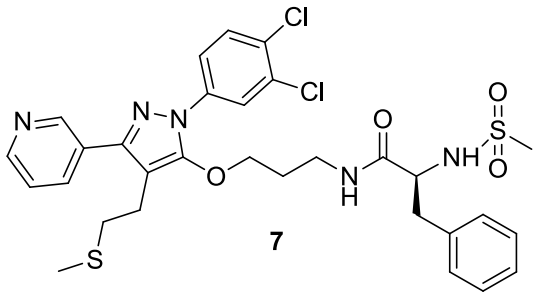

7

Following the same procedure adopted for the synthesis of **2**, the reaction of **58** with **34** gave the title compound **7** as a colorless solid (yield 57%). M. p. 130-131 ^{o}C.$-[\alpha]_{D}^{20}$ = – 38.4 0.0025, EtOH). IR (neat): 3376, 3280, 3062, 2920, 1664. 1592, 1566, 1482, 1457, 1317, 1149 cm^{-1}. ^{1}H NMR (500 MHz, $CDCl_3$): δ 1.95 (pent, 2 H, CH_2*CH_2*CH_2), 2.08 (s, 3 H, SCH_3), 2.54 (s, 3 H, SO_2CH_3), 2.70 (t, *J* = 6.7 Hz, 2 H, SCH_2), 2.89 (dd, *J* = 7.2, 13.7 Hz, 1 H, *CH*$_2$CH), 2.97 (t, *J* = 7.6 Hz, 2 H, Ar*CH*$_2$), 3.31 (m, 2 H, NCH_2), 3.41 (dd, *J* = 5.6, 13.7 Hz, 1 H, *CH*$_2$CH), 4.03 (t, *J* = 6.4 Hz, 2 H, OCH_2), 4.08 (m, 1 H, CH_2*CH*), 5.73 (br. s, 1 H, NH), 7.20-7.24 (m, 2 H, aromatic H), 7.25-7.30 (m, 3 H, aromatic H), 7.57 (d, *J* = 8.8 Hz, 1 H, aromatic H), 7.66 (dd, *J* = 2.4, 8.8 Hz, 1 H, aromatic H), 7.90 (m, 1 H, aromatic H), 7.95 (m, 1 H, aromatic H), 8.49 (d, *J* = 7.6 Hz, 1 H, aromatic H), 8.76 (d, *J* = 6.5 Hz, 1 H, aromatic H), 9.10 (s, 1 H, aromatic H). ^{13}C NMR (125.7 MHz, $CDCl_3$): δ 15.66 (SCH_3), 23.17 (Ar-*CH*$_2$), 29.54 (CH_2*CH_2*CH_2), 33.98 (SCH_2), 36.45 (*CH*$_2$CH), 38.66 (NCH_2), 40.03 (SO_2CH_3), 59.12 (CH_2*CH*), 72.97 (OCH_2), 106.76, 121.03, 123.57, 123.69, 127.63, 129.13, 129.39, 129.62, 130.74, 130.89, 133.14, 134.92, 136.38, 137.66, 147.88, 148.52, 149.34, 151.73 (all C_{arom}), 170.46 (C=O). Anal. Calcd. $C_{30}H_{33}Cl_2N_5O_4S_2$ (662.65): C 54.38, H 5.02, N 10.57; Found C 54.33, H 5.07, N, 10.50.

4.3.28 Synthesis of (S)-2-Acetamido-N-(3-((1-(3,4-dichlorophenyl)-4-(2-(methylthio)ethyl)-3-(pyridin-3-yl)-1H-pyrazol-5-yl)oxy)propyl)-3-(4-fluorophenyl)propanamide (8)

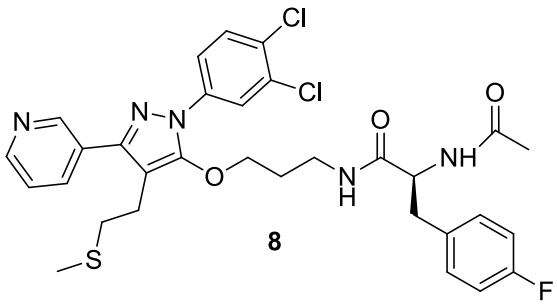

8

Following the same procedure adopted for the synthesis of **2**, the reaction of **58** with **35** gave the title compound **8** as a colorless solid (yield 67%). M. p. 117-118 ^{o}C. – $[\alpha]_D^{20}$ = – 5.6 (c = 0.0.005, EtOH). IR (neat): 3505, 3272, 3066, 2921, 1892, 1654, 1593.3, 1509, 1482, 1368, 1220, 1132 cm^{-1}. ^{1}H NMR (500 MHz, $CDCl_3$): δ 2.06 (s, 3 H, SCH_3), 2.08 (s, 3 H, $COCH_3$), 2.17 (pent, 2 H, $CH_2CH_2CH_2$), 2.70 (t, J = 7.2 Hz, 2 H, SCH_2), 2.89-2.95 (m, 4 H, ArCH_2, CH_2CH), 3.32 (t, J = 6.2 Hz, 2 H, NCH_2), 3.96 (t, J = 7.1 Hz, 2 H, OCH_2), 4.70 (m, 1H, CH_2CH), 6.94 (m, 2 H, aromatic H), 7.20 (m, 2 H, aromatic H), 7.58 (d, J = 8.2 Hz, 1 H, aromatic H), 7.64 (d, J = 8.2 Hz, 1 H, aromatic H), 7.90 (m, 1 H, aromatic H), 7.99 (d, J = 2.6 Hz, 1 H, aromatic H), 8.74-8.79 (m, 2 H, aromatic H), 89.24 (d, J = 2.1 Hz, 1 H, aromatic H). ^{13}C NMR (125.7 MHz, $CDCl_3$): δ 15.69 (SCH_3), 23.17 ($COCH_3$, Ar-CH_2), 29.67 ($CH_2CH_2CH_2$), 34.04 (SCH_2), 36.31 (CH_2CH), 37.57 (NCH_2), 54.79 (CH_2CH), 72.98 (OCH_2) 105.72, 115.42, 115.59, 120.98, 123.63, 129.63, 130.76, 130.89, 132.24, 133.17, 135.00, 137.63, 147.89, 148.45, 149.31, 151.73, 162.88 (all C_{arom}), 170.08 (C=O), 170.92 (C=O). Anal. Calcd. $C_{31}H_{32}Cl_2FN_5O_3S$ (644.59): C 57.76, H 5.00, N 10.86; Found C 57.70, H 5.06, N 10.80.

4.3.29 Synthesis of (S)-N-(3-((1-(3,4-Dichlorophenyl)-4-(2-(methylthio)ethyl)-3-(pyridin-3-yl)-1H-pyrazol-5-yl)oxy)propyl)-3-(4-fluorophenyl)-2-(methylsulfonamido)propanamide (9)

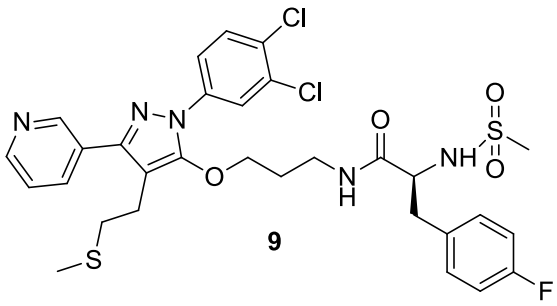

9

Following the same procedure adopted for the synthesis of **2**, the reaction of **58** with **36** gave the title compound **9** as a white crystalline solid (yield 60%). M. p. 126-127 ^{o}C. -$[\alpha]_D^{20}$= –18.0 (c = 0.00455, EtOH). IR (neat): 3663, 3282, 3066, 2921, 1664, 1593, 1511, 1482, 1319, 1223, 1150 cm^{-1}. ^{1}H NMR (500 MHz, $CDCl_3$): δ 1.92 (pent, 2 H, $CH_2CH_2CH_2$), 2.08 (s, 3 H, SCH_3), 2.54 (s, 3H, SO_2CH_3), 2.64 (t, J = 7.3 Hz, 2 H, SCH_2), 2.89-2.93 (m, 3 H, ArCH_2, CH_2CH), 3.20 (dd, J = 5.1, 12.2 Hz, 1 H, CH_2CH), 3.44 (t, J = 6.4 Hz, 2 H, NCH_2), 3.96-3.99 (m, 3 H, OCH_2, CH_2CH), 4.93 (d, J = 5.6 Hz, 1 H, NH), 6.42 (br. s, 1 H, NH), 7.03 (m, 2 H, aromatic H), 7.19 (m, 2 H, aromatic H), 7.38 (dd, J = 2.7, 8.5 Hz, 1 H, aromatic H), 7.55 (d, J = 8.5 Hz, 1 H, aromatic H), 7.65 (dd, J = 2.4, 8.5 Hz, 1 H, aromatic H), 7.93 (d, J = 2.4 Hz, 1 H, aromatic H), 8.00 (m, 1 H, aromatic H), 8.63 (dd, J = 2.1, 7.6 Hz, 1 H, aromatic H), 8.90 (d, J = 2.1, 1 H, aromatic H). ^{13}C NMR (125.7 MHz, $CDCl_3$): δ 15.69 (SCH_3), 23.22 (Ar-CH_2), 29.57 ($CH_2CH_2CH_2$), 34.03 (SCH_2), 36.56 (CH_2CH), 37.97 (NCH_2), 40.50 (SO_2CH_3), 58.94 (CH_2CH), 72.97 (OCH_2), 105.78, 115.92, 116.08, 121.09, 123.58, 123.72, 129.63, 130.81, 130.93, 131.03, 133.17, 134.94, 137.69, 148.56, 149.41 (all C_{arom}), 170.34 (C=O). Anal. Calcd. $C_{30}H_{32}Cl_2FN_5O_4S_2$ (680.64): C 52.94, H 4.74, N 10.29; Found C 52.88, H 4.80, N 10.21.

4.3.30 Synthesis of (S)-2-Acetamido-N-(3-((1-(3,4-dichlorophenyl)-4-(2-(methylthio)ethyl)-3-(pyridin-3-yl)-1H-pyrazol-5-yl)oxy)propyl)-3-(4-methoxyphenyl)propanamide (10)

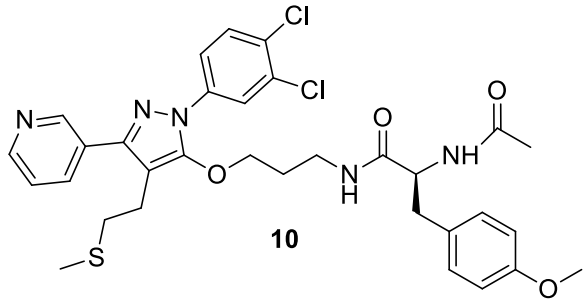

10

Following the same procedure adopted for the synthesis of **2**, the reaction of **58** with **42** gave the title compound **10** as a colorless solid (yield 61%). M. p. 131-132 ^{o}C. – $[\alpha]_D^{20}$ = – 19.1 (c = 0.00335, EtOH). IR (neat): 3275, 3039, 2917, 1652, 1591, 1483, 1368, 1284, 1030 cm^{-1}. ^{1}H NMR (500 MHz, $CDCl_3$): δ 1.82 (pent, 2H, CH_2*CH_2*CH_2), 1.97 (s, 3 H, $COCH_3$), 2.07 (s, 3 H, SCH_3), 2.62 (t, *J* = 7.1 Hz, 2 H, SCH_2), 2.84-2.93 (m, 3 H, Ar*CH_2*, *CH_2*CH), 3.01 (dd, *J* = 5.5, 12.2 Hz, 1 H, *CH_2*CH), 3.32 (m, 2 H, NCH_2), 3.74 (s, 3 H, OCH_3), 3.88 (t, J = 6.2 Hz, 2 H, OCH_2), 4.49 (m, 1 H, CH_2*CH*), 6.05 (br. s, 1 H, NH), 6.18 (d, *J* = 6.7 Hz, 1 H, NH), 6.80 (d, *J* = 8.5 Hz, 2 H, aromatic H), 7.10 (d, *J* = 8.5 Hz, 2 H, aromatic H), 7.39 (m, 1 H, aromatic H), 7.54 (d, *J* = 8.8 Hz, 1 H, aromatic H), 7.65 (dd, *J* = 2.4, 8.8 Hz, 1 H, aromatic H), 7.91 (d, *J* = 2.4 Hz, 1 H, aromatic H), 8.00 (d, *J* = 7.9 Hz, 1 H, aromatic H), 8.63 (d, *J* = 4.9 Hz, 1 H, aromatic H), 8.90 (s, 1 H, aromatic H). ^{13}C NMR (125.7 MHz, $CDCl_3$): δ 15.71 (SCH_3), 23.12 (CO*CH_3*), 23.19 (Ar-*CH_2*), 32.75 (CH_2*CH_2*CH_2), 34.07 (SCH_2), 36.24 (*CH_2*CH), 37.57 (NCH_2), 54.97 (OCH_3), 55.22 (CH_2*CH*), 73.05 (OCH_2), 105.82, 114.07, 120.95, 123.63, 123.92, 128.48, 130.22, 130.90, 133.20, 135.80, 137.58, 147.37, 147.46, 148.20, 151.83, 158.65 (all C_{arom}), 170.00 (C=O),

171.17 (C=O). Anal. Calcd. $C_{32}H_{35}Cl_2N_5O_4S$ (656.62): C 58.53, H 5.37, N 10.67; Found C 58.47, H 5.43, N 10.60.

4.3.31 Synthesis of (S)-N-(3-((1-(3,4-dichlorophenyl)-4-(2-(methylthio)ethyl)-3-(pyridin-3-yl)-1H-pyrazol-5-yl)oxy)propyl)-3-(4-methoxyphenyl)-2-(methylsulfonamido)propanamide (11)

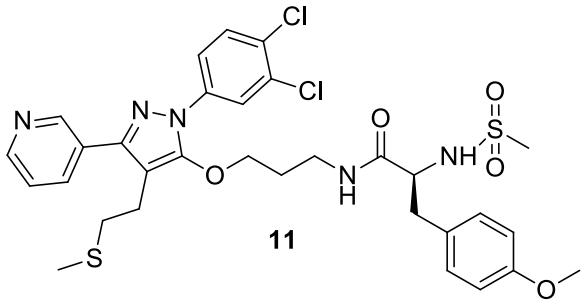

11

Following the same procedure adopted for the synthesis of **2**, the reaction of **58** with **44** gave the title compound **11** as a yellow thick gum (yield 64%). – $[\alpha]_D^{20}$ = –13.9 (c = 0.0049, EtOH). IR (neat): 3403, 3066, 2925, 2835, 1667, 1592, 1514, 1482, 1321, 1248, 1150 cm^{-1}. ^1H NMR (500 MHz, $CDCl_3$): δ 1.92 (pent, 2 H, $CH_2CH_2CH_2$), 2.07 (s, 3 H, SCH_3), 2.50 (s, 3 H, SO_2CH_3), 2.64 (t, J = 7.3 Hz, 2 H, SCH_2), 2.82-2.90 (m, 3 H, ArCH_2, CH_2CH), 3.19 (dd, J = 6.4, 14.0 Hz, 1 H, CH_2CH), 3.40 (m, 2 H, NCH_2), 3.77 (s, 3 H, OCH_3), 3.96 (t, J = 6.4 Hz, 2 H, OCH_2), 4.48 (m, 1 H, CH_2CH), 5.04 (br. s, 1 H, NH), 6.22 (br. s, 1 H, NH), 6.86 (d, J = 8.5 Hz, 2 H, aromatic H), 7.14 (d, J = 8.5 Hz, 2 H, aromatic H), 7.38 (m, 1 H, aromatic H), 7.55 (d, J = 8.8 Hz, 1 H, aromatic H), 7.66 (dd, J = 2.4, 8.8 Hz, 1 H, aromatic-H), 7.92 (d, J = 2.45 Hz, 1 H, aromatic H), 8.00 (d, J = 7.9 Hz, 1 H, aromatic H), 8.63 (m, 1 H, aromatic H), 8.90 (d, J = 2.1 Hz, 1 H, aromatic H). ^{13}C NMR (125.7 MHz, $CDCl_3$): δ 15.67 (SCH_3), 23.19 (Ar-CH_2), 29.61 ($CH_2CH_2CH_2$), 34.02 (SCH_2), 36.48 (CH_2CH), 37.87 (NCH_2), 40.19 (SO_2CH_3), 55.33 (OCH_3), 59.18 (CH_2CH), 73.02 (OCH_2),

114.04, 114.48, 121.06, 123.58, 123.72, 128.10, 129.66, 130.44, 130.75, 130.91, 133.16, 134.96, 137.69, 147.92, 148.54, 149.34, 151.77, 159.09 (all C_{arom}), 170.65 (C=O). Anal. Calcd. $C_{31}H_{35}Cl_2N_5O_5S_2$ (692.68): C 53.75, H 5.09, N 10.11; Found C 53.70, H 5.15, N 10.03.

4.3.32 Synthesis of (S)-tert-Butyl (1-((3-((1-(3,4-dichlorophenyl)-4-(2-(methylthio)ethyl)-3-(pyridin-3-yl)-1H-pyrazol-5-yl)oxy)propyl)amino)-3-(4-methoxyphenyl)-1-oxopropan-2-yl)carbamate (12)

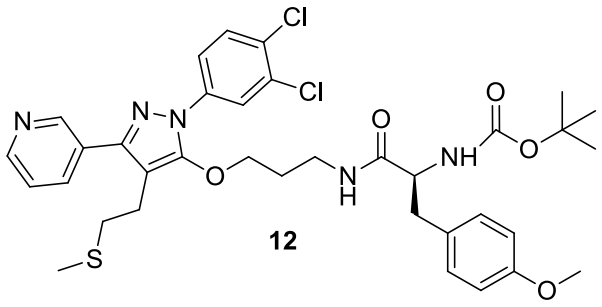

12

Following the same procedure adopted for the synthesis of **2**, the reaction of **58** with **43** yielded compound **12** as a colorless crystalline solid (yield 55%). M. p. 123-124 °C. – $[\alpha]_D^{20}$ = –8.9 (c = 0.00335, EtOH). IR (neat): 3427, 3314, 3042, 2974, 2922, 1714, 1592, 1513, 1366, 1247, 1166 cm^{-1}. ^1H NMR (500 MHz, $CDCl_3$): δ 1.39 (s, 9 H, OC(CH_3)$_3$, 1.84 (pent, 2 H, $CH_2CH_2CH_2$), 2.06 (s, 3 H, SCH_3), 2.62 (t, J = 7.5 Hz, 2 H, SCH_2), 2.86 (t, J = 8.8 Hz, 2 H, ArCH_2), 2.93-3.02 (m, 2 H, CH_2CH), 3.34 (m, 2 H, NCH_2), 3.75 (s, 3 H, OCH_3), 3.91 (t, J = 6.4 Hz, 2 H, OCH_2), 4.42 (m, 1 H, CH_2CH), 5.04 (br. s, 1 H, NH), 6.01 (br. s, 1 H, NH), 6.80 (d, J = 8.5 Hz, 2H, aromatic H), 7.10 (d, J =8.5 Hz, 2 H, aromatic H), 7.39 (m, 1 H, aromatic H), 7.55 (d, J = 8.5 Hz, 1 H, aromatic H), 7.65 (dd, J = 2.4, 8.5 Hz, 1 H, aromatic H), 7.91 (d, J = 2.4 Hz, aromatic H), 8.00 (dd, J = 2.1, 7.6 Hz, 1 H, aromatic H),

8.63 (d, J = 7.9 Hz, 1 H, aromatic H), 8.90 (d, J = 2.1, 7.6 Hz, 1 H, aromatic H). ^{13}C NMR (125.7 MHz, $CDCl_3$): δ 15.66 (SCH_3), 23.12 (Ar-CH_2), 28.26 ($OC(CH_3)_3$), 29.70 ($CH_2CH_2CH_2$), 34.00 (SCH_2), 36.28 (CH_2CH), 37.59 (NCH_2), 55.20 (OCH_3), 55.24 (CH_2CH), 73.12 (OCH_2), 79. 92 ($OC(CH_3)_3$), 105.74, 114.06, 120.95, 123.58, 123.63, 129.60, 130.29, 130.76, 130.88, 133.17, 134.92, 137.62, 147.91, 148.52, 149.37, 151.76 (all C_{arom}), 158.60 (C=O), 171.54 (C=O). Anal. Calcd. $C_{35}H_{41}Cl_2N_5O_5S$ (387.52): C 58.82, H 5.78, N 9.80; Found C 58.77, H 5.82, N 9.74.

4.3.33 Synthesis of *(*S)-2-acetamido-N-(3-((1-(3,4-dichlorophenyl)-4-(2-(methylthio)ethyl)-3-(pyridin-3-yl)-1H-pyrazol-5-yl)oxy)propyl)-3-(pyridin-3-yl)propanamide (13)

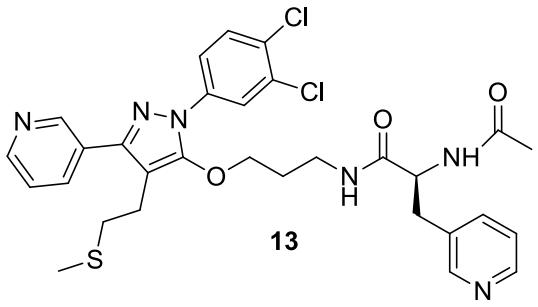

13

Following the same procedure adopted for the synthesis of **2**, the reaction of **58** with **37** yielded compound **13** as a light brown gum (yield 58%). – $[\alpha]_D^{20}$ = –17.5 (c = 0.00365, EtOH). IR (neat): 3442, 3060, 2923, 1653, 1592, 1482, 1369, 1133 cm^{-1}. ^{1}H NMR (500 MHz, $CDCl_3$): δ 1.85 (pent, 2 H, $CH_2CH_2CH_2$), 1.96 (s, 3 H, $COCH_3$), 2.07 (s, 3 H, SCH_3), 2.62 (t, J = 7.0 Hz, 2 H, SCH_2), 2.87 (t, J = 7.3 Hz, 2 H, ArCH_2), 3.01 (dd, J = 5.5, 12.7 Hz, 1 H, CH_2CH), 3.09 (dd, J = 7.3, 12.7 Hz, 1 H, CH_2CH), 3.35 (m, 2 H, NCH_2), 3.93 (t, J = 7.0 Hz, 2 H, OCH_2), 4.61 (m, 1H, CH_2CH), 6.45 (br. s, 1 H, NH), 6.76 (br. s, 1 H, NH), 7.20 (m, 1 H, aromatic H), 7.38 (m, 1 H, aromatic H), 7.54 (d, J = 8.8 Hz, 1 H, aromatic

H), 7.60 (m, 1 H, aromatic H), 7.64 (dd, *J* = 2.4, 8.8 Hz, 1 H, aromatic H), 7.91 (d, *J* = 2.5 Hz, 1 H, aromatic H), 8.00 (m, 1 H, aromatic H), 8.40 (d, *J* = 2.1 Hz, 1 H, aromatic H), 8.45 (dd, *J* = 2.1, 8.0 Hz, 1 H, aromatic H), 8.63 (dd, *J* = 2.1, 8.0 Hz, 1 H, aromatic H), 8.89 (d, *J* = 2.1 Hz, 1 H, aromatic H). ^{13}C NMR (125.7 MHz, $CDCl_3$): δ 15.68 (SCH_3), 23.11 ($CO\mathit{CH_3}$), 23.18 (Ar-$\mathit{CH_2}$), 29.70 ($CH_2\mathit{CH_2}CH_2$), 34.04 (SCH_2), 35.58 ($\mathit{CH_2}CH$), 36.35 (NCH_2), 54.23 ($CH_2\mathit{CH}$), 73.06 (OCH_2), 105.72, 120.98, 123.48, 123.58, 129.59, 130.88, 132.31, 133.15, 134.92, 136.80, 137.66, 147.92, 148.36, 148.52, 149.73, 150.44, 151.75 (all C_{arom}), 170.18 (C=O), 170.69 (C=O). $C_{30}H_{32}Cl_2N_6O_3S$ (627.58): calcd. C 57.41, H 5.14, N 13.39; found C 57.36, H 5.19, N 13.34.

4.3.34 Synthesis of (S)-N-(3-((1-(3,4-dichlorophenyl)-4-(2-(methylthio)ethyl)-3-(pyridin-3-yl)-1H-pyrazol-5-yl)oxy)propyl)-2-(methylsulfonamido)-3-(pyridin-3-yl)propanamide (14)

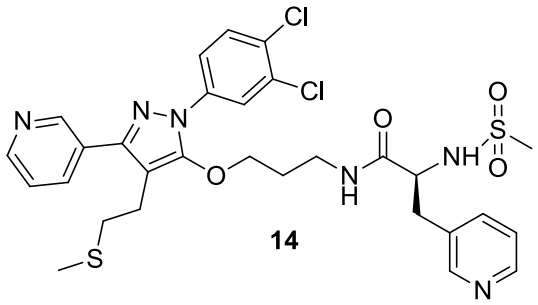

14

Following the same procedure adopted for the synthesis of **2**, the reaction of **58** with **38** yielded compound **14** as a colorless gum (yield 65%). – $[\alpha]_D^{20}$= –28.3 (c = 0.0036, EtOH). IR (neat): 3546, 3386, 3060, 2979, 1674, 1592, 1483, 1318, 1150 cm^{-1}. ^{1}H NMR (500 MHz, $CDCl_3$): δ 1.93 (pent, 2 H, $CH_2\mathit{CH_2}CH_2$), 2.08 (s, 3 H, SCH_3), 2.59 (s, 3 H, SO_2CH_3), 2.64 (t, *J* = 7.6 Hz, 2 H, SCH_2), 2.88 (t, *J* = 6.7 Hz, 2 H, Ar$\mathit{CH_2}$), 2.97 (dd, *J* = 5.8, 14.0 Hz, 1 H, $\mathit{CH_2}CH$), 3.20 (dd, J= 6.1, 14.0 Hz, 1 H, $\mathit{CH_2}CH$), 3.45 (m, 2 H, NCH_2), 3.97 (t, *J* = 5.8

Hz, 2 H, OCH_2), 4.05 (m, 1 H, CH_2CH), 5.36 (d, *J* = 5.8 Hz, 1 H, NH), 6.60 (br. s, 1 H, NH), 7.29 (dd, *J* = 4.9, 7.9 Hz, 1 H, aromatic H), 7.38 (dd, *J* = 4.9, 7.8 Hz, 1 H, aromatic H), 7.55 (d, *J* = 7.9 Hz, 1 H, aromatic H), 7.61 (m, 1 H, aromatic H), 7.65 (dd, *J* = 2.4, 8.8 Hz, 1 H, aromatic H), 7.92 (d, *J* = 2.4 Hz, 1 H aromatic H), 8.00 (m, 1 H, aromatic H), 8.49 (d, *J* = 2.1 Hz, 1 H, aromatic H), 8.52 (dd, *J* = 2.1, 8.1 Hz, 1 H, aromatic H), 8.63 (dd, *J* = 2.1, 8.0 Hz, 1 H, aromatic H), 8.90 (d, *J* = 2.1 Hz, 1 H, aromatic H). ^{13}C NMR (125.7 MHz, $CDCl_3$): δ 15.69 (SCH_3), 23.20 (Ar-CH_2), 29.54 ($CH_2CH_2CH_2$), 34.02 (SCH_2), 36.06 (CH_2CH), 36.62 (NCH_2), 40.95 (SO_2CH_3), 58.45 (CH_2CH), 72.96 (OCH_2), 121.07, 123.60, 123.68, 123.75, 129.61, 130.78, 130.92, 132.15, 133.15, 134.94, 137.19, 137.66, 148.49, 148.77, 149.37, 150.57, 151.71 (all C_{arom}), 170.21 (C=O). Anal. Calcd. $C_{29}H_{32}Cl_2N_6O_4S_2$ (663.64): C 52.48, H 4.86, N 12.66; Found C 52.42, H 4.90, N 12.60.

4.3.35 Synthesis of (S)-2-acetamido-N-(3-((1-(3,4-dichlorophenyl)-4-(2-(methylthio)ethyl)-3-(pyridin-3-yl)-1H-pyrazol-5-yl)oxy)propyl)-3-(pyridin-4-yl)propanamide (15)

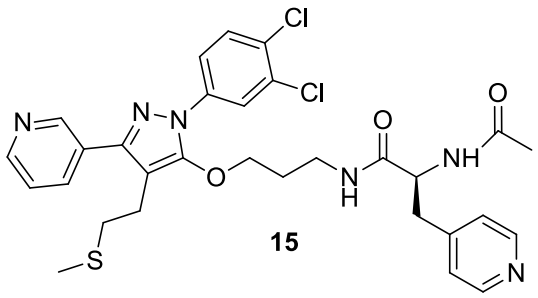

15

Following the same procedure adopted for the synthesis of **2**, the reaction of **58** with **39** yielded compound **15** as a light brown gum (yield 59%). – $[\alpha]_D^{20}$ = –14.6 (c = 0.00315, EtOH). IR (neat): 3478, 3289, 3060, 2919, 1659, 1592, 1482, 1367, 1133 cm^{-1}. ^1H NMR (500 MHz, $CDCl_3$): δ 1.85 (pent, 2 H, $CH_2CH_2CH_2$), 1.96 (s, 3 H, $COCH_3$), 2.08 (s, 3 H,

SCH_3), 2.63 (t, *J* = 7.0 Hz, 2 H, SCH_2), 2.86 (t, *J* = 7.3 Hz, 2H, Ar*CH*$_2$), 3.02 (dd, *J* = 6.4, 12.7 Hz, 1 H, *CH*$_2$CH), 3.06 (dd, *J* = 5.3, 12.7 Hz, 1 H, *CH*$_2$CH), 3.36 (m, 2 H, NCH_2), 3.90 (t, *J* = 7.0 Hz, 2 H, OCH_2), 4.60 (m, 1 H, CH_2*CH*), 6.06 (br. s, 1 H, NH), 6.15 (br. s, 1 H, NH), 7.14 (d, *J* = 6.1 Hz, 1 H, aromatic H), 7.39 (d, *J* = 6.6 Hz, 2 H, aromatic H), 7.54 (d, *J* = 8.8 Hz, 1 H, aromatic H), 7.64 (dd, *J* = 2.4, 8.8 Hz, 1 H, aromatic H), 7.92 (d, *J* = 2.4 Hz, 1 H, aromatic H), 8.00 (m, 1 H, aromatic H), 8.51 (d, *J* = 6.6 Hz, 2 H, aromatic H), 8.62 (m, 1 H, aromatic H), 8.89 (d, *J* = 2.1 Hz, 1 H, aromatic H). ^{13}C NMR (125.7 MHz, $CDCl_3$): δ 15.69 (SCH_3), 23.14 (CO*CH*$_3$), 23.20 (Ar-*CH*$_2$), 29.54 (CH_2*CH*$_2$$CH_2$), 34.02 ($SCH_2$), 36.40 (*CH*$_2$CH), 37.38 ($NCH_2$), 53.82 ($CH_2$*CH*), 72.96 ($OCH_2$), 121.07, 123.60, 123.68, 123.75, 129.61, 130.78, 130.92, 132.15, 133.15, 134.94, 137.19, 137.66, 148.49, 148.77, 149.37, 150.57, 151.71 (all C_{arom}), 170.21 (C=O), 170.71 (C=O). Anal. Calcd. $C_{30}H_{32}Cl_2N_6O_3S$ (627.58): C 57.41, H 5.14, N 13.39; Found C 57.35, H 5.19, N 13.32.

4.3.36 Synthesis of (S)-N-(3-((1-(3,4-dichlorophenyl)-4-(2-(methylthio)ethyl)-3-(pyridin-3-yl)-1H-pyrazol-5-yl)oxy)propyl)-2-(methylsulfonamido)-3-(pyridin-4-yl)propanamide (16)

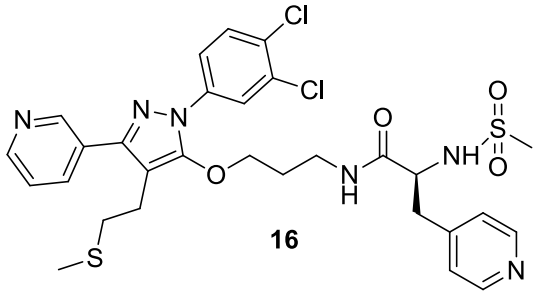

16

Following the same procedure adopted for the synthesis of **2**, the reaction of **58** with **40** yielded compound **16** as a colorless crystalline solid (yield 62%). M. p. 136-137 ^{o}C. – $[\alpha]_D^{20}$ = –20.0 (c = 0.0028, EtOH). IR (neat): 3373, 3281, 3062, 2919, 1675, 1592, 1482, 1415,

1319, 1183, 1150 cm^{-1}. ^{1}H NMR (500 MHz, $CDCl_3$): δ 1.92 (pent, 2 H, $CH_2\mathit{CH_2}CH_2$), 2.08 (s, 3 H, SCH_3), 2.59 (s, 3 H, SO_2CH_3), 2.65 (t, J = 7.7 Hz, 2 H, SCH_2), 2.88 (t, J = 6.7 Hz, 2 H, Ar$\mathit{CH_2}$), 2.97 (dd, J = 5.2, 13.7 Hz, 1 H, $\mathit{CH_2}$CH), 3.20 (dd, J = 6.2, 13.7 Hz, 1 H, $\mathit{CH_2}$CH), 3.47 (m, 2 H, NCH_2), 3.97 (t, J = 5.9 Hz, 2 H, OCH_2), 4.08 (m, 1 H, $CH_2\mathit{CH}$), 5.11 (m, 1 H, NH), 6.44 (br. s, 1 H, NH), 7.19 (d, J = 5.8 Hz, 1 H, aromatic H), 7.38 (d, J = 6.8 Hz, 2 H, aromatic H), 7.56 (d, J = 8.2 Hz, 1 H, aromatic H), 7.64 (dd, J = 2.4, 8.2 Hz, 1 H, aromatic H), 7.92 (d, J = 2.4 Hz, 1 H, aromatic H), 8.00 (m, 1 H, aromatic H), 8.56 (d, J = 6.8 Hz, 2 H, aromatic H), 8.62 (m, 1 H, aromatic H), 8.90 (d, J = 1.5 Hz, 1 H, aromatic H). ^{13}C NMR (125.7 MHz, $CDCl_3$): δ 15.71 (SCH_3), 23.23 (Ar-$\mathit{CH_2}$), 29.71 ($CH_2\mathit{CH_2}CH_2$), 34.02 (SCH_2), 36.65 ($\mathit{CH_2}$CH), 38.16 (NCH_2), 40.95 (SO_2CH_3), 58.02 ($CH_2\mathit{CH}$), 72.91 (OCH_2), 105.77, 121.10, 123.60, 123.70, 124.68, 130.94, 133.17, 134.92, 137.66, 145.44, 148.52, 149.42, 150.35, 151.68 (all C_{arom}), 169.98 (C=O). Anal. Calcd. $C_{29}H_{32}Cl_2N_6O_4S_2$ (663.64): C 52.48, H 4.86, N 12.66; Found C 52.44, H 4.92, N 12.60.

4.4 GGTase-I and FTase assays

Assays were carried out on black bottom 96-well plates and read on Tecon Micro Plate reader. The assay system (100 μl) containing 50 mM Tris-HCl (pH 7.4), 10 μM GGPP (in case of GGTase-I inhibition) or 10 μM FPP (in case of FTase inhibition), 5 μM dansyl-GCVLL, 5 mM DTT, 5 mM $MgCl_2$, 10 mM KCl, 50 μM $ZnCl_2$, 0.04% *n*-Dodecyl β-D-maltoside and indicated concentration of compounds dissolved in 1 μl DMSO. All the mixtures were incubated at 30 °C for 5 minutes for use. The reaction was initiated by the addition of 500 ng of pure GGTase-I or FTase and the fluorescence was measured for 20 min (with readings taken every 1 min) at 30°C with the excitation wavelength at 340 nm and the emission wavelength at 520 nm. Each measurement was performed as triplicate and the IC_{50} values (concentrations resulting in 50% inhibition) were calculated from initial velocity of three independent measurements of five to seven different concentrations. GGTI-DU40 (Duke University) and FTI-277 (Sigma-Aldrich) were used as positive controls for GGTase-I and FTase inhibition, respectively.

4.5 Western blot analysis

MDAMB231 breast cancer cells were seeded at 6×10^4 cells/ well of a 6-well plate 24 hours before drug treatment and incubated at 37°C in 5% CO_2. The total volume in each well was maintained to 2 ml. The inhibitor compounds dissolved in DMSO were added in 5 μM final concentration in each well whereas in the control well was added same volume of DMSO (10 μL of DMSO (0.5%)). After 48 hours, cells were washed twice with cold PBS and lysed using cell extraction buffer 20 mM HEPES, pH 8.0, 1 mM EDTA, 3 mM dithiothreitol, 10 mM $MgSO_4$, 150 mM NaCl, 1% Triton X-100. The protein concentration was quantified using the Pierce BCA Protein Assay kit (Thermo Scientific). Protein

samples (20–30 μg) were separated by 10% SDS-PAGE, transferred onto an Immun-Blot PVDF membrane (Bio-rad) and blotted with Rap1A antibody (Santa Cruz Biotechnology, Inc. CA). GGTI- DU40 was used as the positive control inhibitor, tubulin (Sigma) was used as the loading control for the immunoblot and visualized by Western Lightning-ECL (Millipore).

4.6 Cell proliferation assay

MDA-MB-231 breast cancer cells were cultured in 96-well microplates (5000 cells per well) for 24 h and then treated with compounds at different concentrations ranging from 2 μM -32 μM for 48 h. The cytotoxicity of compounds in MDA-MB-231 cells was evaluated based on its effect on cell growth which was determined by using CellTiter 96® Aqueous One Solution Cell Proliferation Assay (Promega, Madison, WI) at 48 hours. Briefly, 10 μl of CellTiter 96 Aqueous One Solution Reagent was added into each well and incubated for 1 h at 37°C in a humidified 5% CO_2 incubator. The absorbance measurement was done at 490nm (Tecon Micro plate reader) and plotted in the graph using Prism. Each experiment was performed in triplicate and repeated three times. The cytotoxic effects of the extracts were estimated in terms of growth inhibition percentage and expressed as IC_{50} which is the concentration of compound which reduces the absorbance of treated cells by 50% with reference to the control (DMSO treated cells).

4.7 Computational methods

The crystal structure of the GGTase-I complexed with a GGPP Analog and a KKKSKTKCVIL peptide (PDB ID: 1N4Q) was employed in the docking calculations performed with Glide 6.2 (Schrodinger, LLC). Hydrogen atoms were added to the crystal structure, and the complex was submitted to a series of restrained, partial minimizations

using the OPLS-AA force field within the "Protein and Ligand Preparation" module of Glide. Two docking runs were performed, the first keeping the peptide KKKSKTKCVIL and the second by removing the peptide prior to the docking calculation. To compensate for the fixed protein structure, which is not expected to be optimal for a particular ligand, the van der Waals radii for nonpolar ligand atoms were scaled by a factor of 0.8, thereby decreasing penalties for close contacts. Receptor atoms were not scaled. For the protein preparation, grid generation, and ligand docking procedures, the default Glide settings were used. The compound **2** was preprocessed with the Glide module "LigPrep", which ensured proper protonation and tautomerization states. The compounds was docked and scored using the Glide standard precision (SP) mode and subsequently the extra precision (XP) mode. In essence, Glide performs a thorough conformational search for a ligand; then it determines all reasonable orientations ("poses") for each low-energy conformer in the designated binding site. In the process, torsional degrees of the ligand are relaxed, though the protein conformation is fixed. The SP "scoring function" is applied to judge the poses by considering, for example, hydrophobic and electrostatic interactions, hydrogen bonding, steric clashes, desolvation and internal energy of the ligand, and possible trapped or bridging water molecules in the binding site. In XP mode, the poses are further relaxed by complete energy minimizations. The resultant more accurate structures provide a basis for more detailed evaluation of contributions from explicit water molecules in the binding site and hydrophobic interactions.

CONCLUSION

In conclusion, we synthesized a series of pyrazole based GGTase-I inhibitors which are structural analogues of GGT1-DU40, a potent GGTase-I inhibitor. All synthesized compounds were evaluated for their *in vitro* inhibition against GGTase-I and FTase enzyme which revealed a clear trend of decreased inhibitory activity for propanamides (**6-16**) compared to butanamides (**2-5**). Among the tested compounds, **2** (IC_{50} = 2.4 µM) exhibited the highest activity and turned out to be more active than the control compound **1 (**DU40). In addition, the activity of **2** was slightly diminished, but yet comparable to **1**, when the fluoro moiety in **2** was replaced with a methoxy group to produce **5** (IC_{50} = 3.1 µM). The screening results of *in vitro* inhibition against FTase enzyme revealed that all the target compounds were inactive at 100 µM concentration which suggested that they are selective inhibitors of GGTase-I. The efficiency of the target compounds was further validated by western blot analysis in MDA-MB-231 cell line, which highlighted the very high inhibitory cellular activity of **2** and **5** compared to the control compound GGTI-DU40 (IC_{50} = 3.3 µM). The target compounds were also tested for the anti-proliferative efficacies against the MDA-MB-231 cell line which revealed significantly higher activity of **2** (IC_{50} = 7.6 µM) compared to **1** (IC_{50} = 23.0 µM). Molecular docking studies of **2** with the crystal structure of GGTase-I complexed with a GGPP Analog and a KKKSKTKCVIL peptide revealed several hydrogen-bonding interactions and π-π contacts between **2** and the binding pocket of GGTase-I. The optimized scaffold of **2**, showing increased potency merits its extensive in vivo investigation.

REFERENCES

[1] F.L.F. Zhang, P.P.J. Casey, Protein Prenylation: Molecular Mechanisms and Functional Consequences, Annu. Rev. Biochem. 65 (1996) 241–269. doi:10.1146/annurev.bi.65.070196.001325.

[2] M.C. Seabra, Membrane Association and Targeting of Prenylated Ras-like GTPases, Cell. Signal. 10 (1998) 167–172. doi:10.1016/S0898-6568(97)00120-4.

[3] J.A. Glomset, M.H. Gelb, C.C. Farnsworth, Prenyl proteins in eukaryotic cells: a new type of membrane anchor, Trends Biochem. Sci. 15 (1990) 139–142. doi:10.1016/0968-0004(90)90213-U.

[4] P.J. Casey, M.C. Seabra, Protein Prenyltransferases, J. Biol. Chem. 271 (1996) 5289–5292. doi:10.1074/jbc.271.10.5289.

[5] M.H. Gelb, L. Brunsveld, C.A. Hrycyna, S. Michaelis, F. Tamanoi, W.C. Van Voorhis, H. Waldmann, Therapeutic intervention based on protein prenylation and associated modifications, Nat. Chem. Biol. 2 (2006) 518–528. doi:10.1038/nchembio818.

[6] S. Maurer-Stroh, M. Koranda, W. Benetka, G. Schneider, F.L. Sirota, F. Eisenhaber, Towards Complete Sets of Farnesylated and Geranylgeranylated Proteins, PLoS Comput. Biol. 3 (2007) e66. doi:10.1371/journal.pcbi.0030066.

[7] H.W. Fu, P.J. Casey, Enzymology and biology of CaaX protein prenylation., Recent Prog. Horm. Res. 54 (1999) 315-42–3.

[8] J. Glomset, C. Farnsworth, Role of protein modification reactions in programming interactions between ras-related GTPases and cell membranes, Annu. Rev. Cell Biol. (1994).

[9] A.M. Winter-Vann, P.J. Casey, Opinion: Post-prenylation-processing enzymes as new targets in oncogenesis, Nat. Rev. Cancer. 5 (2005) 405–412. doi:10.1038/nrc1612.

[10] K. Yokoyama, M.H. Gelb, Purification of a mammalian protein geranylgeranyltransferase. Formation and catalytic properties of an enzyme-geranylgeranyl pyrophosphate complex., J. Biol. Chem. 268 (1993) 4055–60. http://www.ncbi.nlm.nih.gov/pubmed/8440698 (accessed June 21, 2016).

[11] T. Scott Reid, K.L. Terry, P.J. Casey, L.S. Beese, Crystallographic Analysis of CaaX Prenyltransferases Complexed with Substrates Defines Rules of Protein Substrate Selectivity, J. Mol. Biol. 343 (2004) 417–433. doi:10.1016/j.jmb.2004.08.056.

[12] M. Ashby, CaaX converting enzymes, Curr. Opin. Lipidol. (1998).

[13] N. Berndt, A.D. Hamilton, S.M. Sebti, Targeting protein prenylation for cancer therapy, Nat. Rev. Cancer. 11 (2011) 775–791. doi:10.1038/nrc3151.

[14] J.L. Bos, ras oncogenes in human cancer: a review., Cancer Res. 49 (1989) 4682–9.

[15] K. Kato, A.D. Cox, M.M. Hisaka, S.M. Graham, J.E. Buss, C.J. Der, Isoprenoid addition to Ras protein is the critical modification for its membrane association and transforming activity., Proc. Natl. Acad. Sci. U. S. A. 89 (1992) 6403–7.

[16] A.D. Basso, P. Kirschmeier, W.R. Bishop, Thematic review series: Lipid Posttranslational Modifications. Farnesyl transferase inhibitors, J. Lipid Res. 47 (2005) 15–31. doi:10.1194/jlr.R500012-JLR200.

[17] N.E. Kohl, C.A. Omer, M.W. Conner, N.J. Anthony, J.P. Davide, S.J. Desolms, E.A. Giuliani, R.P. Gomez, S.L. Graham, K. Hamilton, L.K. Handt, G.D. Hartman, K.S. Koblan, A.M. Kral, P.J. Miller, S.D. Mosser, T.J. O'Neill, E. Rands, M.D. Schaber, J.B. Gibbs, A. Oliff, Inhibition of farnesyltransferase induces regression of mammary and salivary carcinomas in ras transgenic mice, Nat. Med. 1 (1995) 792–797. doi:10.1038/nm0895-792.

[18] J.B. Gibbs, A. Oliff, N.E. Kohl, Farnesyltransferase inhibitors: Ras research yields a potential cancer therapeutic, Cell. 77 (1994) 175–178. doi:10.1016/0092-8674(94)90308-5.

[19] M.C. Seabra, Y. Reiss, P.J. Casey, M.S. Brown, J.L. Goldstein, Protein farnesyltransferase and geranylgeranyltransferase share a common α subunit, Cell. 65 (1991) 429–434. doi:10.1016/0092-8674(91)90460-G.

[20] K. Yokoyama, P. McGeady, M.H. Gelb, Mammalian Protein Geranylgeranyltransferase-I: Substrate Specificity, Kinetic Mechanism, Metal Requirements, and Affinity Labeling, (2002).

[21] W.J. Chen, J.F. Moomaw, L. Overton, T.A. Kost, P.J. Casey, High level expression of mammalian protein farnesyltransferase in a baculovirus system. The purified protein contains zinc., J. Biol. Chem. 268 (1993) 9675–80.

[22] P.J. Casey, Evidence for a Catalytic Role of Zinc in Protein Farnesyltransferase. Spectroscopy of Co^{2+}-Farnesyltransferase Indicates Metal Coordination of The Substrate Thiolate, J. Biol. Chem. 272 (1997) 20–23. doi:10.1074/jbc.272.1.20.

[23] D.L. Pompliano, E. Rands, M.D. Schaber, S.D. Mosser, N.J. Anthony, J.B. Gibbs, Steady-state kinetic mechanism of ras farnesyl:protein transferase, (2002).

[24] E.S. Furfine, J.J. Leban, A. Landavazo, J.F. Moomaw, P.J. Casey, Protein farnesyltransferase: kinetics of farnesyl pyrophosphate binding and product release, (2002).

[25] F.L. Zhang, J.F. Moomaw, P.J. Casey, Properties and kinetic mechanism of recombinant mammalian protein geranylgeranyltransferase type I., J. Biol. Chem. 269 (1994) 23465–70.

[26] J.S. Taylor, T.S. Reid, K.L. Terry, P.J. Casey, L.S. Beese, Structure of mammalian protein geranylgeranyltransferase type-I., EMBO J. 22 (2003) 5963–74. doi:10.1093/emboj/cdg571.

[27] E.S. Furfine, E.S. Furfine, P.J. Casey, Substrate Binding Is Required for Release of Product from Mammalian Protein Farnesyltransferase, J. Biol. Chem. 272 (1997) 9989–9993. doi:10.1074/jbc.272.15.9989.

[28] S.B. Long, P.J. Casey, L.S. Beese, Reaction path of protein farnesyltransferase at atomic resolution, Nature. 419 (2002) 645–650. doi:10.1038/nature00986.

[29] H.-W. Park, Crystal Structure of Protein Farnesyltransferase at 2.25 Angstrom Resolution, Science (80) 275 (1997) 1800–1805. doi:10.1126/science.275.5307.1800.

[30] S.B. Long, P.J. Casey, L.S. Beese, The basis for K-Ras4B binding specificity to protein farnesyl-transferase revealed by 2 Å resolution ternary complex structures, Structure. 8 (2000) 209–222. doi:10.1016/S0969-2126(00)00096-4.

[31] D.B.R. and, C.D. Poulter*, Yeast Protein Farnesyltransferase. pKas of Peptide Substrates Bound as Zinc Thiolates†, (1999). doi:10.1021/BI990794Y.

[32] W.-J. Chen$, J.F. Moomaw, L. Overton$, T.A. Kost$, P.J. Caseyfil, THE JOURNAL OF BIOLOGICAL CHEMISTRY High Level Expression of Mammalian Protein Farnesyltransferase in a Baculovirus System, 268 (1393) 9675–9680.

[33] Y. Reiss, M.S. Brown, J.L. Goldstein, Divalent cation and prenyl pyrophosphate specificities of the protein farnesyltransferase from rat brain, a zinc metalloenzyme., J. Biol. Chem. 267 (1992) 6403–8.

[34] C. Huang, K.E. Hightower, C.A. Fierke, Mechanistic studies of rat protein farnesyltransferase indicate an associative transition state., Biochemistry. 39 (2000) 2593–602. http://www.ncbi.nlm.nih.gov/pubmed/10704208 (accessed April 16, 2017).

[35] Y. Reiss, J.L. Goldstein, M.C. Seabra, P.J. Casey, M.S. Brown, Inhibition of purified p21ras farnesyl:protein transferase by Cys-AAX tetrapeptides, Cell. 62 (1990) 81–88. doi:10.1016/0092-8674(90)90242-7.

[36] X. Li, L. Liu, J.C. Tupper, D.D. Bannerman, R.K. Winn, S.M. Sebti, A.D. Hamilton, J.M. Harlan, Inhibition of Protein Geranylgeranylation and RhoA/RhoA Kinase Pathway Induces Apoptosis in Human Endothelial Cells, J. Biol. Chem. 277 (2002) 15309–15316. doi:10.1074/jbc.M201253200.

[37] F.L. Zhang, P.J. Casey, Influence of metal ions on substrate binding and catalytic activity of mammalian protein geranylgeranyltransferase type-I., Biochem. J. (1996) 925–32.

[38] M. Malumbres, M. Barbacid, Timeline: RAS oncogenes: the first 30 years, Nat. Rev. Cancer. 3 (2003) 459–465. doi:10.1038/nrc1097.

[39] E.A. Clark, T.R. Golub, E.S. Lander, R.O. Hynes, Genomic analysis of metastasis reveals an essential role for RhoC., Nature. 406 (2000) 532–5. doi:10.1038/35020106.

[40] A. Hakem, O. Sanchez-Sweatman, A. You-Ten, G. Duncan, A. Wakeham, R. Khokha, T.W. Mak, RhoC is dispensable for embryogenesis and tumor initiation but essential for metastasis., Genes Dev. 19 (2005) 1974–9. doi:10.1101/gad.1310805.

[41] K.-H. Lim, A.T. Baines, J.J. Fiordalisi, M. Shipitsin, L.A. Feig, A.D. Cox, C.J. Der, C.M. Counter, Activation of RalA is critical for Ras-induced tumorigenesis of human cells, Cancer Cell. 7 (2005) 533–545. doi:10.1016/j.ccr.2005.04.030.

[42] J.E. Lancet, J.D. Rosenblatt, J.E. Karp, Farnesyltransferase inhibitors and myeloid malignancies: Phase I evidence of Zarnestra activity in high-risk leukemias, Semin. Hematol. 39 (2002) 31–35. doi:10.1053/shem.2002.35985.

[43] J.E. Karp, J.E. Lancet, Development of Farnesyltransferase Inhibitors for Clinical Cancer Therapy: Focus on Hematologic Malignancies, Cancer Invest. 25 (2007) 484–494. doi:10.1080/07357900701359437.

[44] W.-Z. Gu, I. Joseph, Y.-C. Wang, D. Frost, G.M. Sullivan, L. Wang, N.-H. Lin, J. Cohen, V.S. Stoll, C.G. Jakob, S.W. Muchmore, J.E. Harlan, T. Holzman, K.A. Walten, U.S. Ladror, M.G. Anderson, P. Kroeger, L.E. Rodriguez, K.P. Jarvis, D. Ferguson, K. Marsh, S. Ng, S.H. Rosenberg, H.L. Sham, H. Zhang, A highly potent and selective farnesyltransferase inhibitor ABT-100 in preclinical studies., Anticancer. Drugs. 16 (2005) 1059–69.

[45] R.J. Doll, P. Kirschmeier, W.R. Bishop, Farnesyltransferase inhibitors as anticancer agents: critical crossroads., Curr. Opin. Drug Discov. Devel. 7 (2004) 478–86.

[46] A.D. Cox, C.J. Der, Farnesyltransferase inhibitors: promises and realities., Curr. Opin. Pharmacol. 2 (2002) 388–93.

[47] P.F. Lebowitz, G.C. Prendergast, Non-Ras targets of farnesyltransferase inhibitors: focus on Rho, Oncogene. 17 (1998) 1439–1445. doi:10.1038/sj.onc.1202175.

[48] G.L. James, J.L. Goldstein, M.S. Brown, Polylysine and CVIM sequences of K-RasB dictate specificity of prenylation and confer resistance to benzodiazepine peptidomimetic in vitro., J. Biol. Chem. 270 (1995) 6221–6. doi:10.1074/JBC.270.11.6221.

[49] D.B. Whyte, P. Kirschmeier, T.N. Hockenberry, I. Nunez-Oliva, L. James, J.J. Catino, W.R. Bishop, J.-K. Pai, K- and N-Ras Are Geranylgeranylated in Cells

Treated with Farnesyl Protein Transferase Inhibitors, J. Biol. Chem. 272 (1997) 14459–14464. doi:10.1074/jbc.272.22.14459.

[50] E.C. Lerner, T.-T. Zhang, D.B. Knowles, Y. Qian, A.D. Hamilton, S.M. Sebti, Inhibition of the prenylation of K-Ras, but not H- or N-Ras, is highly resistant to CAAX peptidomimetics and requires both a farnesyltransferase and a geranylgeranyltransferase I inhibitor in human tumor cell lines, Oncogene. 15 (1997) 1283–1288. doi:10.1038/sj.onc.1201296.

[51] S.M. Sebti, A.D. Hamilton, Farnesyltransferase and geranylgeranyltransferase I inhibitors in cancer therapy: important mechanistic and bench to bedside issues, Expert Opin. Investig. Drugs. 9 (2000) 2767–2782. doi:10.1517/13543784.9.12.2767.

[52] F. El Oualid, L. H. Cohen, G.A. van der Marel, M. Overhand, Inhibitors of Protein: Geranylgeranyl Transferases, (n.d.).

[53] D. Chakrabarti, T. Da Silva, J. Barger, S. Paquette, H. Patel, S. Patterson, C.M. Allen, Protein Farnesyltransferase and Protein Prenylation inPlasmodium falciparum, J. Biol. Chem. 277 (2002) 42066–42073. doi:10.1074/jbc.M202860200.

[54] S.M. Sagan, Y. Rouleau, C. Leggiadro, L. Supekova, P.G. Schultz, A.I. Su, J.P. Pezacki, The influence of cholesterol and lipid metabolism on host cell structure and hepatitis C virus replication, Biochem. Cell Biol. 84 (2006) 67–79. doi:10.1139/o05-149.

[55] J. Sun, Y. Qian, Z. Chen, J. Marfurt, A.D. Hamilton, S.M. Sebti, The Geranylgeranyltransferase I Inhibitor GGTI-298 Induces Hypophosphorylation of Retinoblastoma and Partner Switching of Cyclin-dependent Kinase Inhibitors: A potential mechanism for GGTI-298 antitumor activity, J. Biol. Chem. 274 (1999) 6930–6934. doi:10.1074/jbc.274.11.6930.

[56] A. Vogt, J. Sun, Y. Qian, A.D. Hamilton, S.M. Sebti, The Geranylgeranyltransferase-I Inhibitor GGTI-298 Arrests Human Tumor Cells in G0/G1 and Induces p21WAF1/CIP1/SDI1 in a p53-independent Manner, J. Biol. Chem. 272 (1997) 27224–27229. doi:10.1074/jbc.272.43.27224.

[57] H.C. Dan, K. Jiang, D. Coppola, A. Hamilton, S. V Nicosia, S.M. Sebti, J.Q. Cheng, Phosphatidylinositol-3-OH kinase/AKT and survivin pathways as critical targets for geranylgeranyltransferase I inhibitor-induced apoptosis, Oncogene. 23 (2004) 706–715. doi:10.1038/sj.onc.1207171.

[58] M.A. Morgan, J. Wegner, E. Aydilek, A. Ganser, C.W.M. Reuter, Synergistic cytotoxic effects in myeloid leukemia cells upon cotreatment with farnesyltransferase and geranylgeranyl transferase-I inhibitors, Leukemia. 17 (2003) 1508–1520. doi:10.1038/sj.leu.2403022.

[59] P.J. Casey, P.A. Solski, C.J. Der, J.E. Buss, p21ras is modified by a farnesyl isoprenoid., Proc. Natl. Acad. Sci. 86 (1989) 8323–8327. doi:10.1073/pnas.86.21.8323.

[60] A. Kazi, A. Carie, M.A. Blaskovich, C. Bucher, V. Thai, S. Moulder, H. Peng, D. Carrico, E. Pusateri, W.J. Pledger, N. Berndt, A. Hamilton, S.M. Sebti, Blockade of

protein geranylgeranylation inhibits Cdk2-dependent p27Kip1 phosphorylation on Thr187 and accumulates p27Kip1 in the nucleus: implications for breast cancer therapy., Mol. Cell. Biol. 29 (2009) 2254–63. doi:10.1128/MCB.01029-08.

[61] H.-J. Park, D. Kong, L. Iruela-Arispe, U. Begley, D. Tang, J.B. Galper, 3-Hydroxy-3-Methylglutaryl Coenzyme A Reductase Inhibitors Interfere With Angiogenesis by Inhibiting the Geranylgeranylation of RhoA, Circ. Res. 91 (2002) 143–150. doi:10.1161/01.RES.0000028149.15986.4C.

[62] S. Dasgupta, I. Cushman, M. Kpetemey, P.J. Casey, J.K. Vishwanatha, Prenylated C17orf37 Induces Filopodia Formation to Promote Cell Migration and Metastasis, J. Biol. Chem. 286 (2011) 25935–25946. doi:10.1074/jbc.M111.254599.

[63] T.S. Jones, E.C. Holland, Standard of care therapy for malignant glioma and its effect on tumor and stromal cells, Oncogene. 31 (2012) 1995–2006. doi:10.1038/onc.2011.398.

[64] X. Zhou, J. Qian, L. Hua, Q. Shi, Z. Liu, Y. Xu, B. Sang, J. Mo, R. Yu, Geranylgeranyltransferase I Promotes Human Glioma Cell Growth through Rac1 Membrane Association and Activation, J. Mol. Neurosci. 49 (2013) 130–139. doi:10.1007/s12031-012-9905-3.

[65] B. Han, N. Fujimoto, M. Kobayashi, T. Matsumoto, B. Han, N. Fujimoto, M. Kobayashi, T. Matsumoto, Synergistic Effect of Geranylgeranyltransferase Inhibitor, GGTI, and Docetaxel on the Growth of Prostate Cancer Cells, Prostate Cancer. 2012 (2012) 1–6. doi:10.1155/2012/989214.

[66] Y.K. Peterson, P. Kelly, C.A. Weinbaum, P.J. Casey, A Novel Protein Geranylgeranyltransferase-I Inhibitor with High Potency, Selectivity, and Cellular Activity, J. Biol. Chem. 281 (2006) 12445–12450. doi:10.1074/jbc.M600168200.

[67] A.-K.M. Sjogren, K.M.E. Andersson, M. Liu, B.A. Cutts, C. Karlsson, A.M. Wahlstrom, M. Dalin, C. Weinbaum, P.J. Casey, A. Tarkowski, B. Swolin, S.G. Young, M.O. Bergo, GGTase-I deficiency reduces tumor formation and improves survival in mice with K-RAS–induced lung cancer, J. Clin. Invest. 117 (2007) 1294–1304. doi:10.1172/JCI30868.

[68] J. Sun, Y. Qian, A.D. Hamilton, S.M. Sebti, Both farnesyltransferase and geranylgeranyltransferase I inhibitors are required for inhibition of oncogenic K-Ras prenylation but each alone is sufficient to suppress human tumor growth in nude mouse xenografts, 16 (1998) 1467–1473.

[69] J. Sun, M.A. Blaskovich, D. Knowles, Y. Qian, J. Ohkanda, R.D. Bailey, A.D. Hamilton, S.M. Sebti, Antitumor efficacy of a novel class of non-thiol-containing peptidomimetic inhibitors of farnesyltransferase and geranylgeranyltransferase I: combination therapy with the cytotoxic agents cisplatin, Taxol, and gemcitabine., Cancer Res. 59 (1999) 4919–26. doi:10.1016/s0163-7258(97)00014-4.

[70] A.B. Jaffe, A. Hall, Rho GTPases in transformation and metastasis, in: 2002: pp. 57–80. doi:10.1016/S0065-230X(02)84003-9.

[71] E. Sahai, C.J. Marshall, RHO–GTPASES AND CANCER, Nat. Rev. Cancer. 2 (2002) 133–142. doi:10.1038/nrc725.

[72] B. Sivakumar, L.E. Harry, E.M. Paleolog, Modulating Angiogenesis, JAMA. 292 (2004) 972. doi:10.1001/jama.292.8.972.

[73] J. Greenwood, C.E. Walters, G. Pryce, N. Kanuga, E. Beraud, D. Baker, P. Adamson, Lovastatin inhibits brain endothelial cell Rho-mediated lymphocyte migration and attenuates experimental autoimmune encephalomyelitis, FASEB J. 17 (2003) 905–7. doi:10.1096/fj.02-1014fje.

[74] C.E. Walters, G. Pryce, D.J.R. Hankey, S.M. Sebti, A.D. Hamilton, D. Baker, J. Greenwood, P. Adamson, Inhibition of Rho GTPases with protein prenyltransferase inhibitors prevents leukocyte recruitment to the central nervous system and attenuates clinical signs of disease in an animal model of multiple sclerosis., J. Immunol. 168 (2002) 4087–94.

[75] C. Wang, M. Gale, B.C. Keller, H. Huang, M.S. Brown, J.L. Goldstein, J. Ye, Identification of FBL2 As a Geranylgeranylated Cellular Protein Required for Hepatitis C Virus RNA Replication, Mol. Cell. 18 (2005) 425–434. doi:10.1016/j.molcel.2005.04.004.

[76] J. Ye, C. Wang, R. Sumpter, M.S. Brown, J.L. Goldstein, M. Gale, Disruption of hepatitis C virus RNA replication through inhibition of host protein geranylgeranylation, Proc. Natl. Acad. Sci. 100 (2003) 15865–15870. doi:10.1073/pnas.2237238100.

[77] A. Vasudevan, Y. Qian, A. Vogt, M.A. Blaskovich, J. Ohkanda, S.M. Sebti, A.D. Hamilton, Potent, Highly Selective, and Non-Thiol Inhibitors of Protein

Geranylgeranyltransferase-I, J. Med. Chem. 42 (1999) 1333–1340. doi:10.1021/jm9900873.

[78] D. Carrico, M.A. Blaskovich, C.J. Bucher, S.M. Sebti, A.D. Hamilton, Design, synthesis, and evaluation of potent and selective benzoyleneurea-based inhibitors of protein geranylgeranyltransferase-I, Bioorg. Med. Chem. 13 (2005) 677–688. doi:10.1016/j.bmc.2004.10.053.

[79] H. Peng, D. Carrico, V. Thai, M. Blaskovich, C. Bucher, E.E. Pusateri, S.M. Sebti, A.D. Hamilton, L.S. Beese, P.C. Weber, H. Iwmara, S. Yamazaki, Y. Arai, M. Kawamura, D.C. Heimbrook, Synthesis and evaluation of potent, highly-selective, 3-aryl-piperazinone inhibitors of protein geranylgeranyltransferase-I, Org. Biomol. Chem. 4 (2006) 1768. doi:10.1039/b517572k.

[80] Sabrina Castellano, † Hannah D. G. Fiji, † Sape S. Kinderman, ‡ Masaru Watanabe, Pablo de Leon, ‡ and Fuyuhiko Tamanoi, † Ohyun Kwon*, Small-Molecule Inhibitors of Protein Geranylgeranyltransferase Type I, (2007). doi:10.1021/JA070274N.

[81] M. Watanabe, H.D.G. Fiji, L. Guo, L. Chan, S.S. Kinderman, D.J. Slamon, O. Kwon, F. Tamanoi, Inhibitors of Protein Geranylgeranyltransferase I and Rab Geranylgeranyltransferase Identified from a Library of Allenoate-derived Compounds, J. Biol. Chem. 283 (2008) 9571–9579. doi:10.1074/jbc.M706229200.

[82] J. Lu, L. Chan, H.D.G. Fiji, R. Dahl, O. Kwon, F. Tamanoi, In vivo antitumor effect of a novel inhibitor of protein geranylgeranyltransferase-I, Mol. Cancer Ther. 8 (2009) 1218–1226. doi:10.1158/1535-7163.MCT-08-1122.

[83] T.F. McGuire, Y. Qian, A. Vogt, A.D. Hamilton, S.M. Sebti, Platelet-derived growth factor receptor tyrosine phosphorylation requires protein geranylgeranylation but not farnesylation., J. Biol. Chem. 271 (1996) 27402–7. doi:10.1074/JBC.271.44.27402.

[84] S. Machida, K. Usuba, M.A. Blaskovich, A. Yano, K. Harada, S.M. Sebti, N. Kato, J. Ohkanda, Module Assembly for Protein-Surface Recognition: Geranylgeranyltransferase I Bivalent Inhibitors for Simultaneous Targeting of Interior and Exterior Protein Surfaces, Chem. - A Eur. J. 14 (2008) 1392–1401. doi:10.1002/chem.200701634.

[85] M. Thippanna, P.A. Subramani, D. Lomada, V.R. Narala, M.C. Reddy, A Homology Based Model and Virtual Screening of Inhibitors for Human Geranylgeranyl Transferase 1 (GGTase1)., Bioinformation. 9 (2013) 973–7. doi:10.6026/97320630009973.

[86] R.C. Gallo, J. Whang-Peng, R.H. Adamson, Studies on the antitumor activity, mechanism of action, and cell cycle effects of camptothecin., J. Natl. Cancer Inst. 46 (1971) 789–95.

[87] P.A. Subramani, V.R. Narala, Challenges of curcumin bioavailability: novel aerosol remedies., Nat. Prod. Commun. 8 (2013) 121–4. http://www.ncbi.nlm.nih.gov/pubmed/23472475 (accessed April 17, 2017).

[88] Y.K. Peterson, X.S. Wang, P.J. Casey, A. Tropsha, Discovery of Geranylgeranyltransferase-I Inhibitors with Novel Scaffolds by the Means of Quantitative Structure−Activity Relationship Modeling, Virtual Screening, and

Experimental Validation, J. Med. Chem. 52 (2009) 4210–4220. doi:10.1021/jm8013772.

[89] K.M. Sane, M. Mynderse, D.T. LaLonde, I.S. Dean, J.W. Wojtkowiak, F. Fouad, R.F. Borch, J.J. Reiners, R.A. Gibbs, R.R. Mattingly, A Novel Geranylgeranyl Transferase Inhibitor in Combination with Lovastatin Inhibits Proliferation and Induces Autophagy in STS-26T MPNST Cells, J. Pharmacol. Exp. Ther. 333 (2010) 23–33. doi:10.1124/jpet.109.160192.

[90] L.N. Chan, H.D.G. Fiji, M. Watanabe, O. Kwon, F. Tamanoi, Identification and Characterization of Mechanism of Action of P61-E7, a Novel Phosphine Catalysis-Based Inhibitor of Geranylgeranyltransferase-I, PLoS One. 6 (2011) e26135. doi:10.1371/journal.pone.0026135.

[91] M. Hamada, T. Miki, S. Iwai, H. Shimizu, Y. Yura, Involvement of RhoA and RalB in geranylgeranyltransferase I inhibitor-mediated inhibition of proliferation and migration of human oral squamous cell carcinoma cells, Cancer Chemother. Pharmacol. 68 (2011) 559–569. doi:10.1007/s00280-010-1520-9.

[92] S.S. Virtanen, J. Sandholm, G. Yegutkin, H. Kalervo Väänänen, P.L. Härkönen, Inhibition of GGTase-I and FTase disrupts cytoskeletal organization of human PC-3 prostate cancer cells, Cell Biol. Int. 34 (2010) 815–826. doi:10.1042/CBI20090288.

[93] T. Kusama, M. Mukai, M. Tatsuta, Y. Matsumoto, H. Nakamura, M. Inoue, Selective inhibition of cancer cell invasion by a geranylgeranyltransferase-I inhibitor., Clin. Exp. Metastasis. 20 (2003) 561–7.

[94] V. Pries, S. Cotesta, R. Riedl, T. Aust, S. Schuierer, J. Tao, I. Filipuzzi, D. Hoepfner, Advantages and Challenges of Phenotypic Screens, J. Biomol. Screen. 21 (2016) 306–315. doi:10.1177/1087057115610488.

[95] V.S. Wills, J.I. Metzger, C. Allen, M.L. Varney, D.F. Wiemer, S.A. Holstein, Bishomoisoprenoid triazole bisphosphonates as inhibitors of geranylgeranyl diphosphate synthase, Bioorg. Med. Chem. 25 (2017) 2437–2444. doi:10.1016/j.bmc.2017.02.066.

[96] J. Sun, J. Ohkanda, D. Coppola, H. Yin, M. Kothare, B. Busciglio, A.D. Hamilton, S.M. Sebti, Geranylgeranyltransferase I Inhibitor GGTI-2154 Induces Breast Carcinoma Apoptosis and Tumor Regression in H-Ras Transgenic Mice, Cancer Res. 63 (2003) 8922–8929.

[97] N.M.G.M. Appels, M.J. Bolijn, K. Chan, T.C. Stephens, G. Hoctin-Boes, M. Middleton, J.H. Beijnen, J.S. de Bono, A.L. Harris, J.H.M. Schellens, Phase I pharmacokinetic and pharmacodynamic study of the prenyl transferase inhibitor AZD3409 in patients with advanced cancer, Br. J. Cancer. 98 (2008) 1951–1958. doi:10.1038/sj.bjc.6604402.

[98] M.A. Morgan, T. Sebil, E. Aydilek, D. Peest, A. Ganser, C.W.M. Reuter, Combining prenylation inhibitors causes synergistic cytotoxicity, apoptosis and disruption of RAS-to-MAP kinase signalling in multiple myeloma cells, Br. J. Haematol. 130 (2005) 912–925. doi:10.1111/j.1365-2141.2005.05696.x.

[99] H. Edamatsu, C.-L. Gau, T. Nemoto, L. Guo, F. Tamanoi, Cdk inhibitors, roscovitine and olomoucine, synergize with farnesyltransferase inhibitor (FTI) to induce

efficient apoptosis of human cancer cell lines, Oncogene. 19 (2000) 3059–3068. doi:10.1038/sj.onc.1203625.

[100] S.J. Heasman, A.J. Ridley, Mammalian Rho GTPases: new insights into their functions from in vivo studies, Nat. Rev. Mol. Cell Biol. 9 (2008) 690–701. doi:10.1038/nrm2476.

[101] J. Greenwood, L. Steinman, S.S. Zamvil, Statin therapy and autoimmune disease: from protein prenylation to immunomodulation, Nat. Rev. Immunol. 6 (2006) 358–370. doi:10.1038/nri1839.

[102] A.M. Connor, S. Berger, A. Narendran, E.C. Keystone, No Title, Arthritis Res. Ther. 8 (2006) R94. doi:10.1186/ar1968.

[103] T. Nagashima, H. Okazaki, K. Yudoh, H. Matsuno, S. Minota, Apoptosis of rheumatoid synovial cells by statins through the blocking of protein geranylgeranylation: A potential therapeutic approach to rheumatoid arthritis, Arthritis Rheum. 54 (2006) 579–586. doi:10.1002/art.21564.

[104] M.K. Jain, P.M. Ridker, Anti-Inflammatory Effects of Statins: Clinical Evidence and Basic Mechanisms, Nat. Rev. Drug Discov. 4 (2005) 977–987. doi:10.1038/nrd1901.

[105] L. Li, W. Zhang, S. Cheng, D. Cao, M. Parent, Isoprenoids and Related Pharmacological Interventions: Potential Application in Alzheimer's Disease, Mol. Neurobiol. 46 (2012) 64–77. doi:10.1007/s12035-012-8253-1.

[106] O.M. Khan, M.K. Akula, K. Skalen, C. Karlsson, M. Stahlman, S.G. Young, J. Boren, M.O. Bergo, Targeting GGTase-I Activates RHOA, Increases Macrophage

Reverse Cholesterol Transport, and Reduces Atherosclerosis in Mice, Circulation. 127 (2013) 782–790. doi:10.1161/CIRCULATIONAHA.112.000588.

[107] C.B. Nichols, J. Ferreyra, E.R. Ballou, J.A. Alspaugh, Subcellular Localization Directs Signaling Specificity of the Cryptococcus neoformans Ras1 Protein, Eukaryot. Cell. 8 (2009) 181–189. doi:10.1128/EC.00351-08.

[108] K. Selvig, E.R. Ballou, C.B. Nichols, J.A. Alspaugh, Restricted Substrate Specificity for the Geranylgeranyltransferase-I Enzyme in Cryptococcus neoformans: Implications for Virulence, Eukaryot. Cell. 12 (2013) 1462–1471. doi:10.1128/EC.00193-13.

[109] M.A. Hast, L.S. Beese, Structure of Protein Geranylgeranyltransferase-I from the Human Pathogen Candida albicans Complexed with a Lipid Substrate, J. Biol. Chem. 283 (2008) 31933–31940. doi:10.1074/jbc.M805330200.

[110] D.J. Mackay, A. Hall, Rho GTPases., J. Biol. Chem. 273 (1998) 20685–8.

[111] F. Imamura, M. Mukai, M. Ayaki, K. Takemura, T. Horai, K. Shinkai, H. Nakamura, H. Akedo, Involvement of small GTPases Rho and Rac in the invasion of rat ascites hepatoma cells., Clin. Exp. Metastasis. 17 (1999) 141–8.

[112] M.A. Chotani, K. Touhalisky, I.-M. Chiu, The Small GTPases Ras, Rac, and Cdc42 Transcriptionally Regulate Expression of Human Fibroblast Growth Factor 1, J. Biol. Chem. 275 (2000) 30432–30438. doi:10.1074/jbc.M003545200.

[113] A. Vogt, J. Sun, Y. Qian, A.D. Hamilton, S.M. Sebti, The geranylgeranyltransferase-I inhibitor GGTI-298 arrests human tumor cells in G0/G1 and induces

p21(WAF1/CIP1/SDI1) in a p53-independent manner., J. Biol. Chem. 272 (1997) 27224–9.

[114] S.M. Sebti, A.D. Hamilton, Farnesyltransferase and geranylgeranyltransferase I inhibitors and cancer therapy: Lessons from mechanism and bench-to-bedside translational studies, Oncogene. 19 (2000) 6584–6593. doi:10.1038/sj.onc.1204146.

[115] J. Lu, K. Yoshimura, K. Goto, C. Lee, K. Hamura, O. Kwon, F. Tamanoi, Nanoformulation of Geranylgeranyltransferase-I Inhibitors for Cancer Therapy: Liposomal Encapsulation and pH-Dependent Delivery to Cancer Cells, PLoS One. 10 (2015) e0137595. doi:10.1371/journal.pone.0137595.

[116] J. Iqbal, N.D. Tangellamudi, B. Dulla, S. Balasubramanian, Sequential C–N and C–O Bond Formation in a Single Pot: Synthesis of 2 H -Benzo[b][1,4]oxazines from 2,5-Dihydroxybenzaldehyde and Amino acid Precursors, Org. Lett. 14 (2012) 552–555.

[117] O.P. Horlacher, R.C. Hartkoorn, S.T. Cole, K.-H. Altmann, Synthesis and Antimycobacterial Activity of 2,1′-Dihydropyridomycins, ACS Med. Chem. Lett. 4 (2013) 264–268. doi:10.1021/ml300385q.

[118] A. Boyd, Steven, S. Miller, A. Thomas, R. Xu, Y. Lehuerou, I. Gunawardana, G. Zhang, J. Demeese, M. Mclaughlin, M. Yanik, J. Lupher, Mark, L., C. Jacobson, Irina, D. Thorsett, Eugene, S. Farouz, Francine, A. Kasar, Ramesh, Acrylamide Derivatives as Vla-1 Integrin Antagonists and Uses Thereof, (2005) WO2005016883A3.

[119] A.N. Hulme, E.M. Rosser, An Aldol-Based Approach to the Synthesis of the Antibiotic Anisomycin, Org. Lett. 4 (2002) 265–267. doi:10.1021/ol017016u.

[120] M.P. Bosch, F. Campos, I. Niubo, G. Rosell, J.L. Dı, J. Brea, M.I. Loza, Synthesis and Biological Activity of New Potential Agonists for the Human Adenosine A 2A Receptor, J. Med. Chem. 47 (2004) 4041–4053. doi:10.1021/jm031143.

[121] C.L. Millington, A.J. Watson, A.S. Marriott, G.P. Margison, A.C. Povey, D.M. Williams, Convenient and Efficient Syntheses of Oligodeoxyribonucleotides Containing O 6 -(Carboxymethyl)Guanine and O 6 -(4-Oxo-4-(3-Pyridyl)Butyl)Guanine, Nucleosides, Nucleotides and Nucleic Acids. 31 (2012) 328–338. doi:10.1080/15257770.2012.656784.

[122] C.P.V. M. G. Campbell, Z. Guo, F. F. Li, K. S. Rehder, J-P. Strachan, Prenylation inhibitors and methods of their synthesis and use, (2003).

[123] K. Guzow, R. Ganzynkowicz, A. Rzeska, J. Mrozek, M. Szabelski, J. Karolczak, A. Liwo, W. Wiczk, Photophysical Properties of Tyrosine and Its Simple Derivatives Studied by Time-Resolved Fluorescence Spectroscopy, Global Analysis, and Theoretical Calculations, J. Phys. Chem. B. 108 (2004) 3879–3889. doi:10.1021/jp036721c.

[124] N.-N. Liu, S.-M. Zhao, J.-F. Zhao, G.-Z. Zeng, N.-H. Tan, J.-P. Liu, Synthesis and conformation studies of rubiyunnanin B analogs, Tetrahedron. 70 (2014) 6630–6640. doi:10.1016/j.tet.2014.06.108.

[125] G.W. Hardy, L.A. Lowe, G. Mills, P.Y. Sang, D.S.A. Simpkin, R.L. Follenfant, C. Shankley, T.W. Smith, Peripherally acting enkephalin analogs. 2. Polar tri- and tetrapeptides, J. Med. Chem. 32 (1989) 1108–1118. doi:10.1021/jm00125a028.

[126] G. Naturale, M. Lamblin, C. Commandeur, F.-X. Felpin, J. Dessolin, Direct C-H Alkylation of Naphthoquinones with Amino Acids Through a Revisited Kochi-Anderson Radical Decarboxylation: Trends in Reactivity and Applications, European J. Org. Chem. 2012 (2012) 5774–5788. doi:10.1002/ejoc.201200722.

[127] T. Poloński, Optical activity of lactones and lactams-III, Tetrahedron. 41 (1985) 603–609. doi:10.1016/S0040-4020(01)96506-8.

[128] J.A. Olsen, D.W. Banner, P. Seiler, B. Wagner, T. Tschopp, U. Obst-Sander, M. Kansy, K. Müller, F. Diederich, Fluorine Interactions at the Thrombin Active Site: Protein Backbone Fragments H□Cα□C□O Comprise a Favorable C□F Environment and Interactions of C□F with Electrophiles, ChemBioChem. 5 (2004) 666–675. doi:10.1002/cbic.200300907.

[129] R.A. Friesner, J.L. Banks, R.B. Murphy, T.A. Halgren, J.J. Klicic, D.T. Mainz, M.P. Repasky, E.H. Knoll, M. Shelley, J.K. Perry, D.E. Shaw, P. Francis, P.S. Shenkin, Glide: A New Approach for Rapid, Accurate Docking and Scoring. 1. Method and Assessment of Docking Accuracy, J. Med. Chem. 47 (2004) 1739–1749. doi:10.1021/jm0306430.

[130] R.A. Friesner, R.B. Murphy, M.P. Repasky, L.L. Frye, J.R. Greenwood, T.A. Halgren, P.C. Sanschagrin, D.T. Mainz, Extra Precision Glide: Docking and Scoring

Incorporating a Model of Hydrophobic Enclosure for Protein−Ligand Complexes, J. Med. Chem. 49 (2006) 6177–6196. doi:10.1021/jm051256o.

[131] A. Nagai, J. Ishikawa, H. Kudo, T. Endo, Synthesis of optically active polyurethanes by self-polyaddition of tyrosine-based monomers, J. Polym. Sci. Part A Polym. Chem. 42 (2004) 1143–1153. doi:10.1002/pola.11047.

[132] S. Liu, Y. Yang, C. Zhao, J. Huang, C. Han, J. Han, Effect of the 4′-substituted phenylalanine moiety of sansalvamide A peptide on antitumor activity, Medchemcomm. 5 (2014) 463. doi:10.1039/c3md00294b.

[133] H. Liu, L. Zhao, Y. Yuan, Z. Xu, K. Chen, S. Qiu, H. Tan, Potassium Thioacids Mediated Selective Amide and Peptide Constructions Enabled by Visible Light Photoredox Catalysis, ACS Catal. 6 (2016) 1732–1736. doi:10.1021/acscatal.5b02943.

[134] A.J. Pearson, P.R. Bruhn, S.Y. Hsu, Preparation of diaryl ethers from tyrosine or 4-hydroxyphenylglycine using organomanganese chemistry, J. Org. Chem. 51 (1986) 2137–2139. doi:10.1021/jo00361a043.

[135] C. Wolf, C.J. Francis, P.A. Hawes, M. Shah, Enantioselective alkylation of aldehydes promoted by (S)-tyrosine-derived β-amino alcohols, Tetrahedron: Asymmetry. 13 (2002) 1733–1741. doi:10.1016/S0957-4166(02)00469-X.

[136] H.M. Betts, S. Milicevic Sephton, C. Tong, R.O. Awais, P.J. Hill, A.C. Perkins, F.I. Aigbirhio, Synthesis, in Vitro Evaluation, and Radiolabeling of Fluorinated

Puromycin Analogues: Potential Candidates for PET Imaging of Protein Synthesis, J. Med. Chem. 59 (2016) 9422–9430.

ANNEXURE

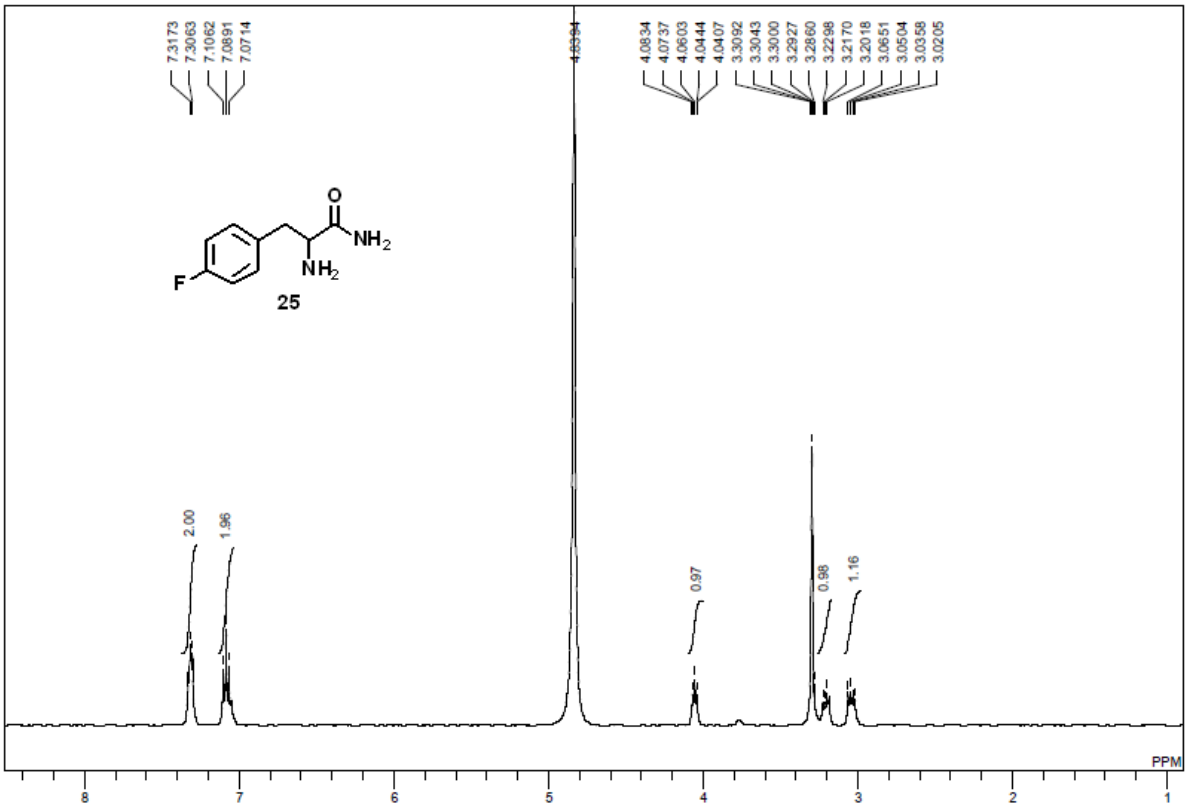
7.3173
7.3063
7.1062
7.0891
7.0714
4.0834
4.0737
4.0603
4.0444
4.0407
3.3092
3.3043
3.3000
3.2927
3.2860
3.2298
3.2170
3.2018
3.0651
3.0504
3.0358
3.0205
2.00
1.96
0.97
0.98
1.16
NH2
NH2
F
O
25
PPM

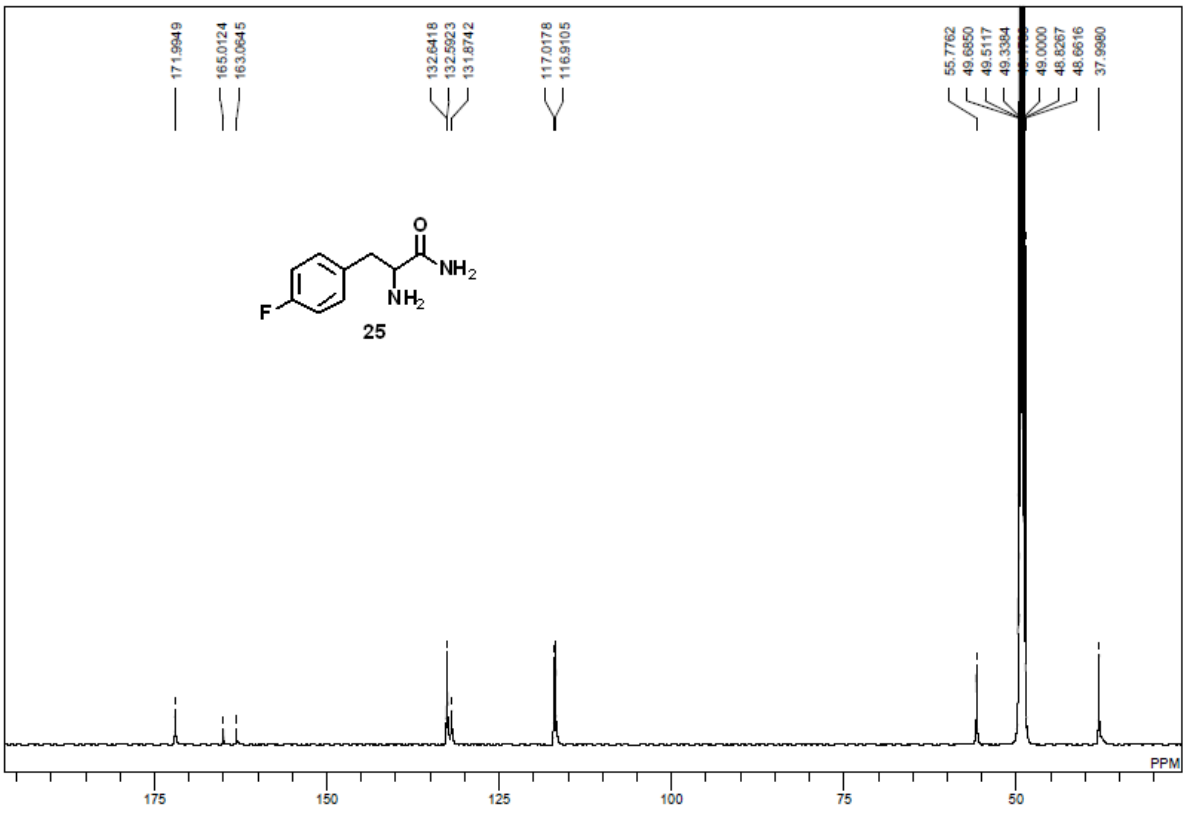
171.9849
165.0124
163.0645
132.6418
132.5923
131.8742
117.0178
116.9105
55.7762
49.6850
49.5117
49.3384
49.0000
48.8267
48.6616
37.9980
NH2
NH2
F
O
25
PPM

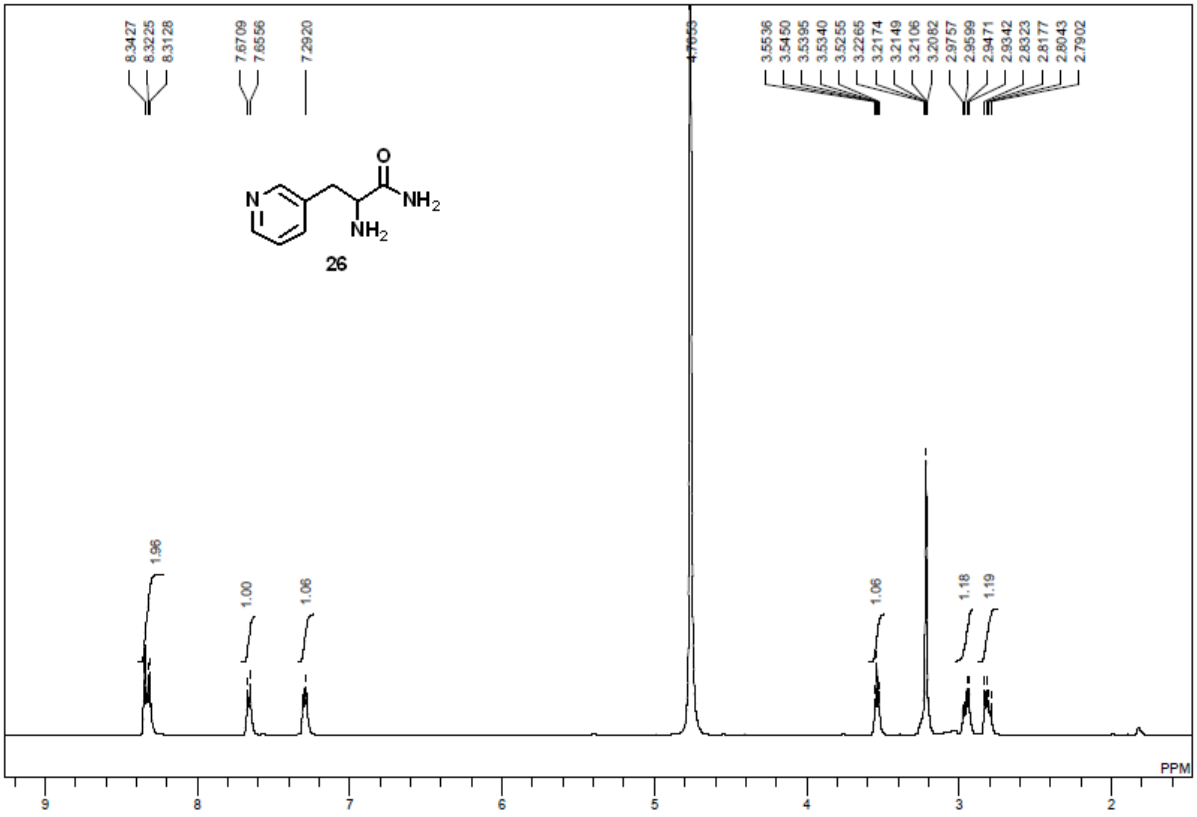
8.3427
8.3225
8.3128
7.6709
7.6556
7.2920
4.7053
3.5536
3.5450
3.5395
3.5340
3.5255
3.2265
3.2174
3.2149
3.2106
3.2082
2.9757
2.9599
2.9471
2.9342
2.8323
2.8177
2.8043
2.7902
1.96
1.00
1.06
1.06
1.18
1.19
PPM
9
8
7
6
5
4
3
2

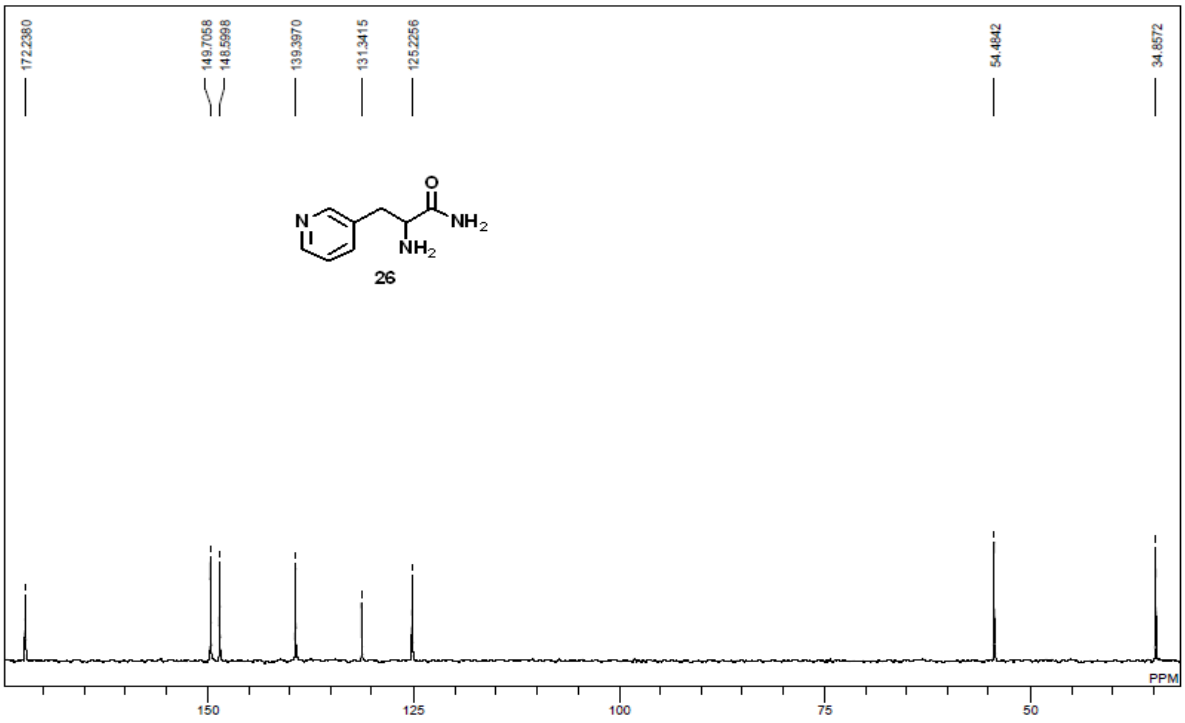
172.2380
149.7058
148.5998
139.3970
131.3415
125.2256
54.4842
34.8572
PPM
150
125
100
75
50

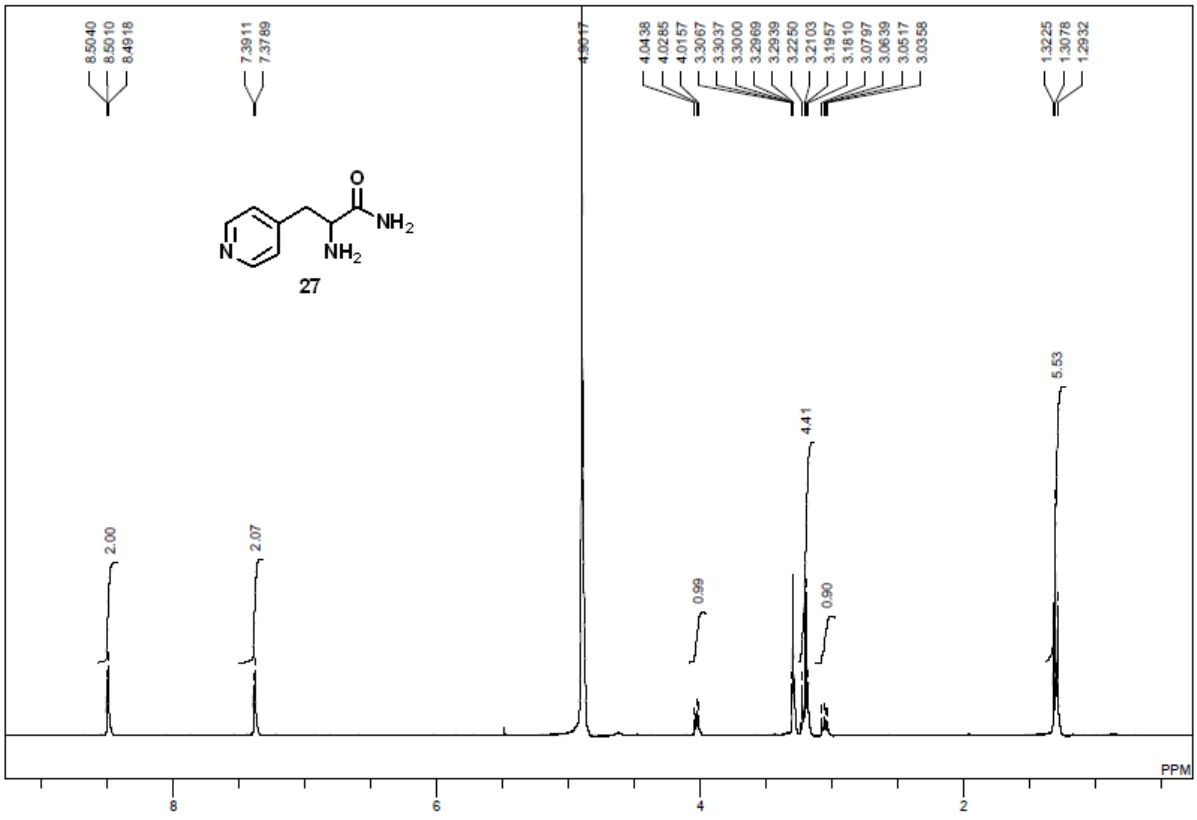
8.5040
8.5010
8.4918
7.3911
7.3789
4.9017
4.0438
4.0285
4.0157
3.3067
3.3037
3.3000
3.2969
3.2939
3.2250
3.2103
3.1957
3.1810
3.0797
3.0639
3.0517
3.0358
1.3225
1.3078
1.2932
2.00
2.07
0.99
4.41
0.90
5.53
PPM
8
6
4
2

27

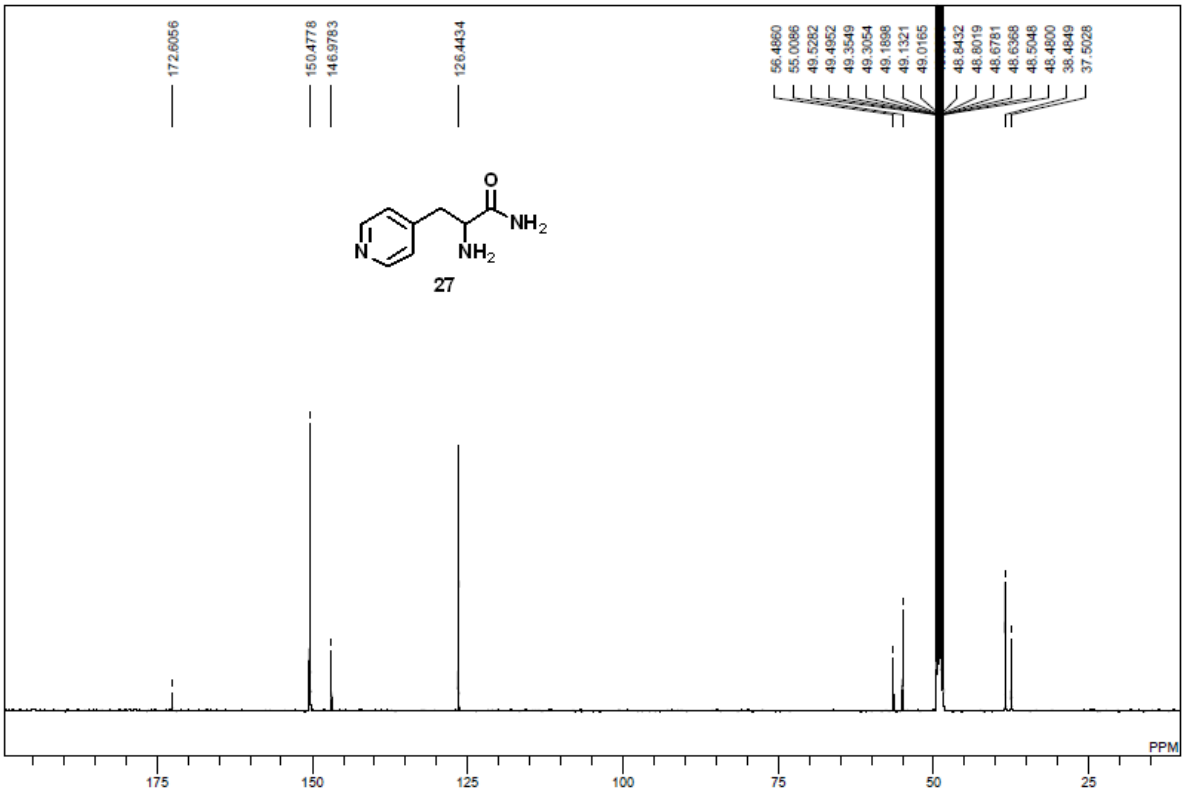
172.6056
150.4778
146.9783
126.4434
56.4860
55.0086
49.5282
49.4962
49.3549
49.3054
49.1898
49.1321
49.0165
48.8432
48.8019
48.6781
48.6368
48.5048
48.4800
38.4849
37.5028
PPM
175
150
125
100
75
50
25

27

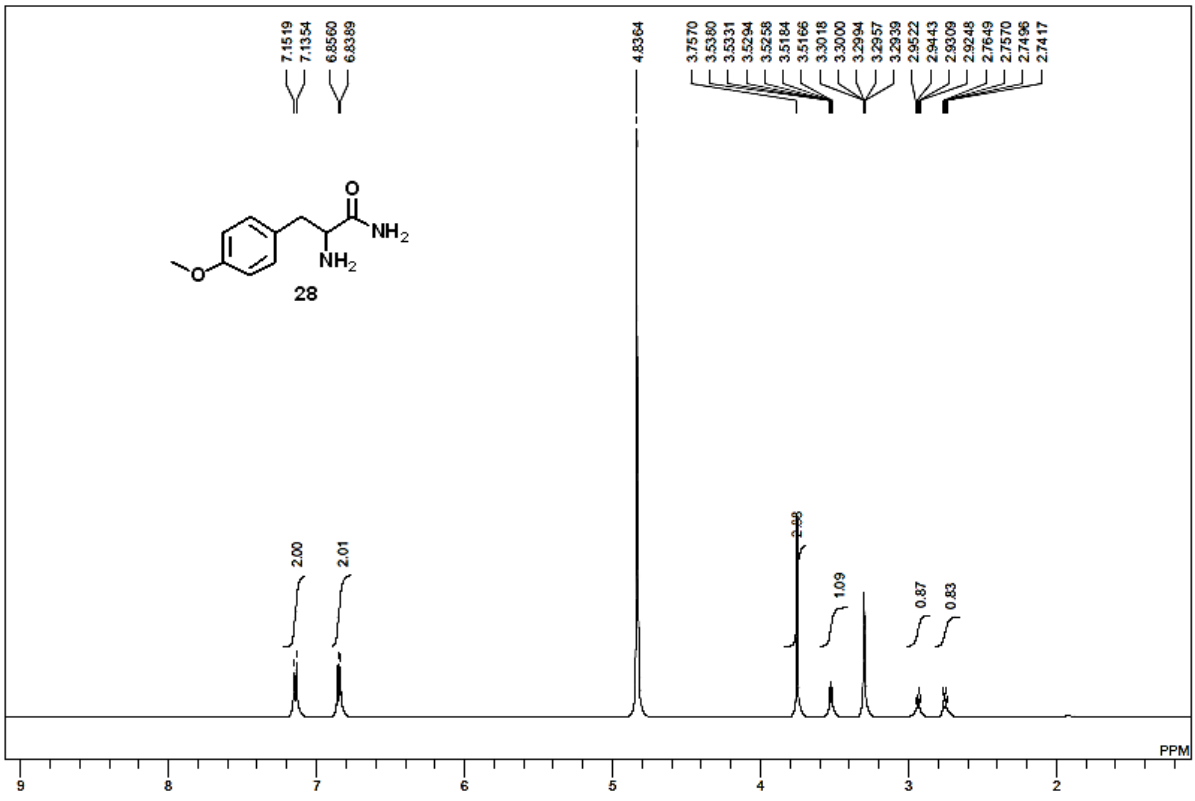
7.1519
7.1354
6.8560
6.8389
4.8364
3.7570
3.5360
3.5331
3.5294
3.5258
3.5184
3.5166
3.3018
3.3000
3.2994
3.2957
3.2939
2.9522
2.9443
2.9309
2.9248
2.7649
2.7570
2.7496
2.7417
O
NH2
NH2
O
28
2.00
2.01
2.98
1.09
0.87
0.83
PPM
9
8
7
6
5
4
3
2

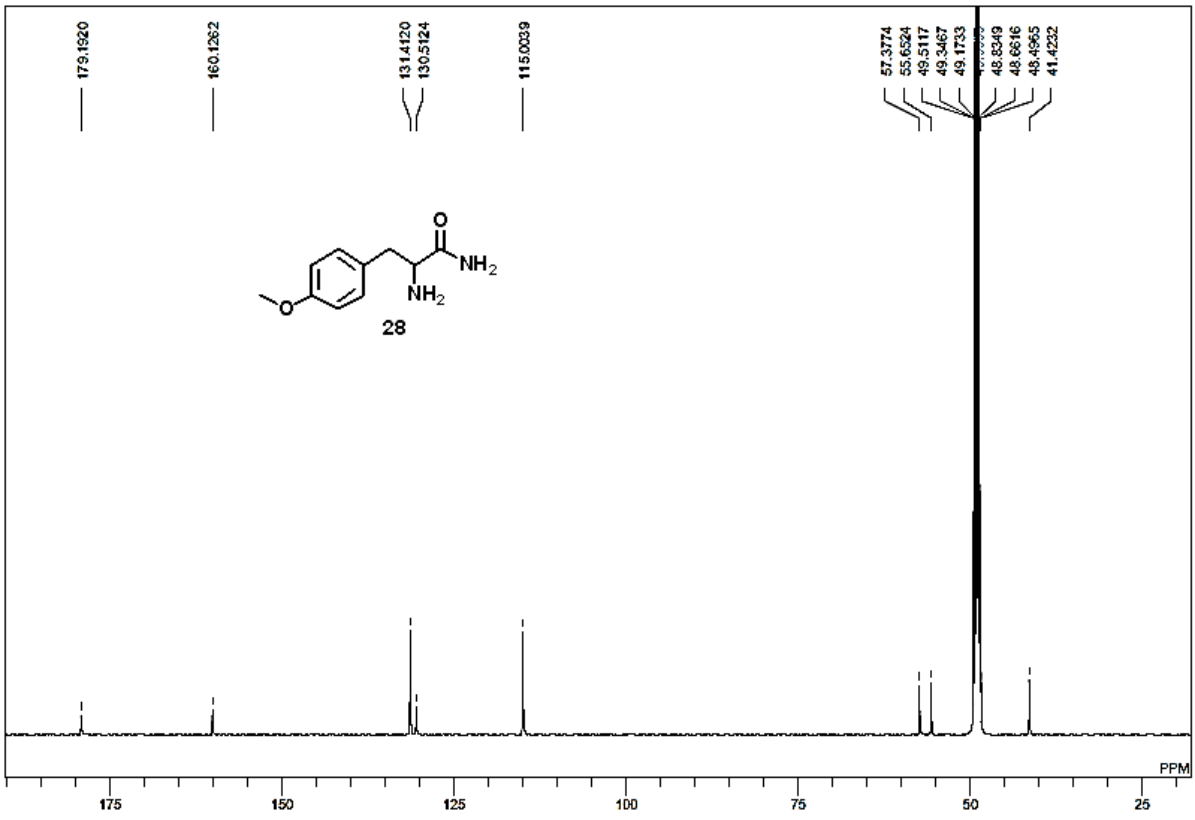
179.1920
160.1262
131.4120
130.5124
115.0039
57.3774
55.6524
49.5117
49.3467
49.1733
48.8349
48.6616
48.4965
41.4232
O
NH2
NH2
O
28
PPM
175
150
125
100
75
50
25

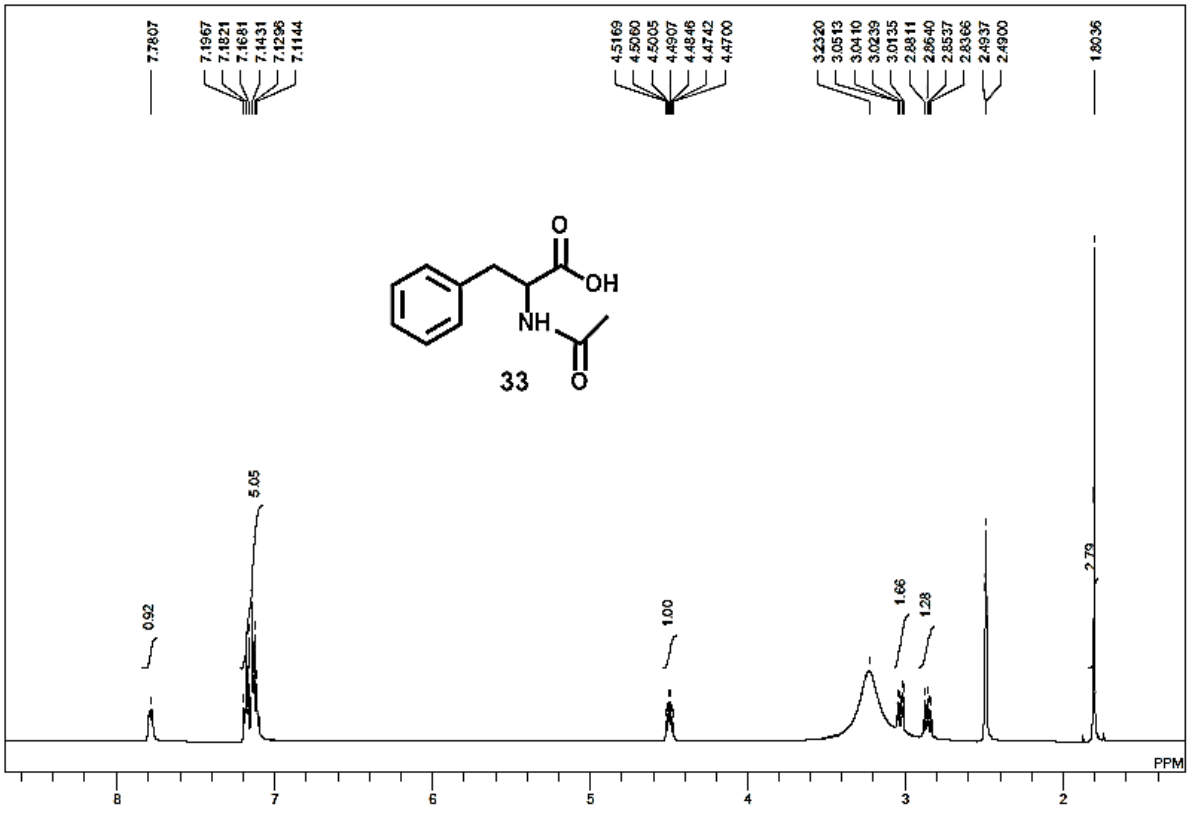
7.7807
7.1967
7.1821
7.1681
7.1431
7.1296
7.1144
4.5169
4.5060
4.5005
4.4907
4.4846
4.4742
4.4700
3.2320
3.0513
3.0410
3.0239
3.0135
2.8811
2.8640
2.8537
2.8366
2.4937
2.4900
1.8036
O
OH
NH
O
33
0.92
5.05
1.00
1.66
1.28
2.79
PPM
8
7
6
5
4
3
2

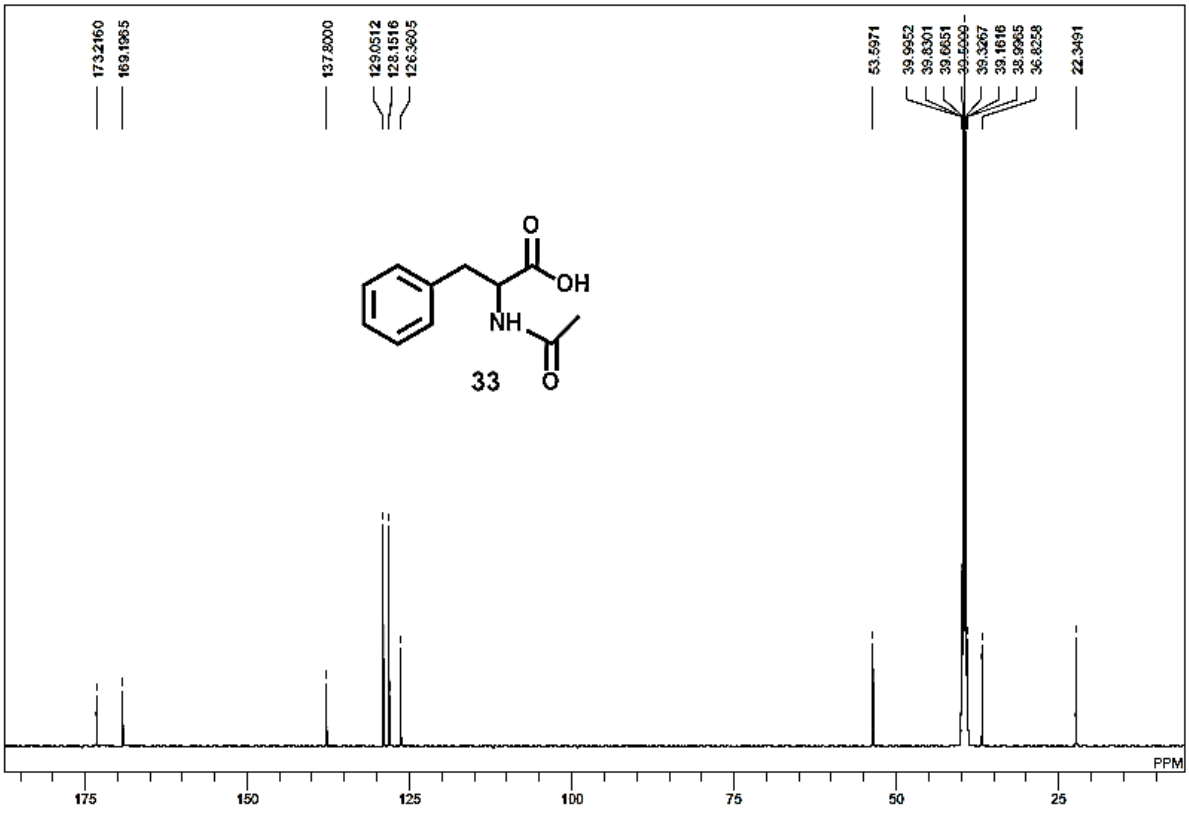
173.2160
169.1965
137.8000
129.0512
128.1516
126.3605
53.5971
39.9952
39.8301
39.6651
39.5000
39.3267
39.1616
38.9965
36.8258
22.3491
O
OH
NH
O
33
PPM
175
150
125
100
75
50
25

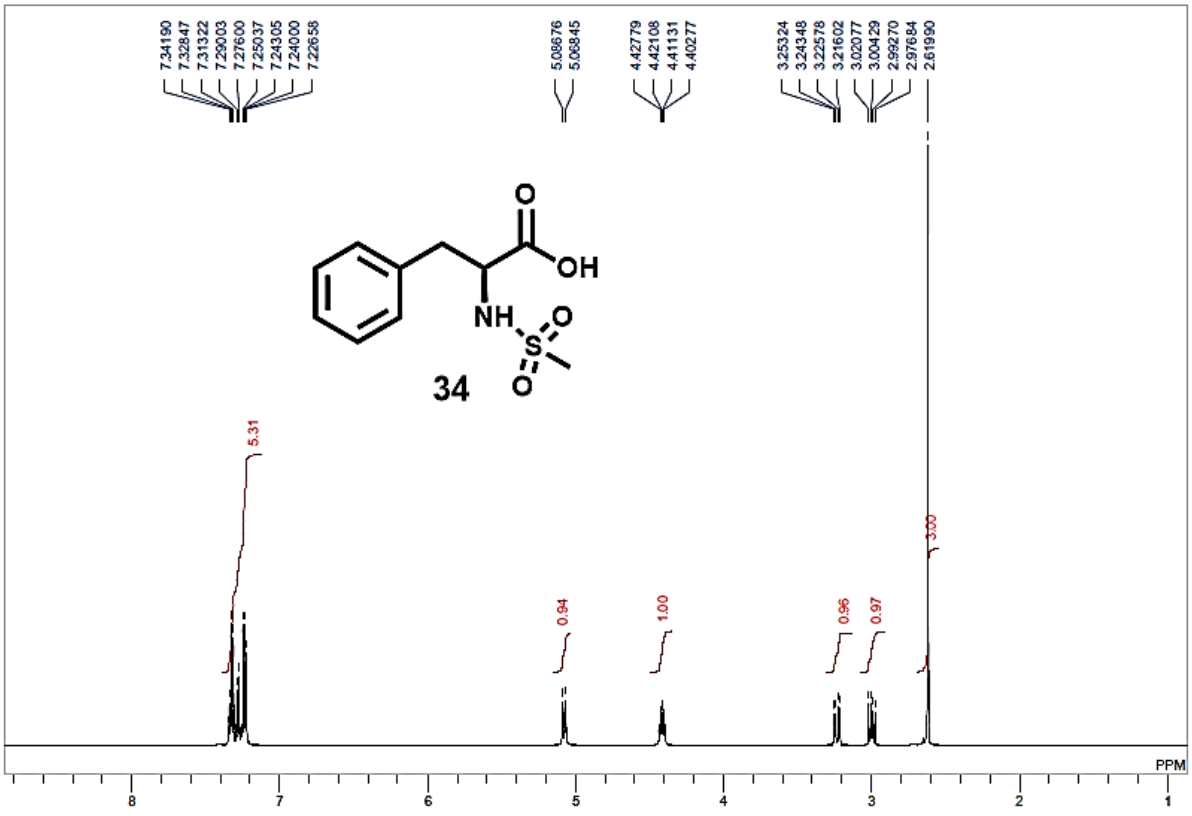
7.34190
7.32847
7.31322
7.29003
7.27600
7.25037
7.24305
7.24000
7.22658
5.09676
5.06845
4.42779
4.42108
4.41131
4.40277
3.25324
3.24348
3.22578
3.21602
3.02077
3.00429
2.99270
2.97684
2.61990
O
OH
NH
S
O
O
34
5.31
0.94
1.00
0.96
0.97
3.00
PPM
8
7
6
5
4
3
2
1

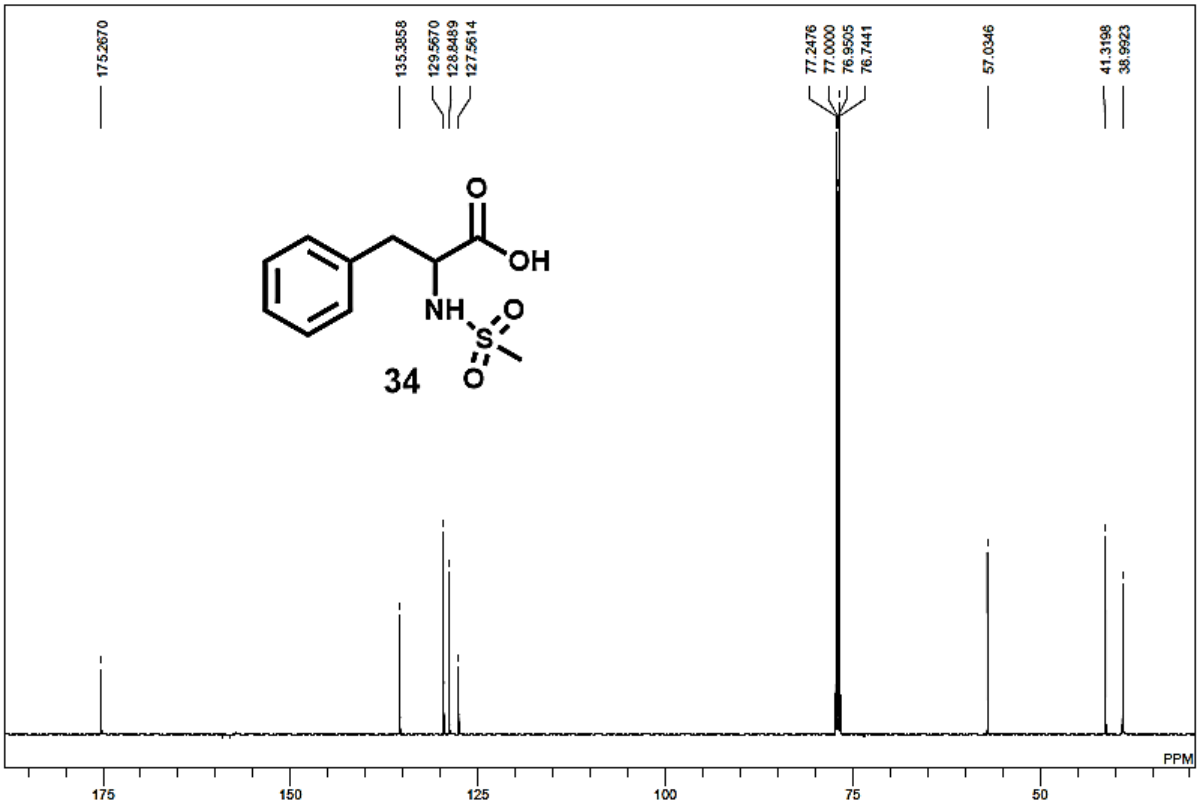
175.2670
135.3858
129.5670
128.8489
127.5614
77.2476
77.0000
76.9505
76.7441
57.0346
41.3198
38.9923
O
OH
NH
S
O
O
34
PPM
175
150
125
100
75
50

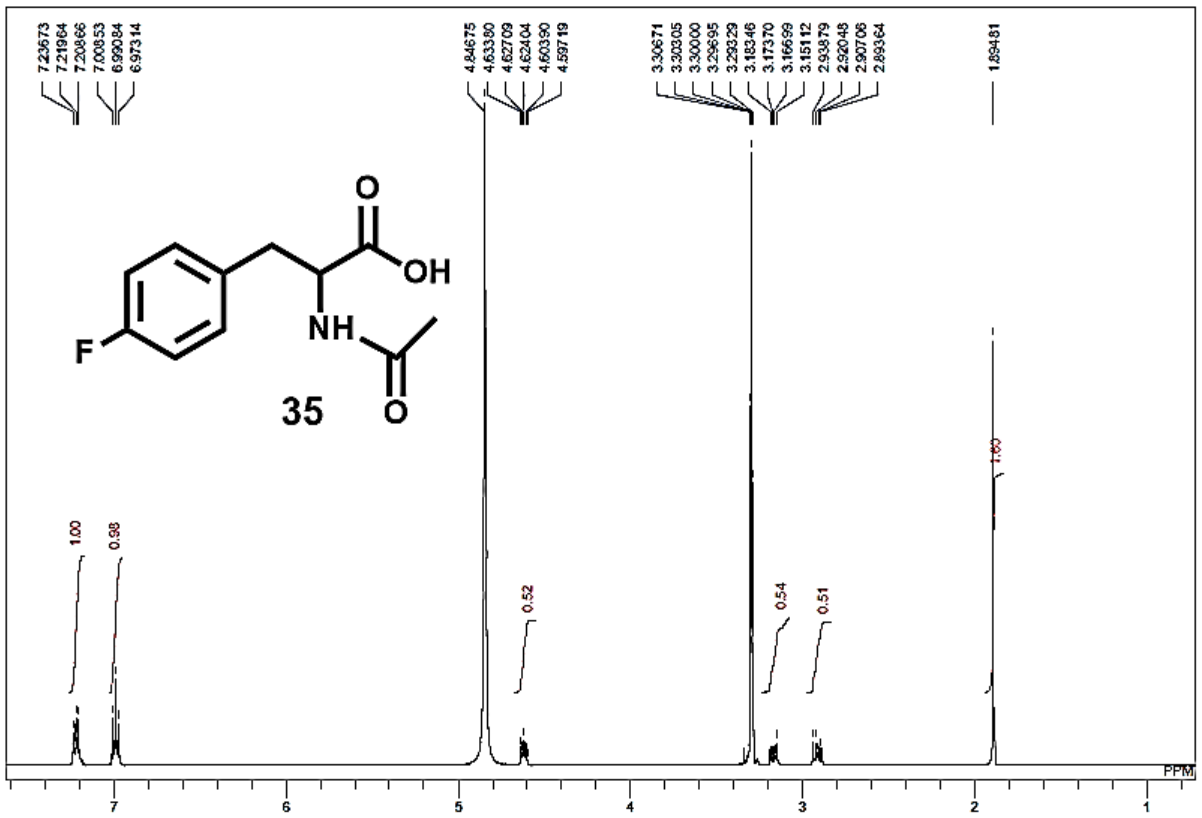
7.23673
7.21964
7.20866
7.00853
6.99084
6.97314
4.64675
4.63380
4.62709
4.62404
4.60390
4.59719
3.30671
3.30305
3.30000
3.29695
3.29329
3.18346
3.17370
3.16699
3.15112
2.93879
2.92048
2.90706
2.89364
1.89481
1.00
0.98
0.52
0.54
0.51
1.60
PPM
7
6
5
4
3
2
1
O
OH
NH
F
O
35

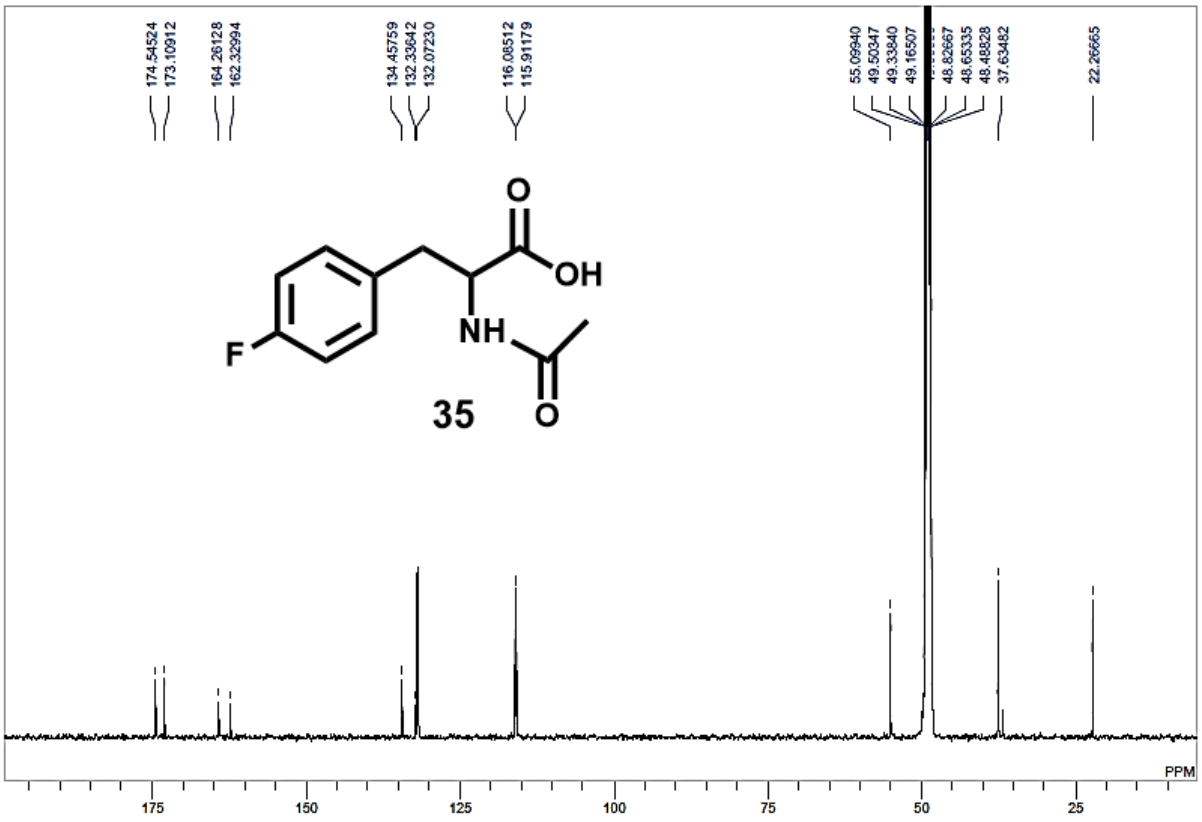
174.54524
173.10912
164.26128
162.32994
134.45759
132.33642
132.07230
116.08512
115.91179
55.09940
49.50347
49.33840
49.16507
48.82667
48.65335
48.48828
37.63482
22.26665
PPM
175
150
125
100
75
50
25
O
OH
NH
F
O
35

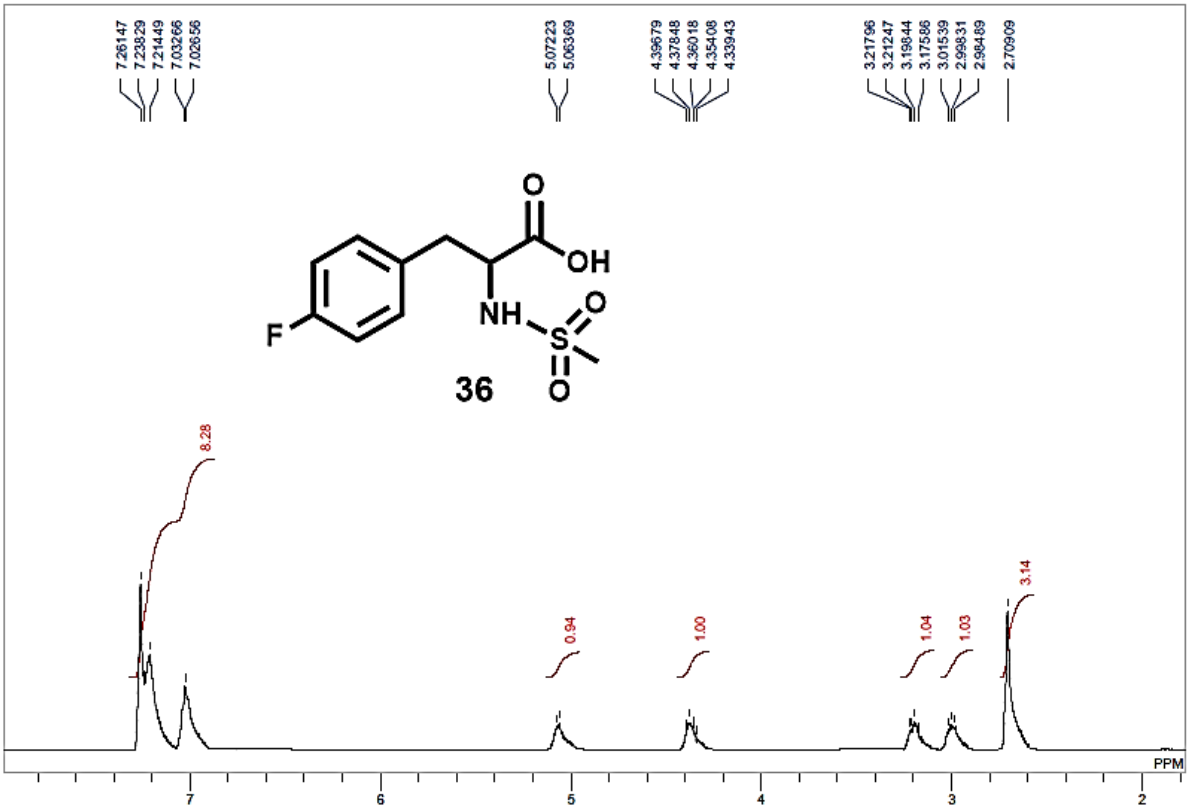
7.26147
7.23829
7.21449
7.03266
7.02656
5.07223
5.06369
4.39679
4.37848
4.36018
4.35408
4.33943
3.21796
3.21247
3.19844
3.17586
3.01539
2.99831
2.98489
2.70909
O
OH
NH
S
O
O
F
36
8.28
0.94
1.00
1.04
1.03
3.14
PPM
7
6
5
4
3
2

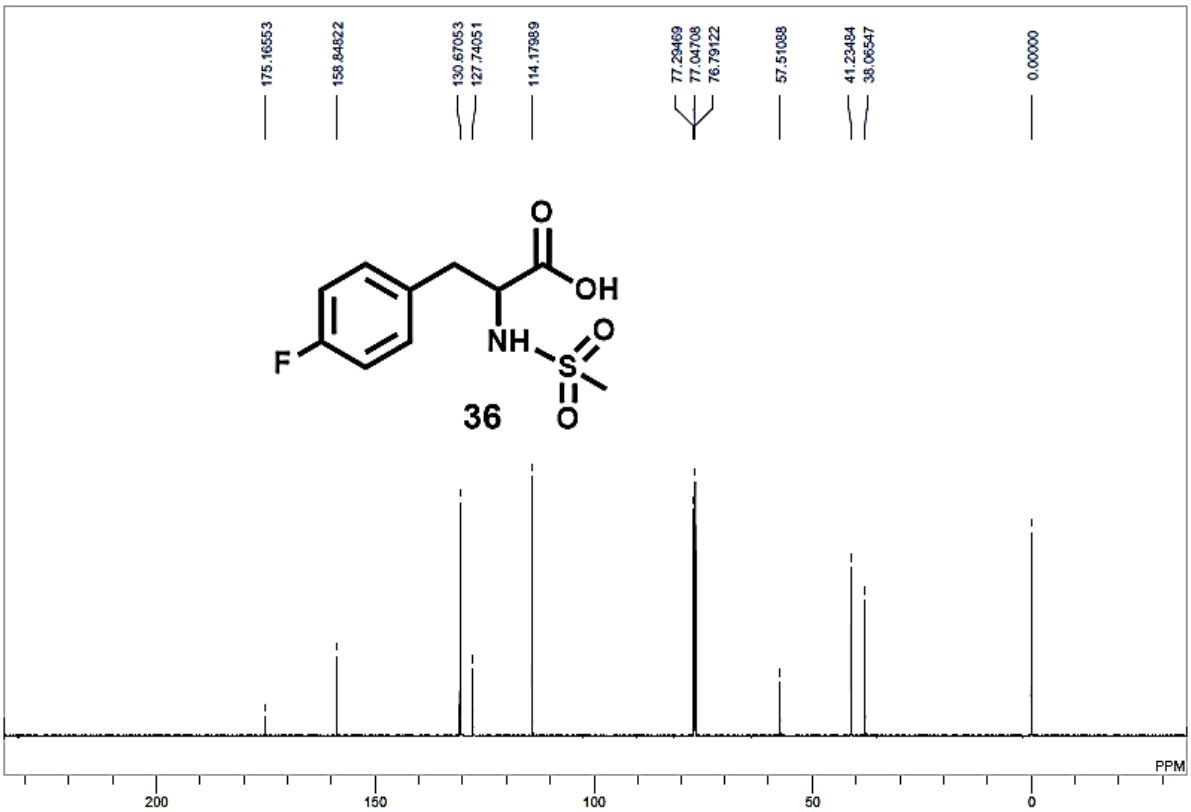
175.16553
158.84822
130.67053
127.74051
114.17989
77.29469
77.04708
76.79122
57.51088
41.23484
38.06547
0.00000
O
OH
NH
S
O
O
F
36
PPM
200
150
100
50
0

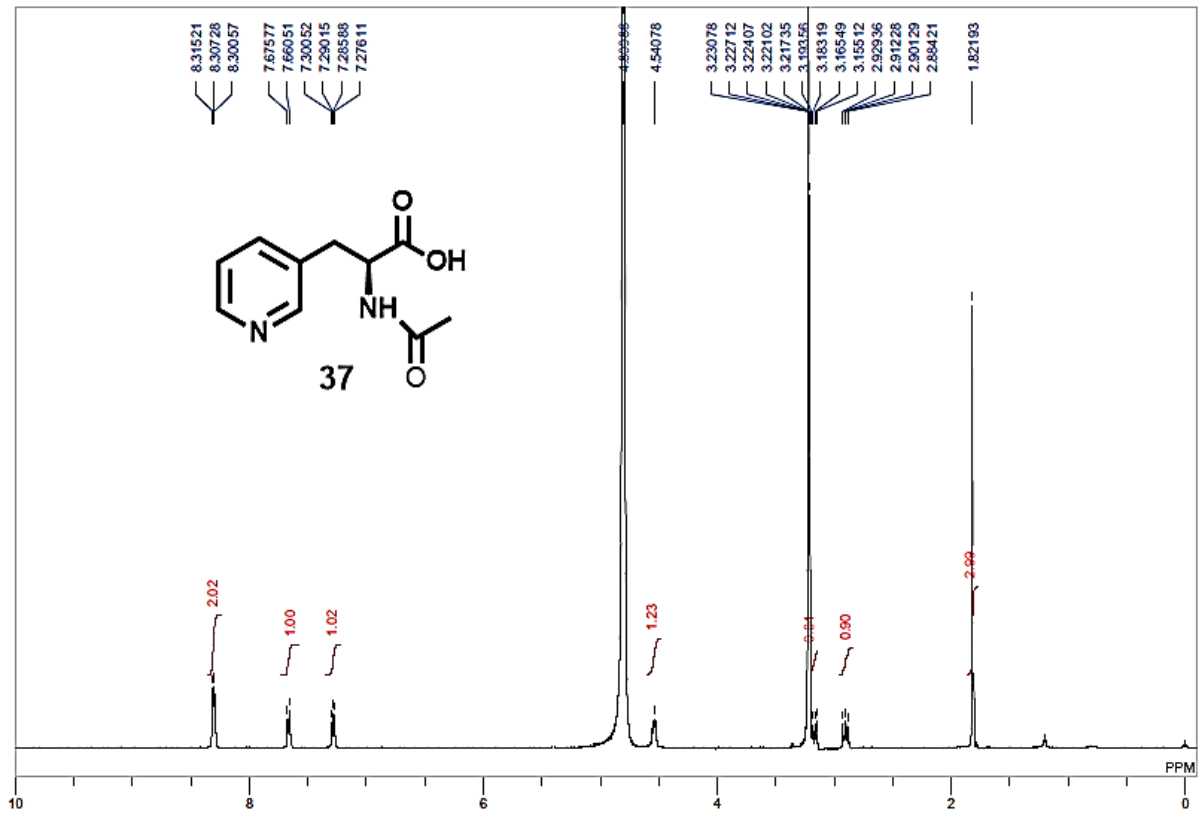
8.31521
8.30728
8.30057
7.67577
7.66051
7.30052
7.29015
7.28588
7.27611
4.54078
3.23078
3.22712
3.22407
3.22102
3.21735
3.18319
3.16549
3.15512
2.92936
2.91228
2.90129
2.88421
1.82193
2.02
1.00
1.02
1.23
0.90
2.99
OH
NH
N
O
37
PPM
10
8
6
4
2
0

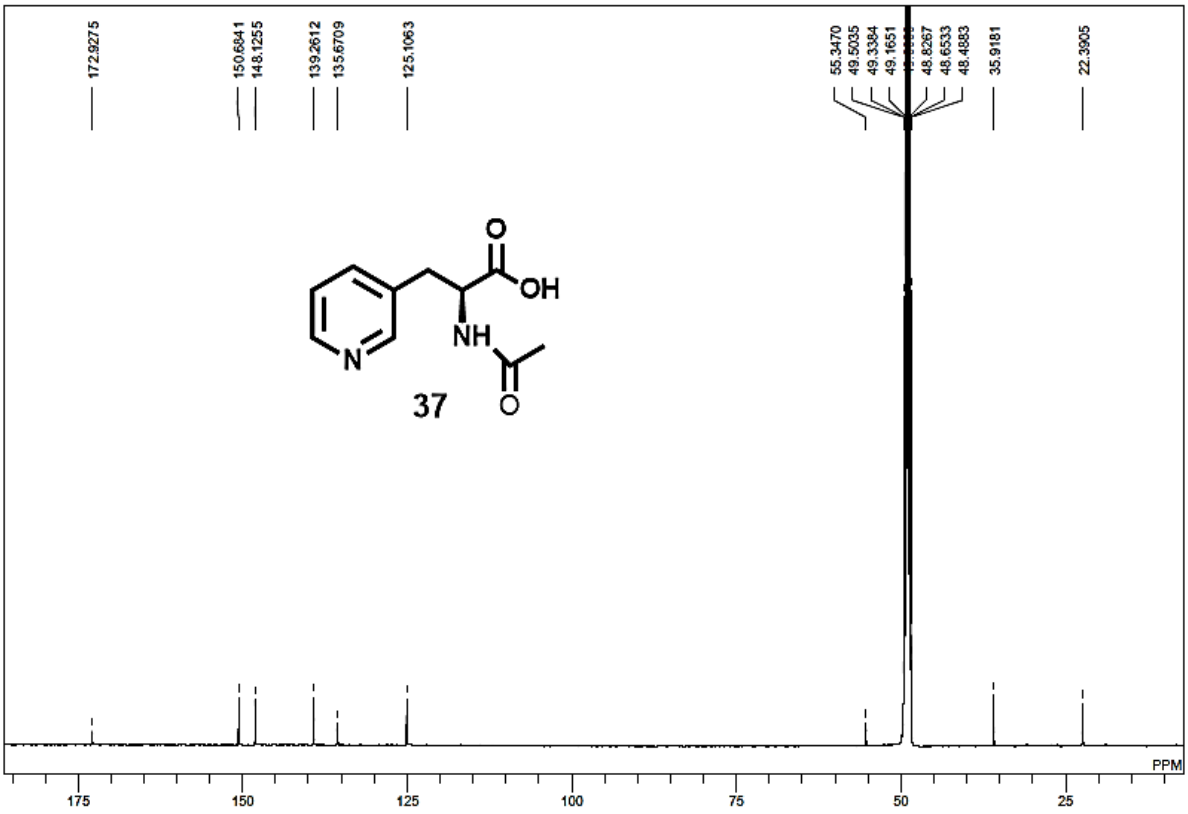
172.9275
150.6841
148.1255
139.2612
135.6709
125.1063
55.3470
49.5035
49.3384
49.1651
48.8267
48.6533
48.4883
35.9181
22.3905
OH
NH
N
O
37
PPM
175
150
125
100
75
50
25

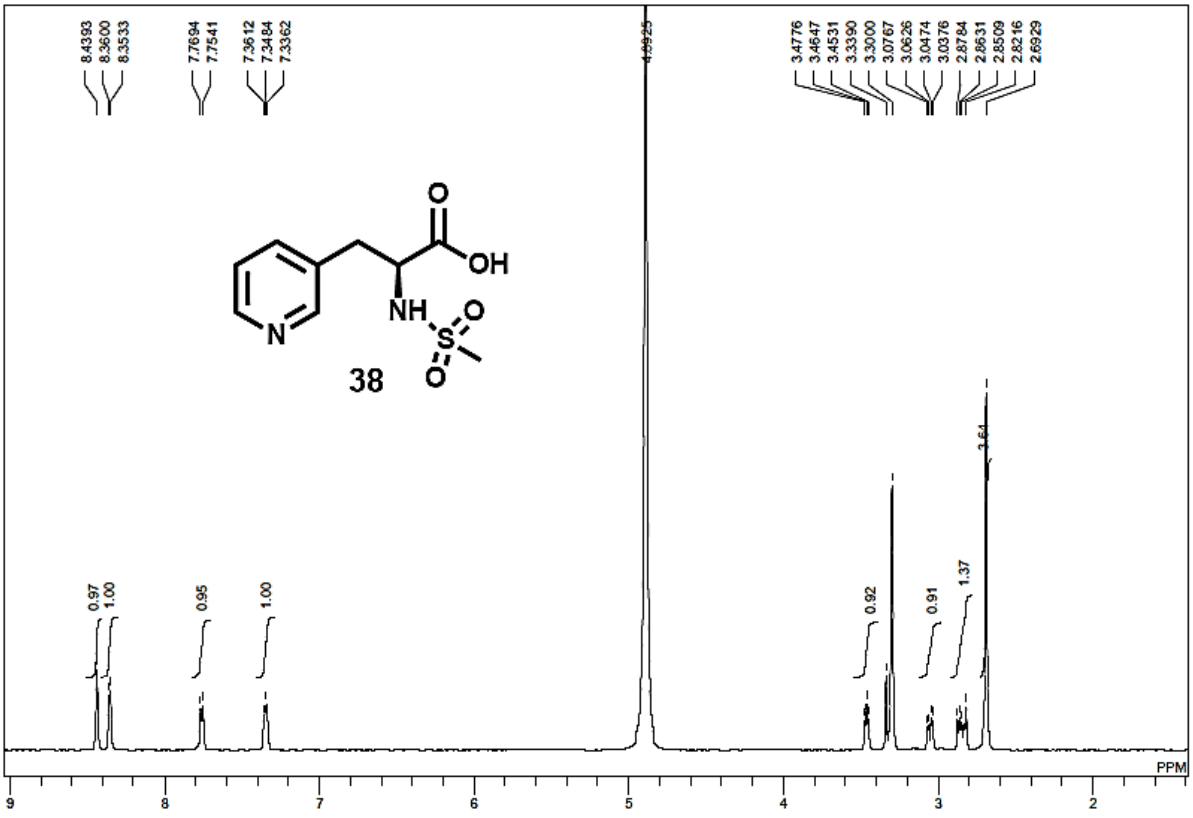
8.4393
8.3600
8.3533
7.7694
7.7541
7.3612
7.3484
7.3362
4.0925
3.4776
3.4647
3.4531
3.3390
3.3000
3.0767
3.0626
3.0474
3.0376
2.8784
2.8631
2.8509
2.8216
2.6929
3.64
0.97
1.00
0.95
1.00
0.92
0.91
1.37
PPM
9
8
7
6
5
4
3
2
O
OH
NH
S
O
O
N
38

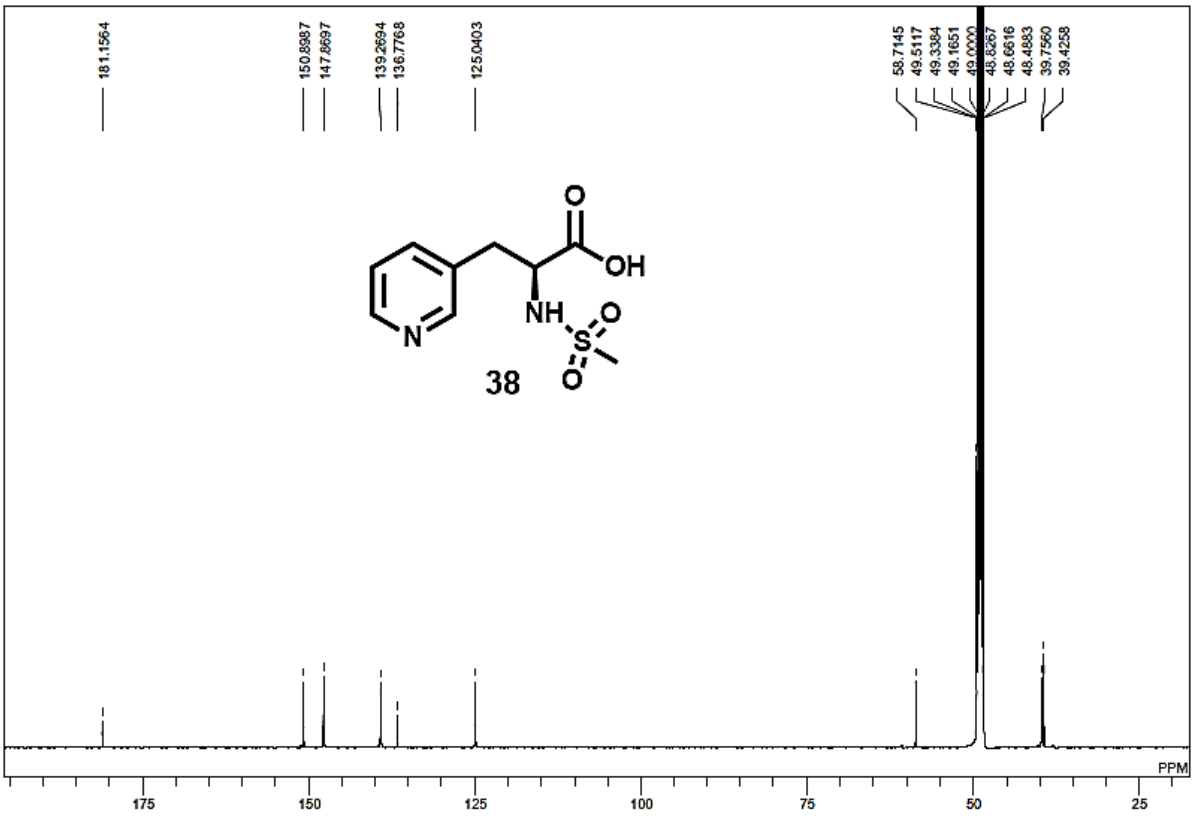
181.1564
150.8987
147.8697
139.2694
136.7768
125.0403
58.7145
49.5117
49.3384
49.1651
48.8267
48.6616
48.4883
39.7560
39.4258
PPM
175
150
125
100
75
50
25
O
OH
NH
S
O
O
N
38

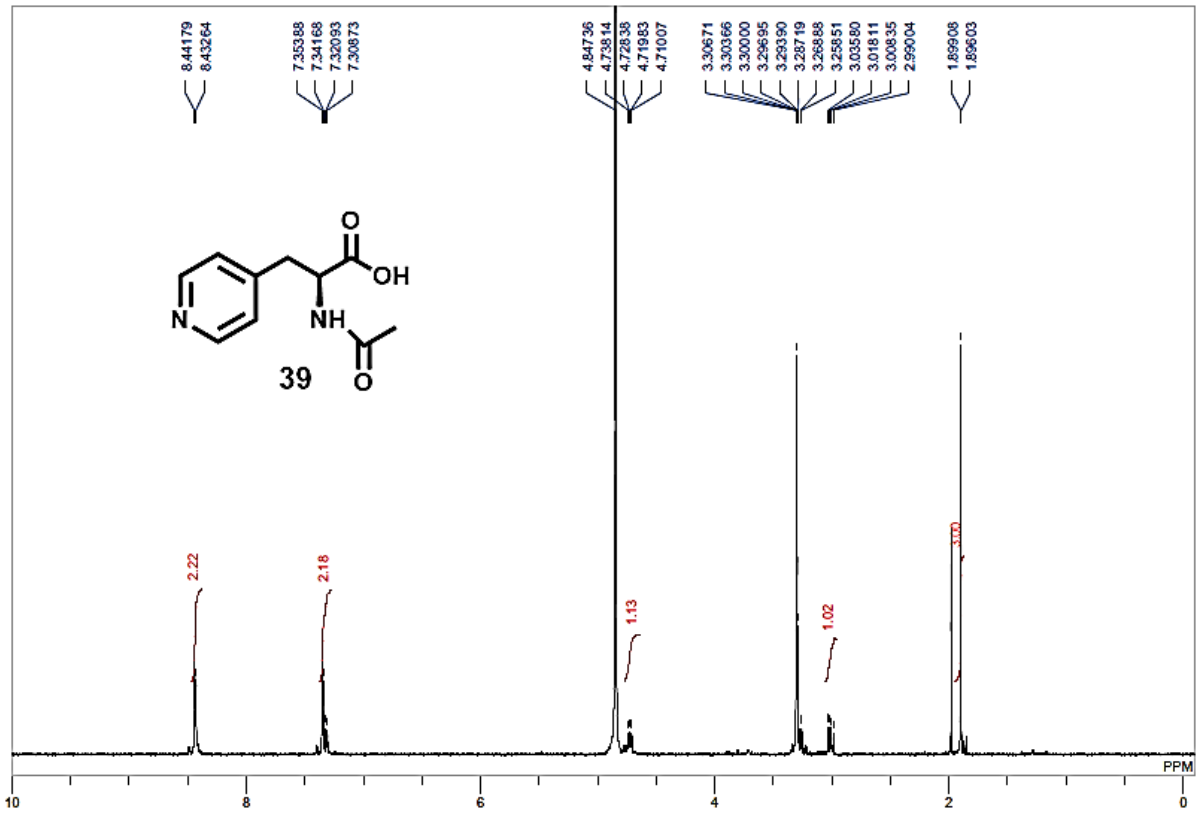
8.44179
8.43264
7.35388
7.34168
7.32093
7.30873
4.84736
4.73814
4.72838
4.71983
4.71007
3.30671
3.30366
3.30000
3.29695
3.29390
3.28719
3.26888
3.25851
3.03580
3.01811
3.00835
2.99004
1.89908
1.89603
O
OH
N
NH
O
39
2.22
2.18
1.13
1.02
3.00
PPM
10
8
6
4
2
0

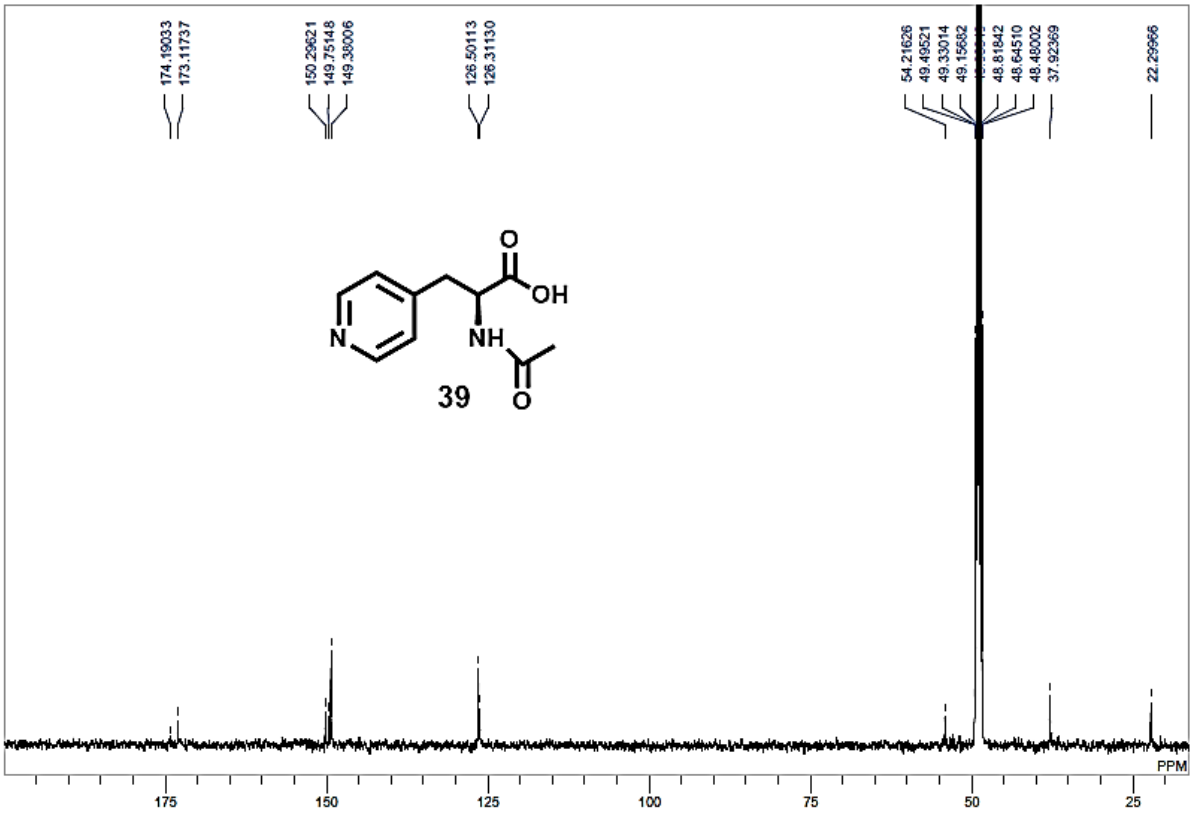
174.19033
173.11737
150.29621
149.75148
149.38006
126.50113
126.31130
54.21626
49.49521
49.33014
49.15682
48.81842
48.64510
48.48002
37.92369
22.29966
O
OH
N
NH
O
39
PPM
175
150
125
100
75
50
25

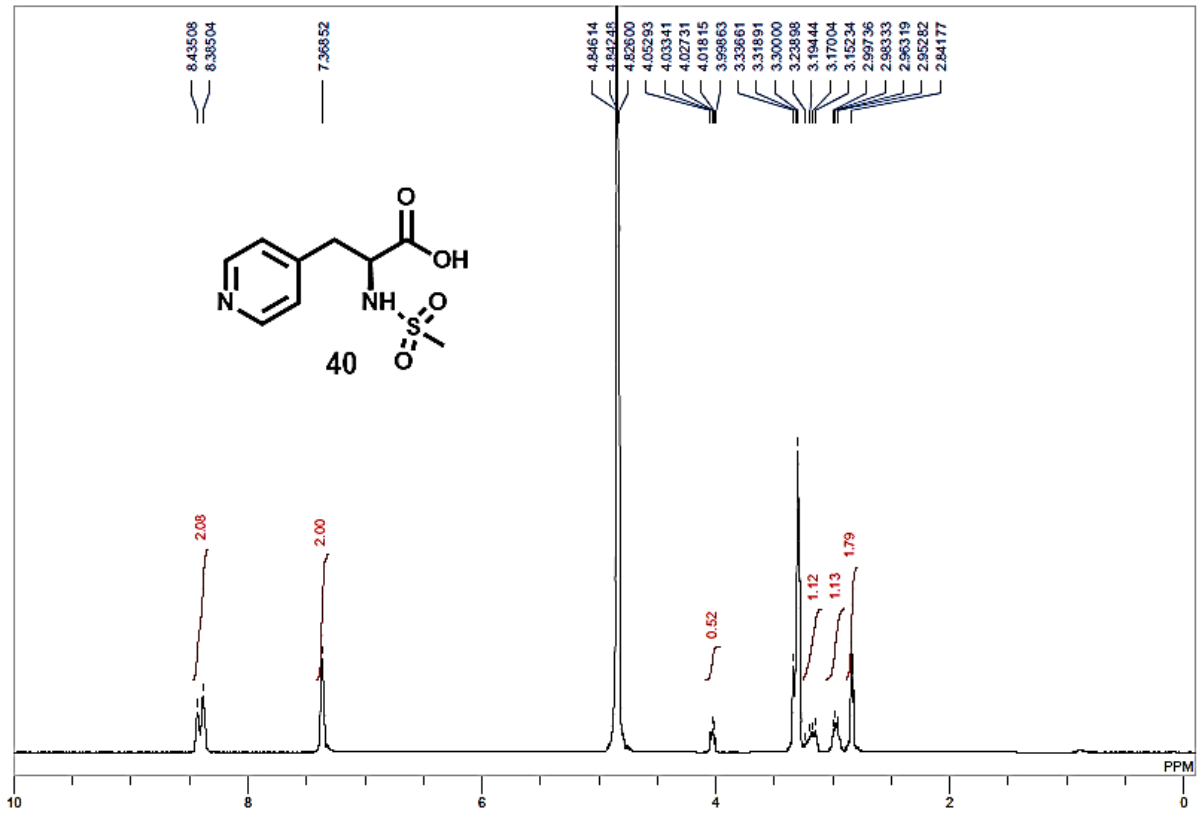
8.43508
8.38504
7.36852
4.84614
4.84248
4.82600
4.05293
4.03341
4.02731
4.01815
3.99863
3.33661
3.31891
3.30000
3.23898
3.19444
3.17004
3.15234
2.99736
2.98333
2.96319
2.95282
2.84177
2.08
2.00
0.52
1.12
1.13
1.79
PPM
10
8
6
4
2
0
40

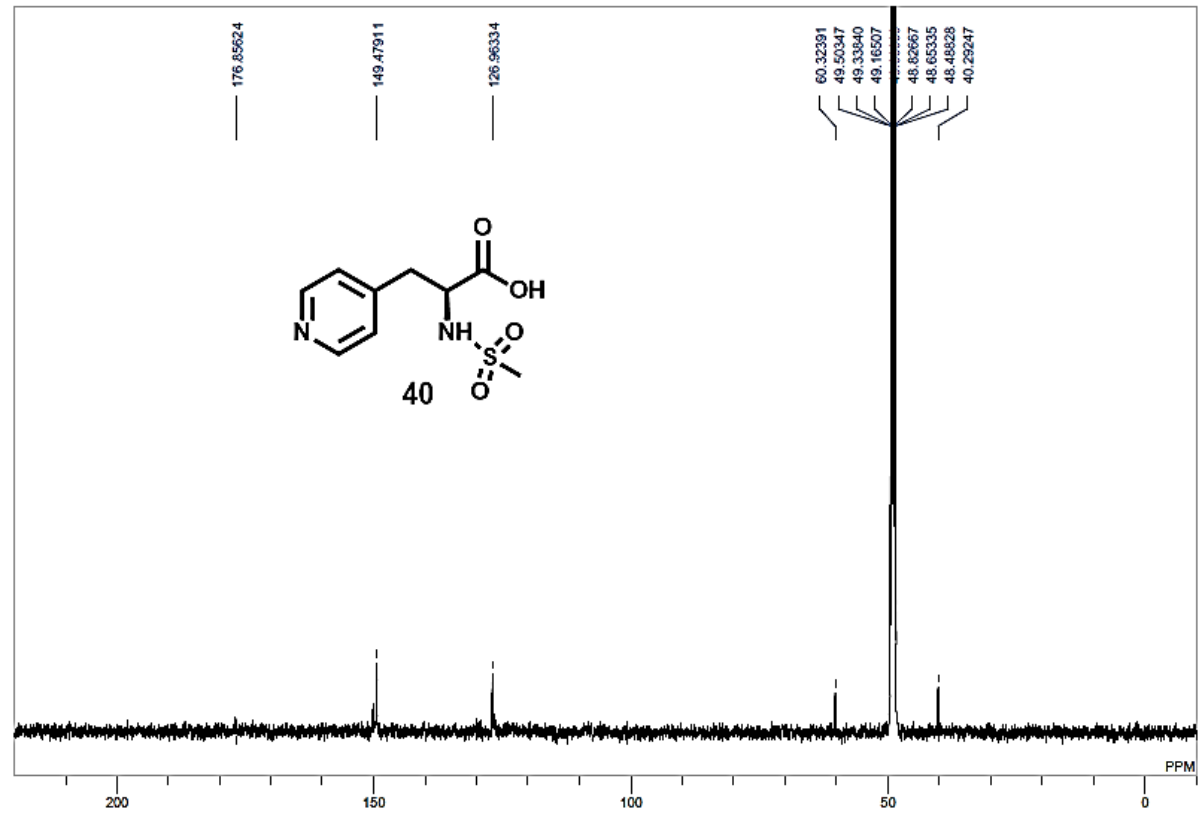
176.85624
149.47911
126.96334
60.32391
49.50347
49.33840
49.16507
48.82667
48.65335
48.48828
40.29247
PPM
200
150
100
50
0
40

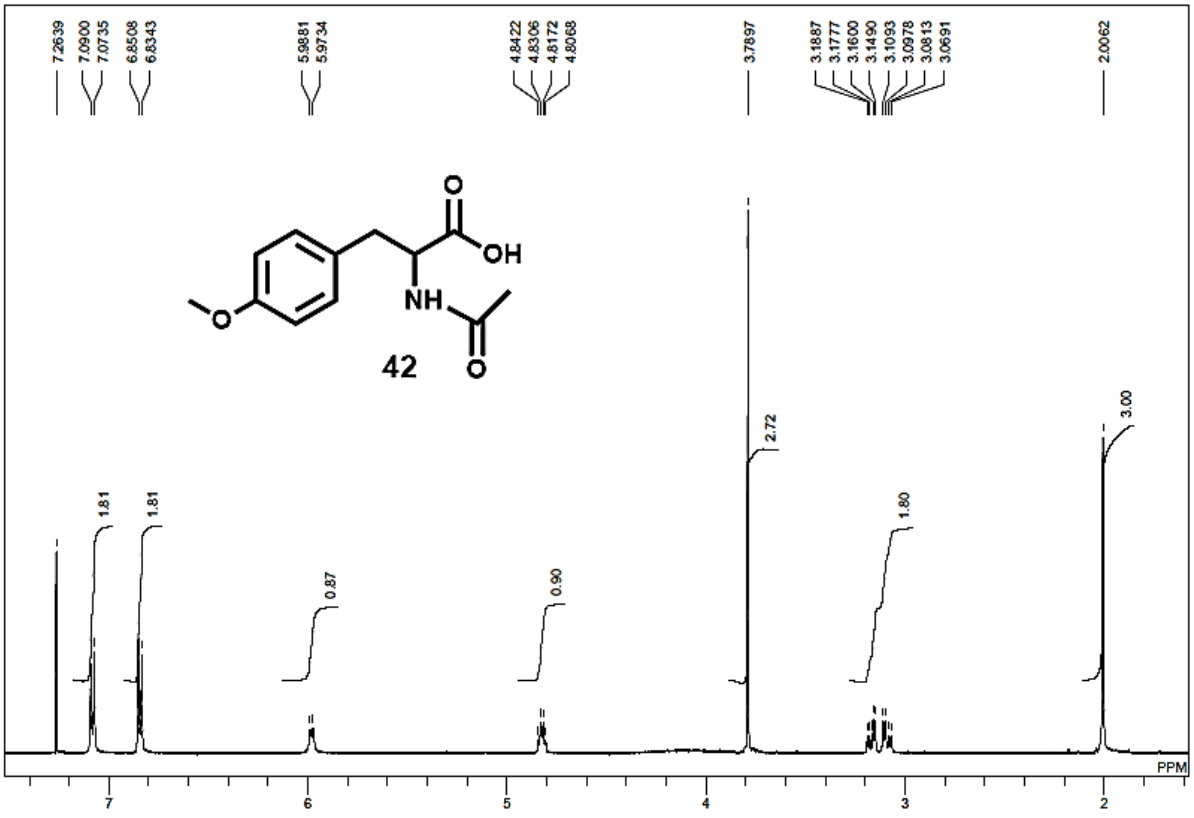
7.26.39
7.0900
7.0735
6.8508
6.8343
5.9881
5.9734
4.8422
4.8306
4.8172
4.8068
3.7897
3.1887
3.1777
3.1600
3.1490
3.1093
3.0978
3.0813
3.0691
2.0062
OH
NH
O
42
1.81
1.81
0.87
0.90
2.72
1.80
3.00
PPM
7
6
5
4
3
2

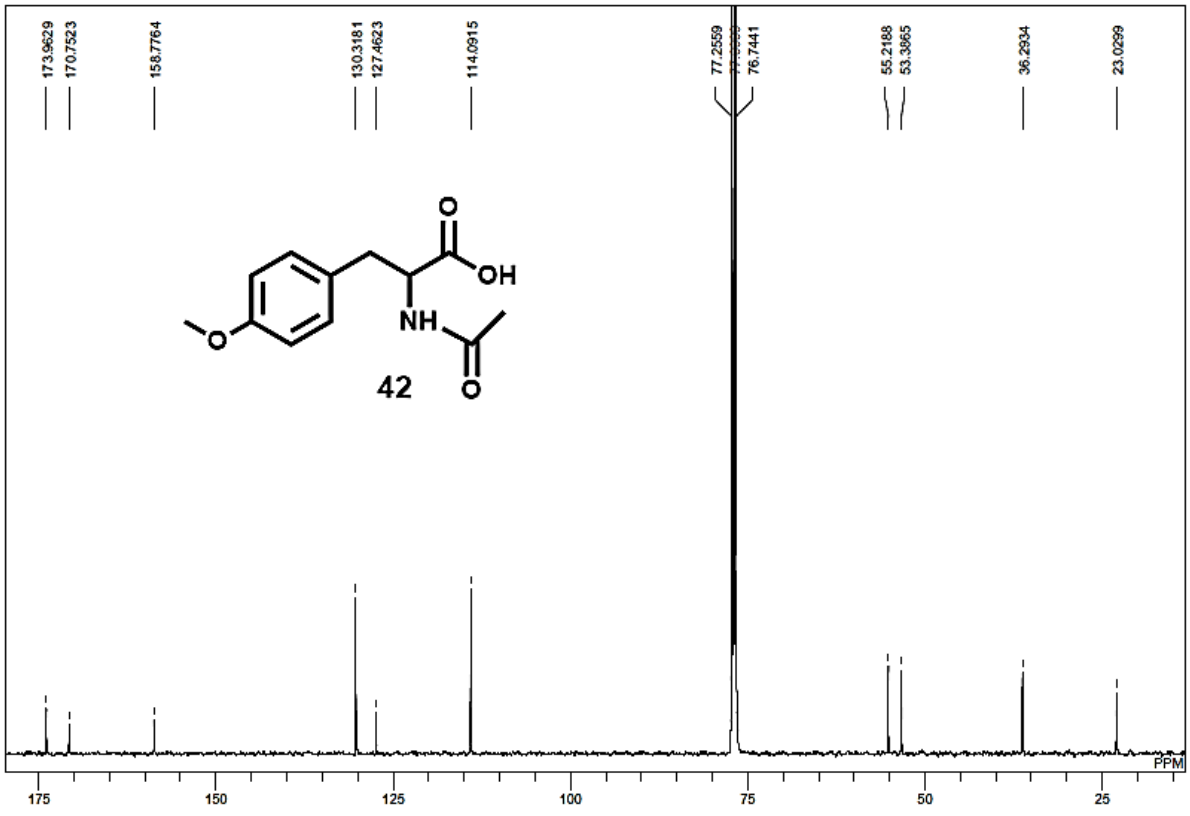
173.9629
170.7523
158.7764
130.3181
127.4623
114.0915
77.2559
76.7441
55.2188
53.3865
36.2934
23.0299
OH
NH
O
42
PPM
175
150
125
100
75
50
25

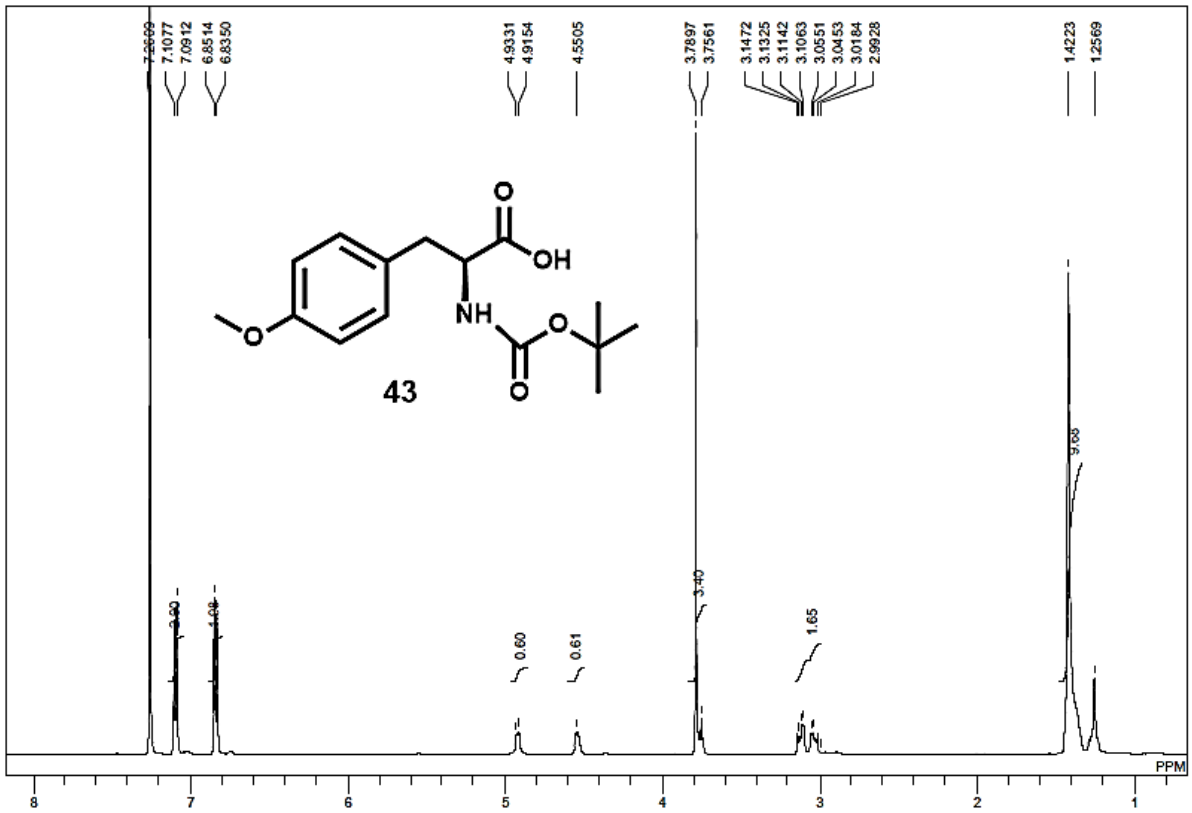
7.2669
7.1077
7.0912
6.8514
6.8350
4.9331
4.9154
4.5505
3.7897
3.7561
3.1472
3.1325
3.1142
3.1063
3.0551
3.0453
3.0184
2.9928
1.4223
1.2569
3.00
1.08
0.60
0.61
3.40
1.65
9.68
OH
NH
O
43
PPM
8
7
6
5
4
3
2
1

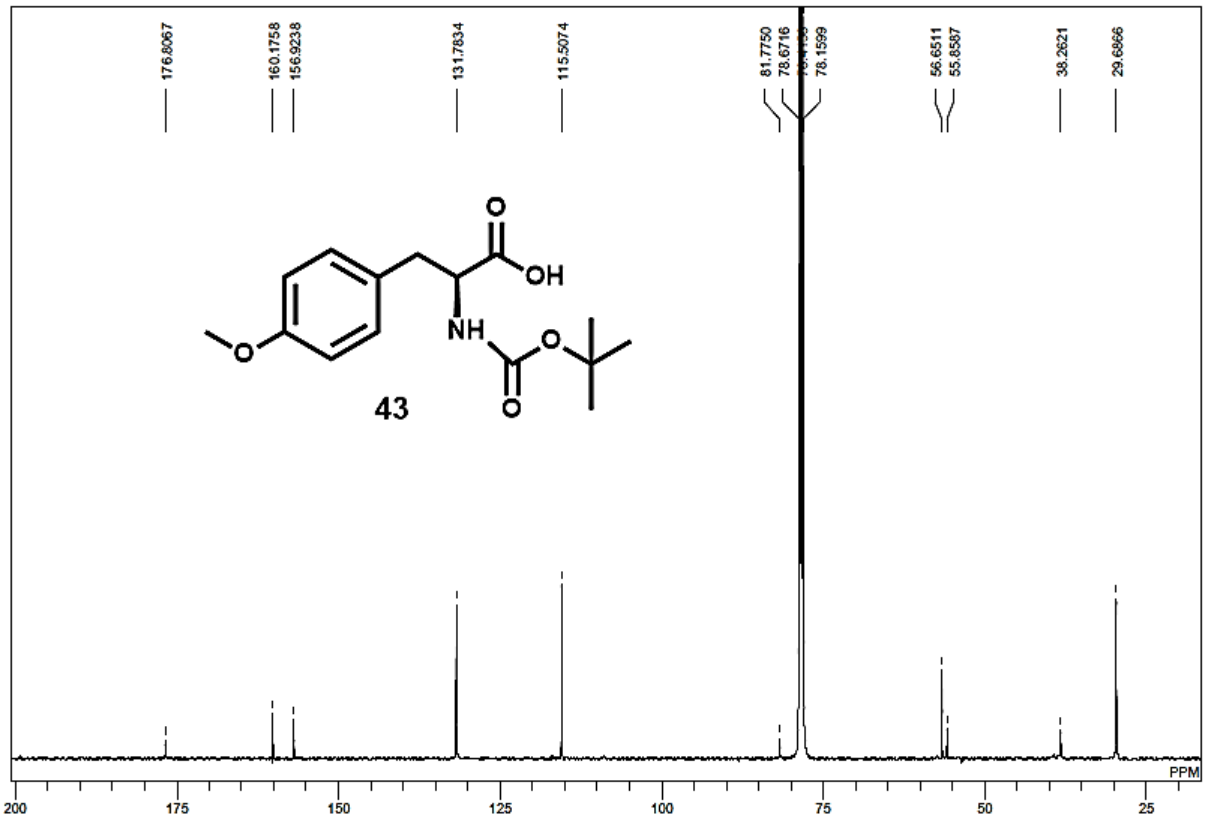
176.8067
160.1758
156.9238
131.7834
115.5074
81.7750
78.6716
78.1599
56.6511
55.8587
38.2621
29.6866
OH
NH
O
43
PPM
200
175
150
125
100
75
50
25

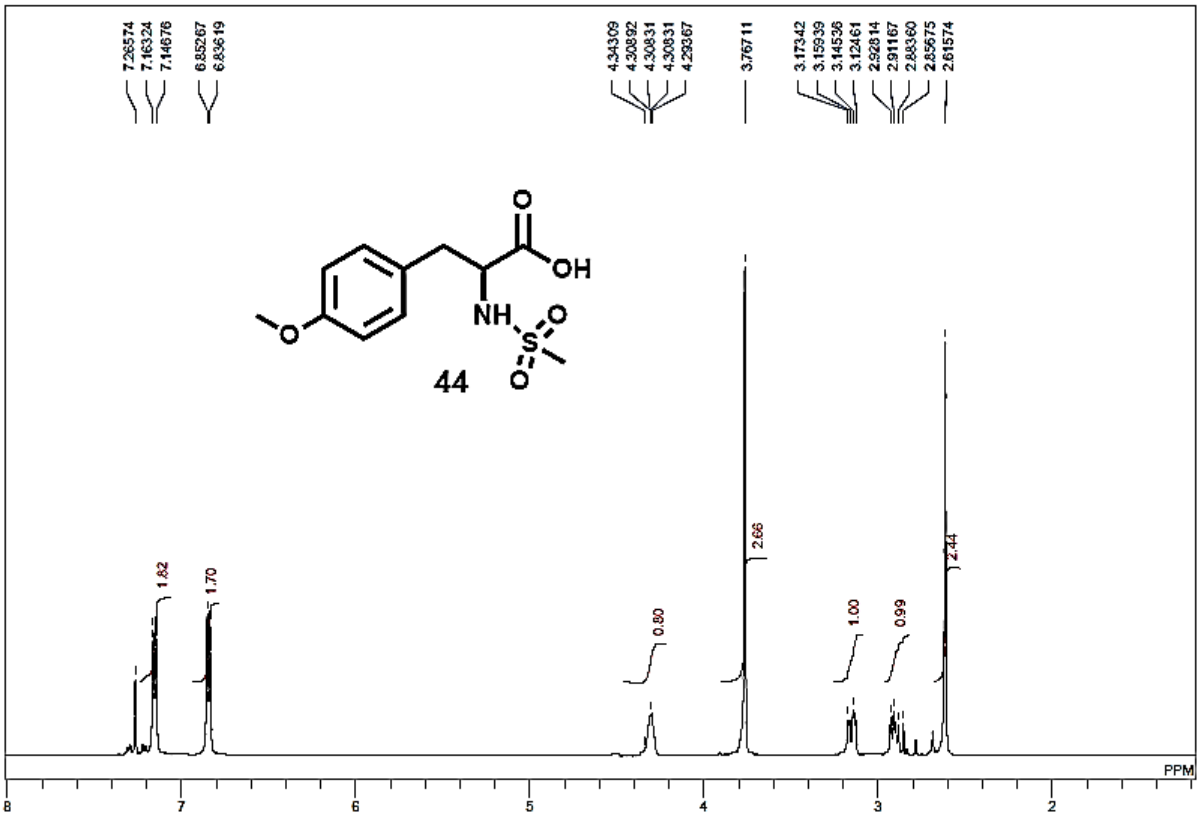
7.26574
7.16324
7.14676
6.85267
6.83619
4.34309
4.30892
4.30831
4.30831
4.29367
3.76711
3.17342
3.15939
3.14536
3.12461
2.92814
2.91167
2.88360
2.85675
2.61574
OH
NH
O
S
O
O
44
1.82
1.70
0.80
2.66
1.00
0.99
2.44
PPM
8
7
6
5
4
3
2

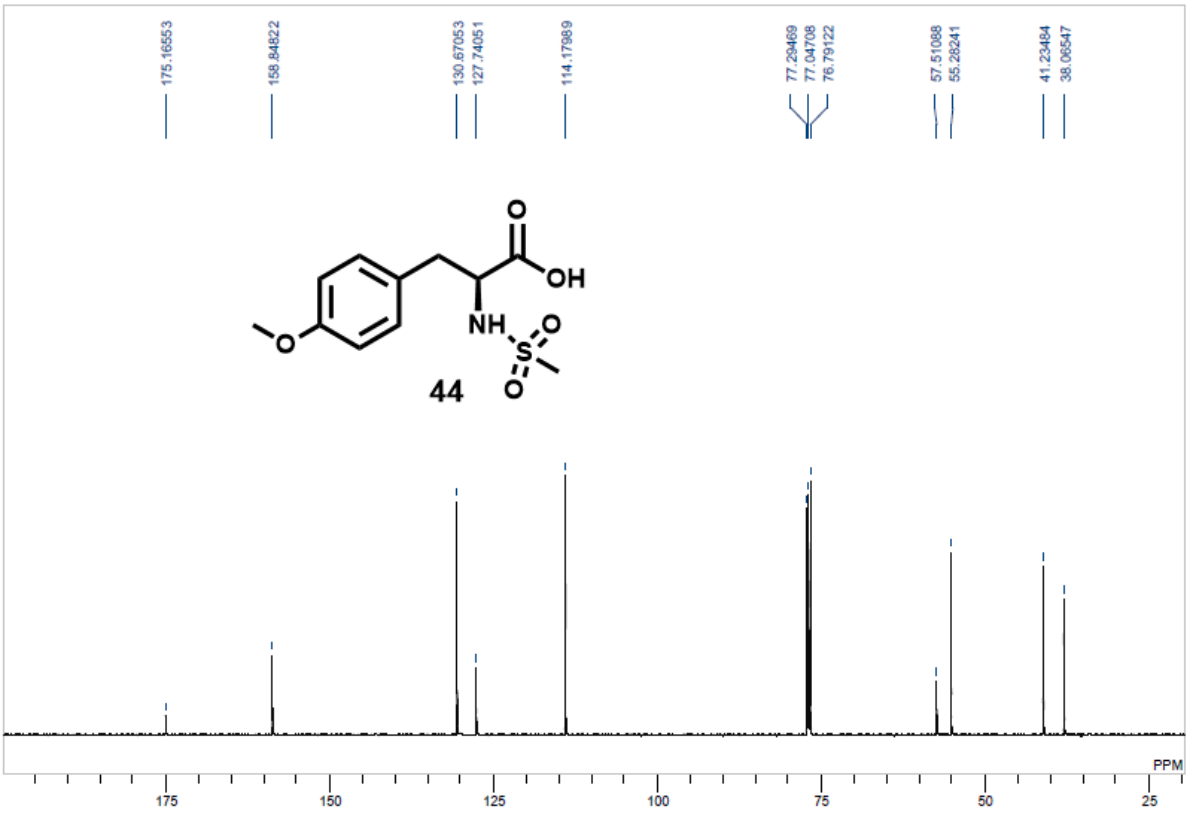
175.16553
158.84822
130.67053
127.74051
114.17989
77.29469
77.04708
76.79122
57.51088
55.28241
41.23484
38.06547
OH
NH
O
S
O
O
44
PPM
175
150
125
100
75
50
25

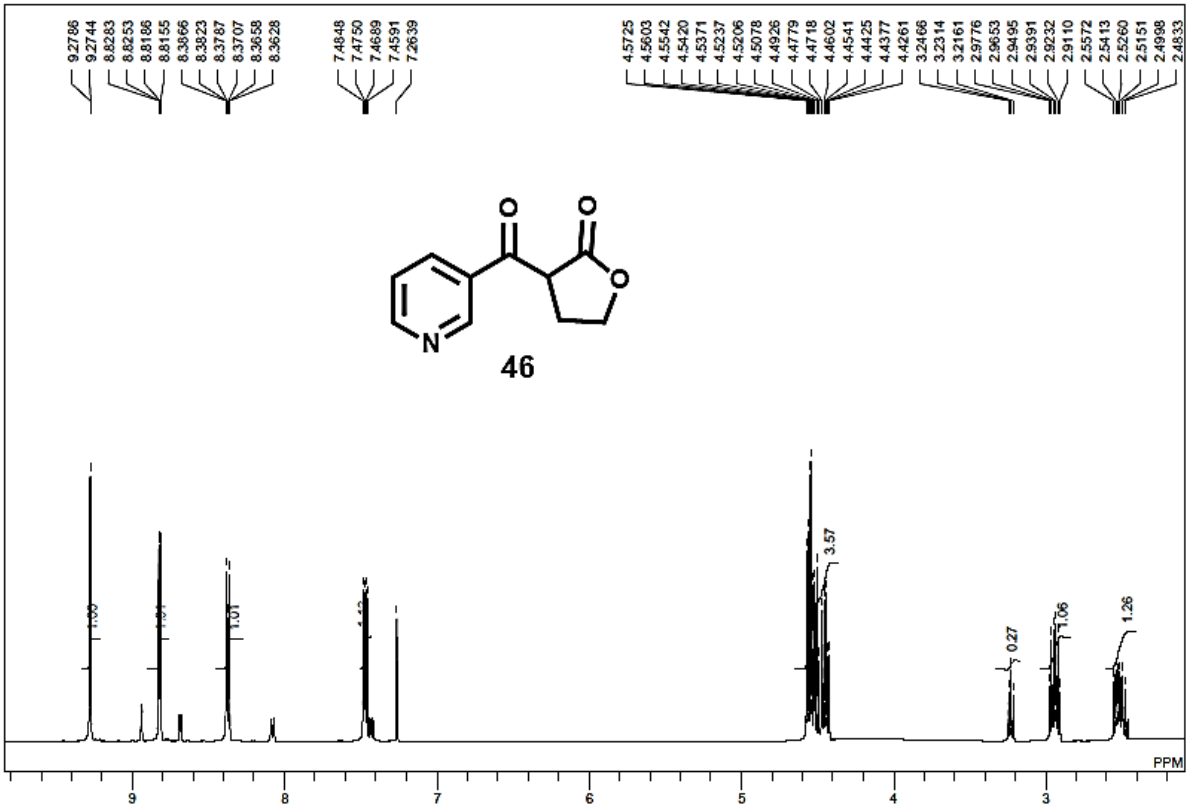
9.2786
9.2744
8.8263
8.8253
8.8186
8.8155
8.3866
8.3823
8.3787
8.3707
8.3658
8.3628
7.4848
7.4750
7.4689
7.4591
7.2639
4.5725
4.5603
4.5542
4.5420
4.5371
4.5237
4.5206
4.5078
4.4926
4.4779
4.4718
4.4602
4.4541
4.4425
4.4377
4.4261
3.2466
3.2314
3.2161
2.9776
2.9653
2.9495
2.9391
2.9232
2.9110
2.5572
2.5413
2.5260
2.5151
2.4998
2.4833
O
O
O
N
46
1.00
1.01
1.01
3.57
0.27
1.06
1.26
PPM
9
8
7
6
5
4
3

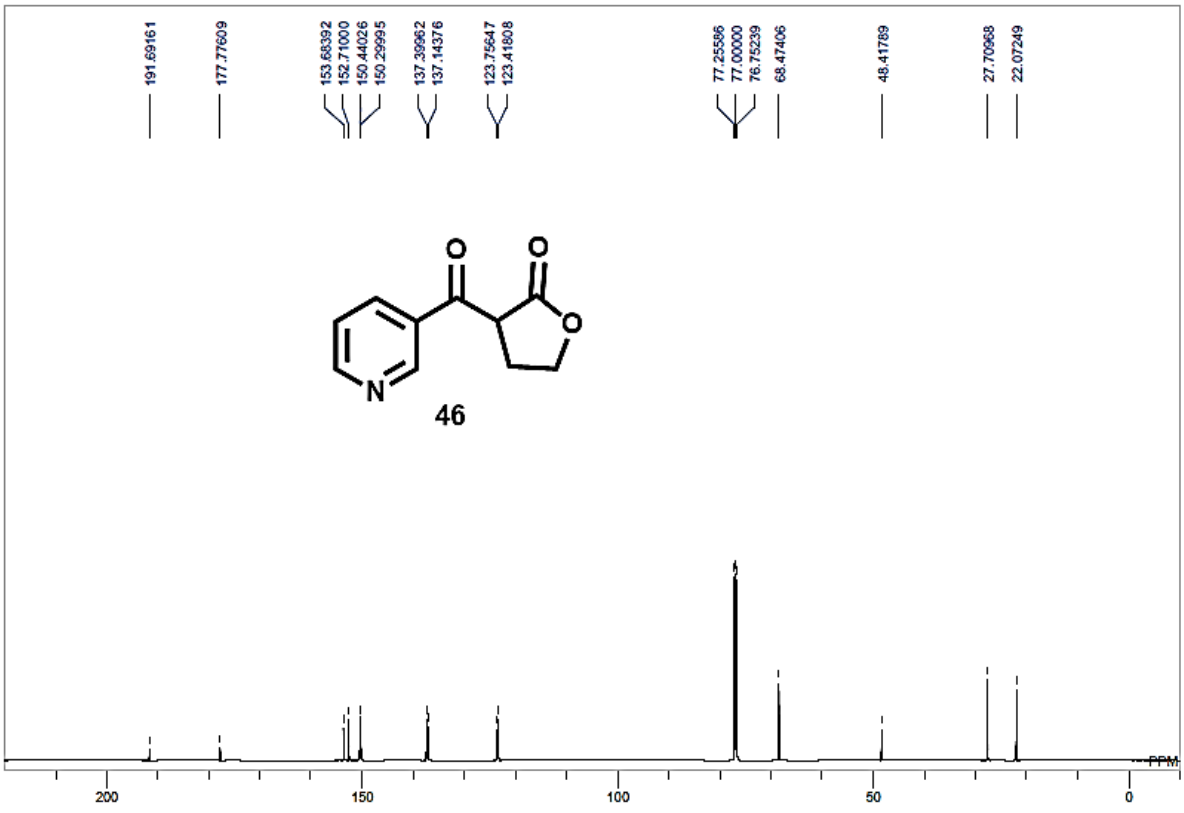
191.69161
177.77609
153.68392
152.71000
150.44026
150.29995
137.39962
137.14376
123.75647
123.41808
77.25586
77.00000
76.75239
68.47406
48.41789
27.70968
22.07249
O
O
O
N
46
PPM
200
150
100
50
0

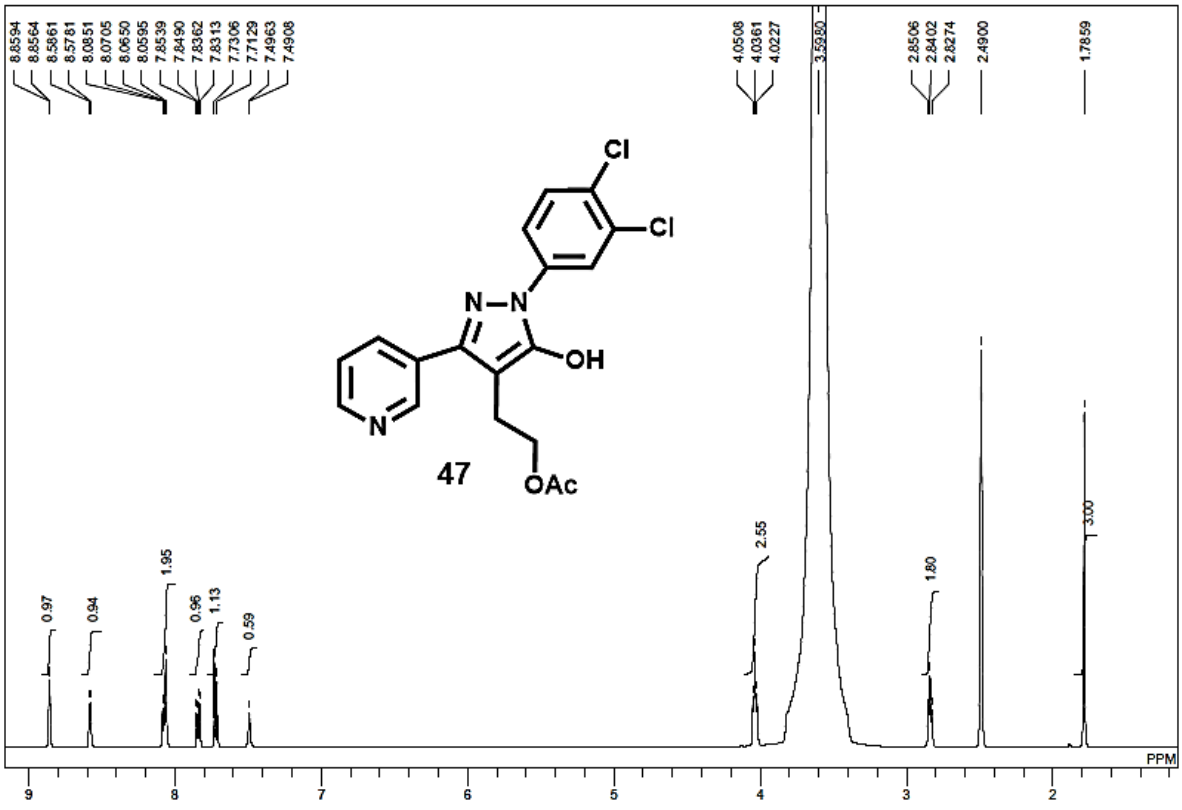
8.8594
8.8564
8.5861
8.5781
8.0851
8.0705
8.0650
8.0595
7.8539
7.8490
7.8362
7.8313
7.7306
7.7129
7.4963
7.4908
4.0508
4.0361
4.0227
3.5980
2.8506
2.8402
2.8274
2.4900
1.7859
Cl
Cl
N–N
OH
N
47
OAc
0.97
0.94
1.95
0.96
1.13
0.59
2.55
1.80
3.00
PPM
9
8
7
6
5
4
3
2

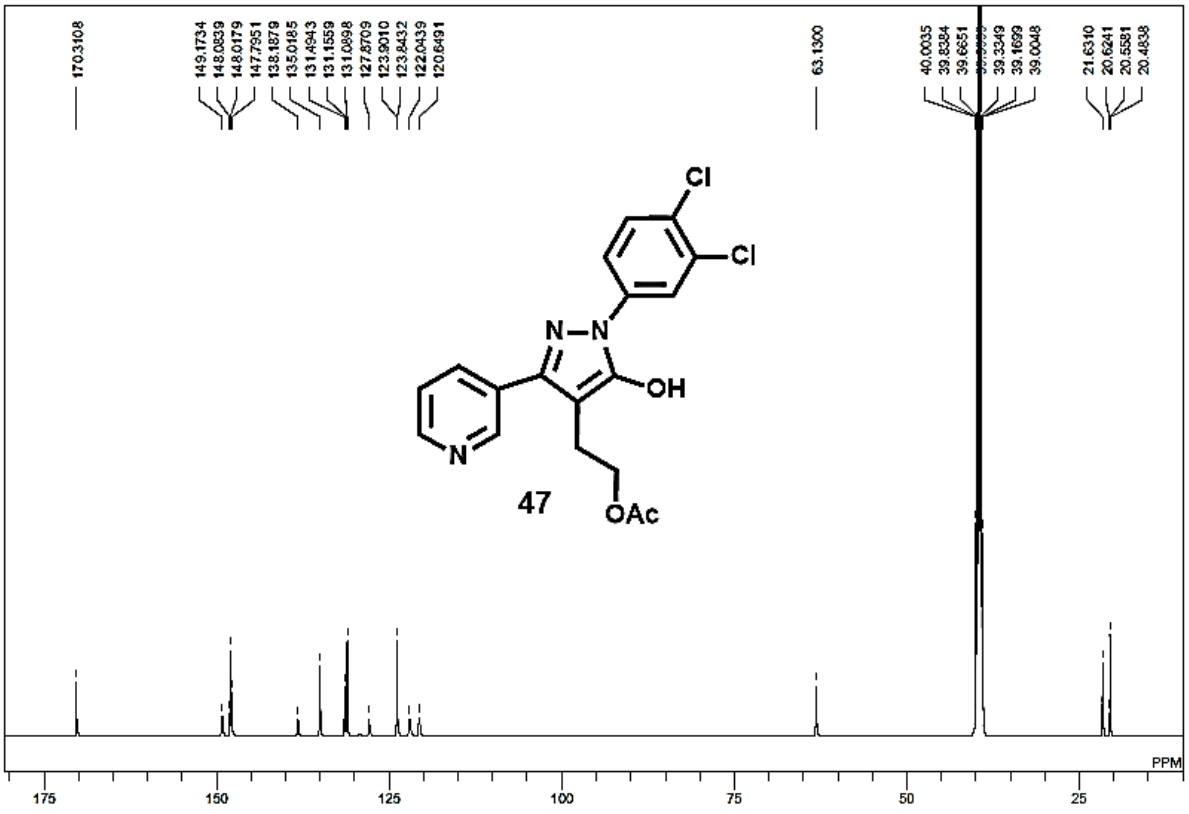
170.3108
149.1734
148.0839
148.0179
147.7951
138.1879
135.0185
131.4943
131.1559
131.0898
127.8709
123.9010
123.8432
122.0439
120.8491
63.1300
40.0035
39.8384
39.6651
39.3349
39.1699
39.0048
21.6310
20.6241
20.5581
20.4838
Cl
Cl
N–N
OH
N
47
OAc
PPM
175
150
125
100
75
50
25

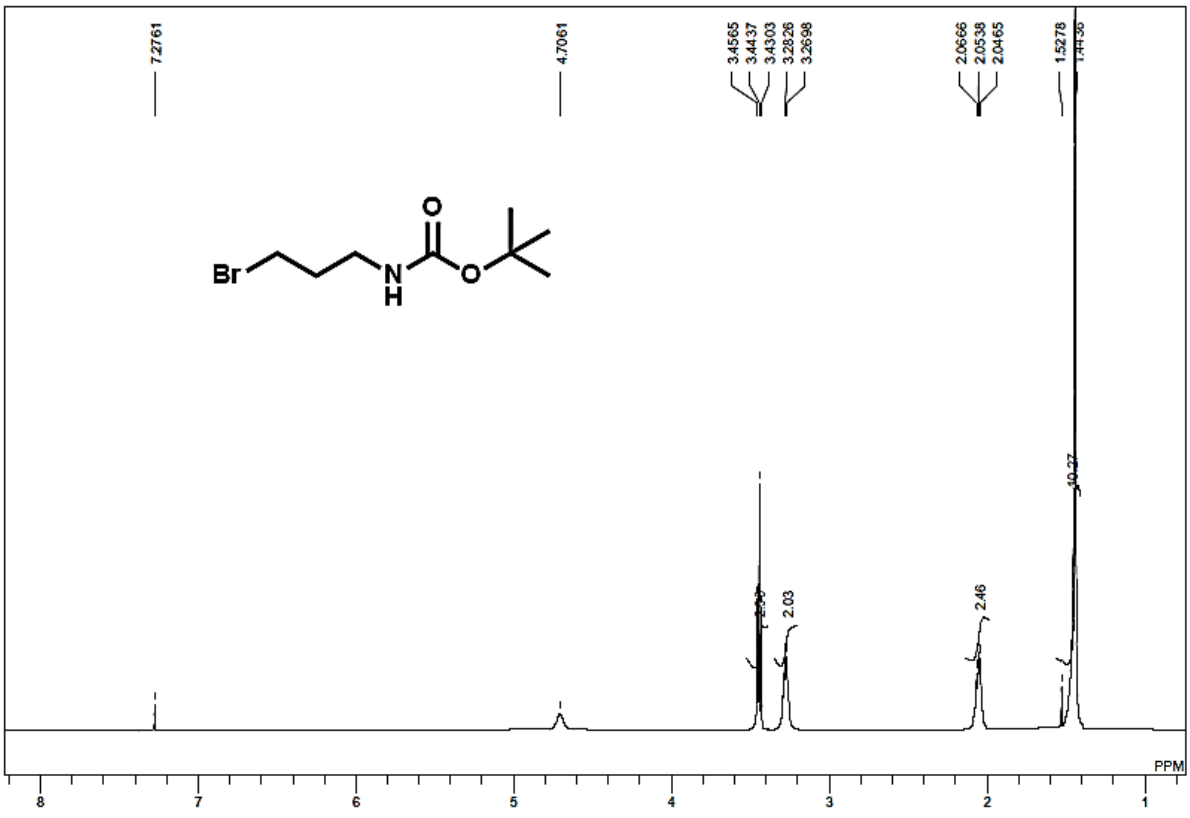
7.2761
4.7061
3.4565
3.4437
3.4303
3.2826
3.2698
2.0666
2.0538
2.0465
1.5278
1.4436
10.37
2.03
2.46
PPM
8
7
6
5
4
3
2
1

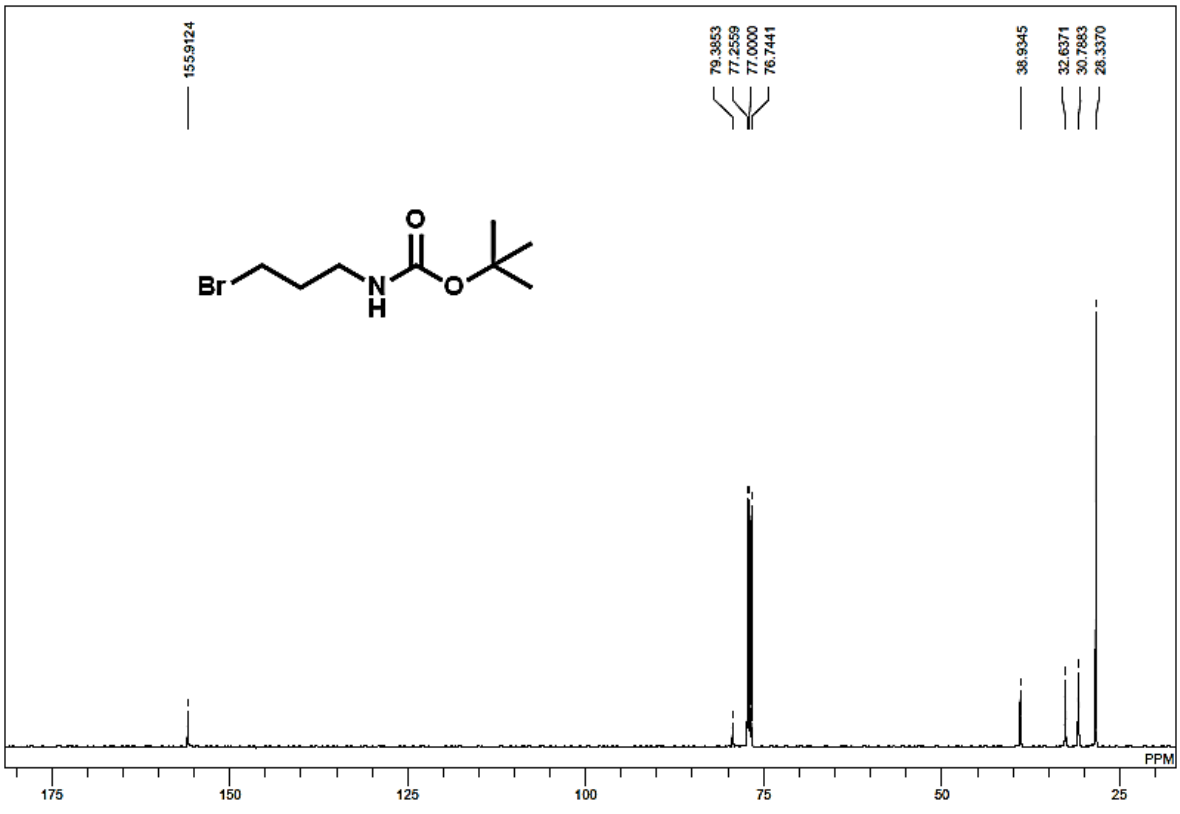
155.9124
79.3853
77.2559
77.0000
76.7441
38.9345
32.6371
30.7883
28.3370
PPM
175
150
125
100
75
50
25

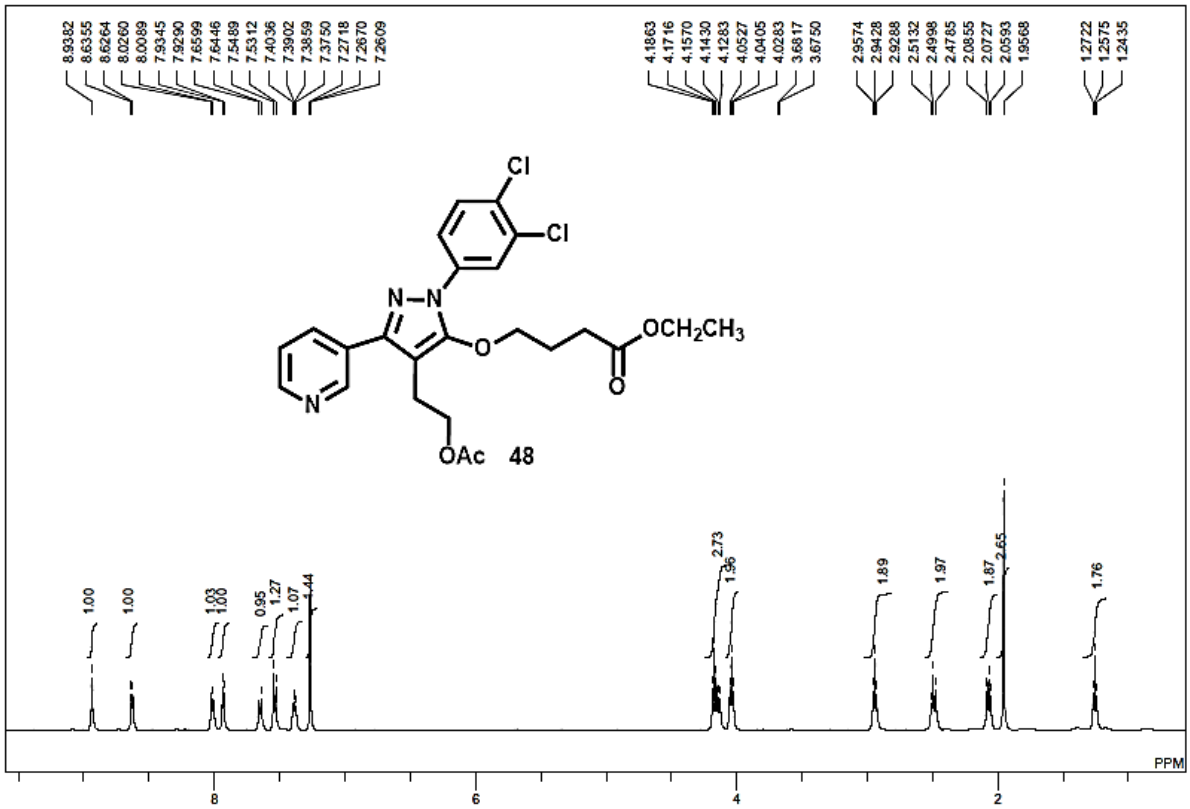
8.9382
8.6355
8.6264
8.0260
8.0089
7.9345
7.9290
7.6599
7.6446
7.5489
7.5312
7.4036
7.3902
7.3859
7.3750
7.2718
7.2670
7.2609
4.1863
4.1716
4.1570
4.1430
4.1283
4.0527
4.0405
4.0283
3.6817
3.6750
2.9574
2.9428
2.9288
2.5132
2.4998
2.4785
2.0855
2.0727
2.0593
1.9568
1.2722
1.2575
1.2435
Cl
Cl
N–N
O
OCH2CH3
O
N
OAc 48
1.00
1.00
1.03
1.00
0.95
1.27
1.07
1.44
2.73
1.36
1.89
1.97
1.87
2.65
1.76
PPM
8
6
4
2

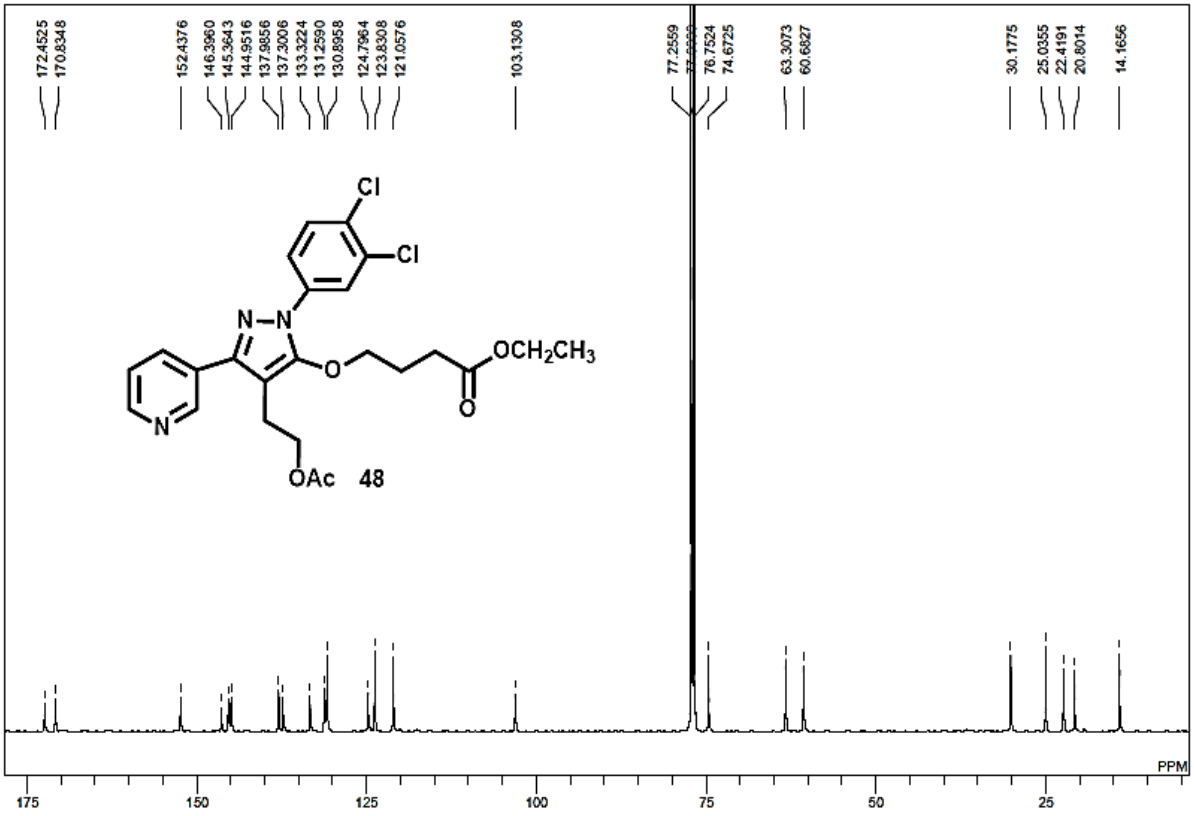
172.4525
170.8348
152.4376
146.3960
145.3643
144.9516
137.9856
137.3006
133.3224
131.2590
130.8958
124.7964
123.8308
121.0576
103.1308
77.2559
76.7524
74.6725
63.3073
60.6827
30.1775
25.0355
22.4191
20.8014
14.1656
Cl
Cl
N–N
O
OCH2CH3
O
N
OAc 48
PPM
175
150
125
100
75
50
25

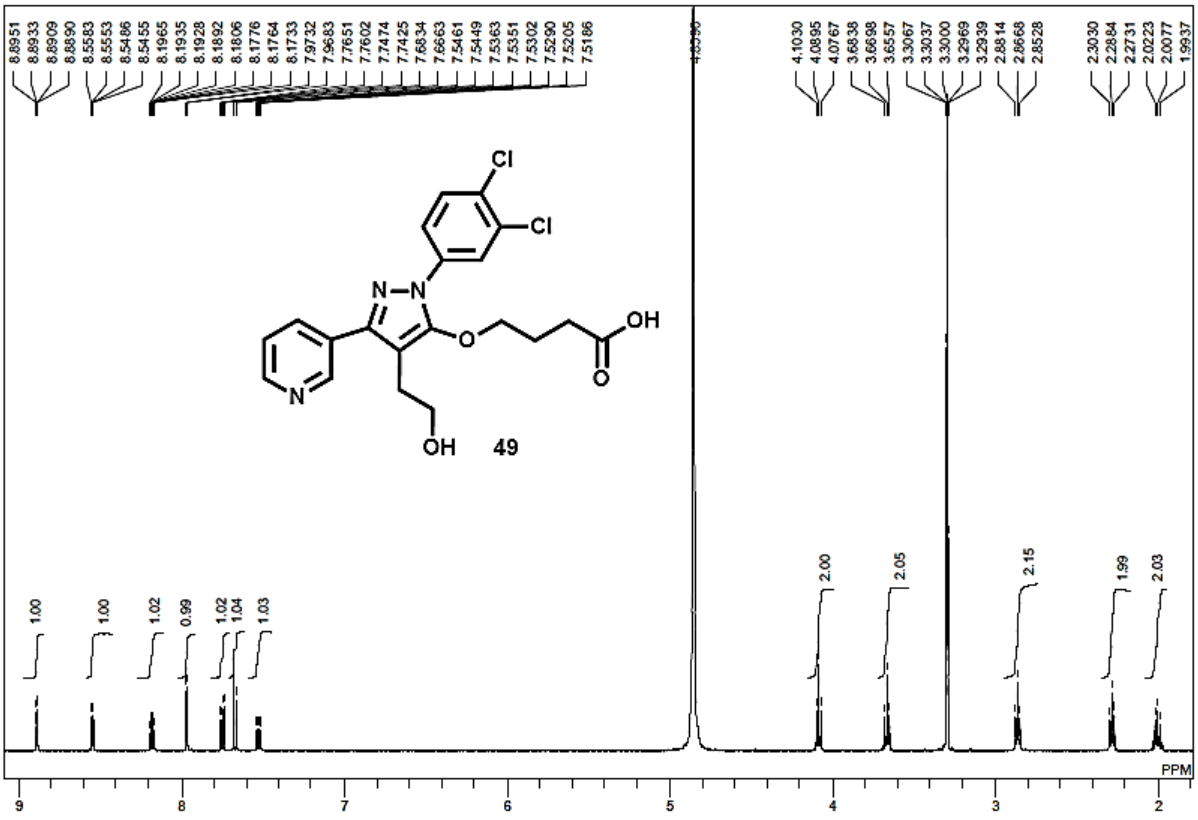
8.8951
8.8933
8.8909
8.8890
8.5583
8.5553
8.5486
8.5455
8.1965
8.1935
8.1928
8.1892
8.1806
8.1776
8.1764
8.1733
7.9732
7.9683
7.7651
7.7602
7.7474
7.7425
7.6834
7.6663
7.5461
7.5449
7.5363
7.5351
7.5302
7.5290
7.5205
7.5186
4.1030
4.0895
4.0767
3.6838
3.6698
3.6557
3.3067
3.3037
3.3000
3.2969
3.2939
2.8814
2.8668
2.8528
2.3030
2.2884
2.2731
2.0223
2.0077
1.9937
Cl
Cl
N
N
O
OH
O
N
OH
49
1.00
1.00
1.02
0.99
1.02
1.04
1.03
2.00
2.05
2.15
1.99
2.03
PPM
9
8
7
6
5
4
3
2

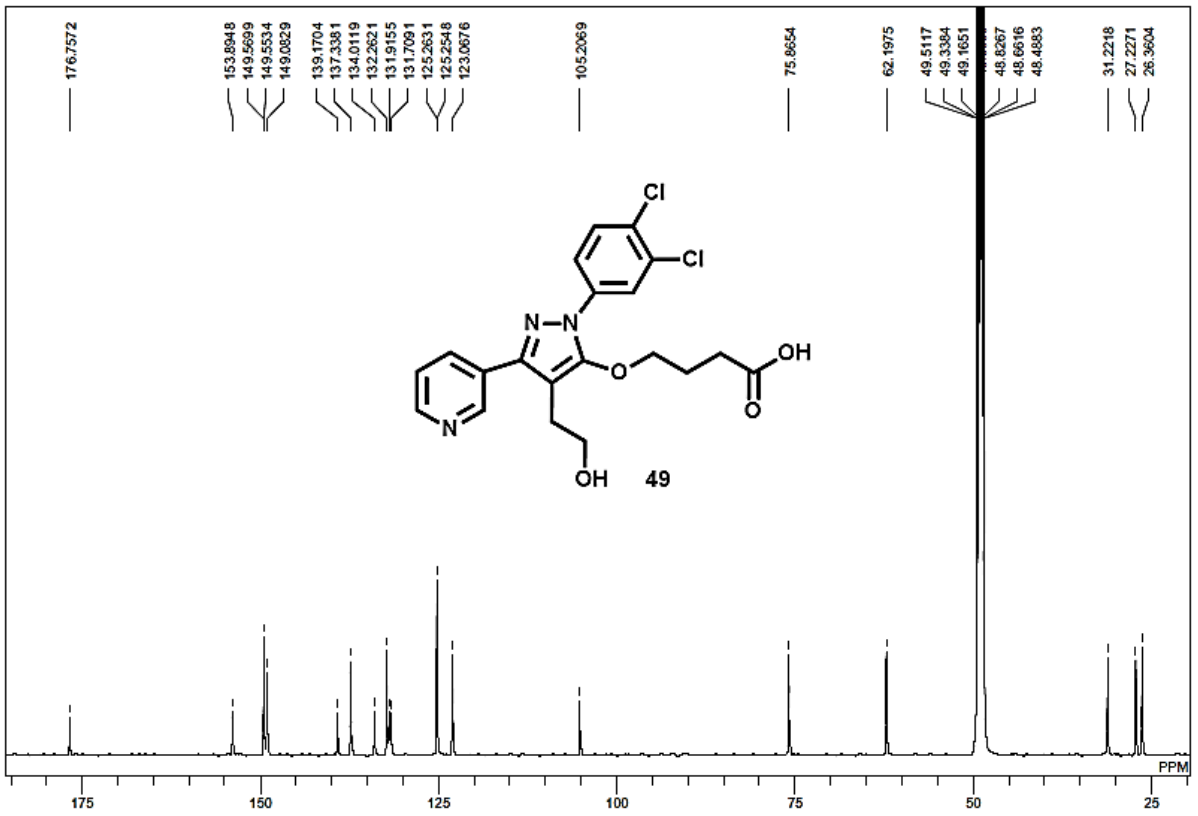
176.7572
153.8948
149.5699
149.5534
149.0829
139.1704
137.3381
134.0119
132.2621
131.9155
131.7091
125.2631
125.2548
123.0676
105.2069
75.8654
62.1975
49.5117
49.3384
49.1651
48.8267
48.6616
48.4883
31.2218
27.2271
26.3604
Cl
Cl
N
N
O
OH
O
N
OH
49
PPM
175
150
125
100
75
50
25

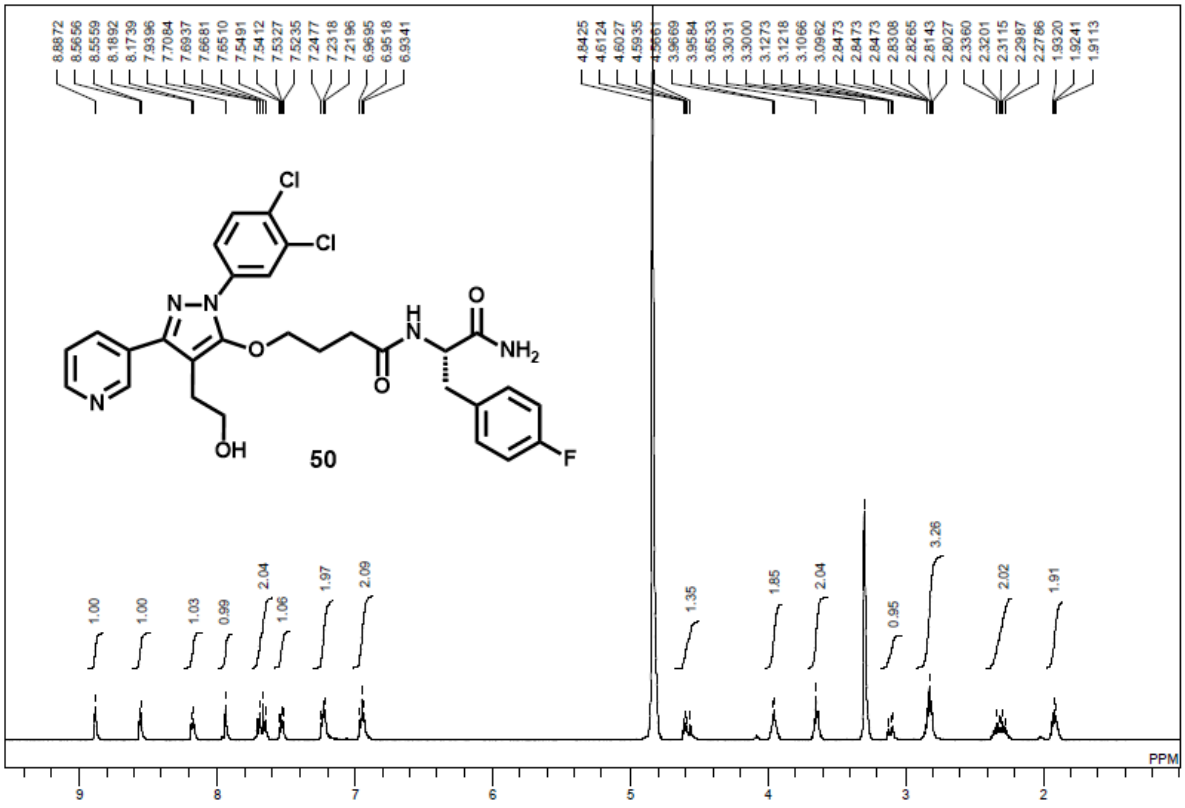
8.8872
8.5656
8.5559
8.1892
8.1739
7.9396
7.7084
7.6937
7.6681
7.6510
7.5491
7.5412
7.5327
7.5235
7.2477
7.2318
7.2196
6.9695
6.9518
6.9341
4.8425
4.6124
4.6027
4.5935
4.5661
3.9669
3.9584
3.6533
3.3031
3.3000
3.1273
3.1218
3.1066
3.0962
2.8473
2.8473
2.8473
2.8308
2.8265
2.8143
2.8027
2.3360
2.3201
2.3115
2.2987
2.2786
1.9320
1.9241
1.9113
Cl
Cl
N
N
O
H
N
O
NH2
O
N
OH
F
50
1.00
1.00
1.03
0.99
2.04
1.06
1.97
2.09
1.35
1.85
2.04
0.95
3.26
2.02
1.91
PPM
9
8
7
6
5
4
3
2

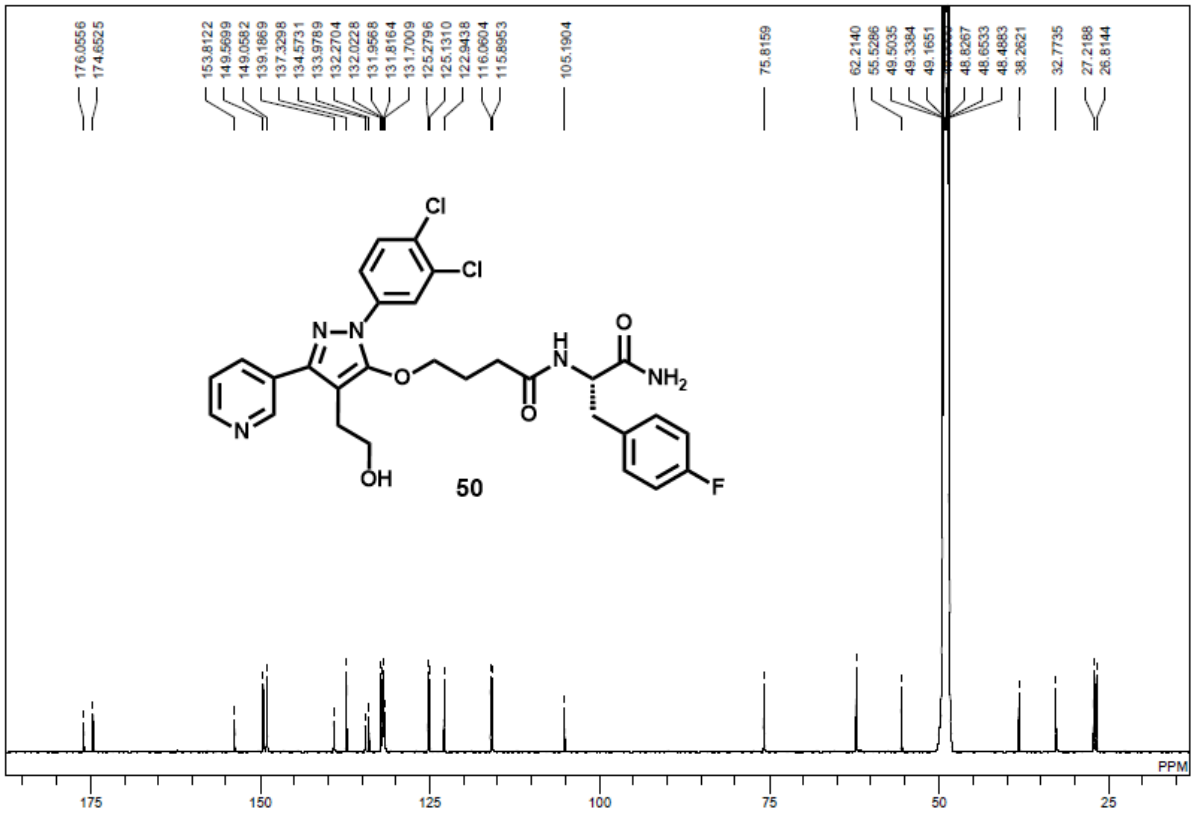
176.0556
174.6525
153.8122
149.5699
149.0582
139.1869
137.3298
134.5731
133.9789
132.2704
132.0228
131.9568
131.8164
131.7009
125.2796
125.1310
122.9438
116.0604
115.8953
105.1904
75.8159
62.2140
55.5286
49.5035
49.3384
49.1651
48.8267
48.6533
48.4883
38.2621
32.7735
27.2188
26.8144
Cl
Cl
N
N
O
H
N
O
NH2
O
N
OH
F
50
PPM
175
150
125
100
75
50
25

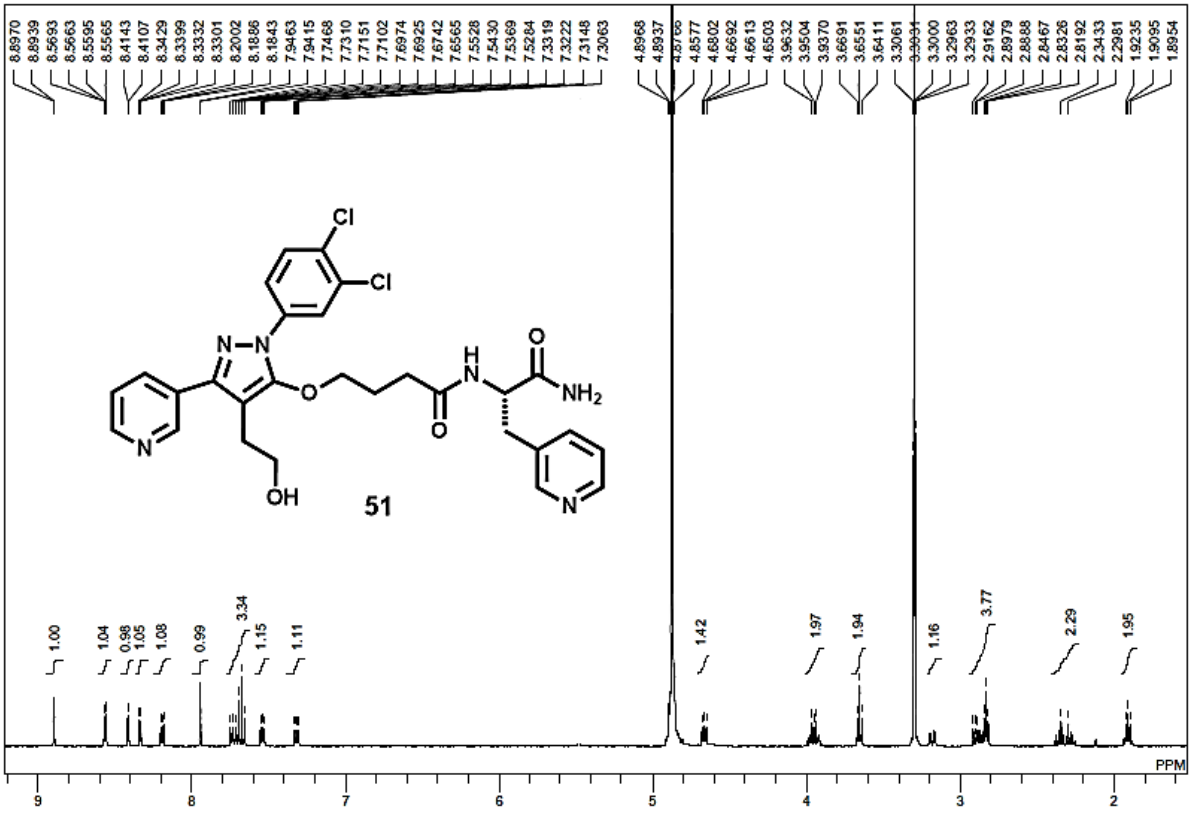
51
PPM

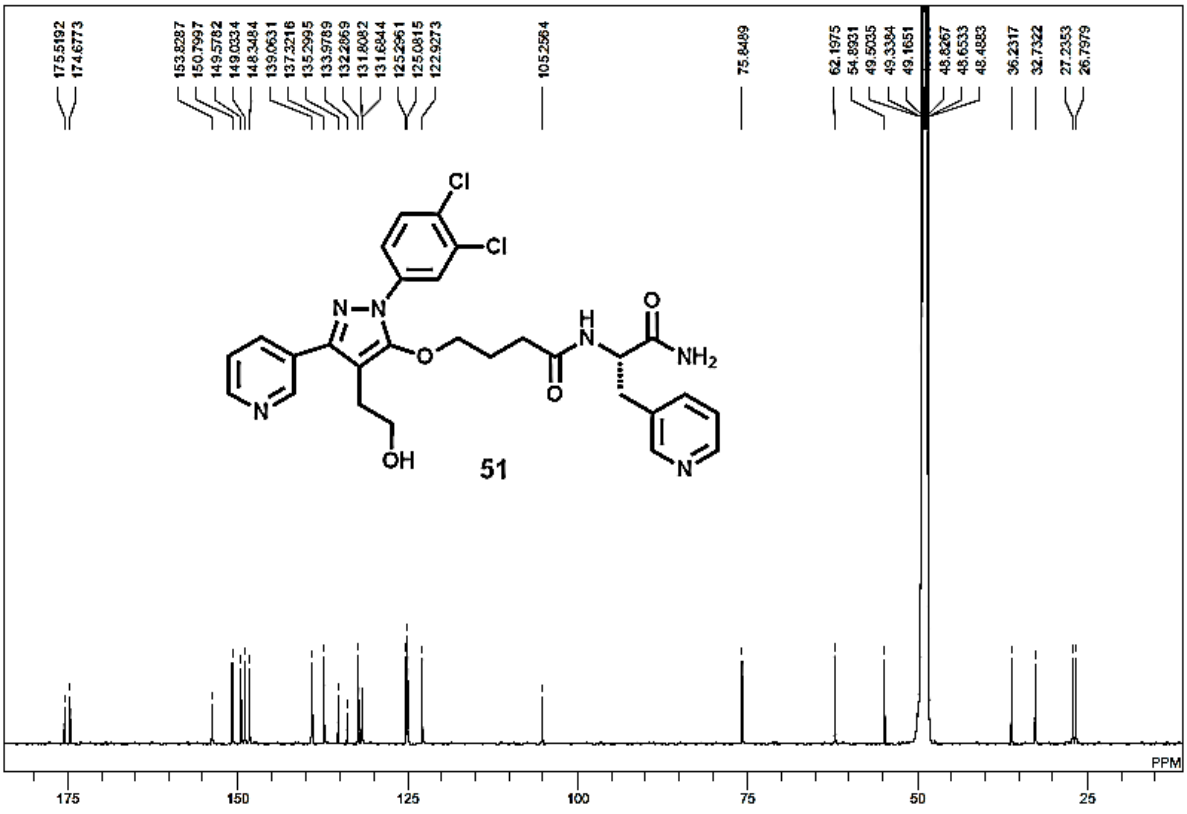
51
PPM

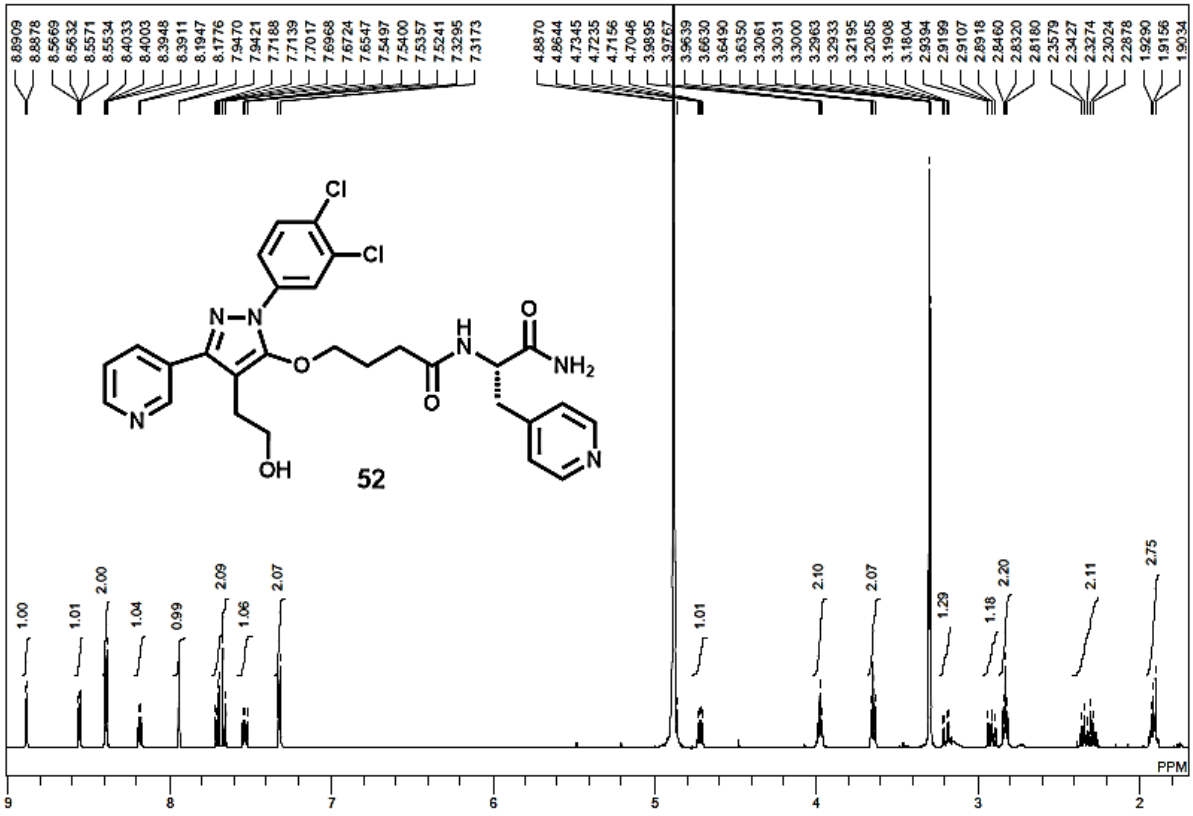
8.8909
8.8878
8.5669
8.5632
8.5571
8.5534
8.4033
8.4003
8.3948
8.3911
8.1947
8.1776
7.9470
7.9421
7.7188
7.7139
7.7017
7.6968
7.6724
7.6547
7.5497
7.5400
7.5357
7.5241
7.3295
7.3173
4.8870
4.8644
4.7345
4.7235
4.7156
4.7046
3.9895
3.9767
3.9639
3.6630
3.6490
3.6350
3.3061
3.3031
3.3000
3.2963
3.2933
3.2195
3.2085
3.1908
3.1804
2.9394
2.9199
2.9107
2.8918
2.8460
2.8320
2.8180
2.3579
2.3427
2.3274
2.3024
2.2878
1.9290
1.9156
1.9034
Cl
Cl
N
N
O
H
N
O
NH2
O
N
OH
52
1.00
1.01
2.00
1.04
0.99
2.09
1.06
2.07
1.01
2.10
2.07
1.29
1.18
2.20
2.11
2.75
PPM
9
8
7
6
5
4
3
2

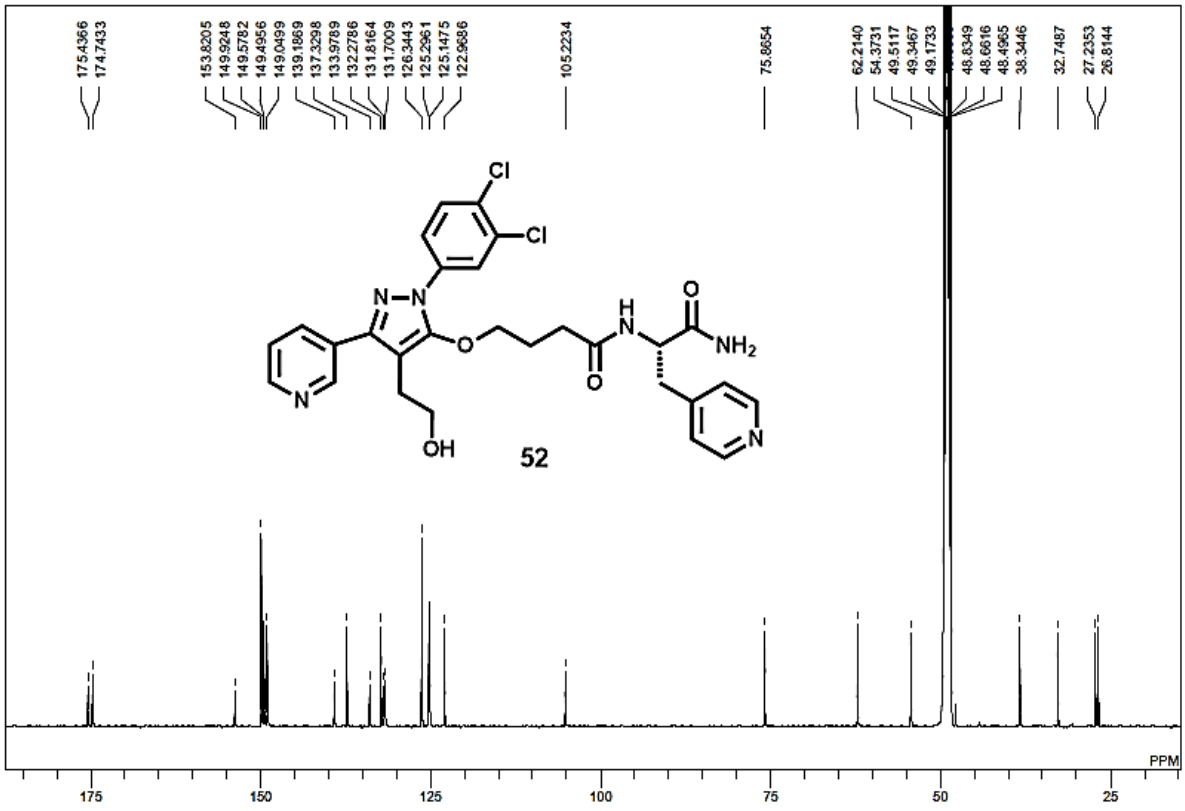
175.4366
174.7433
153.8205
149.9248
149.5782
149.4956
149.0499
139.1869
137.3298
133.9789
132.2786
131.8164
131.7009
126.3443
125.2961
125.1475
122.9686
105.2234
75.8654
62.2140
54.3731
49.5117
49.3467
49.1733
48.8349
48.6616
48.4965
38.3446
32.7487
27.2353
26.8144
Cl
Cl
N
N
O
H
N
O
NH2
O
N
OH
52
PPM
175
150
125
100
75
50
25

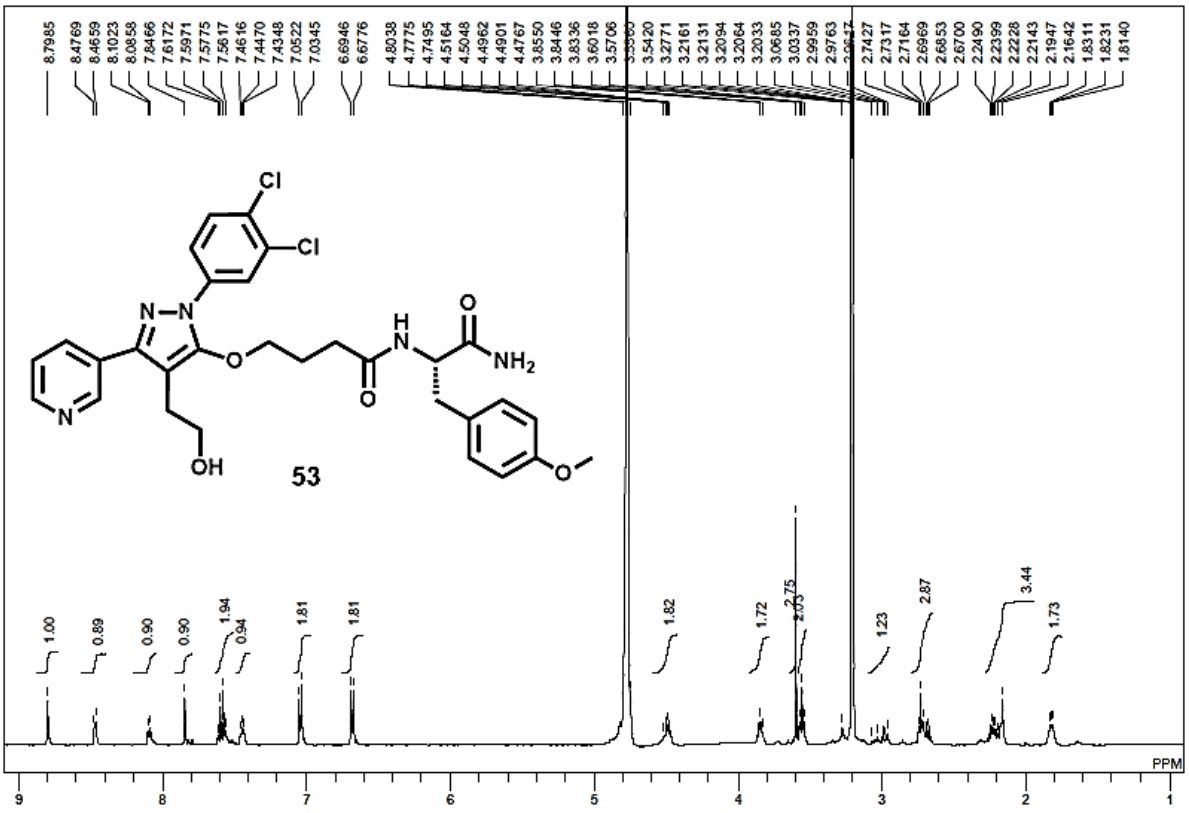
53
PPM

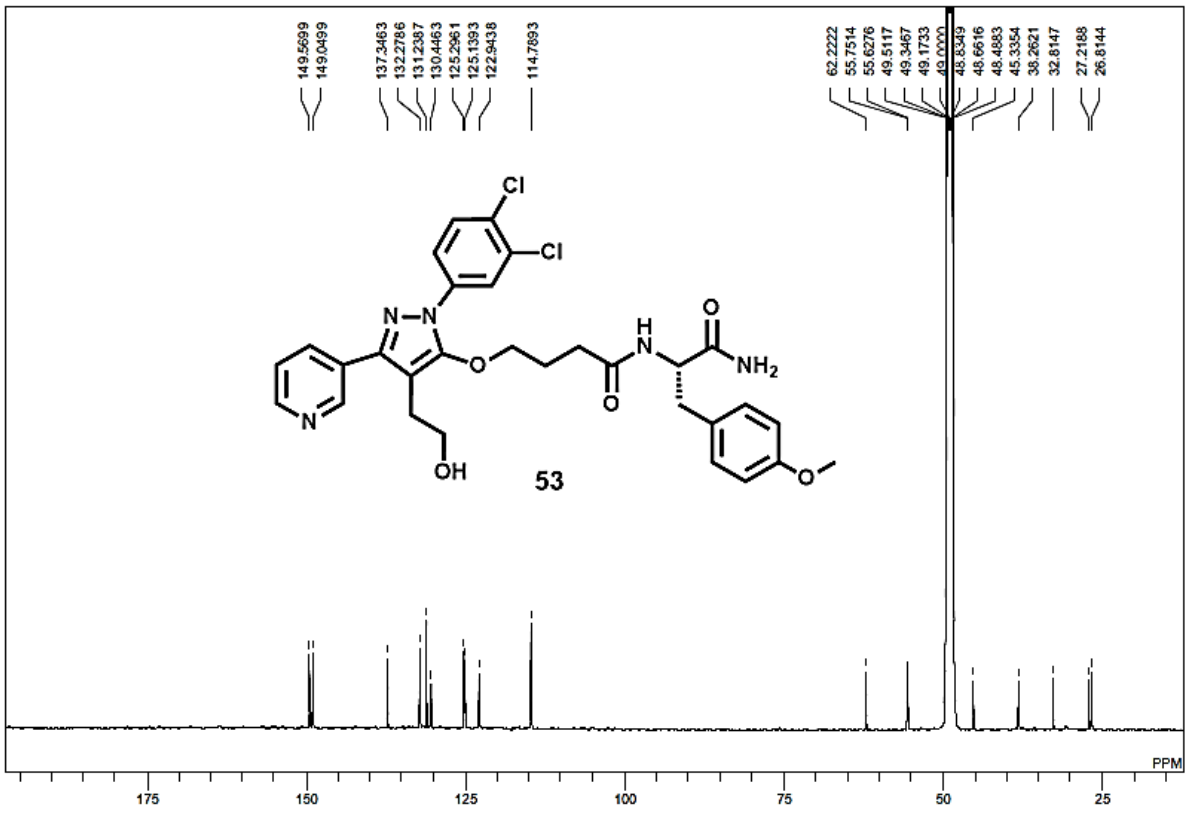
53
PPM

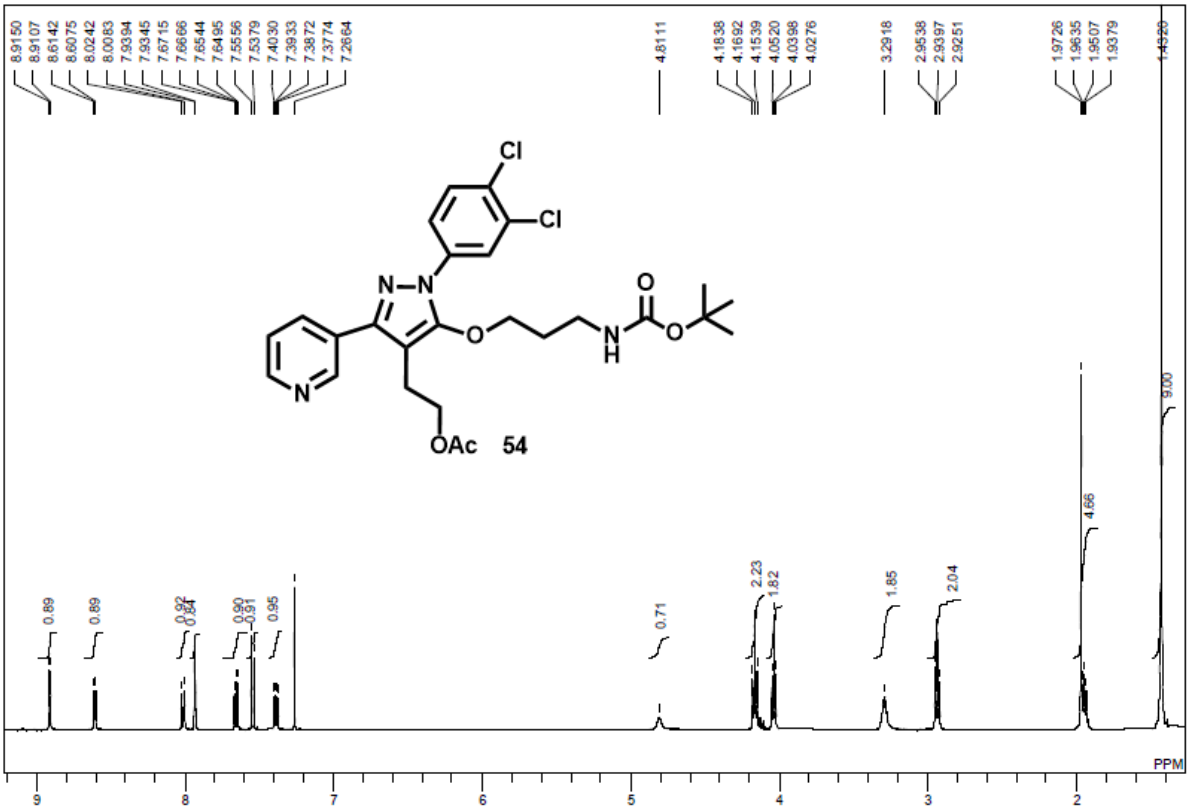
8.9150
8.9107
8.6142
8.6075
8.0242
8.0083
7.9394
7.9345
7.6715
7.6666
7.6544
7.6495
7.5556
7.5379
7.4030
7.3933
7.3872
7.3774
7.2664
4.8111
4.1838
4.1692
4.1539
4.0520
4.0398
4.0276
3.2918
2.9538
2.9397
2.9251
1.9726
1.9635
1.9507
1.9379
1.4320
9.00
4.66
2.23
1.82
1.85
2.04
0.71
0.89
0.89
0.92
0.84
0.90
0.91
0.95
Cl
Cl
N–N
O
N
H
O
O
N
OAc 54
PPM
9
8
7
6
5
4
3
2

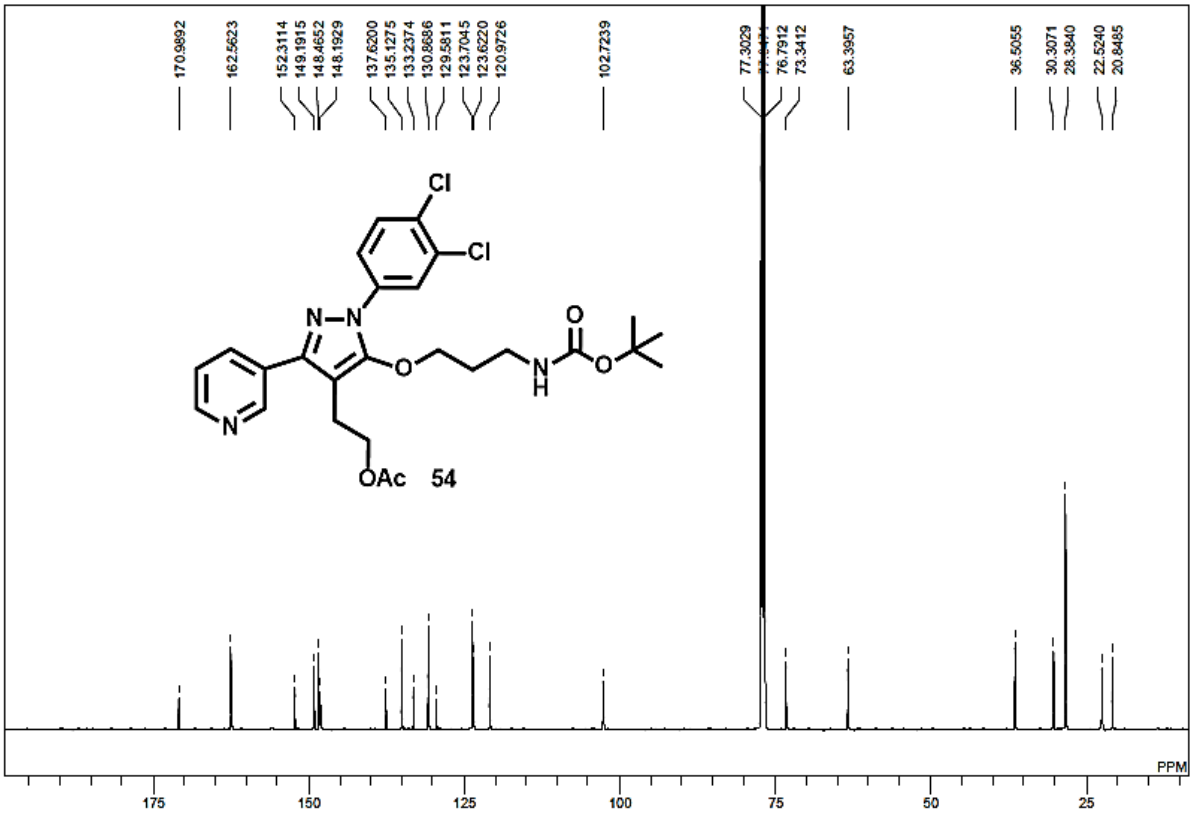
170.9892
162.5623
152.3114
149.1915
148.4652
148.1929
137.6200
135.1275
133.2374
130.8686
129.5811
123.7045
123.6220
120.9726
102.7239
77.3029
76.7912
73.3412
63.3957
36.5055
30.3071
28.3840
22.5240
20.8485
Cl
Cl
N–N
O
N
H
O
O
N
OAc 54
PPM
175
150
125
100
75
50
25

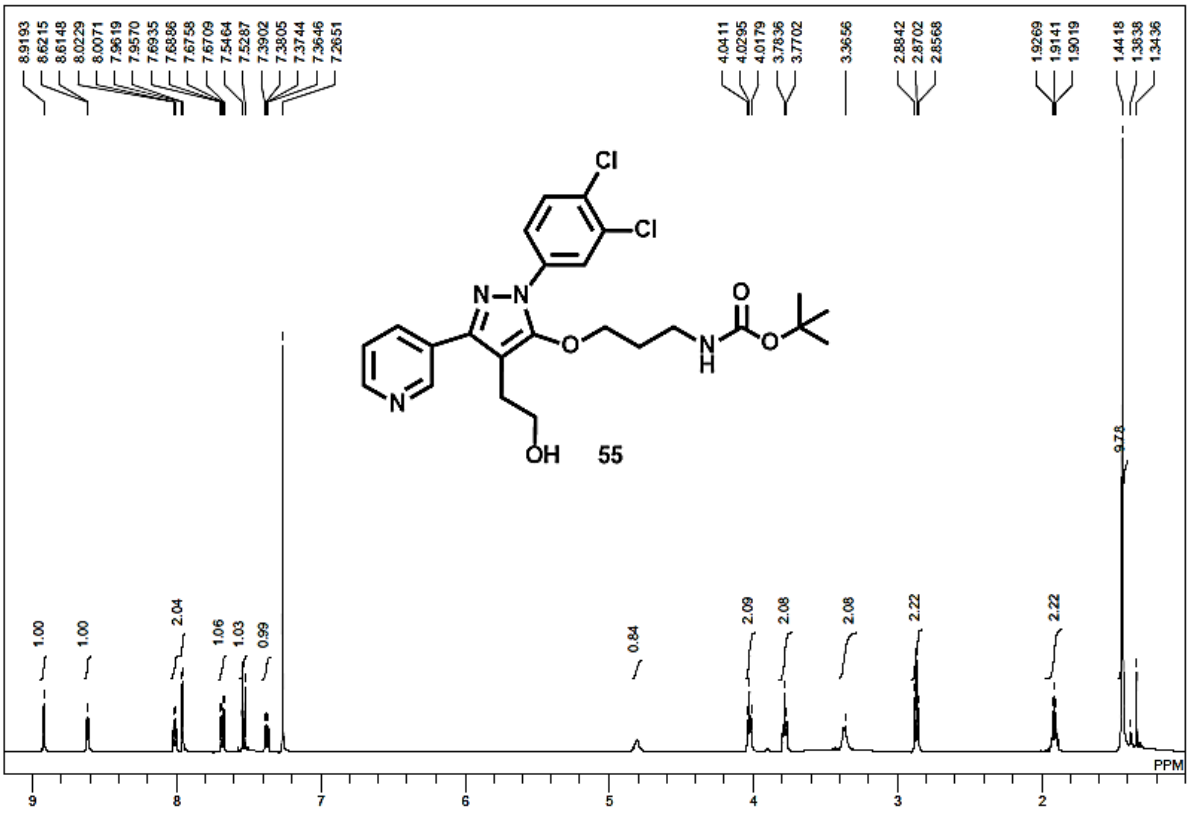
8.9193
8.6215
8.6148
8.0229
8.0071
7.9619
7.9570
7.6935
7.6886
7.6758
7.6709
7.5464
7.5287
7.3902
7.3805
7.3744
7.3646
7.2651
4.0411
4.0295
4.0179
3.7836
3.7702
3.3656
2.8842
2.8702
2.8568
1.9269
1.9141
1.9019
1.4418
1.3838
1.3436
Cl
Cl
N
N
O
O
N
H
O
N
OH
55
1.00
1.00
2.04
1.06
1.03
0.99
0.84
2.09
2.08
2.08
2.22
2.22
9.78
PPM
9
8
7
6
5
4
3
2

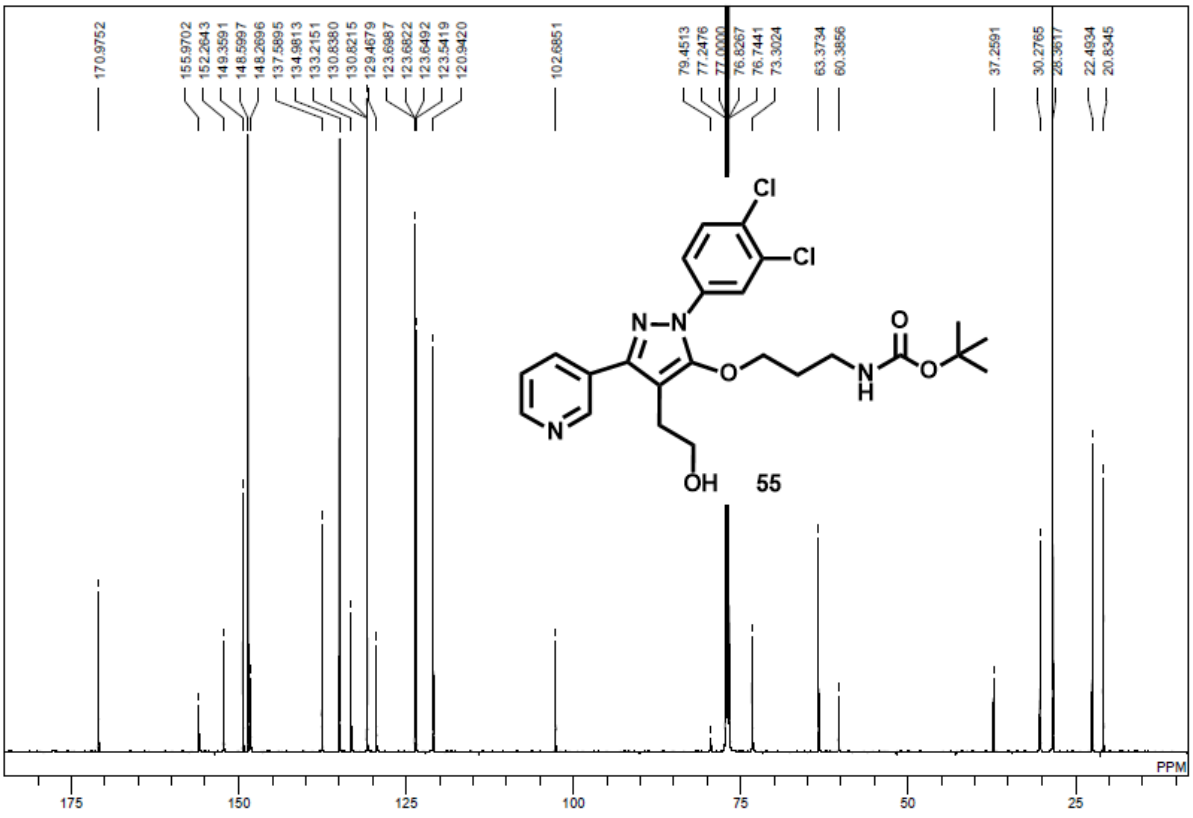
170.9752
155.9702
152.2643
149.3591
148.5997
148.2696
137.5895
134.9813
133.2151
130.8380
130.8215
129.4679
123.6987
123.6822
123.6492
123.5419
120.9420
102.6851
79.4513
77.2476
77.0000
76.8267
76.7441
73.3024
63.3734
60.3856
37.2591
30.2765
28.3617
22.4934
20.8345
Cl
Cl
N
N
O
O
N
H
O
N
OH
55
PPM
175
150
125
100
75
50
25

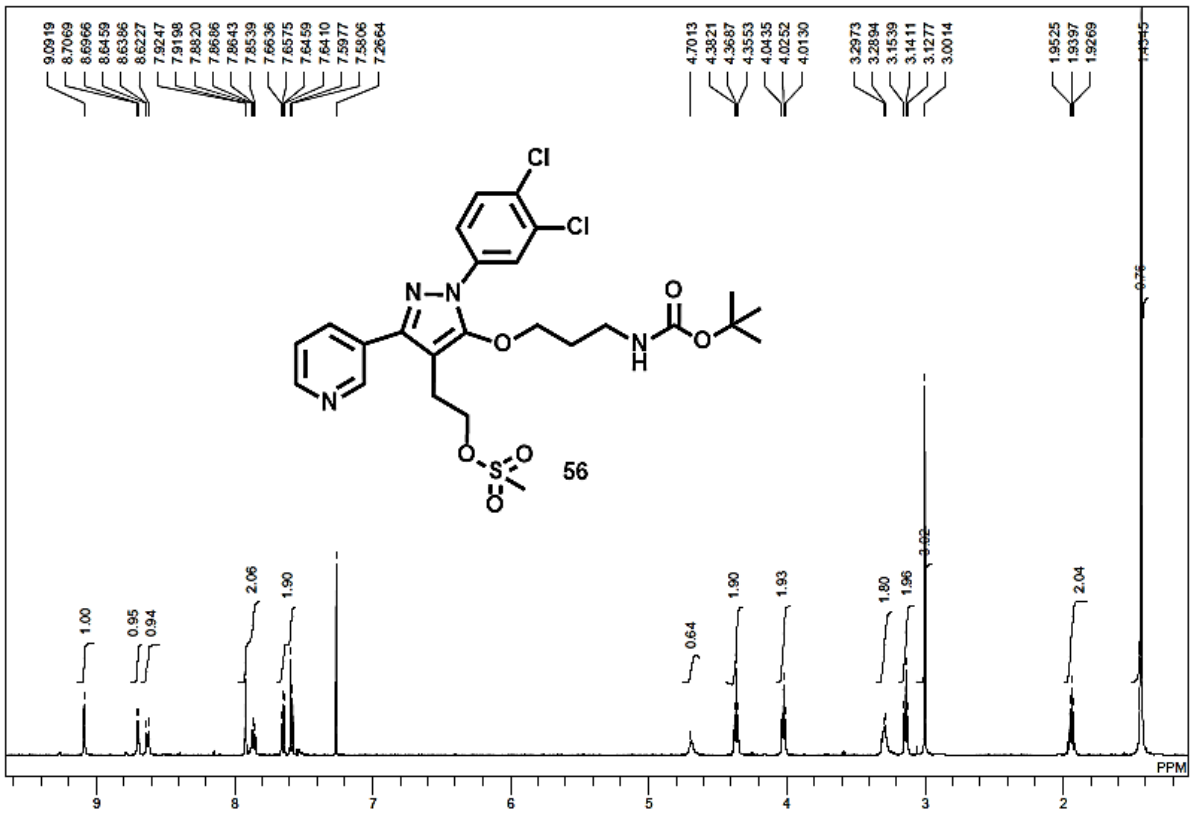
9.0919
8.7069
8.6966
8.6459
8.6386
8.6227
7.9247
7.9198
7.8820
7.8686
7.8643
7.8539
7.6636
7.6575
7.6459
7.6410
7.5977
7.5806
7.2664
4.7013
4.3821
4.3687
4.3553
4.0435
4.0252
4.0130
3.2973
3.2894
3.1539
3.1411
3.1277
3.0014
1.9525
1.9397
1.9269
1.4345
0.76
Cl
Cl
N
N
O
O
N
H
O
O
O
S
O
56
1.00
0.95
0.94
2.06
1.90
0.64
1.90
1.93
1.80
1.96
3.02
2.04
PPM
9
8
7
6
5
4
3
2

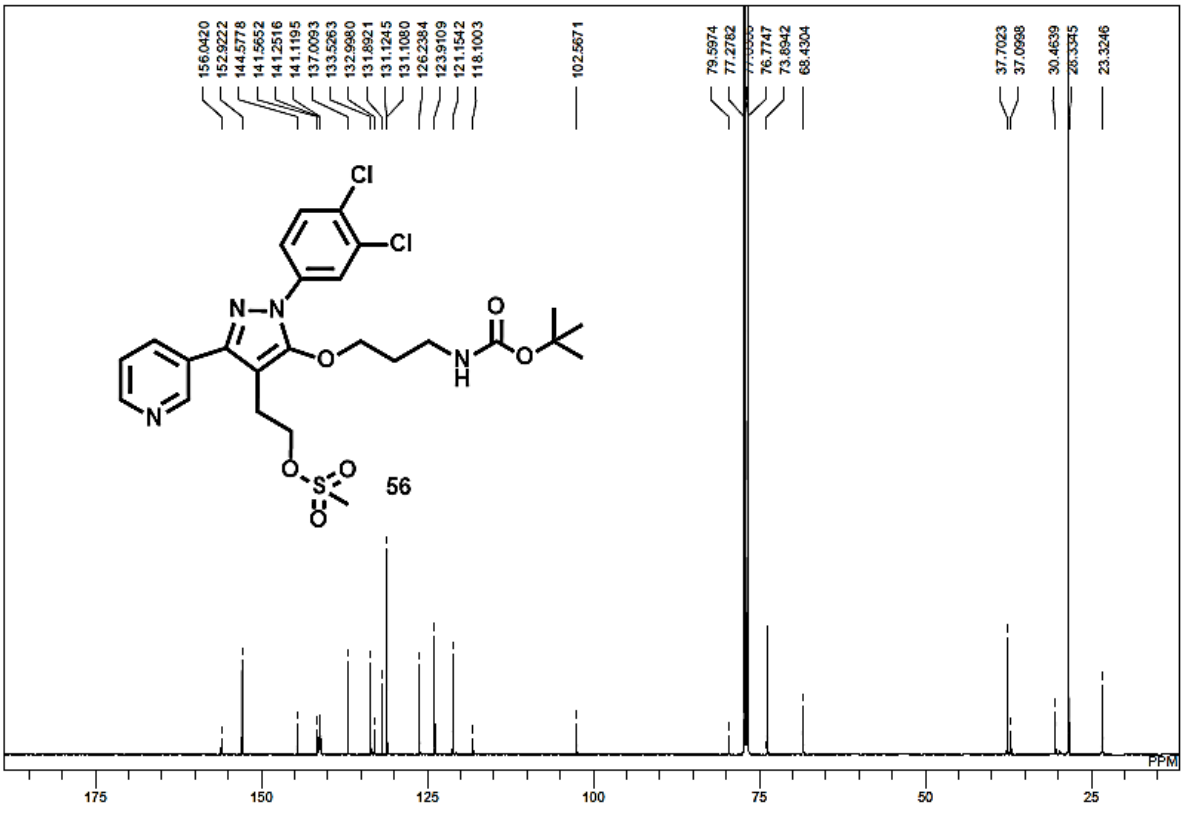
156.0420
152.9222
144.5778
141.5652
141.2516
141.1195
137.0093
133.5263
132.9980
131.8921
131.1245
131.1080
126.2384
123.9109
121.1542
118.1003
102.5671
79.5974
77.2762
76.7747
73.8942
68.4304
37.7023
37.0988
30.4639
28.3345
23.3246
Cl
Cl
N
N
O
O
N
H
O
O
O
S
O
56
PPM
175
150
125
100
75
50
25

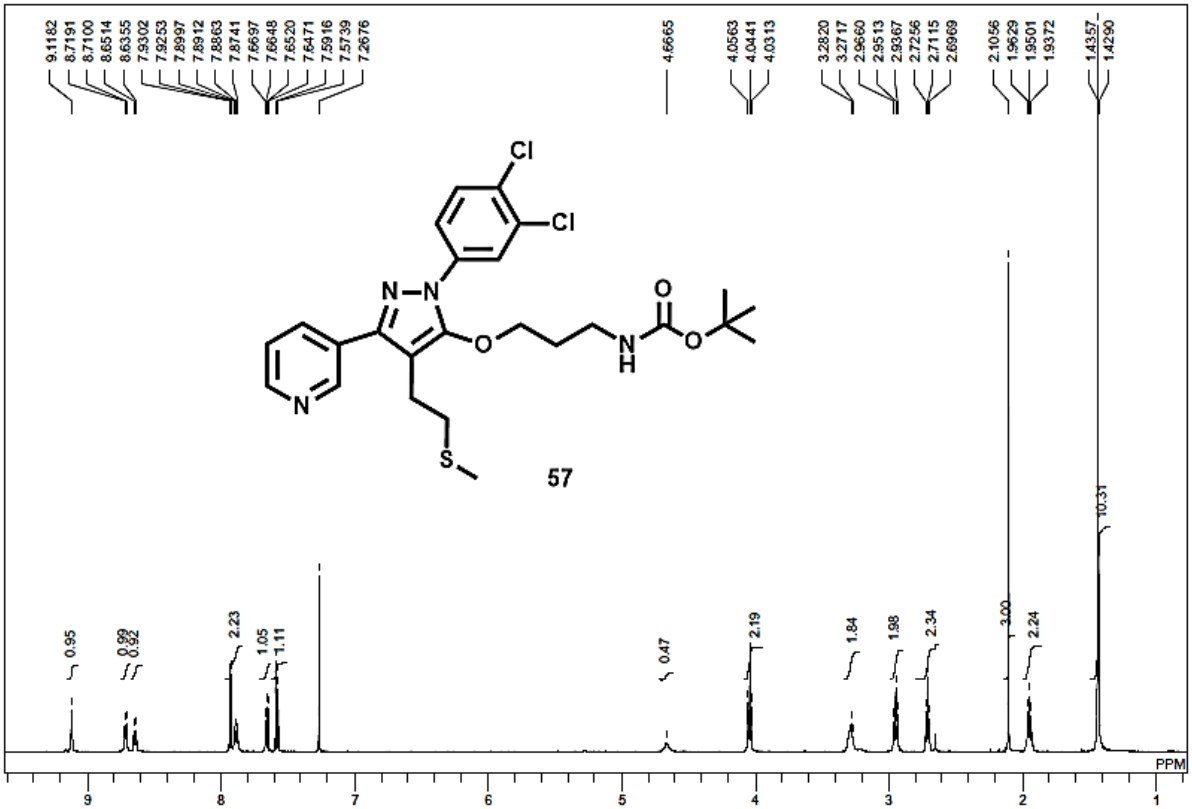
9.1182
8.7191
8.7100
8.6514
8.6355
7.9302
7.9253
7.8997
7.8912
7.8863
7.8741
7.6697
7.6648
7.6520
7.6471
7.5916
7.5739
7.2676
4.6665
4.0563
4.0441
4.0313
3.2820
3.2717
2.9660
2.9513
2.9367
2.7256
2.7115
2.6969
2.1056
1.9629
1.9501
1.9372
1.4357
1.4290
Cl
Cl
N
N
O
O
N
H
O
N
S
57
0.95
0.99
0.92
2.23
1.05
1.11
0.47
2.19
1.84
1.98
2.34
3.00
2.24
10.31
PPM
9
8
7
6
5
4
3
2
1

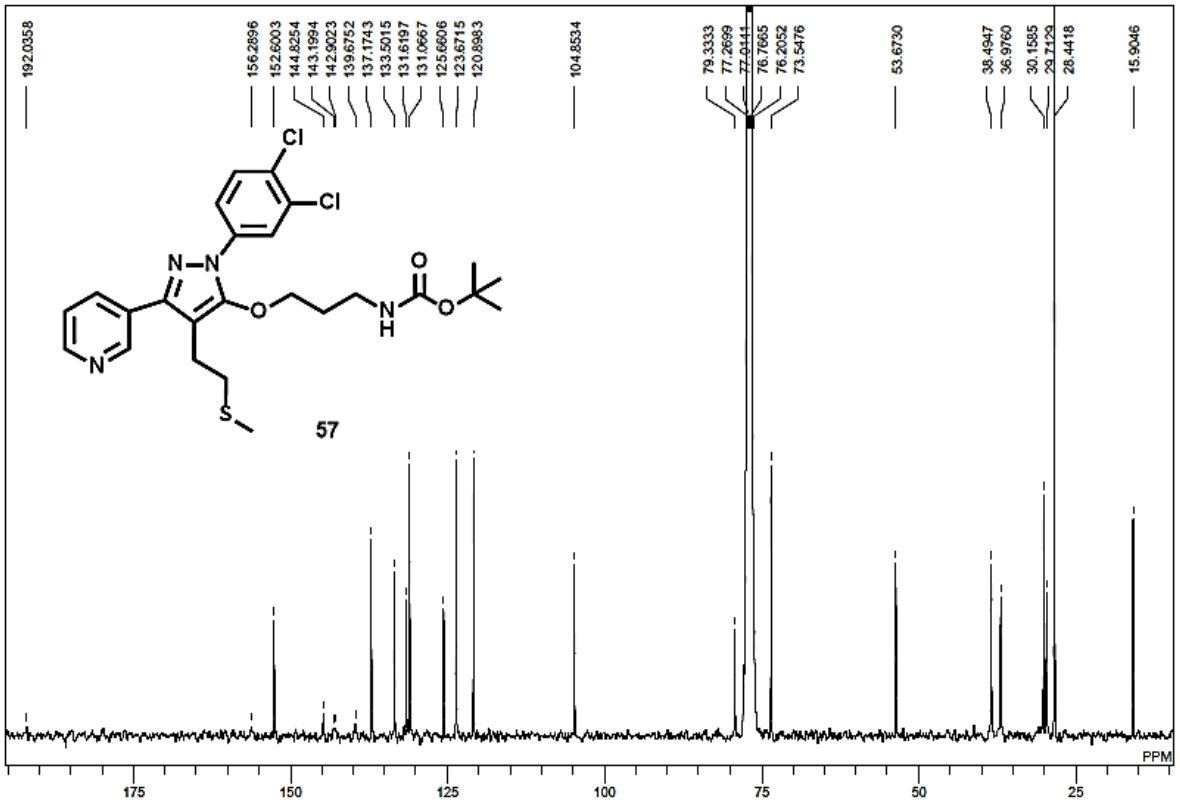
192.0358
156.2896
152.6003
144.8254
143.1994
142.9023
139.6752
137.1743
133.5015
131.6197
131.0667
125.6606
123.6715
120.8983
104.8534
79.3333
77.2699
77.0441
76.7665
76.2052
73.5476
53.6730
38.4947
36.9760
30.1585
29.7129
28.4418
15.9046
Cl
Cl
N
N
O
O
N
H
O
N
S
57
PPM
175
150
125
100
75
50
25

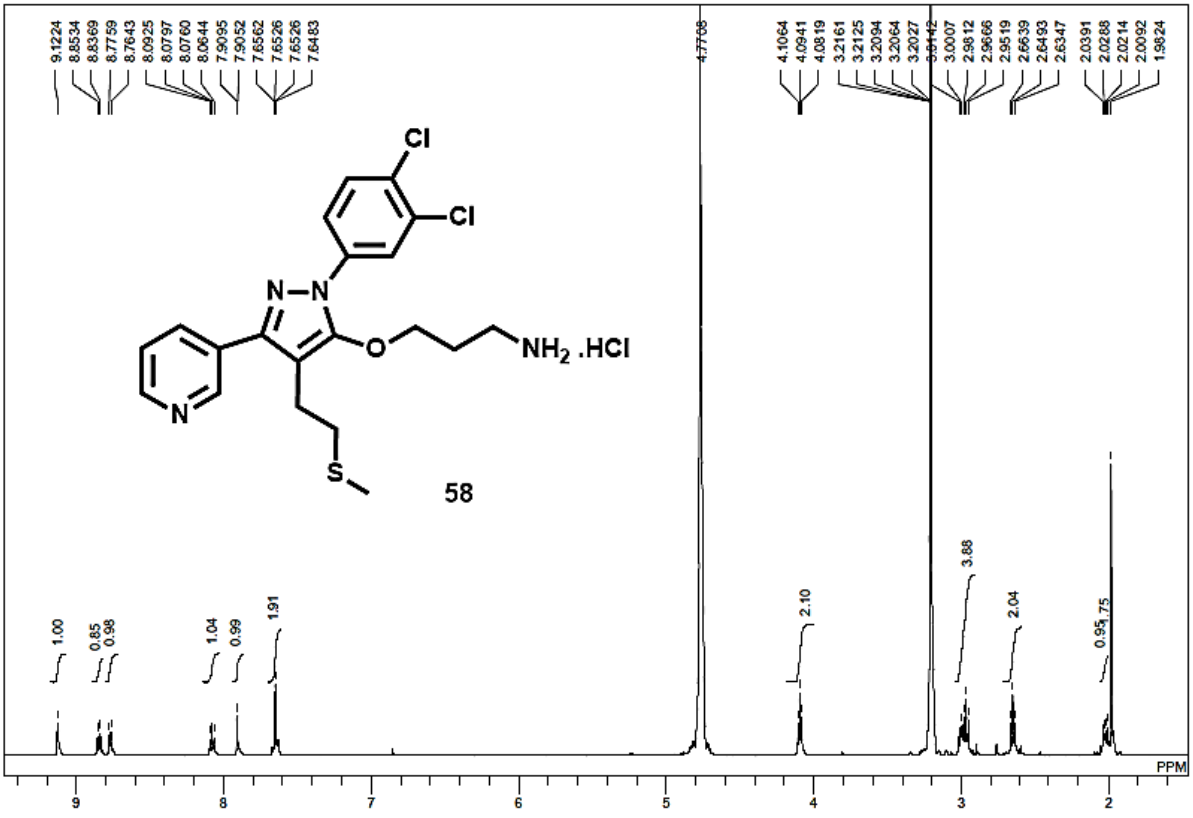
9.1224
8.8534
8.8369
8.7759
8.7643
8.0925
8.0797
8.0760
8.0644
7.9095
7.9052
7.6562
7.6526
7.6526
7.6483
4.7768
4.1064
4.0941
4.0819
3.2161
3.2125
3.2094
3.2064
3.2027
3.0142
3.0007
2.9812
2.9666
2.9519
2.6539
2.6493
2.6347
2.0391
2.0288
2.0214
2.0092
1.9824
Cl
Cl
N
N
O
NH2 .HCl
N
S
58
1.00
0.85
0.98
1.04
0.99
1.91
2.10
3.88
2.04
0.95
1.75
PPM
9
8
7
6
5
4
3
2

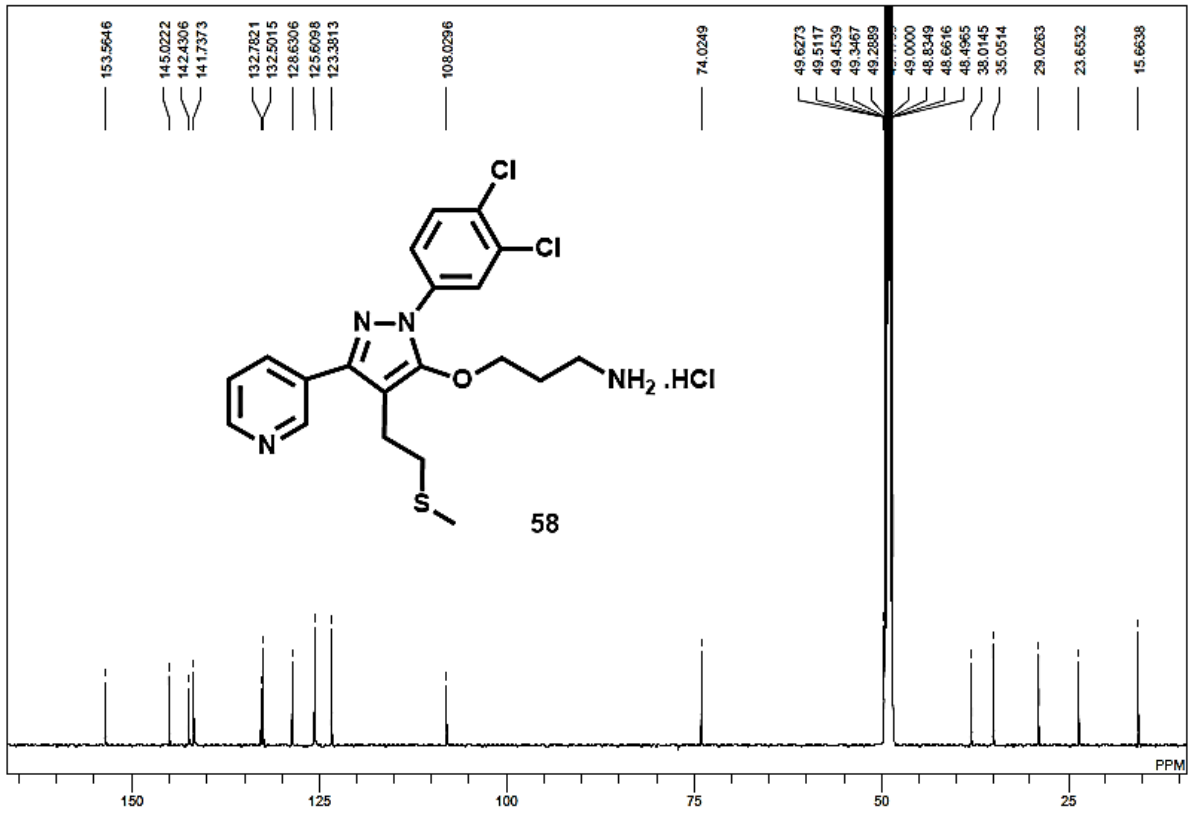
153.5646
145.0222
142.4306
141.7373
132.7821
132.5015
128.6306
125.6098
123.3813
108.0296
74.0249
49.6273
49.5117
49.4539
49.3467
49.2889
49.0000
48.8349
48.6616
48.4965
38.0145
35.0514
29.0263
23.6532
15.6638
Cl
Cl
N
N
O
NH2 .HCl
N
S
58
PPM
150
125
100
75
50
25

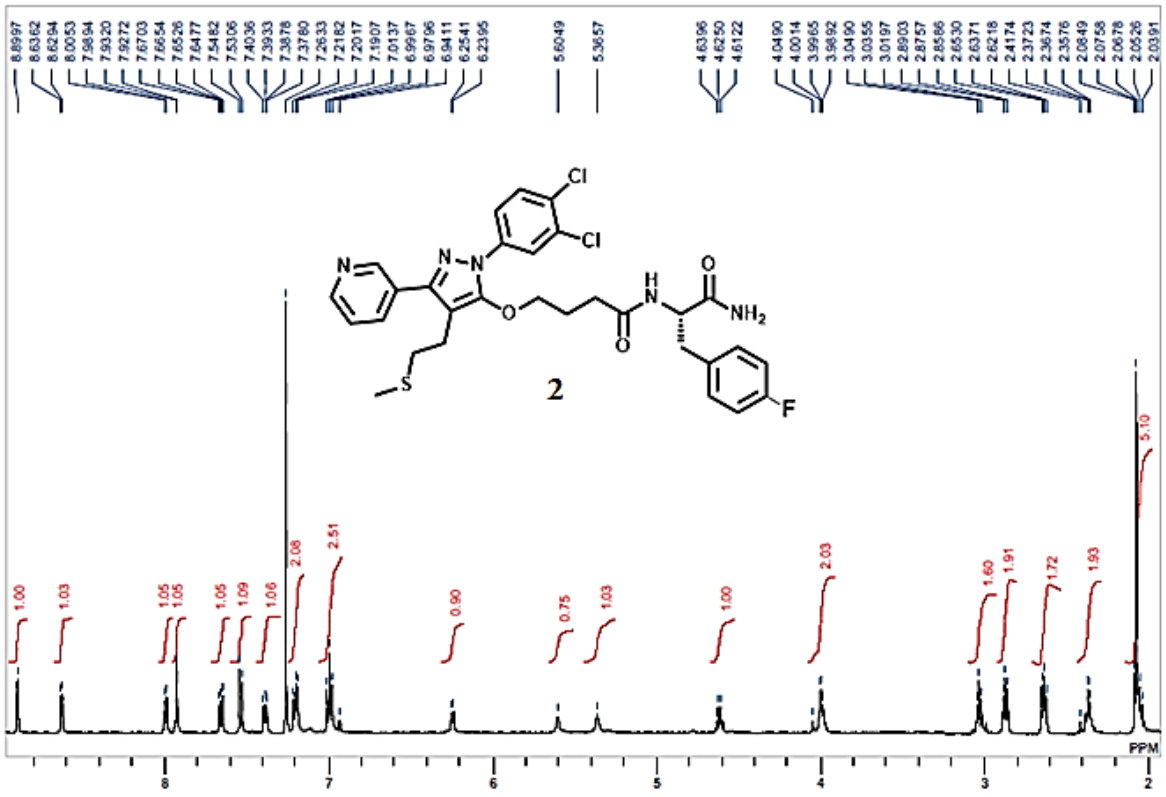
2
PPM

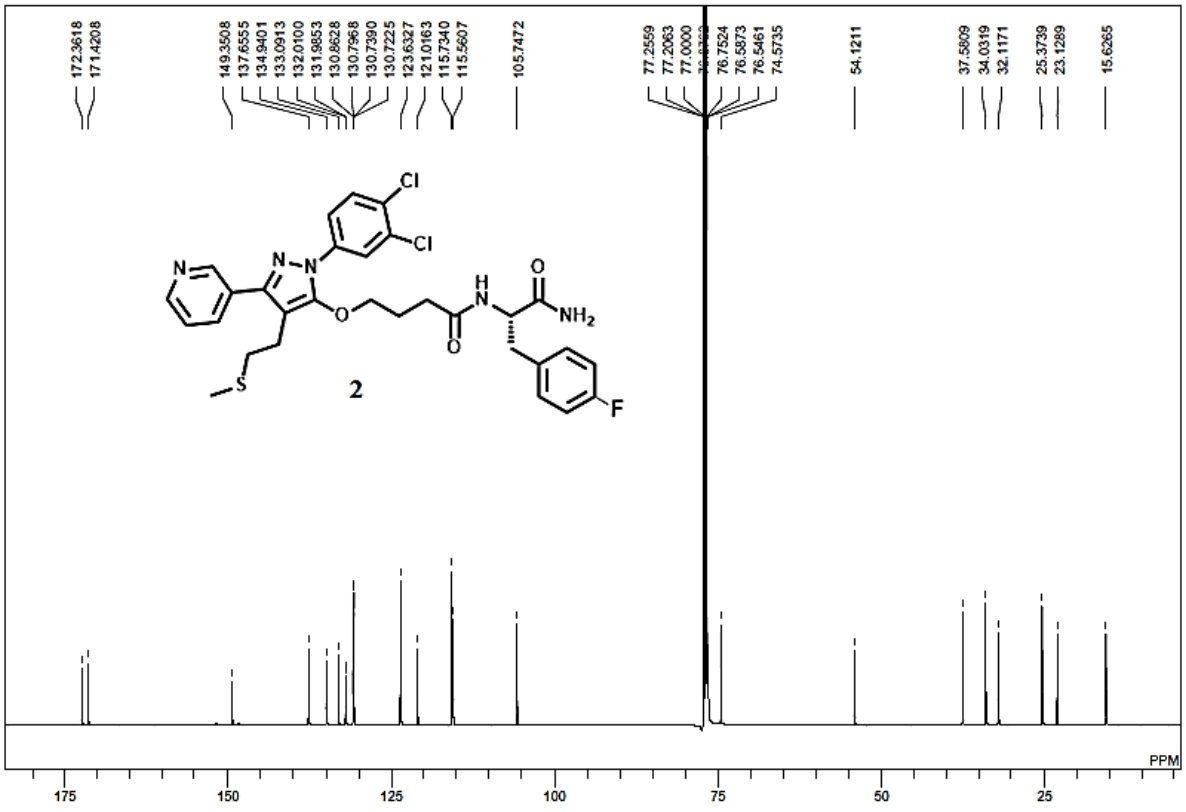
2
PPM

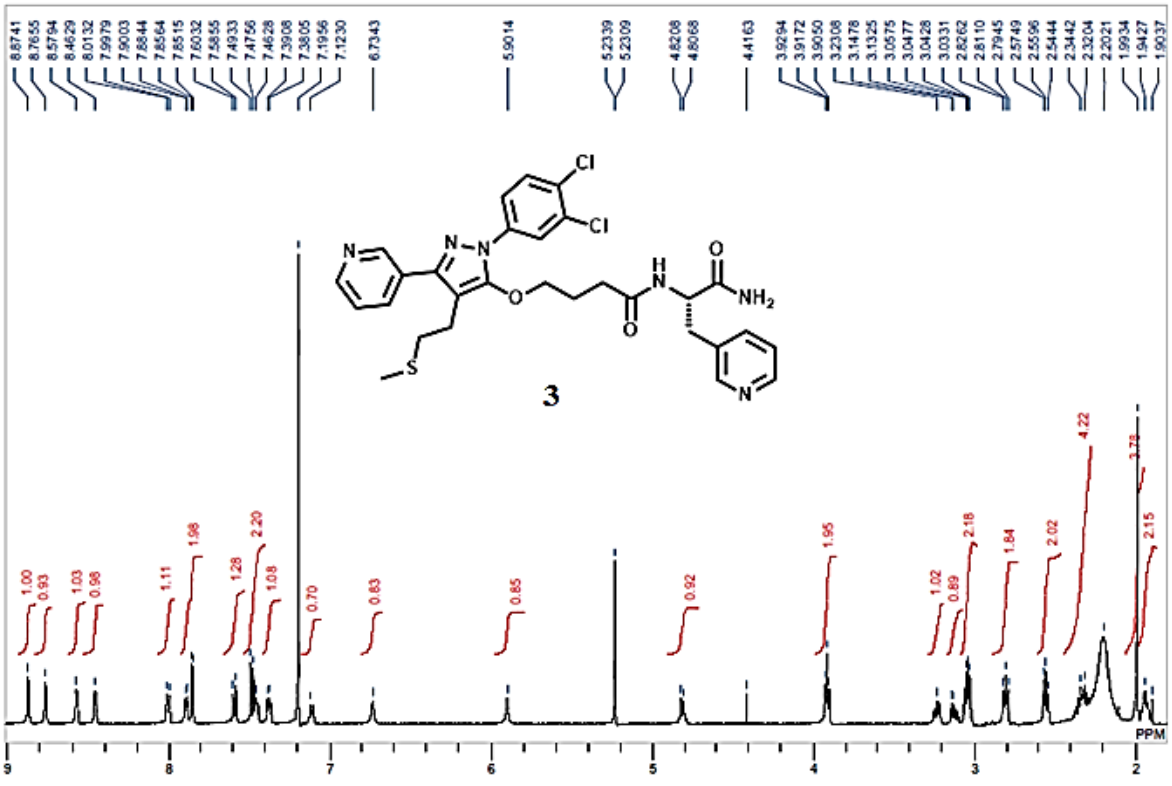
3
PPM

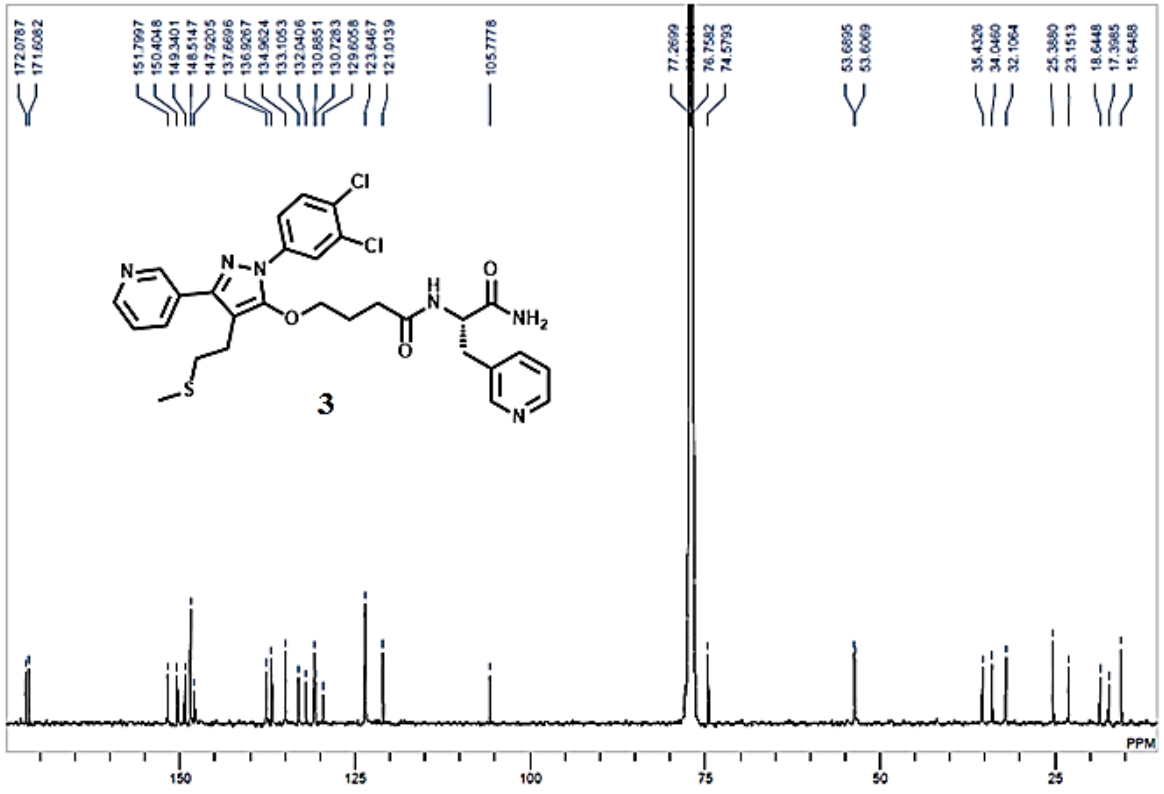
3
PPM

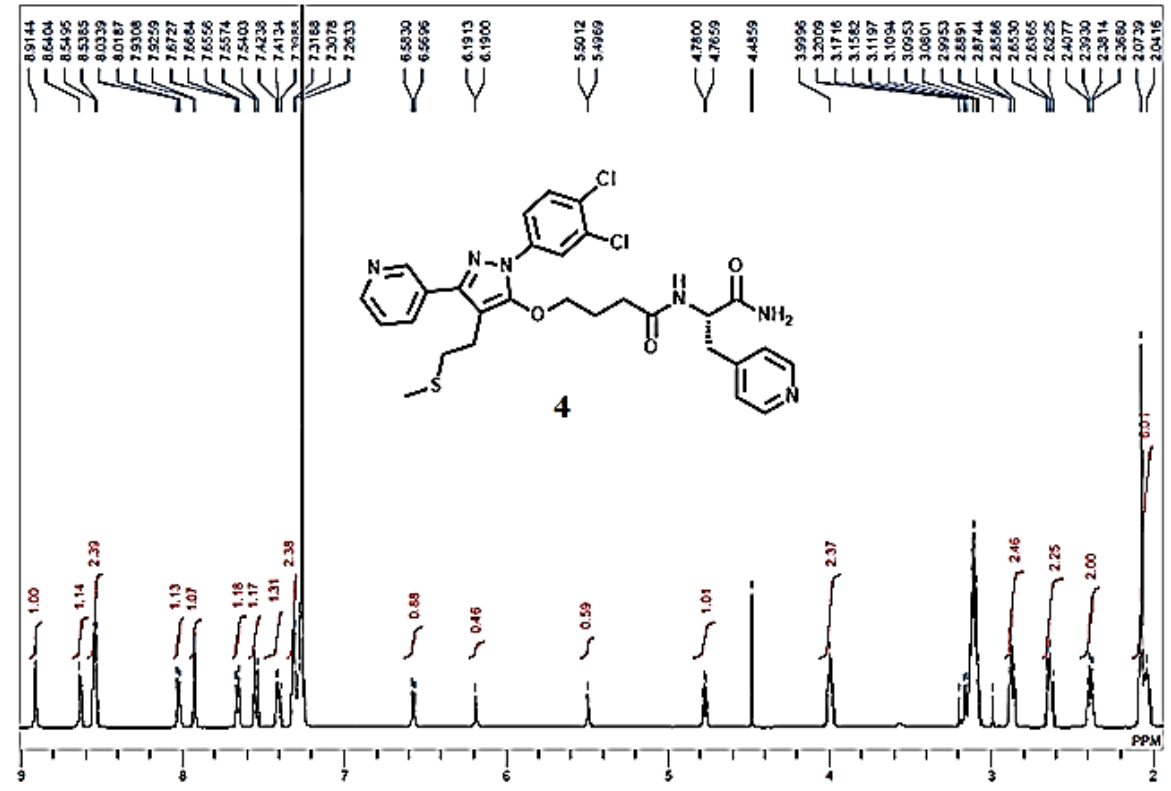
4
PPM

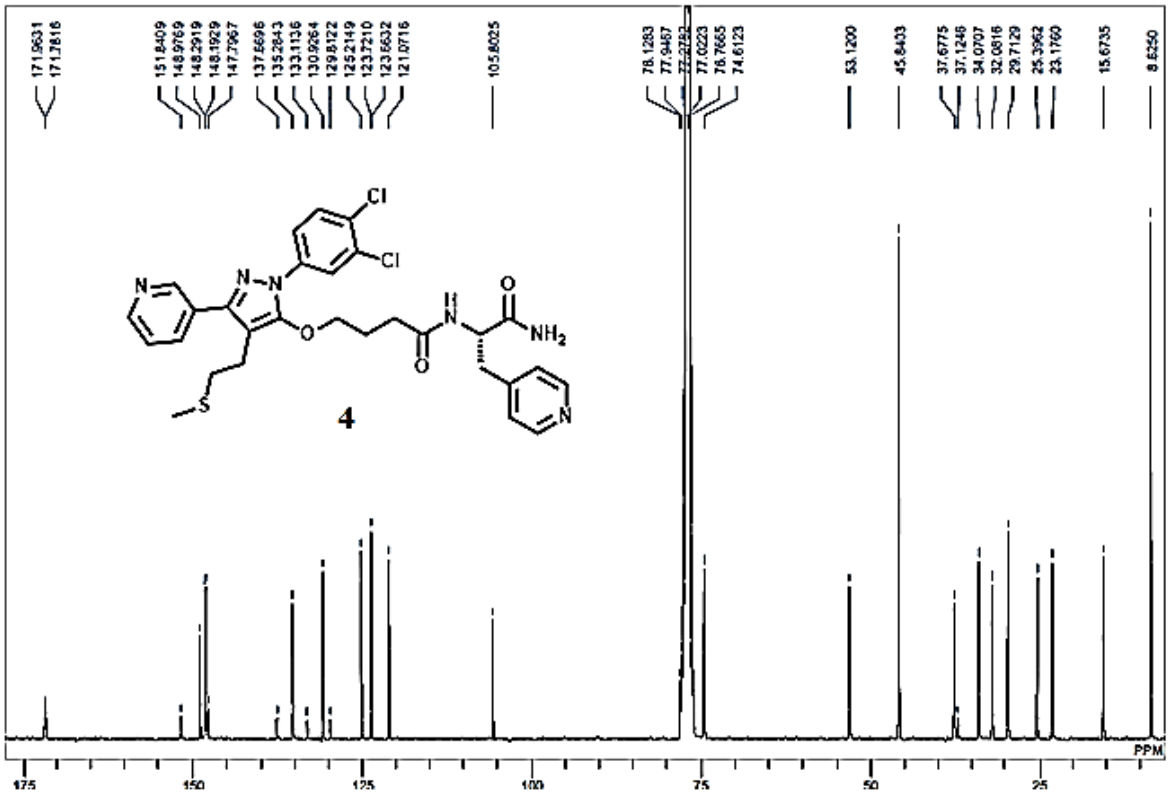
4
PPM

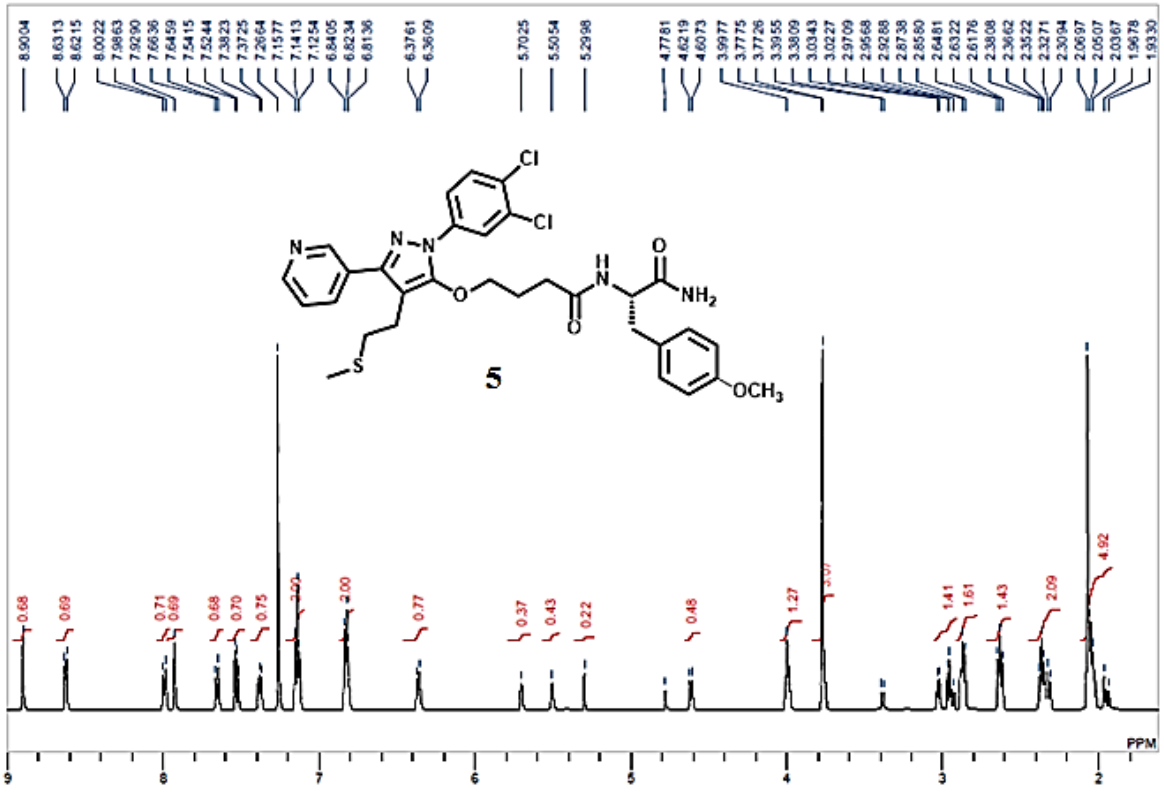
5
PPM

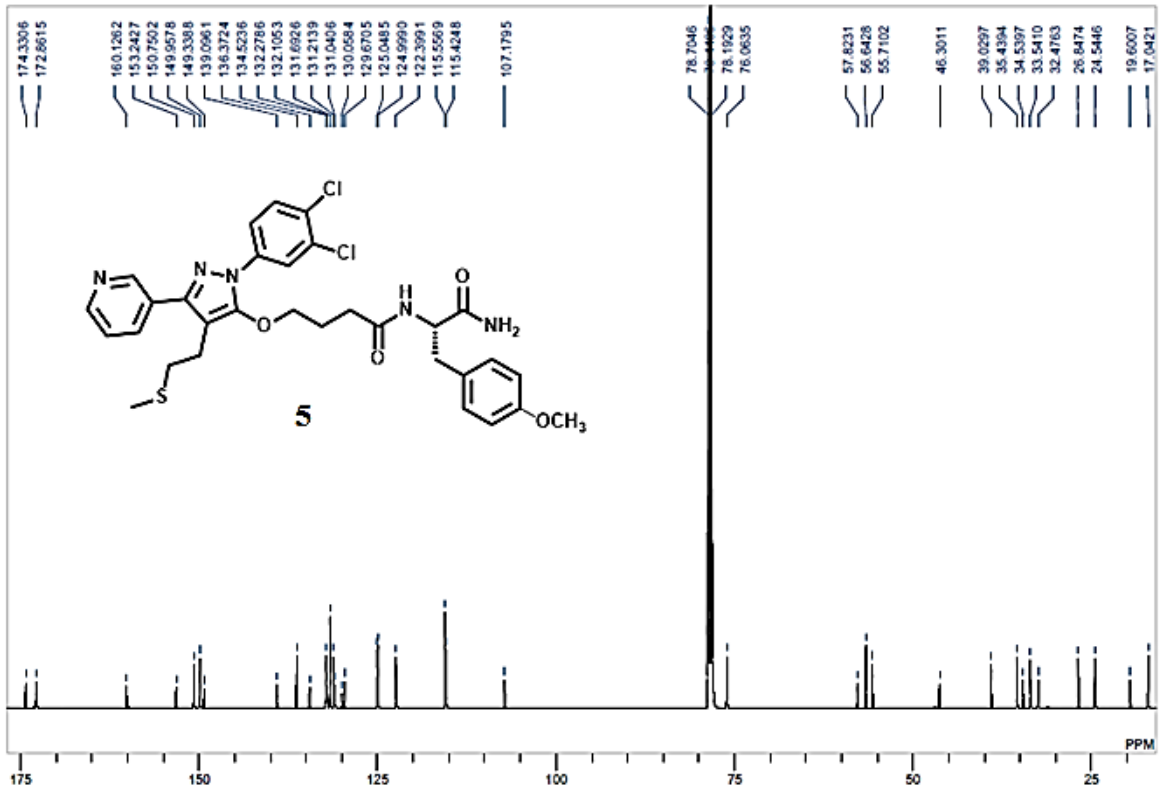
5
PPM

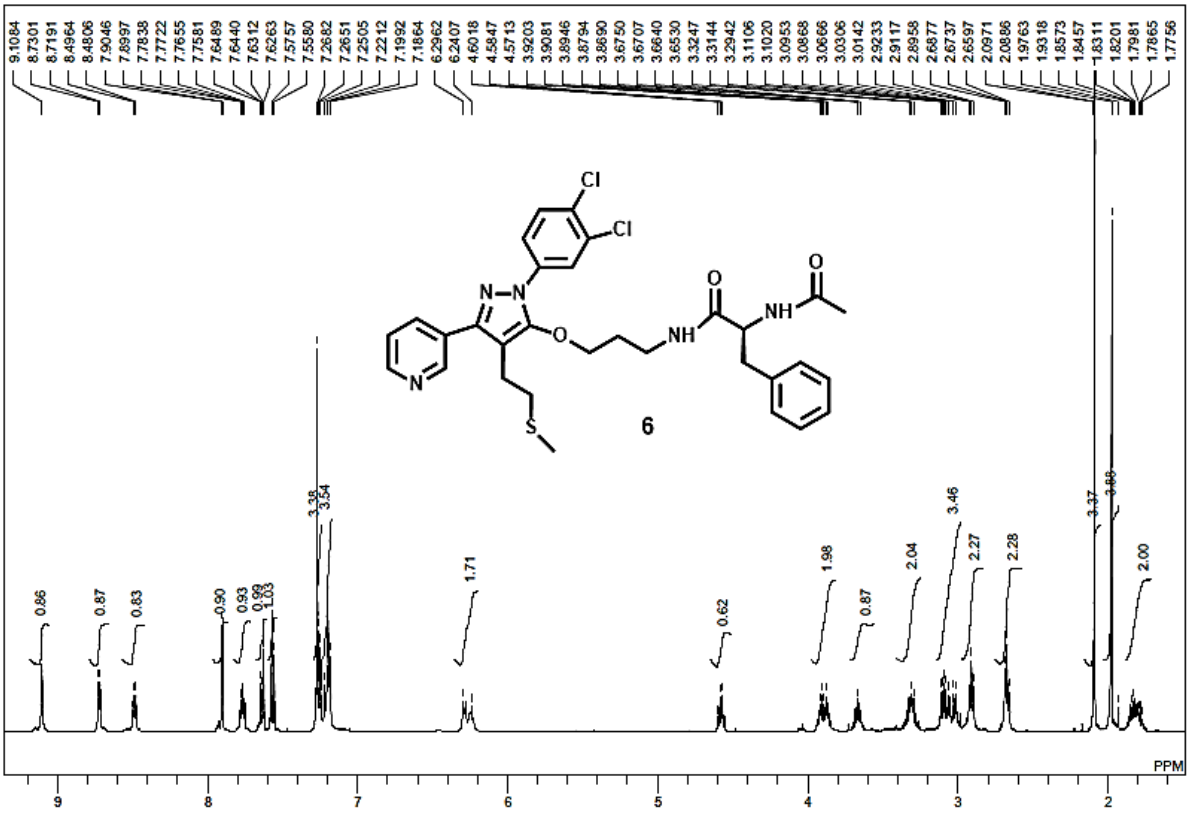
9.1084
8.7301
8.7191
8.4964
8.4806
7.9046
7.8997
7.7838
7.7722
7.7655
7.7581
7.6489
7.6440
7.6312
7.6263
7.5757
7.5580
7.2682
7.2651
7.2505
7.2212
7.1992
7.1864
6.2962
6.2407
4.6018
4.5847
4.5713
3.9203
3.9081
3.8946
3.8794
3.8690
3.6750
3.6707
3.6640
3.6530
3.3247
3.3144
3.2942
3.1106
3.1020
3.0953
3.0868
3.0666
3.0306
3.0142
2.9233
2.9117
2.8958
2.6877
2.6737
2.6597
2.0971
2.0886
1.9763
1.9318
1.8573
1.8457
1.8311
1.8201
1.7981
1.7865
1.7756
Cl
Cl
N
N
O
NH
O
NH
O
N
S
6
0.86
0.87
0.83
0.90
0.93
0.98
1.03
3.38
3.54
1.71
0.62
1.98
0.87
2.04
3.46
2.27
2.28
3.37
3.88
2.00
PPM
9
8
7
6
5
4
3
2

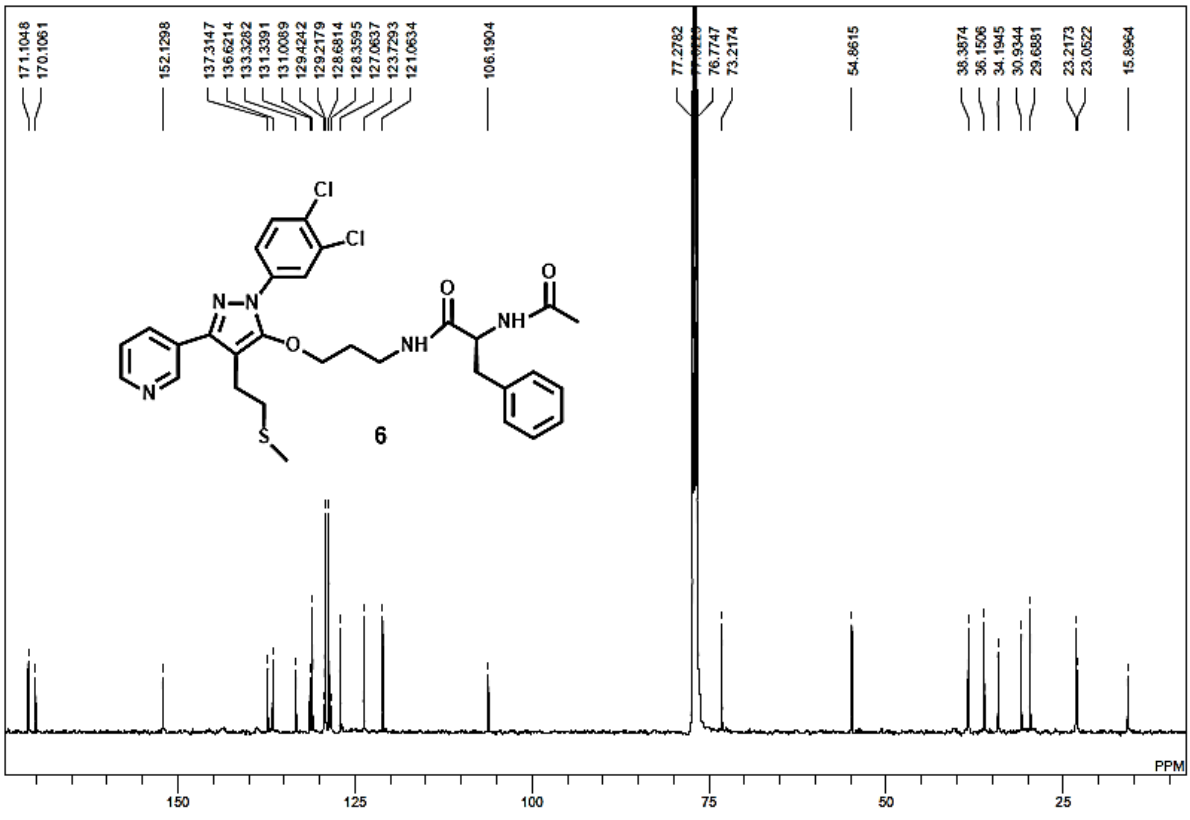
171.1048
170.1061
152.1298
137.3147
136.6214
133.3282
131.3391
131.0089
129.4242
129.2179
128.6814
128.3595
127.0637
123.7293
121.0634
106.1904
77.2782
76.7747
73.2174
54.8615
38.3874
36.1506
34.1945
30.9344
29.6881
23.2173
23.0522
15.8964
Cl
Cl
N
N
O
NH
O
NH
O
N
S
6
PPM
150
125
100
75
50
25

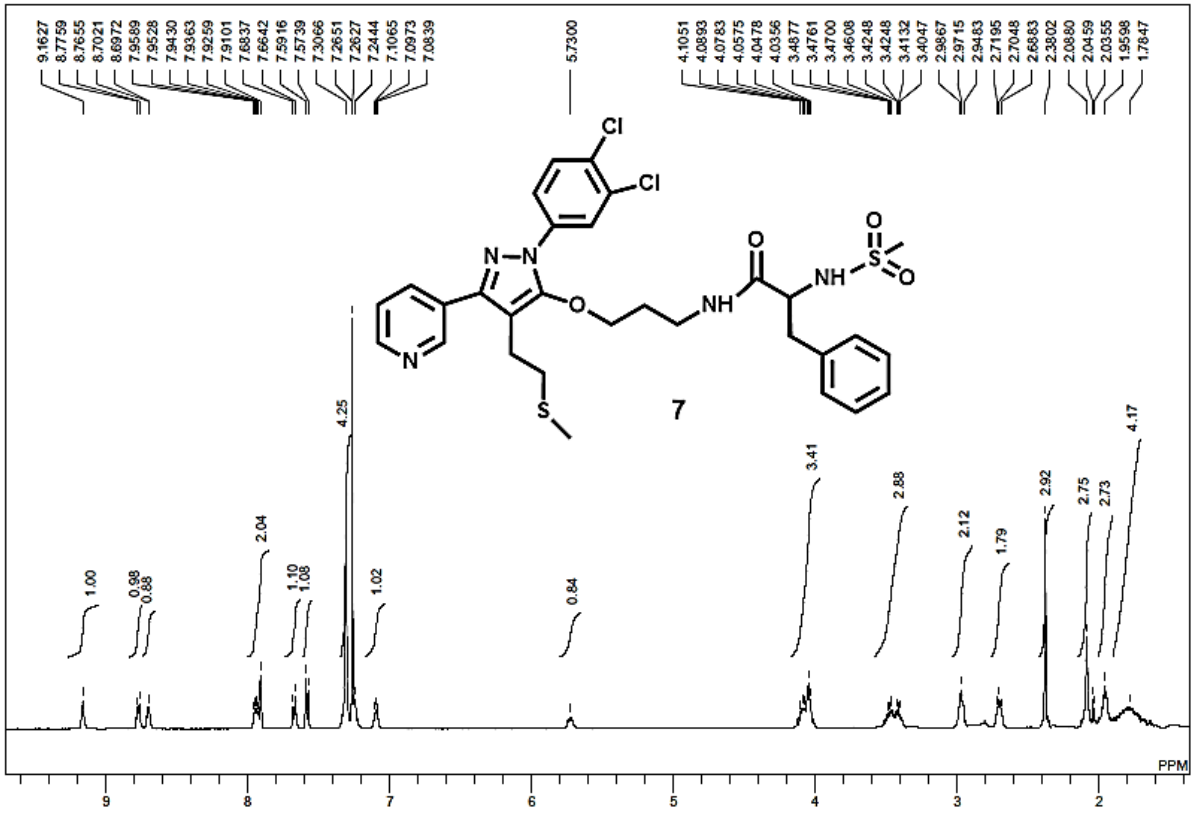
9.1627
8.7759
8.7655
8.7021
8.6972
7.9589
7.9528
7.9430
7.9363
7.9259
7.9101
7.6837
7.6642
7.5916
7.5739
7.3066
7.2651
7.2627
7.2444
7.1065
7.0973
7.0839
5.7300
4.1051
4.0993
4.0783
4.0575
4.0478
4.0356
3.4877
3.4761
3.4700
3.4608
3.4248
3.4132
3.4047
2.9867
2.9715
2.9483
2.7195
2.7048
2.6883
2.3802
2.0880
2.0459
2.0355
1.9598
1.7847
Cl
Cl
N
N
O
NH
O
S
O
O
NH
N
S
7
4.25
3.41
2.88
2.04
2.12
1.79
2.92
2.75
2.73
4.17
1.00
0.98
0.88
1.10
1.08
1.02
0.84
PPM
9
8
7
6
5
4
3
2

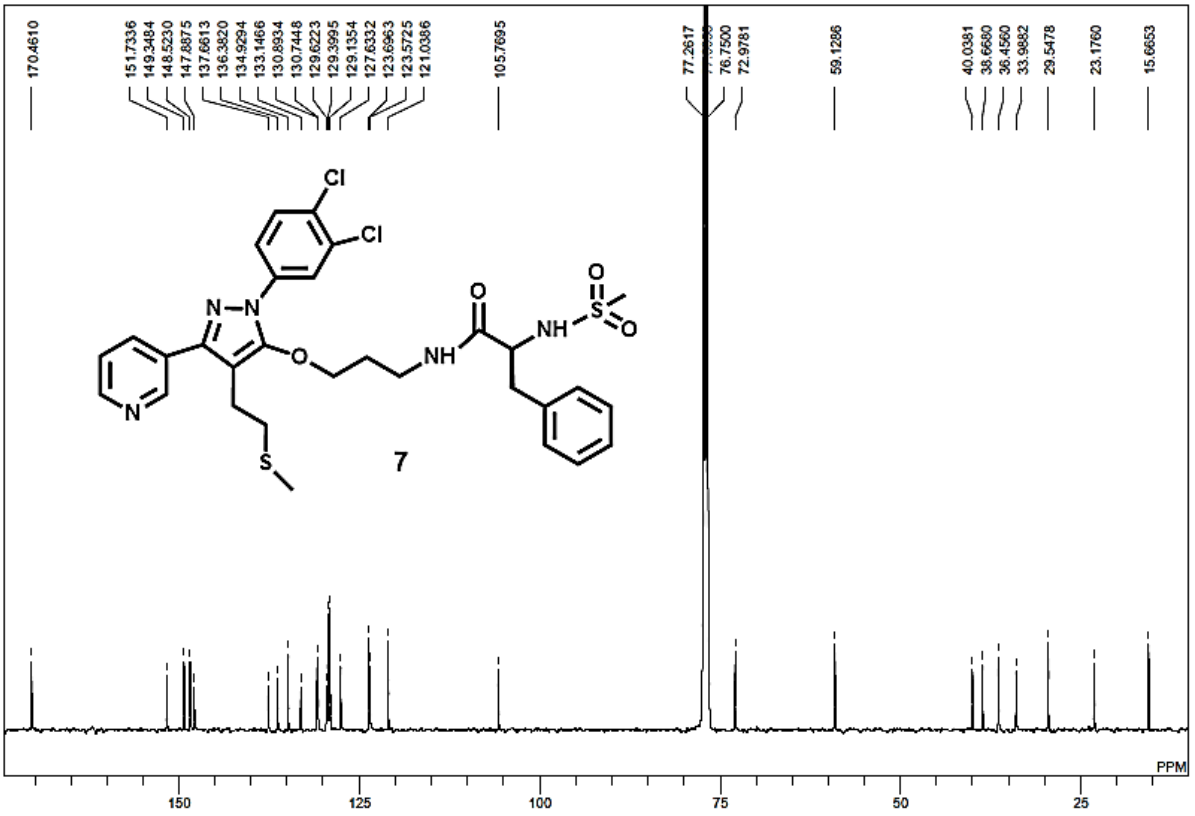
170.4610
151.7336
149.3484
148.5230
147.8875
137.6613
136.3820
134.9294
133.1466
130.8934
130.7448
129.6223
129.3995
129.1354
127.6332
123.6963
123.5725
121.0386
105.7695
77.2617
76.7500
72.9781
59.1286
40.0381
38.6680
36.4560
33.9882
29.5478
23.1760
15.6653
Cl
Cl
N
N
O
NH
O
S
O
O
NH
N
S
7
PPM
150
125
100
75
50
25

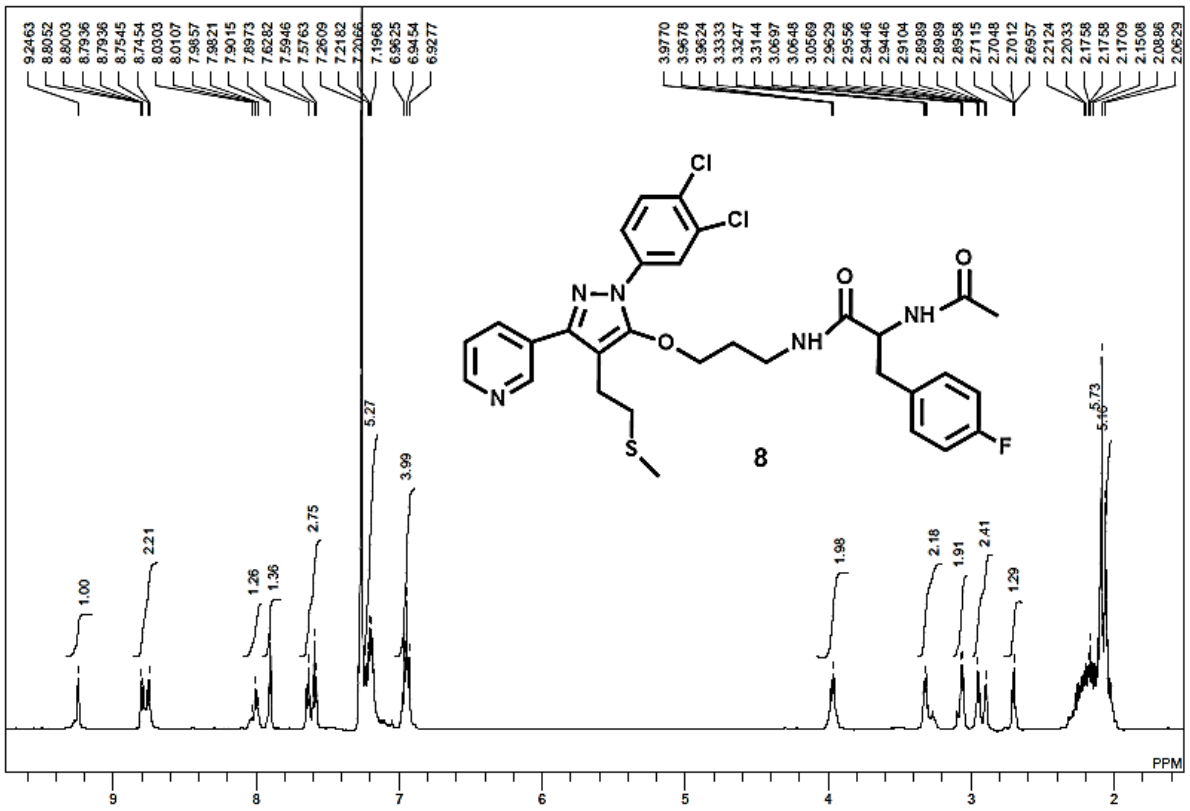
9.2463
8.8052
8.8003
8.7936
8.7936
8.7545
8.7454
8.0303
8.0107
7.9857
7.9821
7.9015
7.8973
7.6282
7.5946
7.5763
7.2609
7.2182
7.2066
7.1968
6.9625
6.9454
6.9277
3.9770
3.9678
3.9624
3.3333
3.3247
3.3144
3.0697
3.0648
3.0569
2.9629
2.9556
2.9446
2.9446
2.9104
2.8989
2.8989
2.8958
2.7115
2.7048
2.7012
2.6957
2.2124
2.2033
2.1758
2.1758
2.1709
2.1508
2.0886
2.0629
1.00
2.21
1.26
1.36
2.75
5.27
3.99
1.98
2.18
1.91
2.41
1.29
5.73
5.18
Cl
Cl
N
N
O
NH
O
NH
O
N
S
F
8
PPM
9
8
7
6
5
4
3
2

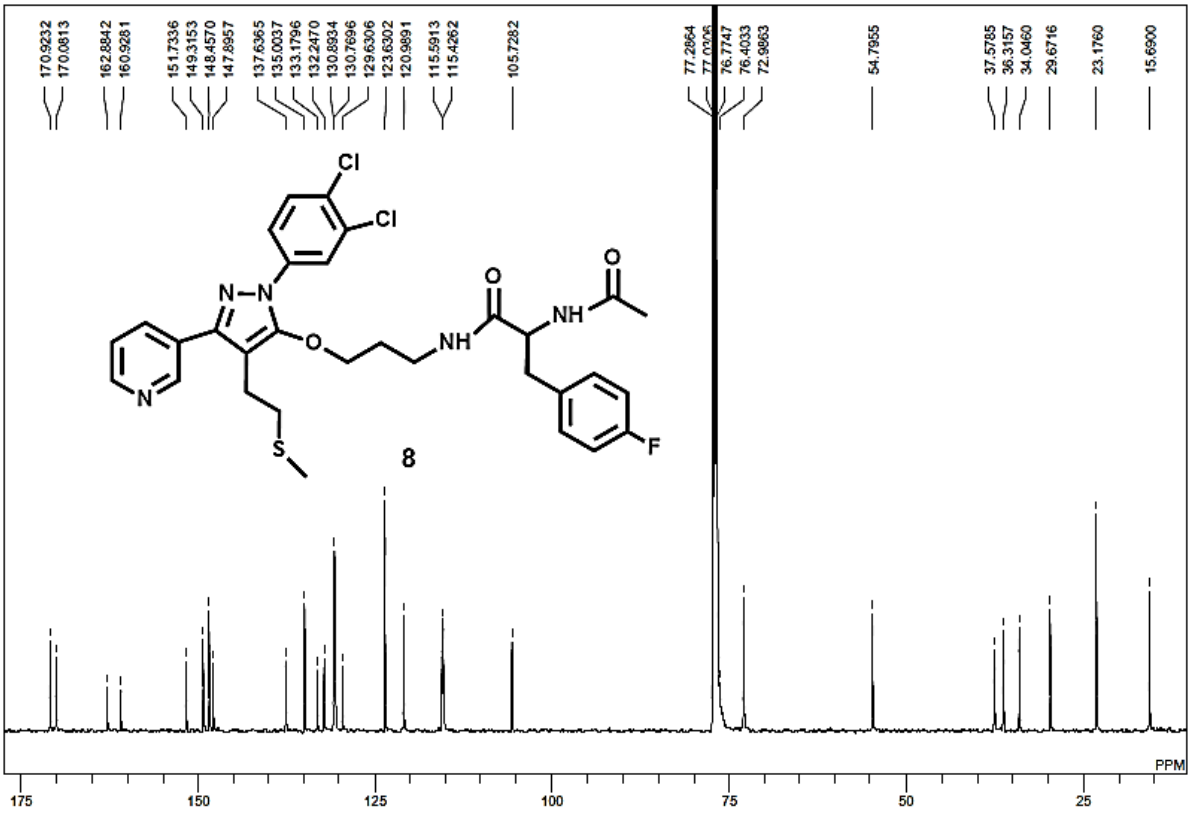
170.9232
170.0813
162.8842
160.9261
151.7336
149.3153
148.4570
147.8957
137.6365
135.0037
133.1796
132.2470
130.8934
130.7696
129.6306
123.6302
120.9891
115.5913
115.4262
105.7282
77.2864
77.0026
76.7747
76.4033
72.9863
54.7955
37.5785
36.3157
34.0460
29.6716
23.1760
15.6900
Cl
Cl
N
N
O
NH
O
NH
O
N
S
F
8
PPM
175
150
125
100
75
50
25

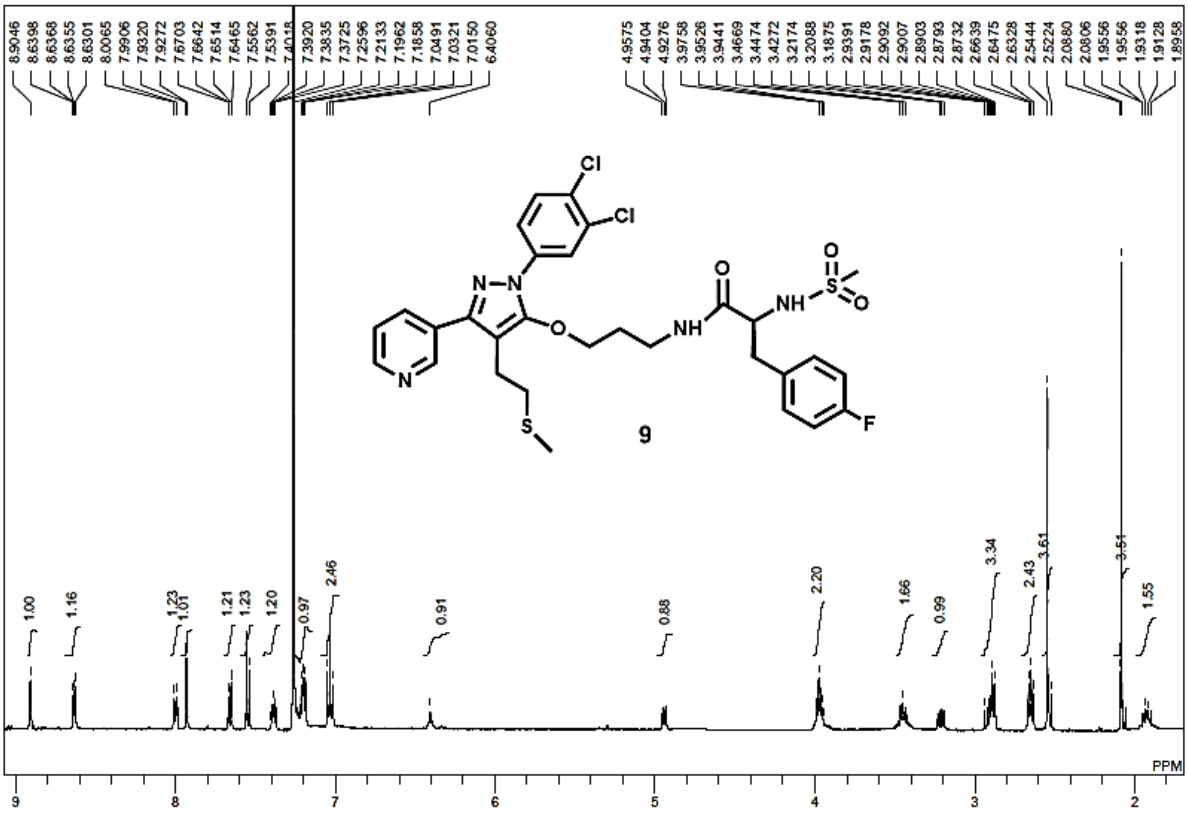
8.9046
8.6398
8.6368
8.6355
8.6301
8.0065
7.9906
7.9320
7.9272
7.6703
7.6642
7.6514
7.6465
7.5562
7.5391
7.4018
7.3920
7.3835
7.3725
7.2596
7.2133
7.1962
7.1858
7.0491
7.0321
7.0150
6.4060
4.9575
4.9404
4.9276
3.9758
3.9526
3.9441
3.4669
3.4474
3.4272
3.2174
3.2088
3.1875
2.9391
2.9178
2.9092
2.9007
2.8903
2.8793
2.8732
2.6639
2.6475
2.6328
2.5444
2.5224
2.0880
2.0806
1.9556
1.9556
1.9318
1.9128
1.8958
1.00
1.16
1.23
1.01
1.21
1.23
1.20
0.97
2.46
0.91
0.88
2.20
1.66
0.99
3.34
2.43
3.61
3.51
1.55
Cl
Cl
N
N
O
NH
O
S
O
NH
O
N
S
F
9
PPM
9
8
7
6
5
4
3
2

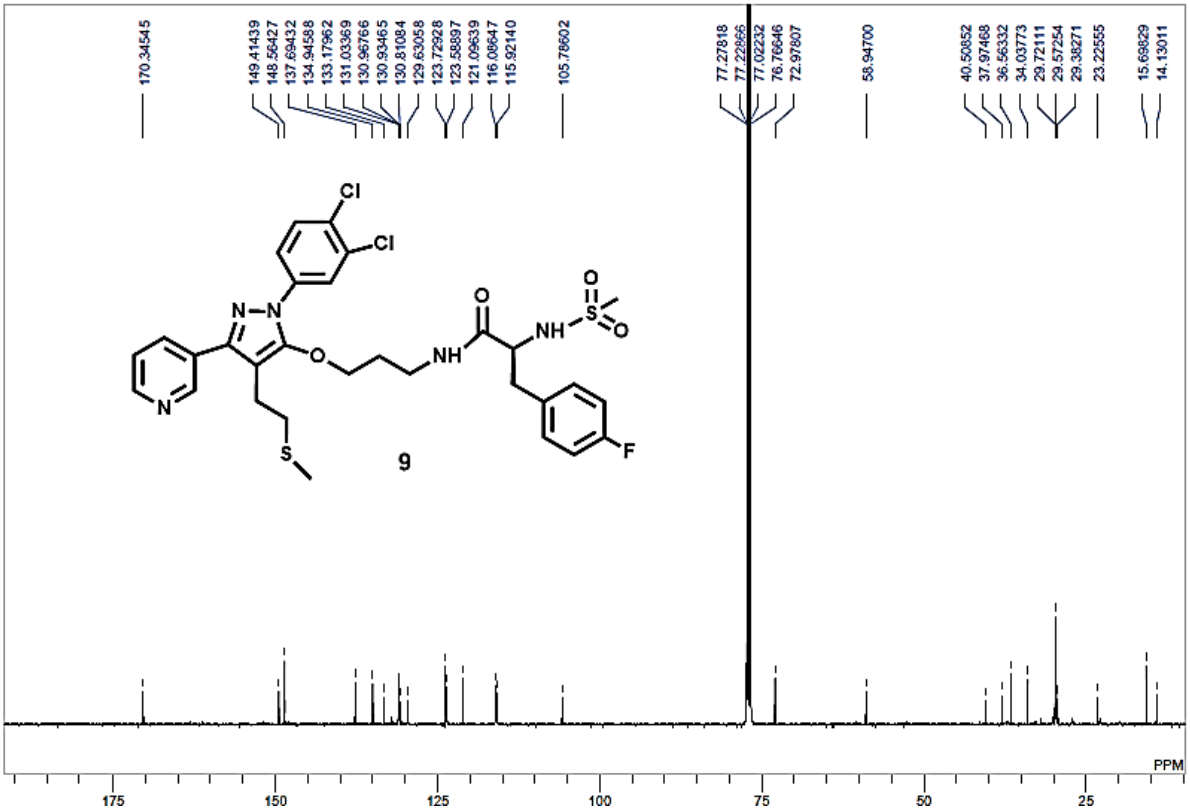
170.34545
149.41439
148.56427
137.69432
134.94588
133.17962
131.03369
130.96766
130.93465
130.81084
129.63058
123.72928
123.58897
121.09639
116.08647
115.92140
105.78602
77.27818
77.22866
77.02232
76.76646
72.97807
58.94700
40.50852
37.97468
36.56332
34.03773
29.72111
29.57254
29.38271
23.22555
15.69829
14.13011
Cl
Cl
N
N
O
NH
O
S
O
NH
O
N
S
F
9
PPM
175
150
125
100
75
50
25

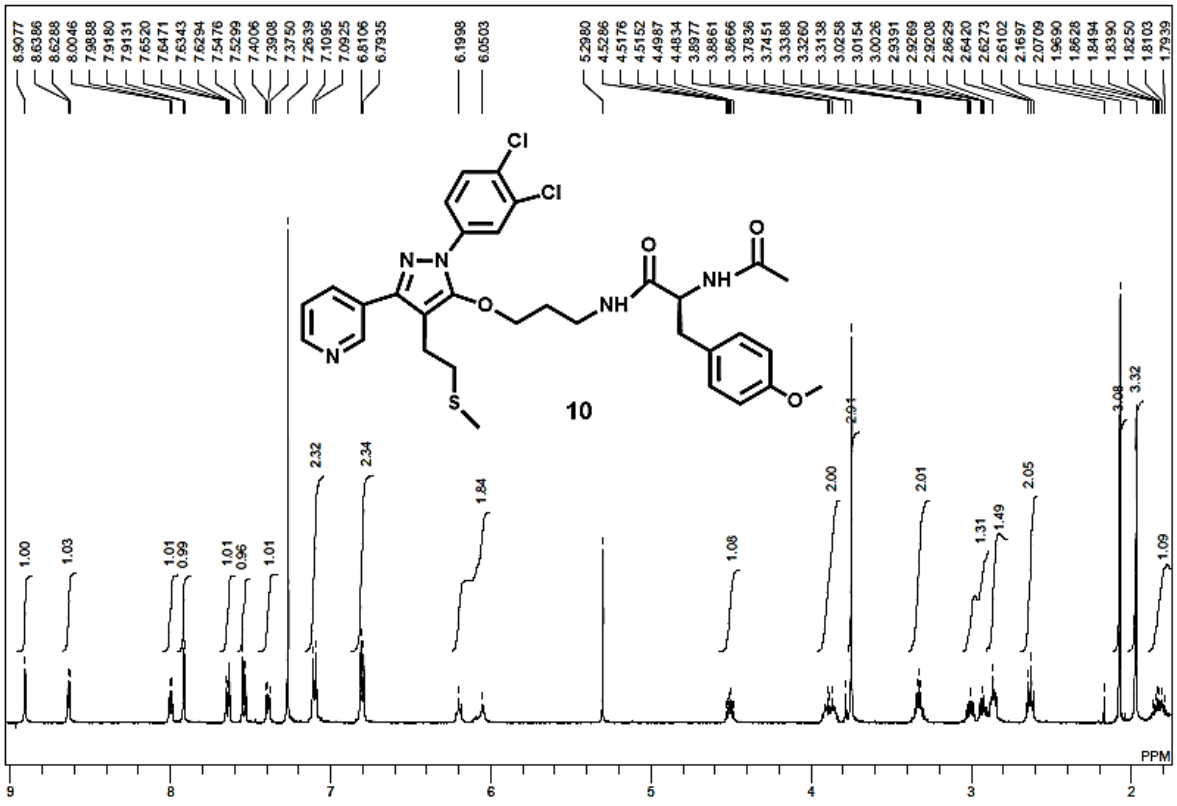
10
PPM

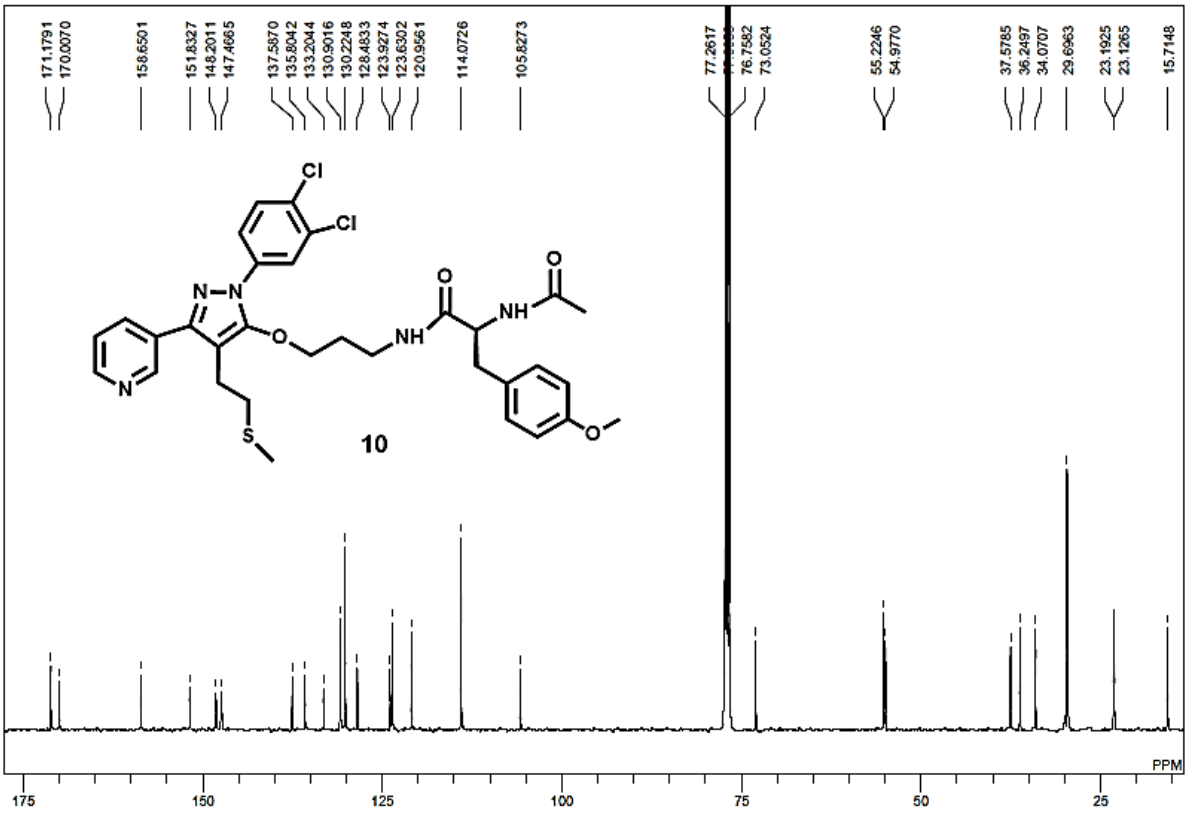
10
PPM

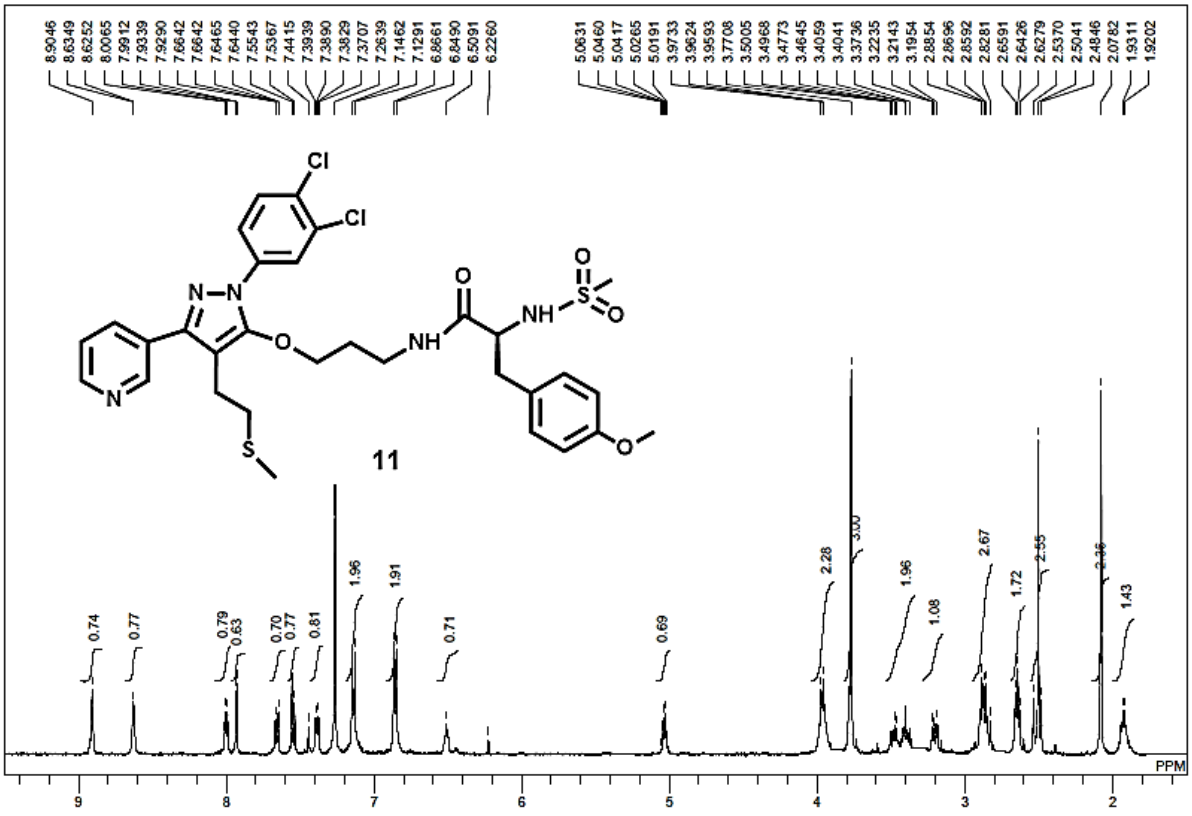
11
PPM

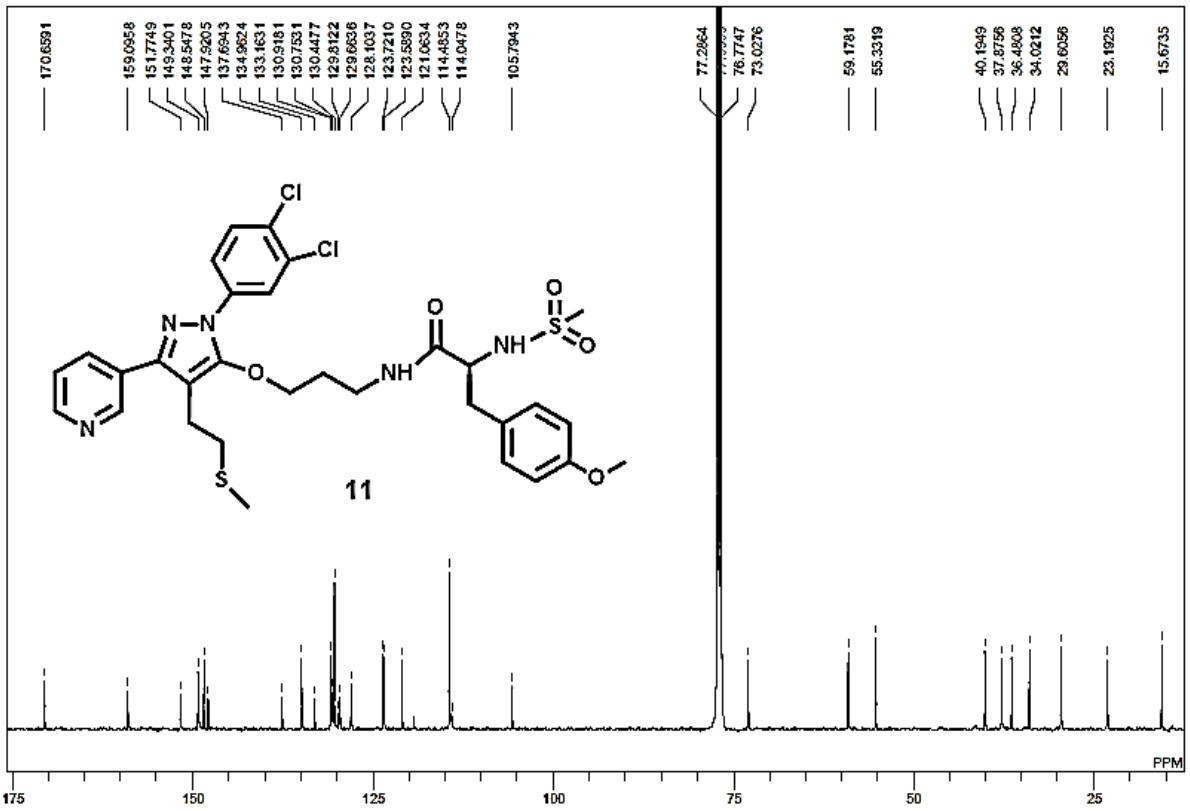
11
PPM

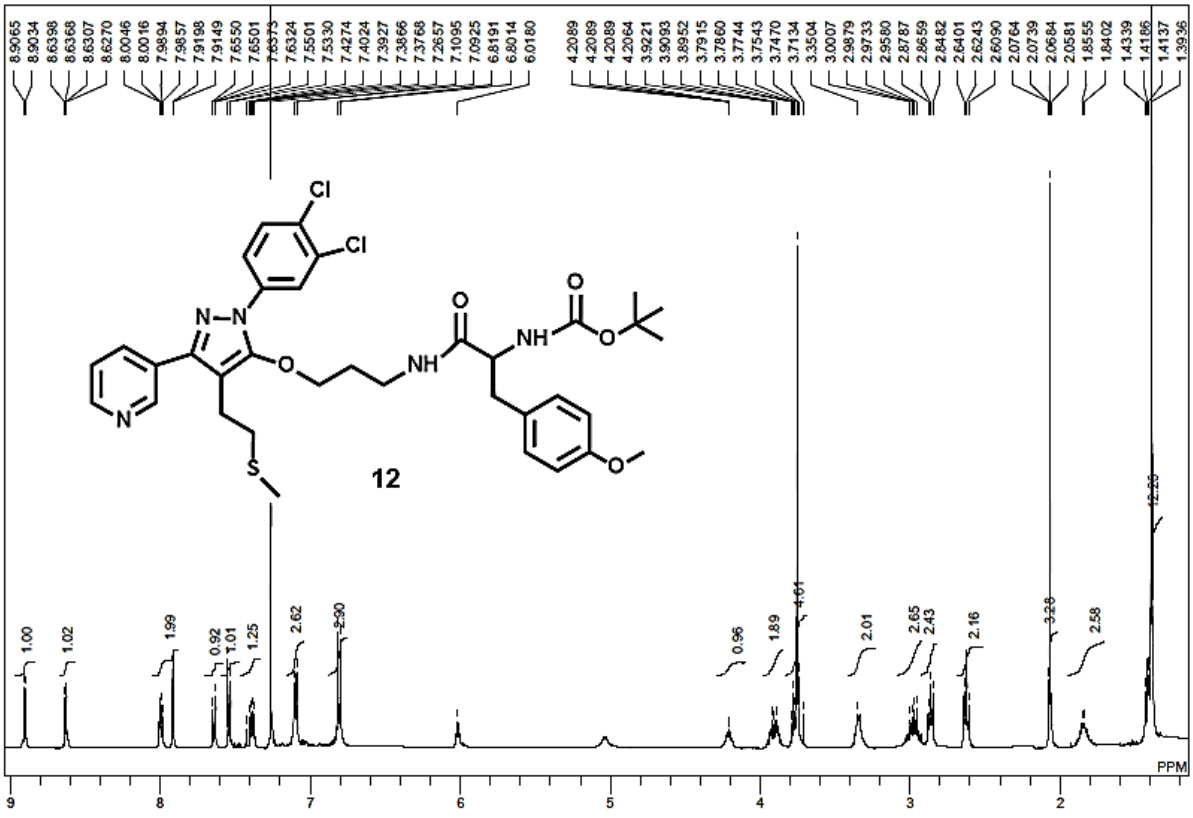
12
PPM

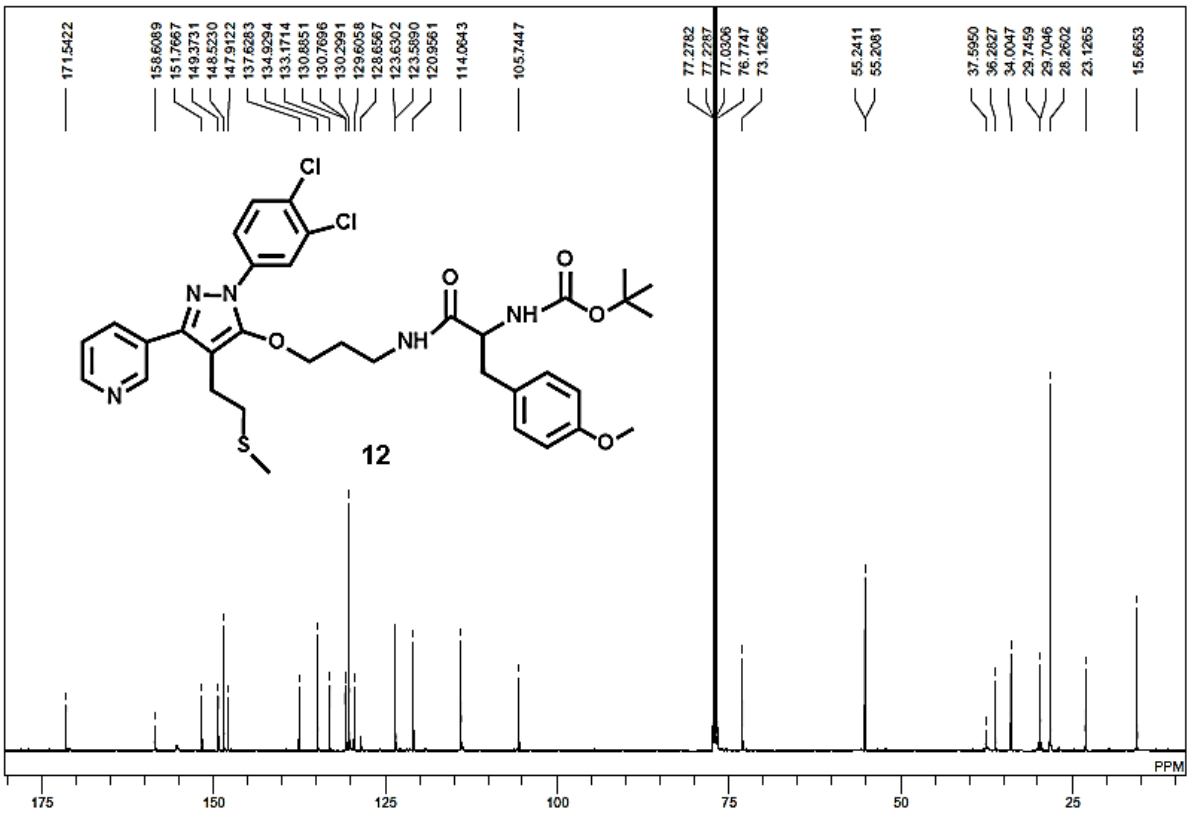
12
PPM

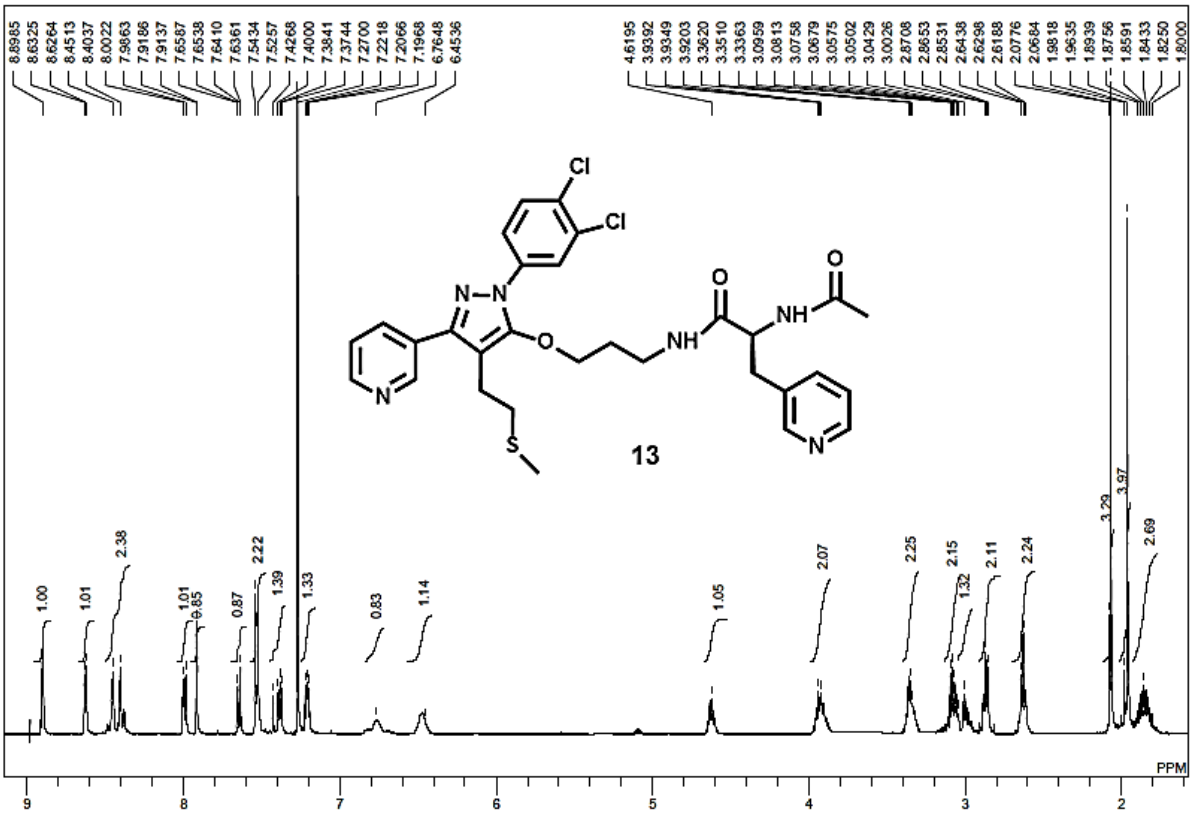
13
PPM

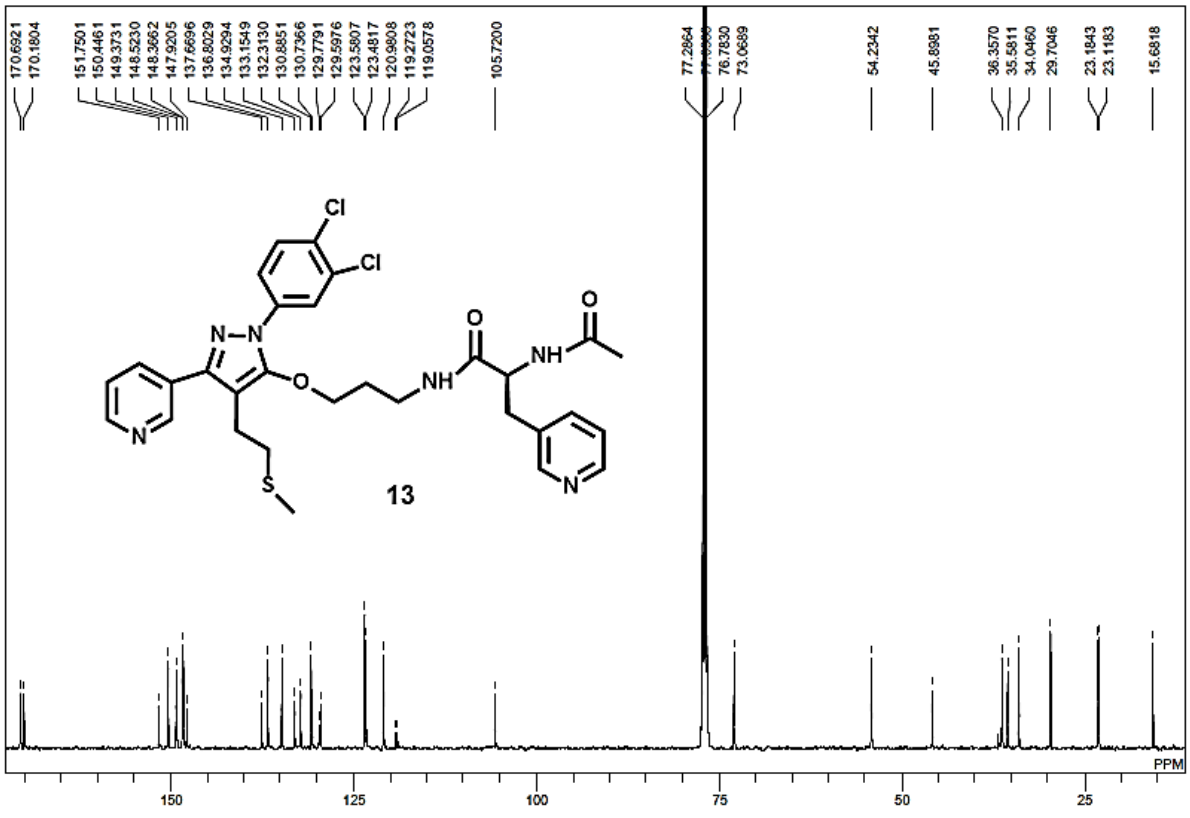
13
PPM

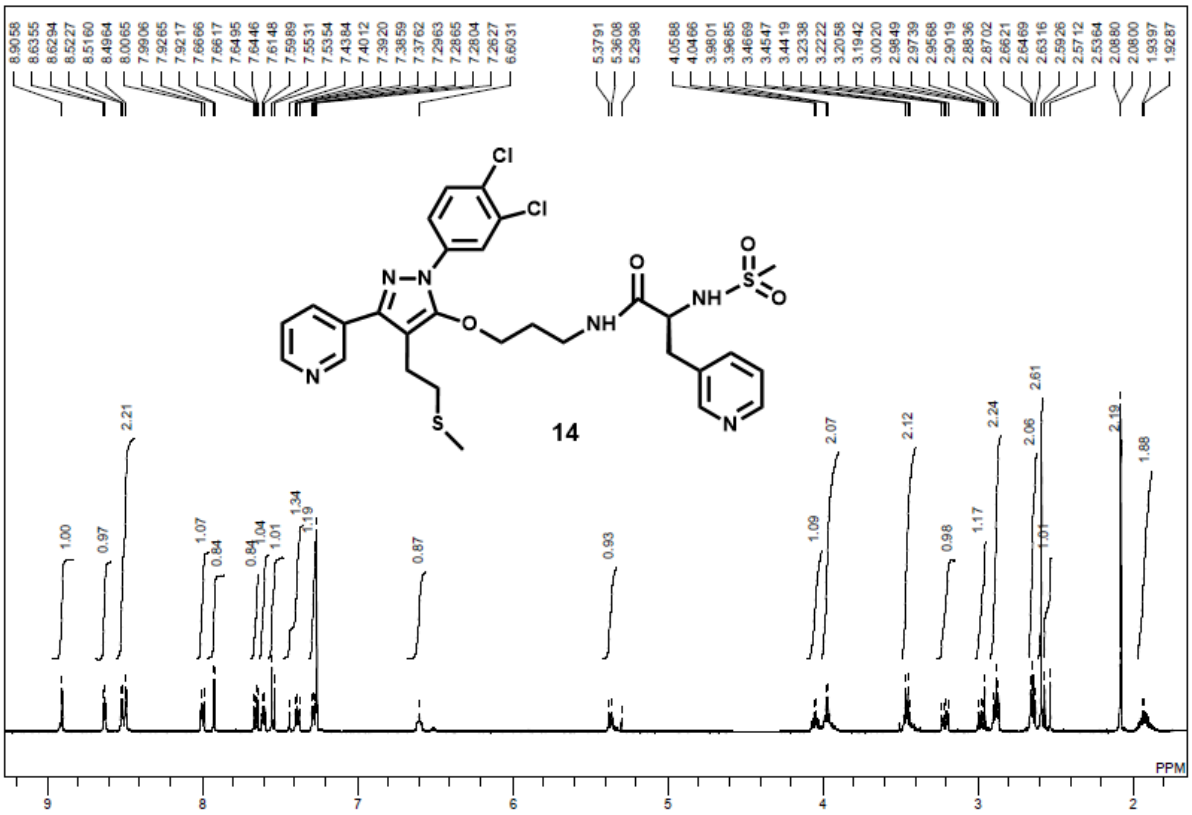
14
PPM

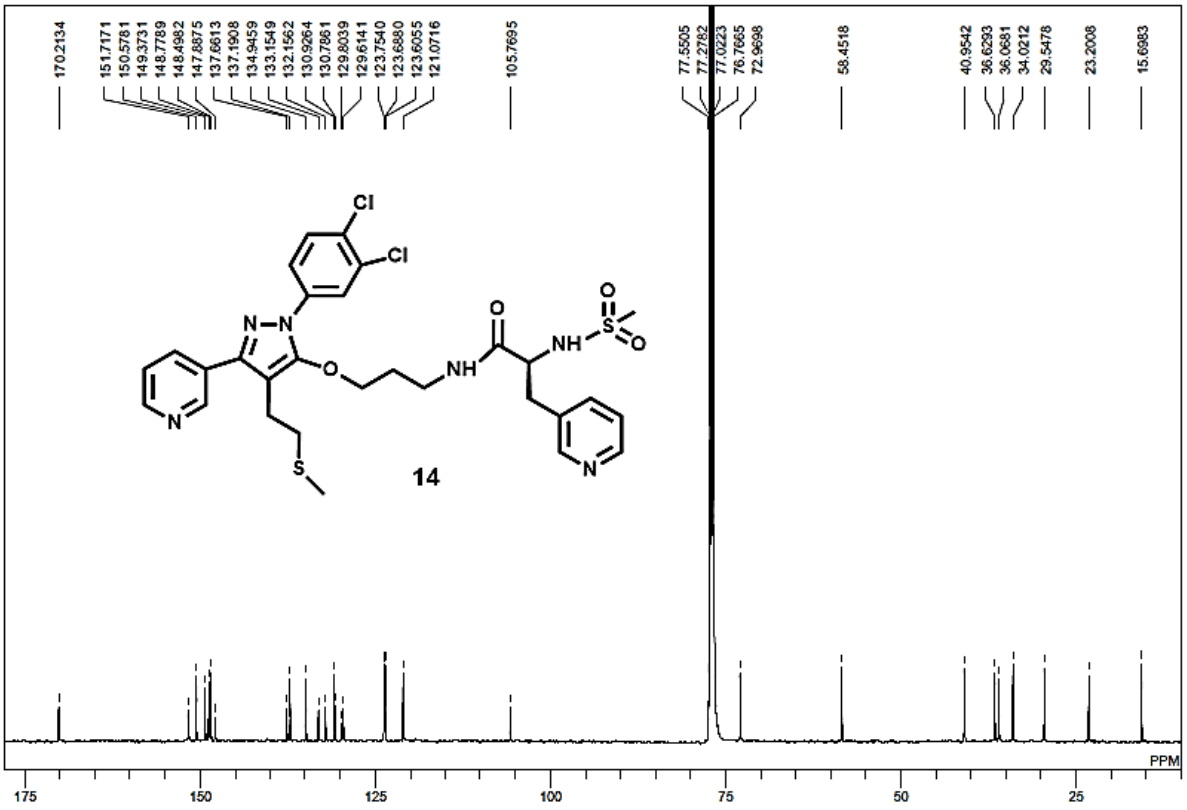
14
PPM

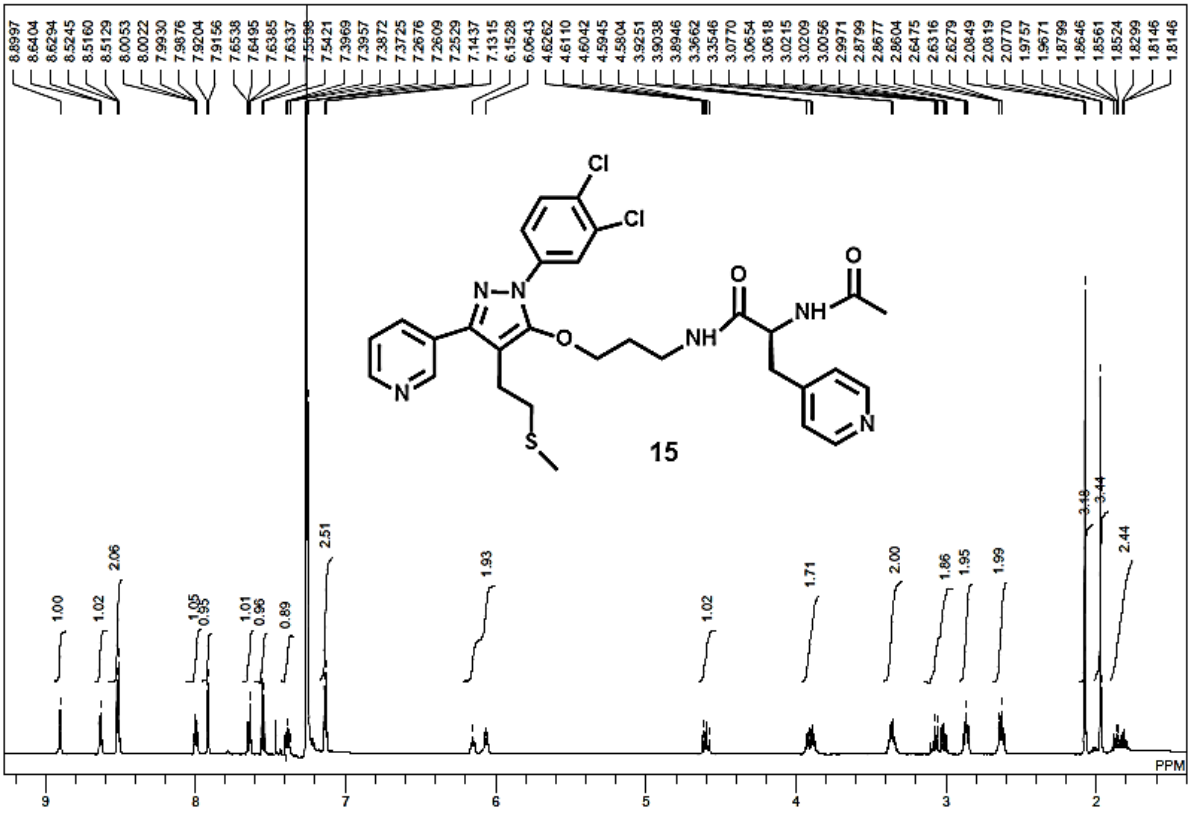
8.8997
8.6404
8.6294
8.5245
8.5160
8.5129
8.0053
8.0022
7.9930
7.9876
7.9204
7.9156
7.6538
7.6495
7.6385
7.6337
7.5598
7.5421
7.3969
7.3957
7.3872
7.3725
7.2676
7.2609
7.2529
7.1437
7.1315
6.1528
6.0643
4.6262
4.6110
4.6042
4.5945
4.5804
3.9251
3.9038
3.8946
3.3662
3.3546
3.0770
3.0654
3.0618
3.0215
3.0209
3.0056
2.9971
2.8799
2.8677
2.8604
2.6475
2.6316
2.6279
2.0849
2.0819
2.0770
1.9757
1.9671
1.8799
1.8646
1.8561
1.8524
1.8299
1.8146
1.8146
Cl
Cl
N
N
O
NH
O
NH
O
N
N
S
15
1.00
1.02
2.06
1.05
0.95
1.01
0.96
0.89
2.51
1.93
1.02
1.71
2.00
1.86
1.95
1.99
3.48
3.44
2.44
PPM
9
8
7
6
5
4
3
2

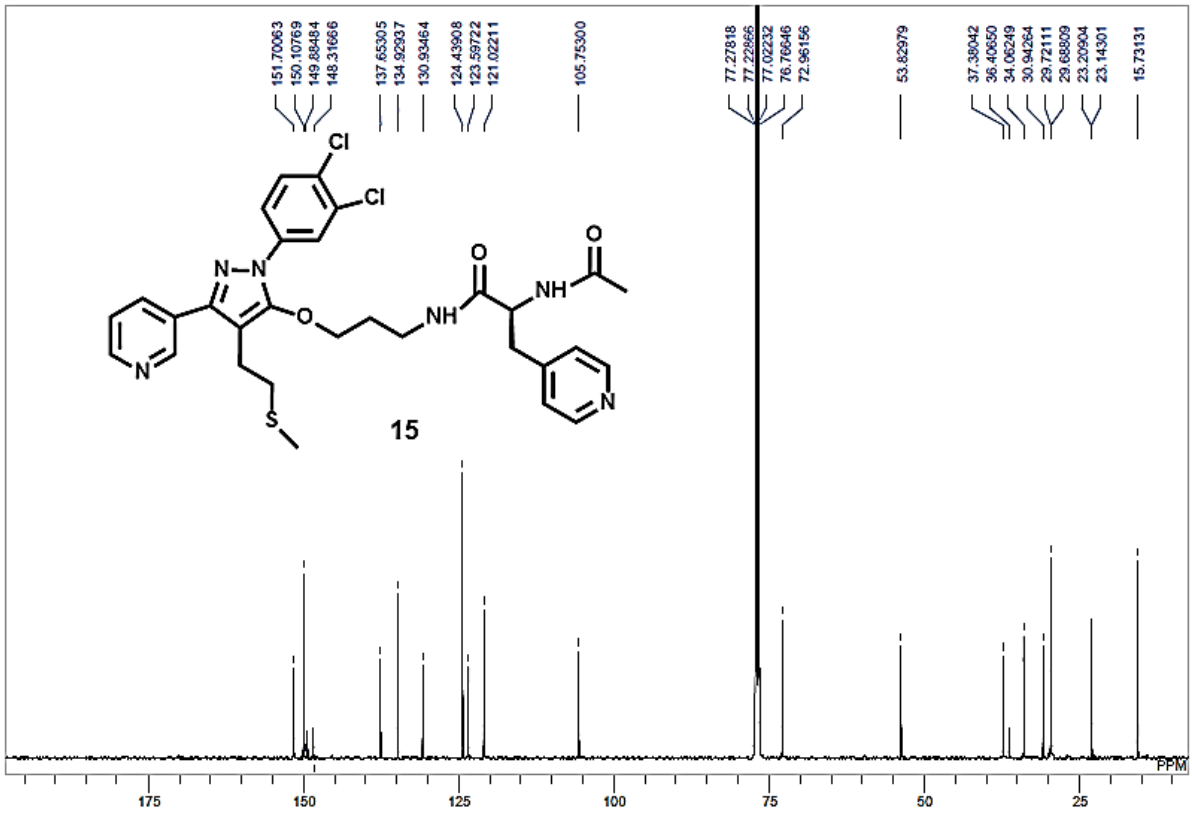
151.70063
150.10769
149.88484
148.31666
137.65305
134.92937
130.93464
124.43908
123.59722
121.02211
105.75300
77.27818
77.22866
77.02232
76.76646
72.96156
53.82979
37.38042
36.40650
34.06249
30.94264
29.72111
29.68809
23.20904
23.14301
15.73131
Cl
Cl
N
N
O
NH
O
NH
O
N
N
S
15
PPM
175
150
125
100
75
50
25

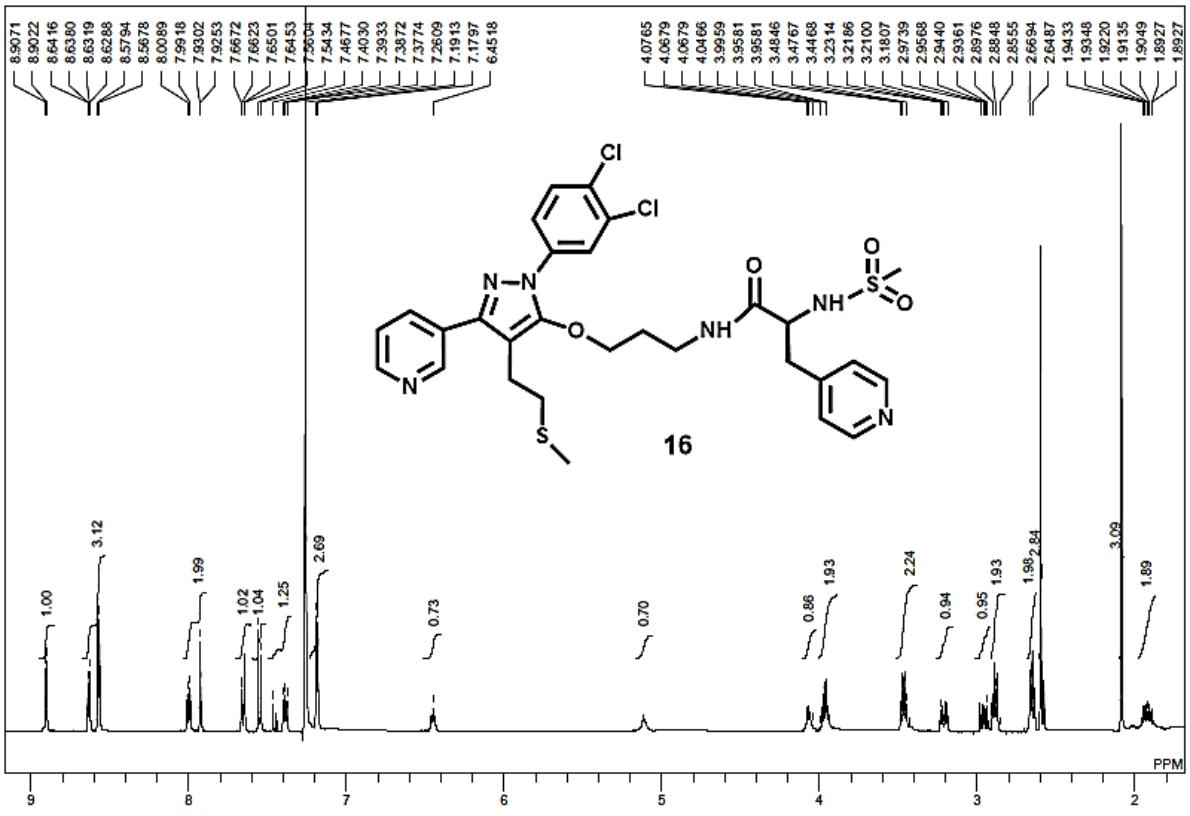
16
PPM

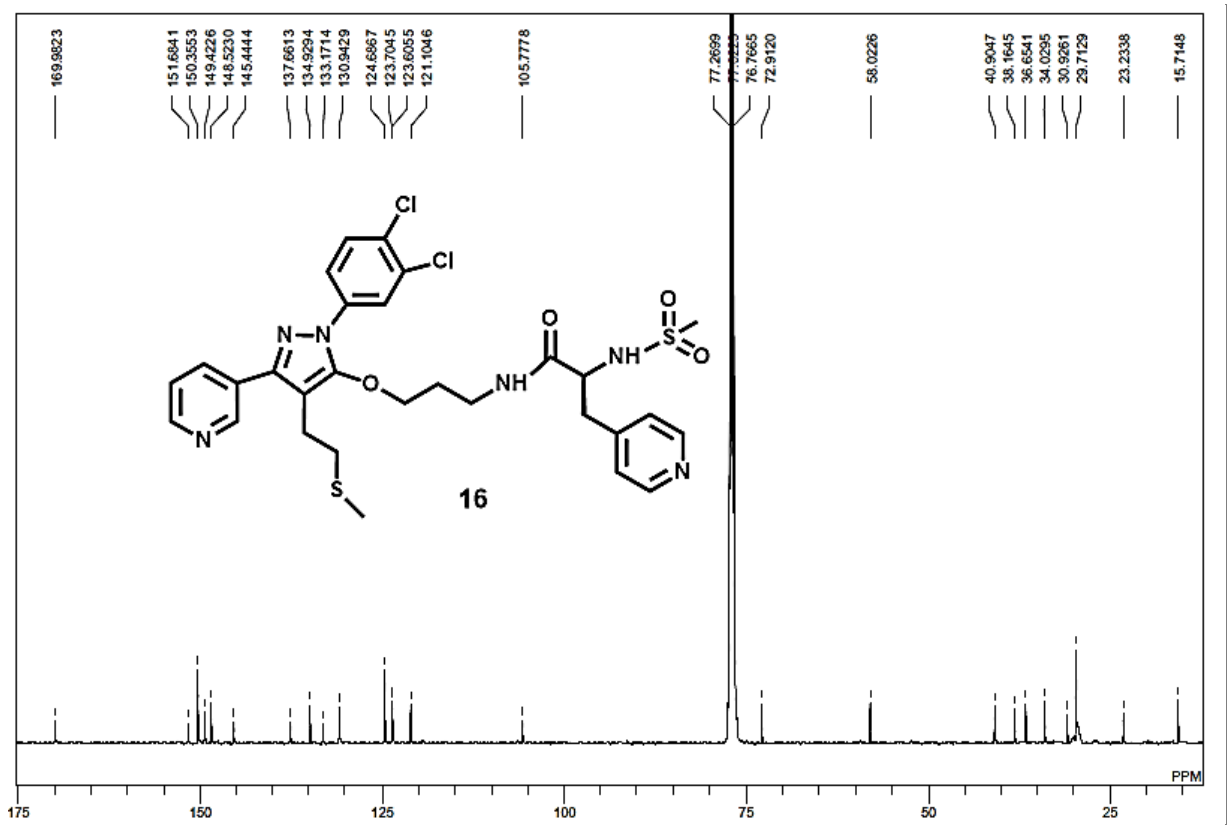
16
PPM

Vitae

Name	:MUHAMMAD MANSHA
Nationality	:PAKISTAN
Date of Birth	:5/11/1985
Email	:manshachohan@gmail.com
Address	:Department of Chemistry, KFUPM. Dhahran, KSA
Academic Background	:PhD in Chemistry
Publications	1). M. Mansha, N. Ullah, and K. Alhooshani, "Synthesis of structural analogues of GGT1-DU40, a potent GGTase-1 inhibitor", Zeitschrift für Naturforschung B 71 (4), 333-344, 2016. 2). M. Mansha, U. U. Kumari, Z. Cournia, and N. Ullah, "Pyrazole-based potent inhibitors of GGTase-I: Synthesis, biological evaluation and molecular docking studies," European Journal of Medicinal Chemistry, 124, 666-676, 2016. 3). N. Ullah, M. Mansha and P. J. Casey, "Protein Geranylgeranyltransferase Type 1 as a Target in Cancer, a review," Current Cancer Drug Targets, 16, 563-571, 2016.